RADIOLOGY AND ONCOLOGY

vol.49 no.2
june 2015

Halaven®
eribulin

NOVA SMER DO PODALJŠANJA **CELOKUPNEGA PREŽIVETJA**

Eisai

Prva in edina samostojna kemoterapija,
ki v primerjavi z ostalimi možnostmi zdravljenja
z enim zdravilom, pri bolnicah s predhodno že
večkratno zdravljenim metastatskim rakom dojke,
dokazano značilno podaljša celokupno preživetje.[1,2]

- **Halaven** (eribulin): ne-taksanski zaviralec dinamike mikrotubulov, prvo zdravilo iz nove skupine kemoterapevtikov, imenovanih *halihondrini*.
- Zdravilo HALAVEN je indicirano za zdravljenje bolnic z lokalno napredovalim ali metastatskim rakom dojke, ki je napredoval po vsaj enem režimu kemoterapije za napredovalo bolezen. Predhodna zdravljenja morajo vključevati antraciklin in taksan, bodisi kot adjuvantno zdravljenje ali za zdravljenje metastatskega raka dojke, razen če to zdravljenje za bolnice ni bilo primerno.[1]
- Priporočeni odmerek 1,23 mg/m^2, intravensko, v obliki 2- do 5-minutne infuzije, 1. in 8. dan vsakega 21-dnevnega cikla.
- Ena 2 ml viala vsebuje 0,88 mg eribulina.
- Raztopina, pripravljena za uporabo, redčenje ni potrebno.

SKRAJŠAN POVZETEK GLAVNIH ZNAČILNOSTI ZDRAVILA

HALAVEN 0,44 mg/ml raztopina za injiciranje (eribulin)
TERAPEVTSKE INDIKACIJE: Zdravljenje lokalno napredovalega ali metastatskega raka dojke, ki je napredoval po vsaj enem režimu kemoterapije za napredovalo bolezen vključno z antraciklinom in taksanom (adjuvantno zdravljenje ali zdravljenje metastatskega raka dojke), razen če to ni bilo primerno. **ODMERJANJE IN NAČIN UPORABE:** Halaven se daje v enotah, specializiranih za dajanje citotoksične kemoterapije, in le pod nadzorom usposobljenega zdravnika z izkušnjami v uporabi citotoksičnih zdravil. Odmerjanje: Priporočeni odmerek eribulina v obliki raztopine je 1,23 mg/m^2 i.v. v obliki 2- do 5-minutne infuzije 1. in 8. dan vsakega 21-dnevnega cikla. Bolnikom je lahko slabo ali bruhajo. Treba je razmisliti o antiemetični profilaksi, vključno s kortikosteroidi. *Preložitev odmerka med zdravljenjem*: Dajanje Halavena je treba preložiti, če se pojavi kaj od naslednjega: absolutno število nevtrofilcev (ANC) < 1 x 10^9/l, trombociti < 75 x 10^9/l ali nehematološki neželeni učinki 3. ali 4. stopnje. *Zmanjšanje odmerka med zdravljenjem*: Za priporočila za zmanjšanje odmerka ob pojavu hematoloških ali nehematoloških neželenih učinkov glejte celoten povzetek glavnih značilnosti zdravila. Okvara jeter zaradi zasevkov: Priporočeni odmerek pri blagi okvari jeter (stopnje A po Child-Pughu) je 0,97 mg/m^2 v obliki 2- do 5-minutne i.v. infuzije 1. in 8. dan 21-dnevnega cikla. Priporočeni odmerek pri zmerni okvari jeter (stopnje B po Child-Pughu) je 0,62 mg/m^2 v obliki 2- do 5-minutne i.v. infuzije 1. in 8. dan 21-dnevnega cikla. Pri hudi okvari jeter (stopnje C po Child-Pughu) se pričakuje, da je treba dati še manjši odmerek eribulina. Okvara jeter zaradi ciroze: Zgornje odmerke se lahko uporabi za blago do zmerno okvaro, vendar se priporoča skrbno nadziranje, saj bo odmerke morda treba ponovno prilagoditi. Okvara ledvic: Pri hudi okvari ledvic (očistek kreatinina < 40 ml/min) bo morda treba odmerek zmanjšati. Priporoča se skrbno nadziranje varnosti. Način uporabe: Odmerek se lahko razredči z do 100 ml 0,9 % raztopine natrijevega klorida (9 mg/ml) za injiciranje. Ne sme se ga redčiti v 5 % infuzijski raztopini glukoze. Pred dajanjem glejte navodila glede redčenja zdravila v celotnem povzetku glavnih značilnosti zdravila ter se prepričajte, da obstaja dober periferni venski dostop ali prehodna centralna linija. Ni znakov, da bi eribulin povzročal mehurje ali dražil. V primeru ekstravazacije mora biti zdravljenje simptomatsko. **KONTRAINDIKACIJE:** Preobčutljivost na zdravilno učinkovino ali katerokoli pomožno snov. Dojenje. **POSEBNA OPOZORILA IN PREVIDNOSTNI UKREPI:** Mielosupresija je odvisna od odmerka in se kaže kot nevtropenija. Pred vsakim odmerkom eribulina je treba opraviti pregled celotne krvne slike. Zdravljenje z eribulinom se lahko uvede le pri bolnikih z vrednostmi ANC ≥ 1,5 x 10^9/l in s trombociti > 100 x 10^9/l. Bolnike, pri katerih se pojavijo febrilna nevtropenija, huda nevtropenija ali trombocitopenija, je treba zdraviti v skladu s priporočili v celotnem povzetku glavnih značilnosti zdravila. Hudo nevtropenijo se lahko zdravi z uporabo G-CSF ali enakovrednim zdravilom v skladu s smernicami. Bolnike je treba skrbno nadzirati za znake periferne motorične in senzorične nevropatije. Pri razvoju hude periferne nevrotoksičnosti je treba odmerek prestaviti ali zmanjšati. Če začnemo zdravljenje pri bolnikih s kongestivnim srčnim popuščanjem, z bradiaritmijami ali sočasno z zdravili, za katera je znano, da podaljšujejo interval QT, vključno z antiaritmiki razreda Ia in III, in z elektrolitskimi motnjami, je priporočljivo spremljanje EKG. Pred začetkom zdravljenja s Halavenom je treba popraviti hipokaliemijo in hipomagneziemijo in te elektrolite je treba občasno kontrolirati med zdravljenjem. Eribulina ne smemo dajati bolnikom s prirojenim sindromom dolgega intervala QT. To zdravilo vsebuje majhne količine etanola (alkohola), manj kot 100 mg na odmerek. Eribulin je pri podganah embriotoksičen, fetotoksičen in teratogen. Halavena se ne sme uporabljati med nosečnostjo, razen kadar je to nujno potrebno. Ženske v rodni dobi naj ne zanosijo v času, ko same ali njihov moški partner dobivajo Halaven, in naj med zdravljenjem in še do 3 mesece po njem uporabljajo učinkovito kontracepcijo. Moški naj se pred zdravljenjem posvetujejo o shranjevanju sperme zaradi možnosti nepopravljive neplodnosti. **INTERAKCIJE:** Eribulin se izloča do 70 % prek žolča. Sočasna uporaba učinkovin, ki zavirajo jetrne transportne beljakovine, kot so beljakovine za prenos organskih anionov in beljakovine, odporne na številna zdravila, z eribulinom se ne priporoča (npr. ciklosporin, ritonavir, sakvinavir, lopinavir in nekateri drugi zaviralci proteaze, efavirenz, emtricitabin, verapamil, klaritromicin, kinin, kinidin, dizopiramid itd). Sočasno zdravljenje z indukcijskimi učinkovinami, kot so rifampicin, karbamazepin, fenitoin, šentjanževka, lahko povzroči znižanje koncentracij eribulina v plazmi, zato je ob sočasni uporabi induktorjev potrebna previdnost. Eribulin je blag inhibitor encima CYP3A4. Priporočljiva je previdnost in spremljanje glede neželenih učinkov pri sočasni uporabi snovi, ki imajo ozko terapevtsko okno in se odstranjujejo iz telesa predvsem preko CYP3A4 (npr. alfentanil, ciklosporin, ergotamin, fentanil, pimozid, kinidin, sirolimus, takrolimus). **NEŽELENI UČINKI:** Povzetek varnostnega profila Neželeni učinek, o katerem najpogosteje poročajo v zvezi s Halavenom, je supresija kostnega mozga, ki se kaže kot nevtropenija, levkopenija, anemija, trombocitopenija s pridruženimi okužbami. Poročali so tudi o novem začetku ali poslabšanju že obstoječe periferne nevropatije. Med neželenimi učinki, o katerih poročajo, je toksičnost za prebavila, ki se kaže kot anoreksija, navzea, bruhanje, driska, zaprtost in stomatitis. Med drugimi neželenimi učinki so utrujenost, alopecija, zvečani jetrni encimi, sepsa in mišičnoskeletni bolečinski sindrom. Seznam neželenih učinkov: *Zelo pogosti (≥ 1/10):* nevtropenija (57,0 %) (3./4. stopnje: 49,7 %), levkopenija (29,3 %) (3./4. stopnje: 17,3 %), anemija (20,6 %) (3./4. stopnje: 2,0 %), zmanjšan apetit (21,9 %) (3./4. stopnje: 0,7 %), periferna nevropatija (35,6 %) (3./4. stopnje: 7,6 %), glavobol (17,2 %) (3./4. stopnje: 0,8 %), dispnea (13,9 %) (3./4. stopnje: 3,1 %), kašelj (13,6 %) (3./4. stopnje: 0,6 %), navzea (33,8 %) (3./4. stopnje: 1,1 %), zaprtost (19,6 %) (3./4. stopnje: 0,6 %), driska (17,9 %) (3./4. stopnje: 0,8 %), bruhanje (17,6 %) (3./4. stopnje: 0,9 %), alopecija, artralgija in mialgija (19,4 %) (3./4. stopnje: 1,1 %), bolečina v hrbtu (13,0 %) (3./4. stopnje: 1,5 %), bolečina v udu (10,0 %) (3./4. stopnje: 0,7 %), utrujenost/astenija (47,9 %) (3./4. stopnje: 7,8 %), pireksija (20,4 %) (3./4. stopnje: 0,6 %), zmanjšanje telesne mase (11,3 %) (3./4. stopnje: 0,3 %). *Pogosti (≥ 1/100 do < 1/10):* okužba sečil (8 %) (3./4. stopnje: 0,5 %), pljučnica (1,2 %) (3./4. stopnje: 0,8 %), ustna kandidiaza, ustni herpes, okužba zgornjih dihal, nazofaringitis, rinitis, limfopenija (4,9 %) (3./4. stopnje: 1,4 %), febrilna nevtropenija (4,7 %) (3./4. stopnje: 4,5 %), trombocitopenija (4,3 %) (3./4. stopnje: 0,7 %), hipokaliemija (6,1 %) (3./4. stopnje: 1,7 %), hipomagneziemija (2,9 %) (3./4. stopnje: 0,2 %), dehidracija (2,8 %) (3./4. stopnje: 0,5 %), hiperglikemija, hipofosfatemija, nespečnost, depresija, disgevzija, omotičnost (7,9 %) (3./4. stopnje: 0,5 %), hipoestezija, letargija, nevrotoksičnost, oslinjenje solzenje (6,0 %) (3./4. stopnje: 0,1 %), konjunktivitis, vrtoglavica, tahikardija, vročinski valovi, orofaringealna bolečina, epistaksa, rinoreja, bolečina v trebuhu, stomatitis (9,3 %) (3./4. stopnje: 0,8 %), suha usta, dispepsija (5,9 %) (3./4. stopnje: 0,2 %), gastroezofagealna refluksna bolezen, razjede v ustih, distenzija trebuha, zvišanje alanin-aminotransferaze (7,6 %) (3./4. stopnje: 2,1 %), zvišanje aspartat-aminotransferaze (7,4 %) (3./4. stopnje: 1,5 %), zvišanje gama-glutamiltransferaze (1,8 %) (3./4. stopnje: 0,9 %), hiperbilirubinemija (1,5 %) (3./4. stopnje: 0,3 %), izpuščaj, pruritus (3,9 %) (3./4. stopnje: 0,1 %), bolezni nohtov, nočno potenje, suha koža, eritem, hiperhidroza, bolečina v kosteh (9,6 %) (3./4. stopnje: 1,7 %), mišični spazmi (5,1 %) (3./4. stopnje: 0,1 %), mišično-skeletna bolečina in mišično-skeletna bolečina v prsih, mišična oslabelost, disurija, vnetje sluznice (8,3 %) (3./4. stopnje: 1,1 %), periferni edem, bolečina, mrzlica, bolečina v prsih, gripi podobna bolezen. *Občasni (≥ 1/1.000 do < 1/100):* sepsa (0,5 %) (3./4. stopnje: 0,2 %), nevtropenična sepsa (0,1 %) (3./4. stopnje: 0,1 %), herpes zoster, tinitus, globoka venska tromboza, pljučna embolija, hepatotoksičnost (1,0 %) (3./4. stopnje: 0.6 %), palmarno-plantarna eritrodisestezija, hematurija, proteinurija, odpoved ledvic. *Redki (≥ 1/10.000 do < 1/1.000):* diseminirana intravaskularna koagulacija, intersticijska pljučna bolezen, pankreatitis, angioedem. Za popoln opis neželenih učinkov glejte celoten povzetek glavnih značilnosti zdravila. Vrsta ovojnine in vsebina: viala z 2 ml raztopine. **Režim izdaje: H Imetnik dovoljenja za promet:** Eisai Europe Ltd, European Knowledge Centre, Mosquito Way, Hatfield, Hertfordshire, AL10 9SN, Velika Britanija
HAL-270614, julij 2014
Pred predpisovanjem in uporabo zdravila prosimo preberite celoten povzetek glavnih značilnosti zdravila!

Viri: (1) Povzetek glavnih značilnosti zdravila Halaven, junij 2014; (2) Cortes J *et al. Lancet* 2011; 377: 914–23.

PharmaSwiss
Choose More Life

Odgovoren za trženje v Sloveniji:
PharmaSwiss d.o.o., Brodišče 32, 1236 Trzin
telefon: +386 1 236 47 00, faks: +386 1 283 38 10
HAL-0714-01, julij 2014

RADIOLOGY AND ONCOLOGY

June 2015
Vol. 49 No. 2
Pages 107-208
ISSN 1318-2099
UDC 616-006
CODEN: RONCEM

Publisher
Association of Radiology and Oncology

Affiliated with
Slovenian Medical Association – Slovenian Association of Radiology, Nuclear Medicine Society,
Slovenian Society for Radiotherapy and Oncology, and Slovenian Cancer Society
Croatian Medical Association – Croatian Society of Radiology
Societas Radiologorum Hungarorum
Friuli-Venezia Giulia regional groups of S.I.R.M.
Italian Society of Medical Radiology

Aims and scope
Radiology and Oncology is a journal devoted to publication of original contributions in diagnostic and interventional radiology, computerized tomography, ultrasound, magnetic resonance, nuclear medicine, radiotherapy, clinical and experimental oncology, radiobiology, radiophysics and radiation protection.

Editorial office

Radiology and Oncology
Zaloška cesta 2
P. O. Box 2217
SI-1000 Ljubljana
Slovenia
Phone: +386 1 5879 369
Phone/Fax: +386 1 5879 434
E-mail: gsersa@onko-i.si

Reader for English
Vida Kološa

Secretary
Mira Klemenčič
Zvezdana Vukmirović

Design
Monika Fink-Serša, Samo Rovan, Ivana Ljubanović

Layout
Matjaž Lužar

Printed by
Tiskarna Ozimek, Slovenia

Published quarterly in 400 copies

Beneficiary name: DRUŠTVO RADIOLOGIJE IN ONKOLOGIJE
Zaloška cesta 2
1000 Ljubljana
Slovenia

Beneficiary bank account number: SI56 02010-0090006751
IBAN: SI56 0201 0009 0006 751
Our bank name: Nova Ljubljanska banka, d.d.,
Ljubljana, Trg republike 2,
1520 Ljubljana; Slovenia

SWIFT: LJBASI2X

Subscription fee for institutions EUR 100, individuals EUR 50

The publication of this journal is subsidized by the Slovenian Research Agency.

Indexed and abstracted by:

- *Celdes*
- *Chemical Abstracts Service (CAS)*
- *Chemical Abstracts Service (CAS) - SciFinder*
- *CNKI Scholar (China National Knowledge Infrastructure)*
- *CNPIEC*
- *DOAJ*
- *EBSCO - Biomedical Reference Collection*
- *EBSCO - Cinahl*
- *EBSCO - TOC Premier*
- *EBSCO Discovery Service*
- *Elsevier - EMBASE*
- *Elsevier - SCOPUS*
- *Google Scholar*
- *J-Gate*
- *JournalTOCs*
- *Naviga (Softweco)*
- *Primo Central (ExLibris)*
- *ProQuest - Advanced Technologies Database with Aerospace*
- *ProQuest - Health & Medical Complete*
- *ProQuest - Illustrata: Health Sciences*
- *ProQuest - Illustrata: Technology*
- *ProQuest - Medical Library*
- *ProQuest - Nursing & Allied Health Source*
- *ProQuest - Pharma Collection*
- *ProQuest - Public Health*
- *ProQuest - Science Journals*
- *ProQuest - SciTech Journals*
- *ProQuest - Technology Journals*
- *PubMed*
- *PubsHub*
- *ReadCube*
- *SCImago (SJR)*
- *Summon (Serials Solutions/ProQuest)*
- *TDOne (TDNet)*
- *Thomson Reuters - Journal Citation Reports/Science Edition*
- *Thomson Reuters - Science Citation Index Expanded*
- *Ulrich's Periodicals Directory/ulrichsweb*
- *WorldCat (OCLC)*

This journal is printed on acid- free paper

On the web: ISSN 1581-3207
http://www.degruyter.com/view/j/raon
http://www.radioloncol.com

contents

clinical oncology

radiophysics

special communication

review

Blood-brain barrier permeability imaging using perfusion computed tomography

Jernej Avsenik[1], Sotirios Bisdas[2], Katarina Surlan Popovic[1]

[1] Institute of Radiology, University Medical Centre Ljubljana, Slovenia
[2] Department of Neuroradiology, Eberhard Karls University, Tubingen, Germany

Radiol Oncol 2015; 49(2): 107-114.

Received 2 December 2013
Accepted 2 March 2014

Correspondence to: Jernej Avsenik, M.D., Institute of Radiology, University Medical Centre Ljubljana, Zaloška cesta 7, SI-1000 Ljubljana, Slovenia. E-mail: jernej.avsenik@gmail.com

Disclosure: No potential conflicts of interest were disclosed.

Background. The blood-brain barrier represents the selective diffusion barrier at the level of the cerebral microvascular endothelium. Other functions of blood-brain barrier include transport, signaling and osmoregulation. Endothelial cells interact with surrounding astrocytes, pericytes and neurons. These interactions are crucial to the development, structural integrity and function of the cerebral microvascular endothelium. Dysfunctional blood-brain barrier has been associated with pathologies such as acute stroke, tumors, inflammatory and neurodegenerative diseases.

Conclusions. Blood-brain barrier permeability can be evaluated *in vivo* by perfusion computed tomography - an efficient diagnostic method that involves the sequential acquisition of tomographic images during the intravenous administration of iodinated contrast material. The major clinical applications of perfusion computed tomography are in acute stroke and in brain tumor imaging.

Key words: blood-brain barrier, permeability imaging, computed tomography; perfusion CT

Introduction

The blood-brain barrier (BBB) is the system of tightly regulated anatomical and biochemical mechanisms that protects the brain from harmful compounds in the peripheral circulation, supplies brain cells with nutrients, functions as a dynamic regulator of ion balance and filters harmful substances from the brain to the bloodstream.[1,2] It also restricts the entering of T-lymphocytes, maintaining the immune-privileged status of the brain.[3] The BBB primarily represents the selective diffusion barrier at the level of the cerebral microvascular endothelium. Capillary lumen is enclosed by a single endothelial cell, characterized by the presence of tight junctions (TJ), the absence of fenestrations, increased number of mitochondria and minimal pinocytic activity in comparison to peripheral endothelium. Pericytes are attached to the abluminal membrane of the endothelium and together they are enclosed by the basal lamina, which is contiguous with the plasma membrane of astrocyte end-feet.[2] Under physiologic conditions, the BBB is relatively impermeable. However, in pathologic conditions such as neoplasm, inflammatory/infectious disease and ischemia, the BBB permeability (BBBP) is increased[4] and the diffusion of molecules into the extravascular space is enhanced.[5,6] The increased BBBP can be evaluated *in vivo* by means of perfusion computed tomography (PCT) imaging.[7,8]

Blood-brain barrier cellular structures

Brain microvasculature endothelial cells

Brain endothelial cells represent the essential component of the BBB, performing functions such as diffusion barrier, transport, signaling, leukocyte transport and osmoregulation.[1] Functional polarity exists between the apical and basolateral surface of the endothelial cell, which is evident by asymmetrical distribution of various transport-related carriers and enzymes present in the luminal and ablu-

minal membranes.[9,10] Endothelial cells are connected at the point of junctional complex, comprised predominantly of TJs and adherent junctions.

TJs, the critical component of BBB, are complex structures of intracellular and trans-membrane proteins, bound to an active cytoskeleton. This structure enables the tightness, as well as preserves the capacity for rapid regulation and functional modulation.[9] Three major trans-membrane protein components of TJs are occludins[11], claudins[12], and the group of immunoglobulin gene superfamily proteins, namely junctional adhesion molecules (JAMs)[13] and the endothelial selective adhesion molecules (ESAMs).[14] These molecules are connected to a group of intracellular proteins called membrane-associated guanylate kinases (MAGUK) which function as a cytoplasmic adaptor proteins.[1,9] First order adaptor proteins are zonula occludens (ZO-1, ZO-2 and ZO-3) and Ca^{2+}-dependent protein serine kinase[15-17], while the second order adapter proteins include cingulin, afadin and function-associated coiled-coil protein (JACOP). Besides providing the structural support, these proteins also interact with a large number of signaling and regulatory molecules, enabling the regulation of BBB permeability through local chemical signals. In addition to tight junctions, endothelial cells are also joined by adherent junctions, composed of transmembrane protein VE-cadherin, connected to cytoskeleton via catenins.[9]

Tightness of the BBB is also provided on the enzymatic level. Numerous enzymes were found to be present in BBB elements in significantly higher concentrations than in peripheral vessels. These enzymes metabolize neuroactive blood-borne products and include γ-glutamyl transpeptidase, alkaline phosphatase, aromatic acid decarboxylase and cytochrome 450 enzymes.[9,18]

Various transport systems are also crucial for the proper functioning of BBB. For instance, carrier-mediated transport represents highly specific system that allows the selective transport of small molecules, such as amino-acids, hexoses, nucleosides, amines and vitamins.[9,18] Intracellular pH of endothelial cells as well as the optimal ion gradient across the membrane are provided by ion transporters, namely the sodium pump, sodium-potassium-two chloride co-transporter, chloride-bicarbonate exchanger and the sodium-hydrogen exchanger.[18] Active efflux systems such as ATP-binding cassette (ABC) transporters, the multidrug resistance transporter P-glycoprotein (P-gp) and the group of multidrug resistance-associated proteins (MDRs) prevent the passage of drugs and toxins across the BBB and facilitate the efflux of neuroactive solutes from brain to blood. The transport across BBB for larger molecules like transferrin, low density lipoprotein, IgG, insulin and insulin like growth factor is provided by receptor mediated transport called transcytosis. Finally, absorptive mediated endocytosis represents less selective form of transport, initiated by polycathionic molecules binding to negatively charged plasma membrane.[9]

Astrocytes, pericytes and neurons

Interactions of endothelial cells with surrounding cells as well as the extracellular matrix are crucial to their development, structural integrity[1] and function.[19,20] Astrocytes are glial cells whose end feet cover over 99% of the outer surface of the BBB endothelium.[1,20] Soluble factors released by astrocytes play important role in enhancing TJs, reducing gap junctional area[21] and also regulating water and electrolyte metabolism in the brain.[22]

Pericytes contribute to the low paracellular permeability of the BBB, perform a regulatory role in brain homeostasis, participate in vascular development and maintenance and also represent the source of adult pluripotent stem cells. Moreover, contractile, immune, phagocytic and migratory functions of pericytes have been described.[20]

Temporally and spatially adjusted blood supply in accordance to metabolic requirements of neurons is provided by intense communication between neurons, astrocytes and BBB. In addition to direct innervation of endothelial cells, neurons can regulate the BBB function through induction of specific enzymes in response to metabolic needs.[20]

Blood-brain barrier in pathology

BBB dysfunction can range from mild and transient TJ opening to chronic barrier breakdown and has been associated with pathologies such as ischemia, tumors, multiple sclerosis, Parkinson's disease, Alzheimer's disease, epilepsy, glaucoma and lysosomal storage diseases.[23]

Hypoxia is the end point in many disorders such as acute stroke, cardiac arrest, carbon monoxide poisoning, respiratory distress and rapid ascent to high altitude and leads to increased BBB permeability, edema and tissue damage.[3] Early interventions to reduce long term disease progression and disability rely on efficient diagnostic methods to identify the site and extent of BBB disturbance.[23,24]

Perfusion computed tomography for the evaluation of blood-brain barrier permeability

The advent of fast computed tomography (CT) scanners in the 1990's, together with the development of sophisticated post-processing software, has made PCT a powerful tool for investigating pathophysiological processes in the human body.[25] *In vivo* evaluation and quantitative analysis of brain perfusion by means of PCT has had considerable impact on patient care in the settings of severe head trauma, acute stroke, and cerebral tumors.[26-30] The determination of tissue perfusion by PCT involves the intravenous injection of tracer and subsequential imaging to monitor the concentration of tracer in the tissue and a feeding artery as functions of time.[27] One important advantage of CT is that the enhancement is linearly proportional to the concentration of tracer in the tissue.[25] Serial CT scans start before the contrast agent arrives to determine the baseline and repeated scans are acquired until the tracer leaves the tissues. Subtraction of the baseline from each of the serial CT scans after the arrival of the contrast agent at the tissue gives the time-density curve (TDC) of the tissue.[25,31] All the physiological information is obtained by mathematical analysis of the tissue TDC. These analyses are based on proposed 'tracer kinetics' models that describe the distribution of contrast in blood vessels and extravascular space of the tissue.[25,31]

Permeability imaging: basic concepts

BBBP describes how easy it is for a tracer molecule to move between the intravascular and extravascular space across the BBB. It is defined as the bulk flow of a tracer normalized for surface area, concentration gradient, and time:

$$\frac{dC_{tissue}}{dt} = P \cdot S \cdot M \cdot \left(C_{plasma} - C_{EES}\right) \qquad [Equation\ 1]$$

where P is the permeability (cm/s); S, the surface area per unit mass (cm^2/g); M, the tissue mass (g); C_{plasma} - C_{EES}, the concentration difference between plasma and extravascular extracellular compartment ($mmol/cm^3$).[6] Blood-brain barrier permeability (BBBP) can be expressed as the permeability surface area product (PS) or as transendothelial transfer constant (K).

PS represents the total diffusional flux across all capillaries and is measured in ml/min/100g of tissue. It can be interpreted as following: the unidirectional flux of solutes from blood plasma to interstitial space is equivalent to the complete transfer of all the solutes in PS ml of blood per minute to interstitial space.

Another parameter, frequently used in the setting of permeability imaging is called extraction fraction (E). E represents the fraction of solutes in arterial blood, with the potential to diffuse into extravascular space that actually becomes transferred from blood to interstitial space during a single passage of blood from the arterial end to the venous end of the capillaries of a tissue.[32]

Different permeability parameters can be calculated by measuring the leakage of an intravascular tracer into the extravascular space.[5,32,33] In the normal brain parenchyma, BBB is intact and tightly regulated. PS is normally 0 for large hydrophilic molecules such as a peripherally injected iodinated contrast agent.[5] As mentioned, many pathologic situations such as tumor, inflammatory/infectious disease, and ischemia can alter BBB integrity and allow the diffusion of fluid, blood or contrast molecules into the extravascular space.[5,6]

Tracer kinetic analysis

The analysis of PCT data for the evaluation of BBB can be done by parametric fitting using tracer kinetic models.[27] Compartmental modelling as exemplified by the Patlak model[33] assumes instantaneous mixing within the compartments[27] and has been used by many authors.[5,8,34-36] Alternatively, distributed parameter model (DPM) as first proposed by Johnson and Wilson[37] describes tracer concentration in the vascular compartment as a function of both time and position along the capillary[27] and is generally considered more accurate for the assessment of BBBP.[7,27,38]

Compartmental modelling: Patlak model

A compartment is defined as a well-mixed space where the concentration is spatially uniform within the volume of distribution. In addition, the out flux at any outlet must be directly proportional to the concentration of tracer.[39]

The Patlak model is a unidirectional 2-compartment model that calculates BBBP via linear regression.[5] Following injection into the blood stream, contrast agent will pass into the extravascular space at a rate that is characterized by transendothelial transfer constant K.[25] The theoretical basis of imaging K is the Patlak graphical analysis[33], which assumes that the injected contrast agent is distributed in two well-mixed compartments: the

intravascular (blood) and the extravascular compartment. At any given time, a voxel of tissue will contain both intravascular and extravascular contrast agent. Assuming that during the time interval 0–t there is virtually no return of contrast agent from the extravascular to blood space, the total concentration of contrast agent in the tissue at time t, can be expressed as:

$$Q(t) = V_b C_a(t) + K \int_0^t C_a(u)du \qquad [Equation\ 2]$$

where Q(t) is the tissue enhancement at time t; $C_a(t)$ is the arterial enhancement at time t; and V_b is the distribution volume, which is typically considered to be equal to the cerebral blood volume (CBV) in the considered region of interest. In Equation 2, the first term on the right side describes the intravascular component of enhancement and the second term describes the extravascular component. The graphical analysis of the Patlak model divides both sides of Equation 2 by $C_a(t)$ to give the following equation, describing the Patlak plot:[25,34]

$$\frac{Q(t)}{C_a(t)} = V_b + K\frac{\int_0^t C_a(u)du}{C_a(t)} \qquad [Equation\ 3]$$

In this equation, the ratio of Q(t) to $C_a(t)$ is plotted on the y-axis and is called "apparent distribution volume". The ratio of the integral of C_a to $C_a(t)$, which is plotted on the x-axis, is called "normalized plasma integral". The slope of a regression line fit to the linear part of the Patlak plot is an approximation of K at that time. This value represents the amount of accumulated tracer in relation to the amount of tracer that has been available in plasma and is a measurement of BBBP expressed in mL /100 g/min. The y-axis intercept is equal to the V_b or CBV.[34]

Theoretic model of blood-brain exchange, described by Patlak *et al*.[33,34], is relatively simple and frequently applied model to quantify BBBP from PCT data.[5,34] It assumes the unidirectional transfer of a tracer from a reversible (arterial) compartment to an irreversible extravascular space (brain parenchyma) for a certain period of time.[34,40] Transfer of tracer is assumed to be unidirectional when a steady-state phase is reached between reversible compartments (intravascular space and the blood-brain barrier complex). However, such a steady-state phase can only occur after the initial rapid changes in tracer concentration have subsided, so the arterial concentration decreases slowly enough for the tissue compartment to follow. Recent data suggest that only the delayed phase of the PCT acquisition (and not the first-pass) respects the assumptions of the Patlak model and that BBBP measurements extracted from first-pass PCT data overestimate BBBP values obtained from the delayed phase.[34]

The assumption that back-flux from extravascular into intravascular can be neglected during early times depends on the relative magnitude of blood flow (F) and the capillary permeability surface area product (PS).[25] Permeability (P) is related to the diffusion coefficient of contrast agent in the assumed water-filled pores of the capillary endothelium. The diffusion flux of contrast agent across the capillary endothelium is dependent on both the diffusion coefficient and the total surface area of the pores or the PS product.[36]

The PS product has the same dimensions as F, and thus the ratio PS/F is dimensionless. PS is related to K by the following:

$$K = EF \qquad [Equation\ 4]$$

If PS/F < 1, then K ~ PS. In normal cerebral vasculature, PS is negligible for all contrast agents presently in use.[36] The relative magnitude of PS and F also determines E, according to the classic Renkin-Crone equation:[25,41]

$$E = 1 - e^{\frac{-PS}{F}} \qquad [Equation\ 5]$$

However, in the setting of various pathologic processes, it is doubtful whether the no back flux assumption will be valid in general. Another major drawback of compartmental models is a fact that F and E (PS) cannot be measured separately because they are determined together as K (EF). All information about the convective transport of solute along the capillaries is lost due to the assumption that intravascular space is a well-mixed compartment.[32]

Distributed parameter model

Perfusion parameters can be derived from the impulse residue function (IRF). The IRF is a theoretical concept, *i.e.* a tissue TDC due to an idealized bolus injection of one unit of tracer into the arterial input.[31,42] It describes the fraction of tracer that remains in the tissue as time evolves.[25] Alternatively, it can be seen as the distribution of transit times in the tissue.[31] For ease of calculation, the IRF is usually constrained in its shape to comprise a plateau followed by a single exponential decay (Figure 1).[42] The duration of the plateau corresponds to the time interval during which all the injected contrast material remains in the capillary network.[28] Contrast agent diffusion appears in the IRF as a residual

enhancement that occurs after the initial impulse response and that decreases exponentially with time. The IRF is used to estimate the fraction of the mass of contrast agent arriving at the tissue that leaks into the extravascular space in a single passage through the vasculature, the extraction fraction (E).[25,36]

A mathematical process that uses arterial and tissue TDC to calculate IRF for the considered region of interest is called deconvolution. The height of the flow corrected IRF will give the tissue perfusion and the area under the curve (AUC) will determine the relative blood volume. This approach can be extended to include a measurement of capillary permeability by use of a distributed parameter model.[42]

In the Patlak model, the tracer concentration gradients within the vasculature are assumed to be zero.[32] DPM on the other hand, takes the tracer concentration gradients within the vascular compartment into account, and may therefore allow more complete analysis of the perfusion parameters from a single PCT study.[25,44] In contrast with compartmental models, it enables the separation of F and E (PS).[32] Moreover, with the adiabatic approximation in time domain[32,45], the model solution can be computed efficiently to generate functional maps of perfusion parameters.[25]

For the evaluation of BBBP, two compartment version of DPM has been used[7] as it can be mathematically expressed in a separable form in time domain, each component describing a physiological process:

$$R(t) = R_v(t) + R_p(t) \qquad [Equation\ 6]$$

where R is IRF for vascular (v) and parenchymal (p) phase.[7,27] For times, shorter than vascular transit time (duration of the plateau; $t < t_1$), the vascular phase of the equation remains constant and is proportional to the total amount of tracer in the injected bolus.[7,44] At t_1, the unextracted tracer exits via outflowing blood, and the detector response registers the fraction of extracted tracer, given by E. Beyond the t_1, the extracted tracer diffuses back into the blood and is cleared by outflowing blood, giving rise to a gradually decreasing parenchymal phase. The parameters that can be directly obtained from fitting experimental curves are F, t_1, rate of transfer from intravascular to extravascular compartment (k_{21}) and rate of transfer from extravascular to intravascular compartment (k_{12}). With the DPM, E can be formally given by:[7,27,44]

$$E(t_1) = 1 - e^{-k_{21}t_1} \qquad [Equation\ 7]$$

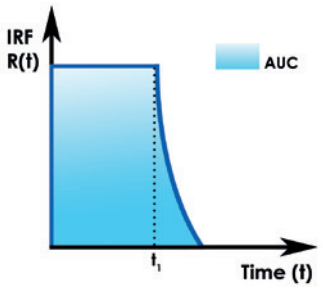

FIGURE 1. Impulse residue function (IRF). The IRF can be interpreted as the fraction of contrast medium that remains in the tissue as time evolves, following a bolus injection into arterial input. The duration of the plateau is the vascular transit time (t_1). The area under the curve (AUC) is the mean transit time (MTT). As the Central Volume Principle states that the product of flow (F) and MTT is blood volume (CBV), the AUC of the flow corrected IRF (FR(t)) is the CBV. R(t) - the IRF at time t.[43]

which is a function of the vascular transit time t_1. This expression for E implies that, for two capillaries with the same outflow (extravasation) rate k21, the fraction of extracted tracer in the first-pass would be larger for the capillary with the longer transit time. The rate constant k_{21} can then be expressed as the ratio of the PS and fractional vascular volume (v_1): $k_{21} = \varrho PS/v_1$. Since v_1 can be estimated by $v_1 = \varrho F t_1$, the PS could then be estimated as $PS = k_{21}v_1/\varrho$, and the latter equation reverts to the classic Renkin-Crone equation (Equation 5).[7,27]

Clinical applications of BBBP imaging

The major clinical applications of PCT are in acute stroke and in brain tumor imaging.[31]

Acute stroke

PCT can be used to demonstrate elevated BBBP as an indicator of ischemia-induced vascular damage.[35] Severe ischemia can alter BBB integrity and allow the diffusion of fluid, blood, or contrast molecules into the interstitium. A nonzero PS represents this diffusion quantitatively, and its functional color map can be generated by dedicated software (Figure 2).[5] Ischemia or reperfusion induced damage to the BBB may lead to hemorrhagic transformation (HT) and poor clinical outcome independent of thrombolytic therapy.[7] Symptomatic HT and malignant edema are feared complications in patients with acute ischemic stroke and occur 10 times more frequently in tPA-treated versus placebo-treated patients.[35] Permeability analysis by means of PCT with DPM, proved to be an efficient tool for predicting HT in acute ischemic stroke.[7] Another study has shown 100% sensitivity and 79 % specificity of admission BBBP imaging (using delayed acquisition PCT and Patlak model) in pre-

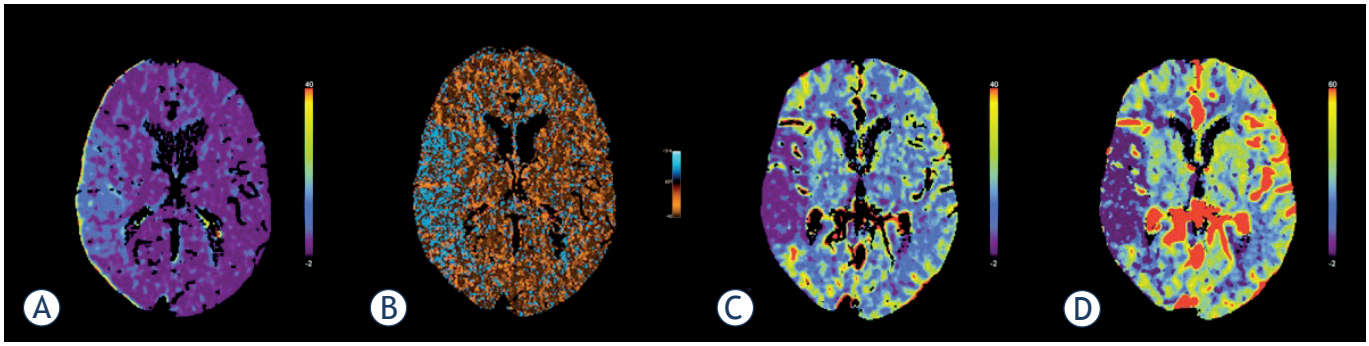

FIGURE 2. Perfusion computed tomography in acute stroke. Parametric maps show increased blood-brain barrier permeability values **(A,B)** in the right middle cerebral artery territory. The main advantage of Patlak's analysis is its conceptual simplicity **(A)**. On the other hand, distributed parameter model takes the tracer concentration gradients within vasculature into account and may allow more complete analysis of kinetic parameters **(B)**. The delineation of ischaemic area is clearly recognized on blood flow **(C)** and blood volume **(D)** parametric maps.

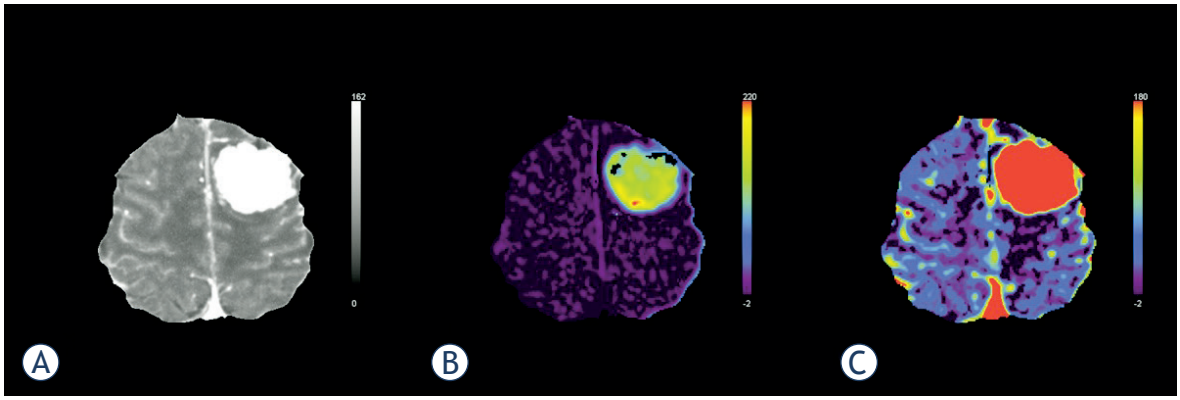

FIGURE 3. Perfusion computed tomography in brain tumours. Tracer kinetic analysis was performed in a patient with a large tumour in left cerebral hemisphere **(A)**, using Patlak model. The tumour tissue presents with significantly higher permeability values, indicating the immature leaky tumour vessels **(B)**. Unlike the blood volume parametric map **(C)**, permeability imaging also shows some local heterogeneity of tumour tissue.

dicting symptomatic HT and malignant edema in acute ischemic stroke.[35]

Brain tumor imaging

The development of a tumor blood supply through the process of angiogenesis is essential for the growth of tumors and also determines the ability of tumors to metastasize.[31] Hypoxia or hypoglycemia that occurs in rapidly growing tumors increases the expression of vascular endothelial growth factor (VEGF), which is a potent permeability factor.[36] Newly formed vessels are immature and have increased permeability to macromolecules due to large endothelial cell gaps, incomplete basement membrane, and absent smooth muscle.[36,46]

Altered permeability of the newly formed tumor vessels can be effectively assessed by the PS and E parametric maps, which offer the additional advantage of tumor segmentation and delineation from surrounding healthy tissue (Figure 3).[47] Both compartmental and distributed parameter modelling for contrast transport and exchange have been developed to quantify tissue F, CBV, MTT and permeability parameters.[32] Significant difference in PS was found between low grade (WHO grade II) and high grade (WHO III or IV) glioma.[48] Recent data even suggest that perfusion parameters, especially PS, can be used to differentiate grade III from grade IV glioma.[36] PCT therefore provides useful information for glioma grading and has the potential to significantly impact clinical management of cerebral gliomas.[48]

Conclusions

The BBB is tightly regulated system, performing functions such as diffusion barrier, transport, signaling and osmoregulation. In the normal brain

parenchyma, BBB is intact and impermeable for large molecules such as iodinated contrast agent. In pathologic situations such as neoplasm, inflammatory/infectious disease, ischemia and some neurodegenerative disorders, the BBBP is altered and the diffusion of fluid, blood or contrast molecules into the extravascular space is enhanced. BBBP can be *in vivo* evaluated by PCT, which uses different mathematical models to calculate physiological information from raw data. An efficient method to identify and quantify the extent of BBB disturbance allows early intervention to reduce the long term disability in some patients. To date, the major clinical applications of PCT have been in acute stroke and in brain tumor imaging.

References

1. Persidsky Y, Ramirez SH, Haorah J, Kanmogne GD. Blood-brain barrier: structural components and function under physiologic and pathologic conditions. *J Neuroimmune Pharmacol* 2006; **1:** 223-36.
2. Hawkins BT, Davis TP. The blood-brain barrier/neurovascular unit in health and disease. *Pharmacol Rev* 2005; **57:** 173-85.
3. Kaur C, Ling EA. Blood brain barrier in hypoxic-ischemic conditions. *Curr Neurovasc Res* 2008; **5:** 71-81.
4. Ballabh P, Braun A, Nedergaard M. The blood-brain barrier: an overview: structure, regulation, and clinical implications. *Neurobiol Dis* 2004; **16:** 1-13.
5. Lin K, Kazmi KS, Law M, Babb J, Peccerelli N, Pramanik BK. Measuring elevated microvascular permeability and predicting hemorrhagic transformation in acute ischemic stroke using first-pass dynamic perfusion CT imaging. AJNR *Am J Neuroradiol* 2007; **28:** 1292-8.
6. Zaharchuk G. Theoretical basis of hemodynamic MR imaging techniques to measure cerebral blood volume, cerebral blood flow, and permeability. AJNR *Am J Neuroradiol* 2007; **28:** 1850-8.
7. Bisdas S, Hartel M, Cheong LH, Koh TS, Vogl TJ. Prediction of subsequent hemorrhage in acute ischemic stroke using permeability CT imaging and a distributed parameter tracer kinetic model. *J Neuroradiol* 2007; **34:** 101-8.
8. Dankbaar JW, Hom J, Schneider T, Cheng SC, Lau BC, van der Schaaf I, et al. Accuracy and anatomical coverage of perfusion CT assessment of the blood-brain barrier permeability: one bolus versus two boluses. *Cerebrovasc Dis* 2008; **26:** 600-5.
9. Correale J, Villa A. Cellular elements of the blood-brain barrier. *Neurochem Res* 2009; **34:** 2067-77.
10. Farrell CL, Pardridge WM. Blood-brain barrier glucose transporter is asymmetrically distributed on brain capillary endothelial lumenal and ablumenal membranes: an electron microscopic immunogold study. *Proc Natl Acad Sci USA* 1991; **88:** 5779-83.
11. Furuse M, Hirase T, Itoh M, Nagafuchi A, Yonemura S, Tsukita S. Occludin: a novel integral membrane protein localizing at tight junctions. *J Cell Biol* 1993; **123:** 1777-88.
12. Furuse M, Fujita K, Hiiragi T, Fujimoto K, Tsukita S. Claudin-1 and -2: novel integral membrane proteins localizing at tight junctions with no sequence similarity to occludin. *J Cell Biol* 1998; **141:** 1539-50.
13. Bazzoni G, Tonetti P, Manzi L, Cera MR, Balconi G, Dejana E. Expression of junctional adhesion molecule-A prevents spontaneous and random motility. *J Cell Sci* 2005; **118:** 623-32.
14. Nasdala I, Wolburg-Buchholz K, Wolburg H, Kuhn A, Ebnet K, Brachtendorf G, et al. A transmembrane tight junction protein selectively expressed on endothelial cells and platelets. *J Biol Chem* 2002; **277:** 16294-303.
15. Fanning AS, Jameson BJ, Jesaitis LA, Anderson JM. The tight junction protein ZO-1 establishes a link between the transmembrane protein occludin and the actin cytoskeleton. *J Biol Chem* 1998; **273:** 29745-53.
16. Haskins J, Gu L, Wittchen ES, Hibbard J, Stevenson BR. ZO-3, a novel member of the MAGUK protein family found at the tight junction, interacts with ZO-1 and occludin. *J Cell Biol* 1998; **141:** 199-208.
17. Ebnet K, Schulz CU, Meyer Zu Brickwedde MK, Pendl GG, Vestweber D. Junctional adhesion molecule interacts with the PDZ domain-containing proteins AF-6 and ZO-1. *J Biol Chem* 2000; **275:** 27979-88.
18. Pardridge WM. Molecular biology of the blood-brain barrier. *Mol Biotechnol* 2005; **30:** 57-70.
19. Hamm S, Dehouck B, Kraus J, Wolburg-Buchholz K, Wolburg H, Risau W, et al. Astrocyte mediated modulation of blood-brain barrier permeability does not correlate with a loss of tight junction proteins from the cellular contacts. *Cell Tissue Res* 2004; **315:** 157-66.
20. Sa-Pereira I, Brites D, Brito MA. Neurovascular unit: a focus on pericytes. *Mol Neurobiol* 2012; **45:** 327-47.
21. Tao-Cheng JH, Brightman MW. Development of membrane interactions between brain endothelial cells and astrocytes in vitro. *Int J Dev Neurosci* 1988; **6:** 25-37.
22. Zlokovic BV. The blood-brain barrier in health and chronic eurodegenerative disorders. *Neuron* 2008; **57:** 178-201.
23. Abbott NJ, Patabendige AA, Dolman DE, Yusof SR, Begley DJ. Structure and function of the blood-brain barrier. *Neurobiol Dis* 2010; **37:** 13-25.
24. Abbott NJ, Ronnback L, Hansson E. Astrocyte-endothelial interactions at the blood-brain barrier. *Nat Rev Neurosci* 2006; **7:** 41-53.
25. Kellogg GE, Fornabaio M, Chen DL, Abraham DJ, Spyrakis F, Cozzini P, et al. Tools for building a comprehensive modeling system for virtual screening under real biological conditions: the computational titration algorithm. *J Mol Graph Model* 2006; **24:** 434-9.
26. Bisdas S, Donnerstag F, Ahl B, Bohrer I, Weissenborn K, Becker H. Comparison of perfusion computed tomography with diffusion-weighted magnetic resonance imaging in hyperacute ischemic stroke. *J Comput Assist Tomogr* 2004; **28:** 747-55.
27. Bisdas S, Donnerstag F, Berding G, Vogl TJ, Thng CH, Koh TS. Computed tomography assessment of cerebral perfusion using a distributed parameter tracer kinetics model: validation with H(2)((15))O positron emission tomography measurements and initial clinical experience in patients with acute stroke. *J Cereb Blood Flow Metab* 2008; **28:** 402-11.
28. Cenic A, Nabavi DG, Craen RA, Gelb AW, Lee TY. A CT method to measure hemodynamics in brain tumors: validation and application of cerebral blood flow maps. *Am J Neuroradiol* 2000; **21:** 462-70.
29. Hoeffner EG, Case I, Jain R, Gujar SK, Shah GV, Deveikis JP, et al. Cerebral perfusion CT: technique and clinical applications. *Radiology* 2004; **231:** 632-44.
30. Wintermark M. Brain perfusion-CT in acute stroke patients. *Eur Radiol* 2005; **15(Suppl 4):** D28-31.
31. Miles KA, Griffiths MR. Perfusion CT: a worthwhile enhancement? *Br J Radiol* 2003; **76:** 220-31.
32. Lee TY, Purdie TG, Stewart E. CT imaging of angiogenesis. *Q J Nucl Med* 2003; **47:** 171-87.
33. Patlak CS, Blasberg RG, Fenstermacher JD. Graphical evaluation of blood-to-brain transfer constants from multiple-time uptake data. *J Cereb Blood Flow Metab* 1983; **3:** 1-7.
34. Dankbaar JW, Hom J, Schneider T, Cheng SC, Lau BC, van der Schaaf I, et al. Dynamic perfusion CT assessment of the blood-brain barrier permeability: first pass versus delayed acquisition. *Am J Neuroradiol* 2008; **29:** 1671-6.
35. Hom J, Dankbaar JW, Schneider T, Cheng SC, Bredno J, Wintermark M. Optimal duration of acquisition for dynamic perfusion CT assessment of blood-brain barrier permeability using the Patlak model. *Am J Neuroradiol* 2009; **30:** 1366-70.
36. Jain R, Ellika SK, Scarpace L, Schultz LR, Rock JP, Gutierrez J, et al. Quantitative estimation of permeability surface-area product in astroglial brain tumors using perfusion CT and correlation with histopathologic grade. *Am J Neuroradiol* 2008; **29:** 694-700.

37. Johnson JA, Wilson TA. A model for capillary exchange. *Am J Physiol* 1966; **210:** 1299-303.

38. Koh TS, Cheong LH, Tan CK, Lim CC. A distributed parameter model of cerebral blood-tissue exchange with account of capillary transit time distribution. *Neuroimage* 2006; **30:** 426-35.

39. Sourbron SP, Buckley DL. Tracer kinetic modelling in MRI: estimating perfusion and capillary permeability. *Phys Med Biol* 2012; **57:** R1-33.

40. Schneider T, Hom J, Bredno J, Dankbaar JW, Cheng SC, Wintermark M. Delay correction for the assessment of blood-brain barrier permeability using first-pass dynamic perfusion CT. *Am J Neuroradiol* 2011; **32:** E134-8.

41. Crone C. The Permeability of Capillaries in Various Organs as Determined by Use of the 'Indicator Diffusion' Method. *Acta Physiol Scand* 1963; **58:** 292-305.

42. Miles KA. Perfusion CT for the assessment of tumour vascularity: which protocol? *Br J Radiol* 2003; **76 (Spec No 1):** S36-42.

43. Lee TY. Functional CT: physiological models. *Trends Biotechnol* 2002; **20 (Suppl 8):** S3-S10.

44. Larson KB, Markham J, Raichle ME. Tracer-kinetic models for measuring cerebral blood flow using externally detected radiotracers. *J Cereb Blood Flow Metab* 1987; **7:** 443-63.

45. St Lawrence KS, Lee TY. An adiabatic approximation to the tissue homogeneity model for water exchange in the brain: I. Theoretical derivation. *J Cereb Blood Flow Metab* 1998; **18:** 1365-77.

46. Hashizume H, Baluk P, Morikawa S, McLean JW, Thurston G, Roberge S, et al. Openings between defective endothelial cells explain tumor vessel leakiness. *Am J Pathol* 2000; **156:** 1363-80.

47. Bisdas S, Yang X, Lim CC, Vogl TJ, Koh TS. Delineation and segmentation of cerebral tumors by mapping blood-brain barrier disruption with dynamic contrast-enhanced CT and tracer kinetics modeling-a feasibility study. *Eur Radiol* 2008; **18:** 143-51.

48. Ding B, Ling HW, Chen KM, Jiang H, Zhu YB. Comparison of cerebral blood volume and permeability in preoperative grading of intracranial glioma using CT perfusion imaging. *Neuroradiol* 2006; **48:** 773-81.

research article

Evaluation of radiographic and metabolic changes in bone metastases in response to systemic therapy with ^{18}FDG-PET/CT

Bengul Gunalp[1], Ali Ozan Oner[2], Semra Ince[1], Engin Alagoz[1], Aslı Ayan[1], Nuri Arslan[1]

[1] Gulhane Military Medical Academy and Faculty, Department of Nuclear Medicine, Ankara, Turkey
[2] Kocatepe University Medical Faculty, Department of Nuclear Medicine, Afyon, Turkey

Radiol Oncol 2015; 49(2): 115-120.

Received 18 December 2014
Accepted 9 February 2015

Correspondence to: Dr. Bengul Gunalp, Gulhane Military Medical Academy and Faculty, Department of Nuclear Medicine, 06018 Ankara, Turkey. Phone: +90 312 3044806; Fax: +90 312 304 4800; E-mail: bgunalp@yahoo.com

Disclosure: No potential conflicts of interest were disclosed.

Background. The aim of the study was to retrospectively evaluate radiographic and metabolic changes in bone metastases in response to systemic therapy with ^{18}FDG-PET/CT and determine their roles on the evaluation of therapy response.

Patients and methods. We retrospectively evaluated radiographic and metabolic characteristics of bone metastases in 30 patients who were referred for the evaluation of response to systemic therapy with ^{18}FDG-PET/CT. All patients underwent integrated ^{18}FDG-PET/CT before and after treatment.

Results. The baseline radiographic patterns of the target lesions in responders group were lytic, sclerotic, mixed and CT negative; after treatment the radiographic patterns of all target lesions changed to a sclerotic pattern and attenuation increased ($p = 0.012$) and metabolic activity decreased ($p = 0.012$). A correlation was found between decreasing metabolic activity and increasing attenuation of the target lesions ($r = -0.55$) ($p = 0.026$). However, in non-responders group, the baseline radiologic patterns of the target lesions were lytic, blastic, mixed and CT negative; after treatment all lytic target lesions remained the same and one CT negative lesion turned to lytic pattern and the attenuation of the target lesions decreased ($p \pm 0.12$) and metabolic activity increased ($p = 0.012$). A correlation was found between increasing metabolic activity and decreasing attenuation ($r = -0.65$) ($p = 0.032$). An exception of this rule was seen in baseline blastic metastases which progressed with increasing in size, metabolic activity and attenuation.

Conclusions. This study shows that the metabolic activity of lesions is a more reliable parameter than the radiographic patterns for the evaluation of therapy response.

Key words: bone metastases; therapy response; ^{18}FDG-PET/CT

Introduction

A significant fraction of patients with known malignancy develop osseous metastases and this usually mandates a radical change to the therapeutic approach. Early detection and evaluation of the treatment response is essential for making correct treatment decisions. Therefore, techniques are required to identify patients with active bone metastases and to monitor the treatment response in a timely manner.

Bone scintigraphy using technetium-99m-labeled diphosphonates has been the method of choice for the detection of bone metastases for many years but it is considered to be unsuitable for evaluating treatment response, because it has a poor specificity for detecting metastases, and positive lesions on a bone scan tend to remain positive even after effective treatment.[1,2]

On the basis of radiographic appearance, bone metastases are classified as osteolytic, osteoblastic (sclerotic), or mixed pattern. The sclerosis of a

lytic component on computed tomography (CT) or plain radiographs is generally considered to suggest a response to treatment[1-4], but if there are no baseline studies it is not possible to differentiate osteoblastic active metastases from sclerotic unviable metastases.

^{18}F-fluorodeoxyglucose positron emission tomography/CT (^{18}FDG-PET/CT) is widely used for the diagnosis and staging of various malignant tumors and evaluating responses to therapy.[5-7] Abnormal bone ^{18}FDG uptake by tumor cells is in proportion to levels of glucose metabolism. ^{18}FDG is transported into tumor cells by glucose transporter proteins and phosphorylated by hexokinase to ^{18}FDG-6-phosphate, which is retained in the malignant cells. Because FDG uptake is related to the metabolic activity of the tumor itself, ^{18}FDG may detect metastases before bone destruction on a CT or osteoblastic healing on a bone scan.[8-10]

In previous investigations, it has been reported that in osteolytic metastases, ^{18}FDG is more likely to be positive, while sclerotic metastases are less likely to be positive[11-14], but changes of the radiographic and functional characteristics of the metastatic lesions during the treatment has not been investigated adequately. The clinical significance of ^{18}FDG-positive/CT-negative lesions and CT-positive/^{18}FDG-negative lesions pre and post-therapy conditions were unclear. In this retrospective study we tried to elucidate this issue determining functional and anatomic characteristics of bone metastases on pre and post-therapy conditions and their role on the evaluation of response to therapy.

Patients and methods

Patients

We retrospectively evaluated the radiographic and metabolic characteristics of bone metastases in 30 patients (mean age 58 years; age range 27–82) who were referred for the evaluation of response to systemic therapy with ^{18}FDG-PET/CT between January 2013 and April 2014. All patients underwent integrated ^{18}FDG-PET/CT before and after treatment. Two reviewers analyzed the images in consensus. Bone metastases in 15 patients with breast carcinoma, 10 patients with lung cancer, 2 patients with neuroendocrine tumor, 2 patients with lymphoma and 1 patient with sarcoma were included in this study (Table 1).

All patients received systemic therapy after baseline ^{18}FDG-PET/CT imaging. Systemic therapy for breast carcinoma patients included the use of endocrine therapy, chemotherapy and/or biologic agents. A choice between them had been made depending on the status of hormone receptors (estrogen, progesterone receptor positive patients received anti-estrogen treatment with tamoxifen or letrazole), status of human epidermal growth factor 2 (HER2) overexpression (HER2 positive patients received biological treatment with trastuzumab or lapatinib). Chemotherapy was combined if patient hadn't responded to endocrine or biological treatment. For metastatic lung carcinoma patients systemic therapy generally consisted of cytotoxic chemotherapy using cisplatin or carboplatin based doublet.

TABLE 1. Baseline characteristics of patients

Characteristic	Value
Mean age (y)	58 ± 13 (27-82)*
Sex	
Female	21 (70)**
Male	9 (30)
Type of cancer	
Breast cancer	15 (50)
Lung cancer	10 (33)
Neuroendocrine tumor	2 (6)
Lymphoma	2 (6)
Sarcoma	1 (3)

* Data are mean ± standard deviation. Data in parentheses are range; ** Data are numbers of patients and data in parentheses are percentages

The response assessment was made according to biochemical, radiologic and clinical follow-up and ^{18}FDG-PET/CT findings. Sixteen patients were classified as responders and 14 patients classified as non-responders or progressive disease. The morphologic appearance of the most prominent (target) lesion in each patient was classified as lytic, blastic (sclerotic), mixed or hypermetabolic bone lesion without CT findings (bone marrow) and lesion attenuation was measured as in Hounsfield units (HU) in axial CT images. The metabolic activity of the same lesion was calculated as the maximum standardized uptake value (SUV Max). The mean follow-up duration of the patients was 7 months, range 3 months to 18 months.

The institutional review board approved this study and for this type of study formal consent is not required (No. 50687469-1491-1311-13/1648.4-1472).

Imaging

^{18}FDG-PET/CT was performed prior to systemic therapy as a baseline study and after treatment (mean 28 days; range 24–32 days) in all patients.

^{18}FDG-PET/CT images were acquired with an integrated PET/CT device (GE Discovery 690). Before ^{18}FDG-PET/CT, patients fasted for at least 6 hours. All patients were tested to confirm that their glucose level was within the normal range [80–120 mg/dL (4.4–6.6 mmol/L)] before ^{18}FDG administration. Before PET, unenhanced CT was performed from vertex to the mid-thigh according to a standardized protocol with the following settings: 120 kVp, 85 mA, Pitch 1.375 and slice thickness 3.75 mm.

Emission scans were obtained 60 minutes after intravenous administration of ^{18}FDG (mean dose, 370 MBq; range 259–444 MBq). The acquisition time was 3 minutes per bed position in the two dimensional mode. Images were reconstructed with attenuation –weighted ordered –subset expectation maximization filter.

Image interpretation and radiographic analysis

PET and CT images obtained in all standard planes were reviewed by two experienced nuclear medicine physicians. Images were analyzed visually and quantitatively. Only the lesion that exhibited the most prominent uptake was selected as the target lesion for response evaluation to the treatment. The exact anatomic location of the target lesion was identified on CT images and classified as lytic, blastic (sclerotic), mixed and no CT finding (bone marrow metastases without identifiable bone destruction on CT).

The change in CT attenuation (ΔAtt) (measured in Hounsfield units) in the region of interest (ROI) of the entire lesion before and after treatment was calculated with the following equation: $\Delta Att = (Att_{post} - Att_{pre})$, where Att_{pre} and Att_{post} denote pre- and post-treatment attenuation, respectively.

The maximum standardized uptake value (SUV) was calculated with the following equation: $SUV = A(ID/BW)$, where A is the decay-corrected mean activity in tissue (measured in millicuries per milliliter), ID is the injected dose of FDG (measured in millicuries), and BW is the patient's body weight (measured in grams). Changes in SUV (ΔSUV) after treatment were calculated with the following equation: $\Delta SUV = (SUV_{post} - SUV_{pre})$, where SUV_{pre} and SUV_{post} denote pre and post-treatment SUV, respectively.

Therapy response evaluation

Patients' medical records and follow-up ^{18}FDG-PET/CT findings were evaluated retrospectively.

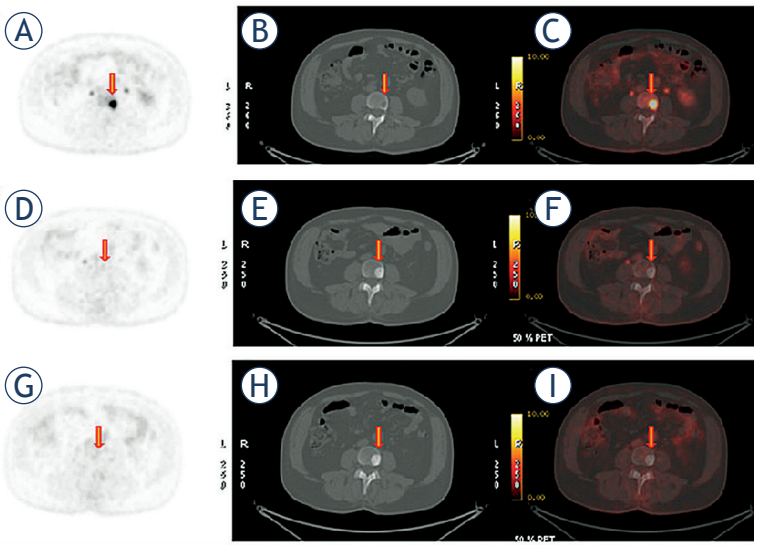

FIGURE 1. Baseline lytic lesion is healing with sclerosis. Baseline transaxial **(A)** ^{18}FDG PET, **(B)** CT, and ^{18}FDG-PET/CT images 65 years old man with lung carcinoma show lytic bone metastasis in vertebra (arrow). Maximum standardized uptake value (SUV) Max: 14.8, Hounsfield units (HU): 58; **(D)**, **(E)**, **(F)** 9 months after therapy lesion metabolic activity decreased SUV Max: 1.6, attenuation increased HU: 780; **(G)**, **(H)**, **(I)** 12 months after therapy. Inactive sclerotic metastasis with no metabolic activity and sclerotic appearance on CT with increased attenuation HU: 934.

In patients who were designated as responders, the target lesion showed decreased uptake when compared with the same lesion depicted on baseline images and all biochemical, radiologic and clinical follow-up findings confirmed the response to therapy. In non-responders, a follow-up examination revealed substantially increased ^{18}FDG uptake in the target lesion or additional new metastatic foci were identified on ^{18}FDG-PET/CT images and all biochemical, radiologic and clinical findings confirmed a progression of the disease.

Statistical analysis

Comparison of mean values between groups was performed with the Student t test. Spearman's rho test was performed to investigate any correlation between attenuation (HU) and metabolic activity (SUV Max) of the lesions. $P<0.05$ was considered to indicate a significant difference. IBM SPSS statistics software (Version 21) was used for the statistical analysis.

Results

The radiographic pattern of the target lesions on the baseline PET/CT images was classified as lytic

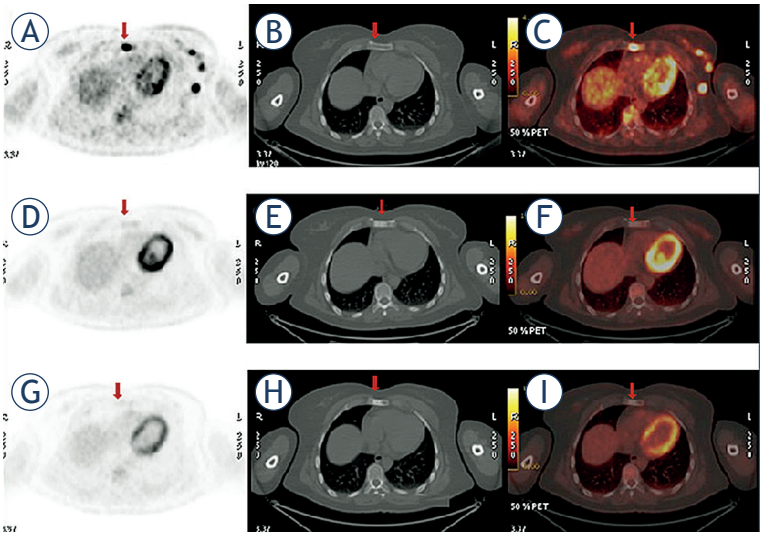

FIGURE 2. Baseline CT-negative ^{18}FDG-positive bone marrow metastasis is becoming sclerotic (CT-positive) while decreasing metabolic activity (^{18}FDG-negative) as a response to therapy. Baseline transaxial **(A)** ^{18}FDG- PET, **(B)** CT, and ^{18}FDG-PET/CT images in 45 years old woman with breast carcinoma show bone marrow metastasis in sternum (arrow) without corresponding CT abnormalities. Maximum standardized uptake value (SUV Max): 11, Hounsfield units (HU): 73; **(D)**, **(E)**, **(F)** 6 months after therapy lesion metabolic activity decreased SUV Max: 2.7, attenuation increased HU: 551; **(G)**, **(H)**, **(I)** 9 months after therapy. Inactive sclerotic metastasis with no increase metabolic activity and sclerotic appearance on CT with increased attenuation HU: 693.

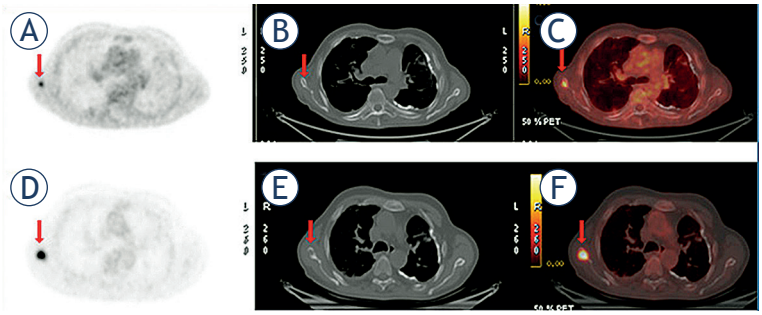

FIGURE 3. Progression of CT-negative ^{18}FDG-positive bone marrow metastasis with becoming lytic lesion on CT. Pre-treatment transaxial **(A)** ^{18}FDG-PET, **(B)** CT, and **(C)** ^{18}FDG-PET/CT images in 67 years old man with lung carcinoma show hypermetabolic bone metastasis in scapula (arrow) without any evidence on CT. Maximum standardized uptake value (SUV Max): 2.6, Hounsfield units (HU): 165; **(D)**, **(E)**, **(F)** 6 months after therapy bone metastasis did not respond to the therapy and the disease progressed. The lesion became lytic, its attenuation decreased HU: 84 and metabolic activity increased SUV Max: 19.9.

in 13 (43%) patients, blastic (sclerotic) in 7 (23%) patients, mixed in 3 (10%) patients and no CT abnormality on target lesion (bone marrow metastases) in 7 (23%) patients.

Responders group

There were 16 (53%) patients whose metabolic activity of the target lesion decreased after treatment

TABLE 2. Summary of the results

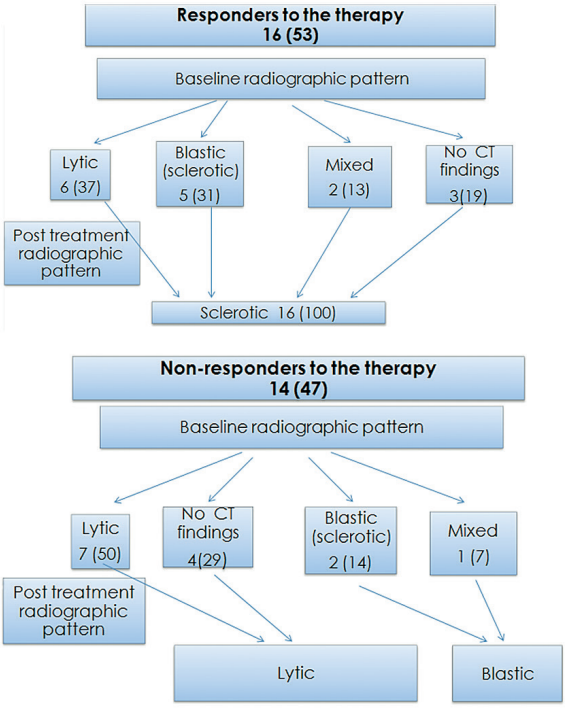

Data are numbers of patients and data in parentheses are percentages

and clinical follow-up confirmed the therapy response. The baseline radiographic patterns of the target lesions were lytic in 6 (37%) patients, blastic (sclerotic) in 5 (31%) patients, mixed in 2 (13%), bone marrow in 3(19%) and the mean attenuation was HU = 190 ± 137; the mean metabolic activity was SUV Max = 8.78 ± 3.09; after treatment the radiographic patterns of all target lesions turned to a sclerotic pattern, as shown in Figures 1, 2, attenuation increased (mean HU = 622 ± 273) ($p = 0.012$) and metabolic activity decreased (SUV Max: 2.92 ± 1.07) ($p = 0.012$). A negative correlation was found between decreasing metabolic activity (SUV Max) and increasing attenuation (HU) of the target lesions ($r = -0.55$) ($p = 0.026$). Three patients with increased metabolic activity on PET and any corresponding radiographic pathologic finding on CT turn to sclerotic lesion after treatment. Bone metastases of all tumor types with different radiological patterns on baseline CT scan showed sclerotic pattern on post-therapy scan if therapy response was achieved.

Non-responders group

There were 14 (47%) patients whose metabolic activity of the target lesion increased after therapy and progression of disease was confirmed by

biochemical, radiologic and clinical findings. The baseline radiographic patterns of the target lesions were lytic (n = 7), blastic (n = 2), mixed (n = 1), CT negative (bone marrow) (n = 4), the mean attenuation was HU = 349 ± 290 and mean metabolic activity was SUV Max = 7.6 ± 2.95; after treatment radiographic patterns of all lytic target lesions remained the same and one bone marrow lesion turned to a lytic pattern and attenuation of the target lesions decreased (HU 168 ± 212) (p = 0.12) and metabolic activity increased (SUV Max:11.0 ± 5.3) (p = 0.012) as shown in Figure 3. A negative correlation was found between increasing metabolic activity and decreasing attenuation (r = -0.65) (p = 0.032).

There were 3 (21%) patients with blastic and mixed metastases on their baseline study that progressed with increasing in size, metabolic activity and attenuation as shown in Figure 4. A summary of the results is illustrated in Table 2.

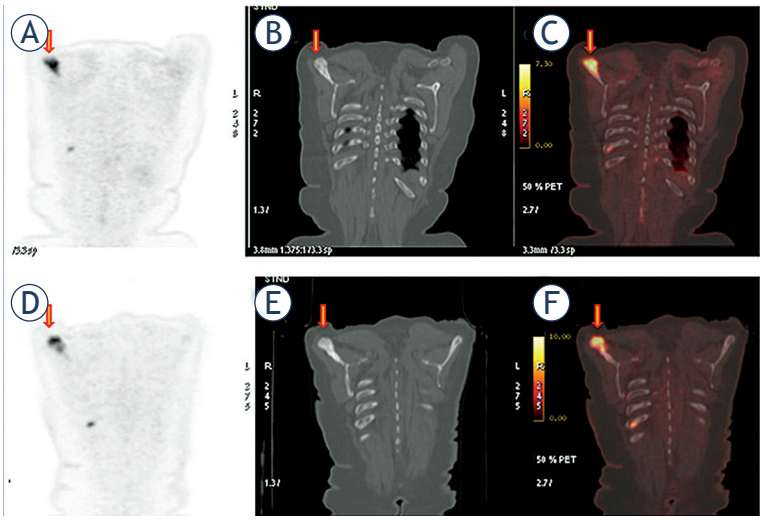

FIGURE 4. Progression of blastic metastasis with increasing metabolic activity and density. Pre-treatment coronal **(A)** ^{18}FDG-PET, **(B)** CT, and **(C)** ^{18}FDG-PET/CT images in 57 years old woman with breast carcinoma show blastic metastasis in scapula (arrow). Maximum standardized uptake value (SUV Max): 7.5, Hounsfield units (HU): 917; **(D)**, **(E)**, **(F)** 4 months after therapy bone metastasis did not respond to the therapy and the disease progressed. The lesion metabolic activity increased SUV Max: 11.1 and attenuation increased HU: 1056

Discussion

Our results show that an increase in attenuation and a decrease in SUV of bone metastases after systemic treatment are associated with therapy response as reported in previous studies.[15,16] All morphologic types of baseline metastatic lesions turned to sclerotic lesions if a therapy response was achieved. On the other hand, if a therapy response was not achieved different patterns were recognized which were not described in previous studies. If therapy response was not achieved while all baseline lytic lesions remained as lytic and CT-negative bone marrow lesions turned to lytic lesions but blastic lesions remained as blastic with increased metabolic activity, density and size. These findings were found to be highly correlated with the pathophysiology of bone metastases. In osteolytic bone metastases, tumor cells release humoral factors that stimulate osteoclastic activity and osteoclasts start to break down bone. Bone resorption results in the release of growth factors that stimulate tumor cell growth. In osteoblastic bone metastases, tumor cells secrete growth factors that stimulate the activity of osteoblasts. Excessive new bone formation occurs around tumor-cell deposits. Osteoblastic activation releases unidentified osteoblastic growth factors that also stimulate tumor cell growth.[17] Although we had very a few numbers of patients in non-responders group with blastic metastases our findings also confirmed continuing excessive new bone formation if therapy response was not achieved.

Our findings suggest that ^{18}FDG uptake reflects the tumor activity of bone metastases independent of the radiographic characteristics. Since both blastic metastases and sclerotic lesions show increased attenuation on CT, it is not possible to differentiate them based on their CT characteristics. ^{18}FDG-PET/CT enables the clinician to differentiate metabolically active tumor tissue in "blastic metastases" from scar tissue in sclerotic lesions. The radiographic changes vary greatly among individual patients and do not seem to correlate with the presence of an active tumor. This study also shows that sequential ^{18}FDG-PET/CT can provide vital information in monitoring the response of bone metastases to therapy.

In this study we observed "early marrow-based" metastases in 7 (23%) patients with increased metabolic activity confined to bone marrow without corresponding morphologic changes on CT. This finding is consistent with previous reports which documented that ^{18}FDG-PET/CT detects bone metastases earlier than CT when there are a substantial number of metabolically active tumor cells present in bone marrow but still tumor invasion of the bone matrix doesn't occur.[18,19]

In the previous studies ^{18}FDG-PET has been found less sensitive than CT and bone scan in the detection of sclerotic metastases, however, most of the patients included in these studies had been

treated with a systemic therapy[20-24], and it has been suggested that osteolytic bone metastases may become sclerotic after effective treatment.[25] ^{18}FDG-PET/CT combines both metabolic and anatomic information on the same image and provides more accurate assessment of bone metastases than does either PET and CT alone.

Hybrid ^{18}FDG-PET/CT provides us with a simultaneous comparison of functional and morphologic changes in bone metastases during the therapy and our study showed that if therapy response is achieved the most of the FDG positive bone metastases on pre-treatment study are becoming ^{18}FDG negative and sclerotic on CT. Our study confirmed that pre-treatment ^{18}FDG positive, post-treatment ^{18}FDG negative sclerotic lesions belong to scar tissue which is developing during the healing process of bone metastases.

Conclusions

This study shows radiographic patterns of bone metastases on CT changing during the therapy and the therapy response cannot be evaluated with the radiographic appearance of the lesion on CT. PET/CT has been found more sensitive and specific than CT both in detecting and evaluating the therapy response of bone metastases.

References

1. Du Y, Cullum I, Illidge TM, Ell PJ. Fusion of metabolic function and morphology: sequential [^{18}F]fluorodeoxyglucose positronemission tomography/computed tomography studies yield new insights into the natural history of bone metastases in breast cancer. *J Clin Oncol* 2007; **25:** 3440-7.
2. Hamaoka T, Madewell JE, Podoloff DA, Hortobagyi GN, Ueno NT. Bone imaging in metastatic breast cancer. *J Clin Oncol* 2004; **22:** 2942-53.
3. Tateishi U, Gamez C, Dawood S, Yeung HW, Cristofanilli M, Macapinlac HA. Bone metastases in patients with metastatic breast cancer: morphologic and metabolic monitoring of response to systemic therapy with integrated PET/CT. *Radiology* 2008; **247:** 189-96.
4. Bellamy EA, Nicholas D, Ward M, Coombes RC, Powles TJ, Husband JE. Comparison of computed tomography and conventional radiology in the assessment of treatment response of lytic bony metastases in patients with carcinoma of the breast. *Clin Radiol* 1987; **38:** 351-5.
5. Eisenhauer EA, Therasse P, Bogaerts J, Schwartz LH, Sargent D, Ford R, et al. New response evaluation criteria in solid tumours: revised RECIST guideline (version 1.1). *Eur J Cancer* 2009; **45:** 228-47.
6. Wahl RL, Jacene H, Kasamon Y, Lodge MA. From RECIST to PERCIST: evolving considerations for PET response criteria in solid tumors. *J Nucl Med* 2009; **50:** 122S-50S.
7. Juweid ME, Cheson BD. Positron-emission tomography and assessment of cancer therapy. *N Engl J Med* 2006; **354:** 496-507.
8. Evangelista L, Panunzio A, Polverosi R, Ferretti A, Chondrogiannis S, Pomerri F, et al. Early bone marrow metastasis detection: the additional value of FDG-PET/CT vs. CT imaging. *Biomed Pharmacother* 2012; **66:** 448-53.
9. Qu X, Huang X, Yan W, Wu L, Dai K. A meta-analysis of ^{18}FDG-PET-CT, ^{18}FDG-PET, MRI and bone scintigraphy for diagnosis of bone metastases in patients with lung cancer. *Eur J Radiol* 2012; **81:** 1007-15.
10. Yang HL, Liu T, Wang XM, Xu Y, Deng SM. Diagnosis of bone metastases: a meta-analysis comparing ^{18}FDG PET, CT, MRI and bone scintigraphy. *Eur Radiol* 2011; **21:** 2604-17.
11. Ben-Haim S, Israel O. Breast cancer: Role of SPECT and PET in imaging bone metastases. *Semin Nucl Med* 2009; **39:** 408-15.
12. Cook GJ, Houston S, Rubens R, Maisey MN, Fogelman I. Detection of bone metastases in breast cancer by ^{18}FDG PET: Differing metabolic activity in osteoblastic and osteolytic lesions. *J Clin Oncol* 1998; **16:** 3375-9.
13. Schirrmeister H. Detection of bone metastases in breast cancer by positron emission tomography. *Radiol Clin North Am* 2007; **45:** 669-76.
14. Uematsu T, Yuen S, Yukisawa S, Aramaki T, Morimoto N, Endo M. Comparison of FDG PET and SPECT for detection of bone metastases in breast cancer. *AJR Am J Roentgenol* 2005; **184:** 1266-73.
15. Tateishi U, Gamez C, Dawood S, Yeung HW, Cristofanilli M, Macapinlac HA. Bone metastases in patients with metastatic breast cancer: morphologic and metabolic monitoring of response to systemic therapy with integrated PET/CT. *Radiology* 2008; **247:** 189-96.
16. Du Y, Cullum I, Illidge TM, Ell PJ. Fusion of metabolic function and morphology: sequential [^{18}F]fluorodeoxyglucose positron-emission tomography/computed tomography studies yield new insights into the natural history of bone metastases in breast cancer. *J Clin Oncol* 2007; **25:** 3440-7.
17. Lipton A. Pathophysiology of bone metastases: How this knowledge may lead to therapeutic intervention. *J Support Oncol* 2004; **2:** 205-22.
18. Basu S,Torigian D, Alavi A. Evolving concept of imaging bone marrow metastasis in the twenty-first century: critical role of FDG-PET. *Eur J Nucl Med Mol Imaging* 2008; **35:** 465-71.
19. Ben-Haim S, Israel O. Breast cancer: Role of SPECT and PET in imaging bone metastases. *Semin Nucl Med* 2009; **39:** 408-15.
20. Cook GJ, Houston S, Rubens R, Maisey MN, Fogelman I. Detection of bone metastases in breast cancer by ^{18}FDG PET: Differing metabolic activity in osteoblastic and osteolytic lesions. *J Clin Oncol* 1998; **16:** 3375-9.
21. Uematsu T, Yuen S, Yukisawa S, Aramaki T, Morimoto N, Endo M, et al: Comparison of FDG PET and SPECT for detection of bone metastases in breast cancer. *AJR Am J Roentgenol* 2005; **184:** 1266-73.
22. Nakai T, Okuyama C, Kubota T, Yamada K, Ushijima Y, Taniike K, et al: Pitfalls of FDG-PET for the diagnosis of osteoblastic bone metastases in patients with breast cancer. *Eur J Nucl Med Mol Imaging* 2005; **32:** 1253-8.
23. Abe K, Sasaki M, Kuwabara Y, Koga H, Baba S, Hayashi K, et al: Comparison of ^{18}FDG-PET with 99mTc-HMDP scintigraphy for the detection of bone metastases in patients with breast cancer. *Ann Nucl Med* 2005; **19:** 573-79.
24. An YS, Yoon JK, Lee MH, Joh CW, Yoon SN. False negative F-18 FDG PET/CT in nonsmall cell lung cancer bone metastases. *Clin Nucl Med* 2005; **30:** 203-4.
25. von Schulthess GK, Steinert HC, Hany TF: Integrated PET/CT: Current applications and future directions. *Radiology* 2006; **238:** 405-22.

research article

Thyroid lesions incidentally detected by ^{18}F-FDG PET-CT — a two centre retrospective study

Jan Jamsek[1], Ivana Zagar[2], Simona Gaberscek[1,3], Marko Grmek[3]

[1] Faculty of Medicine, University of Ljubljana, Ljubljana, Slovenia
[2] Department for Nuclear Medicine, Institute of Oncology Ljubljana, Ljubljana, Slovenia
[3] Department for Nuclear Medicine, University Medical Centre Ljubljana, Ljubljana, Slovenia

Radiol Oncol 2015; 49(2): 121-127.

Received 29 June 2014
Accepted 22 September 2014

Correspondence to: Assist. Prof. Marko Grmek, M.D., Ph.D., Department for Nuclear Medicine, University Medical Centre Ljubljana, Zaloška cesta 2, 1000 Ljubljana, Slovenia. E-mail: marko.grmek@kclj.si

Disclosure: No potential conflicts of interest were disclosed.

Background. Incidental ^{18}F-FDG uptake in the thyroid on PET-CT examinations represents a diagnostic challenge. The maximal standardized uptake value (SUV_{max}) is one possible parameter that can help in distinguishing between benign and malignant thyroid PET lesions.

Patients and methods. We retrospectively evaluated ^{18}F-FDG PET-CT examinations of 5,911 patients performed at two different medical centres from 2010 to 2011. If pathologically increased activity was accidentally detected in the thyroid, the SUV_{max} of the thyroid lesion was calculated. Patients with incidental ^{18}F-FDG uptake in the thyroid were instructed to visit a thyroidologist, who performed further investigation including fine needle aspiration cytology (FNAC) if needed. Lesions deemed suspicious after FNAC were referred for surgery.

Results. Incidental ^{18}F-FDG uptake in the thyroid was found in 3.89% — in 230 out of 5,911 patients investigated on PET-CT. Malignant thyroid lesions (represented with focal thyroid uptake) were detected in 10 of 66 patients (in 15.2%). In the first medical centre the SUV_{max} of 36 benign lesions was 5.6 ± 2.8 compared to 15.8 ± 9.2 of 5 malignant lesions ($p < 0.001$). In the second centre the SUV_{max} of 20 benign lesions was 3.7 ± 2.2 compared to 5.1 ± 2.3 of 5 malignant lesions ($p = 0.217$). All 29 further investigated diffuse thyroid lesions were benign.

Conclusions. Incidental ^{18}F-FDG uptake in the thyroid was found in 3.89% of patients who had a PET-CT examination. Only focal thyroid uptake represented a malignant lesion in our study — in 15.2% of all focal thyroid lesions. SUV_{max} should only serve as one of several parameters that alert the clinician on the possibility of thyroid malignancy.

Key words: thyroid; ^{18}F-FDG; PET-CT; PET incidentaloma; thyroid cancer

Introduction

Incidental uptake of ^{18}F-fluorodeoxyglucose (^{18}F-FDG) in the thyroid is sometimes found during positron emission tomography - computed tomography (PET-CT)[1-3], which is mostly used in cancer staging and diagnostics.[4-6] Throughout the literature the reported incidence of incidental thyroid uptake of ^{18}F-FDG on PET-CT varies between 0.2% and 8.9%.[2] Thyroid lesions on PET-CT can be either diffuse or focal (Figure 1). Diffuse ^{18}F-FDG uptake is usually associated with autoimmune thyroiditis or Graves' disease[7-9], whereas focal ^{18}F-FDG uptake can be either due to a benign or malignant process in the thyroid.[10-19]

A semi-quantitative parameter that could help in differentiating thyroid lesions on PET-CT is the standardized uptake value (SUV), often expressed as the maximal SUV (SUV_{max}) or mean SUV (SUV_{mean}).[20] However, the discriminating power of this parameter is still unclear, as some studies have reported a statistically significant difference between SUV values of benign and malignant thyroid lesions[13,16,21,22],whilst others have shown no statistically significant difference.[17,23-28] Moreover, the SUV of benign and malignant thyroid lesions varied greatly between these studies. We also know that the calculated SUV is highly dependent on the scanner type, reconstruction algorithms and

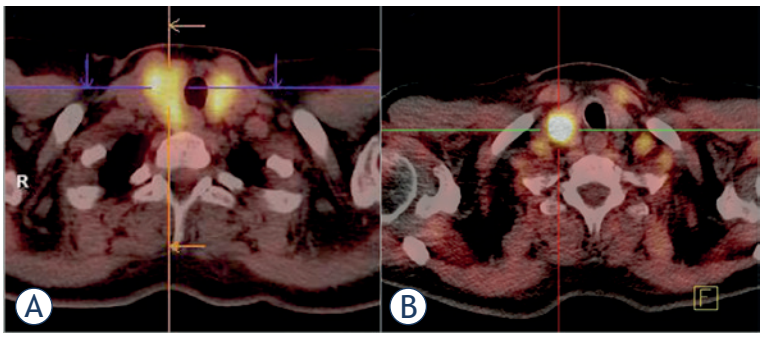

FIGURE 1. Fusion (PET-CT) scans of the thyroid. A diffuse ^{18}F-FDG accumulation in the thyroid is presented on scan **(A)** (this scan was done at the Institute of Oncology Ljubljana). A focal ^{18}F-FDG accumulation in the thyroid is presented on scan **(B)** (this scan was done at the University Medical Centre Ljubljana).

software packages used, which prevents the comparisons of studies conducted at different centres using different equipment.[29-31] This represented a challenge for our study.

The aims of this study were to (i) determine the incidence of thyroid lesions incidentally found on ^{18}F-FDG PET-CT, (ii) identify what diffuse and focal thyroid lesions represent, and (iii) what is the optimal SUV_{max} that can discriminate between benign and malignant focal thyroid lesions incidentally found on PET-CT. This study was conducted at two PET-CT centres (having different PET-CT scanners) in Slovenia: the Department of nuclear medicine at the University Medical Centre Ljubljana (UMC) and the Institute of Oncology Ljubljana (IO).

Patients and methods

Subjects and study design

We retrospectively evaluated the medical records of 5,911 patients (2,840 patients from UMC and 3,071 patients from IO) who underwent an ^{18}F-FDG PET-CT investigation between January 2010 and December 2011. Only patients (males and non-pregnant females) aged 18 years or more were included in this study. The ^{18}F-FDG PET-CT investigation of patients included in the study was performed for different purposes, mainly because of oncologic indications. The study was approved by the Ethics Committee at the Ministry of Health, Republic of Slovenia (No.: 53/04/12).

Methods employed

Patients from both centres fasted for at least 6 hours, ideally having a blood glucose level less than 7 mmol/l, before receiving 370 MBq of ^{18}F-FDG. The acquisition on the PET-CT scanner started 60 minutes after the radiotracer administration. The PET-CT scanners used were different: at UMC a Siemens Biograph mCT and at IO a Philips Gemini 16 GXL. In all patients, the localisation and attenuation correction CT was first done, followed by the PET scan itself. The CT acquisition parameters in both centres were fairly similar. Also, the PET acquisition parameters did not differ a lot; at UMC a bed position of 2 min with 45% overlap and at IO a bed position of 2 min with 50% overlap was used. The acquired PET-CT data was processed using similar iterative reconstruction algorithms.

Nuclear medicine doctors at both centres used visual and semi-quantitative data analysis (SUV_{max}) for creating a final report. They had access to relevant patient history and previous examination reports. Patients with thyroid lesion incidentally found on ^{18}F-FDG PET-CT were referred to a thyroidologist.

Thyroid investigation normally included the patient's history, clinical examination, relevant laboratory workup, ultrasound examination and ^{99m}Tc scintigraphy of the thyroid. For a final diagnosis of suspicious thyroid lesions, patients were further investigated using fine needle aspiration cytology (FNAC). A histological report was obtained for lesions that were surgically removed. All data (PET-CT reports, reports of thyroid examinations, cytological and histological reports) were obtained only from patients treated and followed-up at UMC and IO.

Statistical analyses

Statistical analysis was performed using IBM SPSS Statistics 22.0 and Microsoft Excel for Mac 14.1. The SUV_{max} of benign and malignant thyroid lesions were compared using Student's *t*-test. Results were deemed statistically significant for $p < 0.05$. A receiver operating characteristic (ROC) analysis was performed to determine a SUV_{max} cut-off point that differentiates between suspicious and unsuspicious focal thyroid lesions.

Results

Characteristics of patients

The mean age of 2,840 patients who had a PET-CT investigation at UMC was 61.2 ± 12.9 years; the mean age of 3,071 patients at IO was 64.4 ± 12.1

years. Fifty per cent of UMC patients were males and 50% females. The percentage of males and females in the IO group was 52.5% and 47.5% respectively. Patients at UMC underwent an ^{18}F-FDG PET-CT investigation mainly for cancer-related diagnostics or inflammatory/infection problems. On the other side, patients at IO underwent an ^{18}F-FDG PET-CT investigation almost exclusively because of cancer-related diagnostics.

Incidentally detected thyroid lesions

Incidental ^{18}F-FDG uptake in the thyroid was found in 230 out of 5,911 investigated patients (in 3.89%). Focal thyroid uptake represented 64.3% and diffuse thyroid uptake 35.7% of detected thyroid lesions. 56.1% of all focal lesions and 81.7% of all diffuse lesions were detected in female patients. More detailed information about patients with incidentally found thyroid lesions on ^{18}F-FDG PET-CT is presented in Table 1.

Data of further treatment were found for 58 out of 82 patients (in 70.7%) with increased ^{18}F-FDG uptake in the thyroid investigated at UMC and for 46 out of 148 patients (in 31.1%) investigated at IO. Diffuse thyroid lesions in 14/58 patients (24.1%) from UMC (SUV_{max} range from 3.5 to 10.3) and in 15/46 (32.6%) patients from IO (SUV_{max} range from 1.9 to 9.2) were all benign. Hashimoto's thyroiditis was diagnosed in 92.9% and 73.3% respectively.

At UMC, 44 patients with focal ^{18}F-FDG uptake in the thyroid (SUV_{max} range from 2.3 to 31.9) were further investigated. Thyroid nodules were found in 30 patients (in 68.2%). Autoimmune thyroid disease was diagnosed in 29.5% – in 12 patients with Hashimoto's thyroiditis and in one patient with Graves' disease. One patient was diagnosed to have benign diffuse goitre. FNAC was performed in 28 of 44 patients (63.6%). Results of FNAC are presented in Table 2.

Out of 31 focal thyroid lesions diagnosed on PET-CT in patients from IO (SUV_{max} range from 1.5 to 8.7) thyroid nodules were found in 28 cases (in 90.3%). In two patients the focal lesion was caused by Hashimoto's thyroiditis and in one by Graves' disease. FNAC diagnostics were performed in 24 of 31 patients (77.4%) (Table 2).

The optimal SUV_{max} cut-off point for differentiating between suspicious and unsuspicious focal thyroid lesions incidentally detected on PET-CT, calculated using ROC analysis, was 5.4 for patients investigated at UMC (sensitivity 76.9%, specificity 61.3%, AUC = 0.785); the optimal differentiating SUV_{max} for patients investigated at IO was 4.0 (sensitivity 66.7%, specificity 73.7%, AUC = 0.754).

TABLE 1. Patients and characteristics of incidental ^{18}F-FDG uptake in the thyroid detected by PET-CT

	Patients with incidental thyroid uptake			Incidental thyroid uptake	
	Number (m/f)	Incidence (%)	Age (year) (average ± SD)	Type	SUV_{max} (average ± SD)
UMC	61 (24/37)	2.15	63.6 ± 12.1	Focal	6.6 ± 4.4
	21 (4/17)	0.74	57.5 ± 14.4	Diffuse	7.9 ± 4.0
(all)	**82 (28/54)**	**2.89**	**62 ± 12.9**		**6.9 ± 4.3**
IO	87 (41/46)	2.83	64.2 ± 12.3	Focal	4.2 ± 2.1
	61 (11/50)	1.99	64.9 ± 11.2	Diffuse	4.3 ± 2.7
(all)	**148 (52/96)**	**4.82**	**64.5 ± 11.8**		**4.2 ± 2.3**

UMC = University Medical Centre Ljubljana; IO = Institute of Oncology Ljubljana; SUV_{max} = maximal standardised uptake value

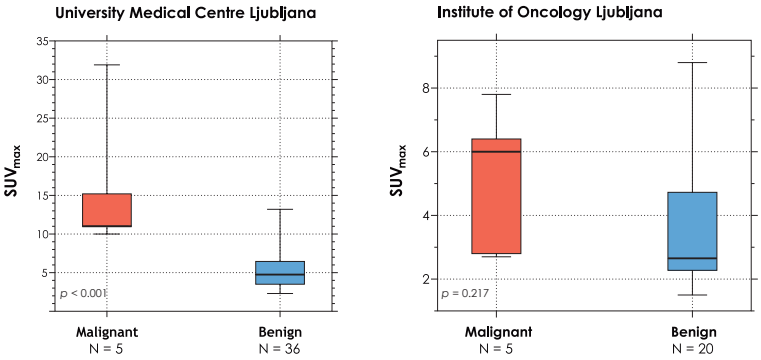

FIGURE 2. SUV_{max} of malignant and benign focal thyroid lesions (median, IQR and MIN/MAX values).

TABLE 2. Results of fine needle aspiration cytology for focal thyroid lesions, classified according to the Bethesda classification

Centre	FNAC (No.)	ND or UnS (No. (%))	BEN (No. (%))	AUS or FLUS (No. (%))	FN (No. (%))	SM (No. (%))	M (No. (%))
UMC	28	2 (7.1)	17 (60.8)	2 (7.1)	5 (17.9)	0	2 (7.1)
IO	24	5 (20.8)	7 (29.2)	1 (4.2)	3 (12.5)	3 (12.5)	5 (20.8)
All	52	7 (13.4)	24 (46.2)	3 (5.8)	8 (15.4)	3 (5.8)	7 (13.4)

FNAC = fine needle aspiration cytology, ND or UnS = non-diagnostic or unsatisfactory; BEN = benign; AUS or FLUS = atypia of undetermined significance or follicular lesion of undetermined significance; FN = follicular neoplasms and oncocytic tumours; SM = suspicious for malignancy; M = malignant

Surgically removed focal thyroid lesions

Malignant thyroid disease was found in 10 out of 18 patients (55.6%) who underwent surgery. Malignant thyroid disease was more common in males (8 cases) than in females (2 cases). Nine patients with focal thyroid lesions who were referred for surgery were lost to follow-up. Therefore in 10 out of 66 patients (15.2%) with focal thyroid lesion incidentally detected on ^{18}F-FDG PET-CT malignant thyroid disease was confirmed. Detailed characteristics of all surgically removed thyroid lesions are presented in Table 3.

SUV_{max} of malignant and benign focal thyroid lesions

SUV_{max} of malignant focal lesions (histologically confirmed) was compared to SUV_{max} of benign focal lesions (the benign nature of a lesion was established either after a thorough thyroid examination with ultrasound, FNAC or surgical treatment) (Figure 2). A statistically significant ($p < 0.001$) difference was observed between 36 benign (SUV_{max} from 2.3 to 13.2) and 5 malignant (SUV_{max} from 10 to 31.9) focal thyroid lesions incidentally detected on PET-CT in patients from UMC. No statistically significant difference ($p = 0.217$) was observed between 20 benign (SUV_{max} from 1.5 to 8.8) and 5 malignant (SUV_{max} from 2.7 to 7.8) focal thyroid lesions in patients from IO.

Discussion

Incidental ^{18}F-FDG uptake in the thyroid was observed in 3.89% of 5,911 patients investigated; in 2.89% of patients investigated at UMC and in 4.82% of patients investigated at IO. This is in accordance with the present literature, where the incidence of such lesions varied from 0.2 to 8.9%, with most studies reporting a incidence between 2 and 3%.[2,3,11-13,16,17,19,21-28,32-36] In a review article by Bertagna *et al.*[2], the authors postulated that this variability in incidence could be attributed to population characteristics and background risk of thyroid disease related to specific geographic areas.

Slovenia, although not an endemic goitre region, still has a significant incidence of thyroid nodules in the general population.[37] This could in part explain the slightly higher incidence of thyroid lesions incidentally found on PET-CT compared to some studies, where authors found a smaller incidence of thyroid lesions.[11,12,17]

According to the *American Thyroid Association Guidelines Taskforce*[38] further investigation of incidentally found thyroid nodules is recommended. Adhering to these guidelines, all patients from our practices with an incidentally detected thyroid lesion on PET-CT were referred to a thyroidologist. Due to different reasons, not all patients had a consultation, mainly because of the management of their primary illness. In our study, 71% of patients from UMC and only 31% of patients from IO received additional thyroid diagnostics. Our explanation for this difference is that PET-CT examinations in patients at IO were done almost exclusively for staging of known primary malignant diseases – many of these patients had more severe primary malignancies that required more prompt treatment than potential thyroid neoplasms. In comparison at UMC, approximately one third of PET-CT examinations were done for non-oncologic indications in which cases additional thyroid diagnostics were more likely than in oncologic patients with more severe primary disease. Other studies also reported a similar percentage of patients with incidentally discovered thyroid PET lesions who were further investigated, with follow-up rates in the ranks of 50%.[11-13,16-18,23-25,28]

Experts agree that diffuse thyroid uptake of ^{18}F-FDG on PET-CT is associated with Hashimoto's thyroiditis.[9] This was also confirmed by our results, where most diffuse lesions were caused by Hashimoto's thyroiditis and no malignancy was found in patients with diffuse thyroid PET lesions.

According to the literature, the rate of focal lesions ranges from 14% to 73% of all thyroid PET lesions[8,16,24,32] with a risk of malignancy in further investigated lesions of about 33%.[2,38] In our study, focal thyroid lesions were present in 64.3% of all cases with incidental thyroid uptake. These lesions represented a thyroid nodule in 68.2% (UMC patients) and in 90.3% (IO patients). We histologically confirmed thyroid malignancy in 5 of 10 surgically treated patients from UMC and in 5 of 8 patients from IO. Altogether, malignant disease was observed in 10 of 66 patients (in 15.2%) with a focal ^{18}F-FDG uptake in the thyroid. In comparison to other reports, the incidence of thyroid malignancy in our study was somewhat lower.[2,12,13,16,17,21-28,34] This is, in our opinion, mainly due to higher goitre prevalence in our population.[37]

Autoimmune thyroid disease was present in 29.5% of focal thyroid lesions from UMC patients. This finding is quite different from data published in the literature.[18,23] Our explanation for this discrepancy is in the different diagnostic process

TABLE 3. Characteristics of surgically removed thyroid lesions

Centre	Referral diagnosis	Sex (m/f)	Age (year)	SUV_{max}	Size (mm)	Cytology	Histology
UMC	Gastric carcinoma	f	71	5.5	10	Oncocytic cells	Hürthle adenoma
	Suspicious lesion in the right lungs	m	68	4.8	12	Unsatisfactory	Nodular goitre
	Tumour of the cardia	f	48	8.9	9	Oncocytic cells	Hürthle adenoma
	Erythema nodosum and pharyngitis	f	40	7.5	22	Unsatisfactory	Hürthle adenoma
	Pelvic inflammatory disease	f	61	6.4	10	Oncocytic cells	Nodular goitre
	Lung carcinoma	m	70	15.2	30	Oncocytic cells	Follicular carcinoma
	Origo ignota malignant disease	m	48	11	21	Atypia of undetermined significance	Medullary carcinoma
	Histiocytosis	m	41	11	10	Papillary carcinoma	Papillary carcinoma
	GIT malignancy	f	64	31.9	52	Atypia of undetermined significance	Papillary carcinoma
	Metastatic lesion on the left side of the neck	m	74	10	30	Planocelluar metastasis	Planocellular subglottic carcinoma — metastasis
IO	Hodgkin's lymphoma	f	64	3.2	15	Suspicious for malignancy (follicular or Hürthle)	Hyperplastic follicular benign nodule
	Malignant melanoma	m	71	2	23	Suspicious for malignancy (follicular or papillary)	Multinodular colloid goitre
	Tumour of the GE junction	f	62	8.7	35	Oncocytic cells	Hürthle adenoma
	Tumour mass in the thigh	m	22	7.8	9	Papillary carcinoma	Follicular carcinoma
	Rectal carcinoma	m	71	2.7	40	Suspicious for follicular malignancy	Follicular carcinoma
	Malignant melanoma	f	55	6	10	Papillary carcinoma	Thyroid malignancy with elements of follicular, papillary and Hürthle carcinoma
	Rectal carcinoma	m	59	6.4	10	Papillary carcinoma	Papillary carcinoma
	Rectal carcinoma	m	58	2.8	15	Oncocytic cells	Papillary carcinoma

UMC = University Medical Centre Ljubljana; IO = Institute of Oncology Ljubljana; SUV_{max} = maximal standardised uptake value; GE = gastro-oesophageal; GIT = gastro-intestinal tract

that was used in different institutions. At UMC, a thorough thyroid examination with relevant laboratory workup and an ultrasound examination of the thyroid, irrespective of the use of FNAC, was in most patients enough to make a final diagnosis of thyroid disease. The decision regarding FNAC examination was undertaken by the consulting thyroidologist on a patient by patient basis. Most studies, like the one conducted by Chu *et al.*[12], were more in line with the IO group, where only 3 of 31 focal PET lesions proved to be of autoimmune origin.

According to the literature, Graves' disease is demonstrated most commonly by diffusely increased ^{18}F-FDG uptake in the thyroid.[39,40] However, in our study, we found two cases of Graves' disease with focal ^{18}F-FDG uptake.

One of the main goals of our study was to determine whether it would be possible to differentiate between benign and malignant thyroid le-

sions using SUV_{max}. The literature is quite divided on this topic, with studies claiming to being able to differentiate between benign and malignant lesions[13,21,22,41] and others whose conclusions were the exact opposite.[17,23-28] This was also the case in our study, where the UMC group presented a statistically significant difference between benign and malignant lesions, whereas no such difference was found in the IO group. Even though the mean SUV_{max} of malignant lesions were on average higher than benign lesions, the overlap between both sets of lesions was considerable. For example, a Hürthle adenoma had a relatively high SUV_{max} of 8.9 while on the other side; a papillary thyroid carcinoma had a SUV_{max} of only 2.8.

It should also be noted, that calculated SUV_{max} is highly dependent on the type of PET-CT scanner, reconstruction algorithms and software packages used[20,29-31], as was the case in our study, which included two centres with different equipment. The newer Siemens Biograph® mCT used at UMC had a better detector system and time of flight technology compared to the older Philips Gemini 16 GXL. These might be some of the factors resulting in different SUV_{max} readings at both centres. Therefore, the SUV_{max} of a thyroid lesion should only serve as one of several parameters that alert the clinician on the possibility of thyroid malignancy. The correct protocol in this situation is, as recommended by the *American Thyroid Association Guidelines*, to promptly investigate all focal thyroid PET lesions with additional diagnostics.[38]

Conclusions

Incidental ^{18}F-FDG uptake in the thyroid on PET-CT was found in 3.89%. Only focal thyroid uptake represented a malignant lesion in our study – in 15.2% of all focal thyroid lesions. SUV_{max} should only serve as one of several parameters that alert the clinician on the possibility of thyroid malignancy and as such must be used with caution in the interpretation of PET-CT studies.

References

1. Jin J, McHenry CR. Thyroid incidentaloma. *Best Pract Res Clin Endocrinol Met*a 2012; **26:** 83-96.
2. Bertagna F, Treglia G, Piccardo A, Giubbini R. Diagnostic and clinical significance of F-18-FDG-PET/CT thyroid incidentalomas. *J Clin Endocrinol Metab* 2012; **97:** 3866-75.
3. Treglia G, Muoio B, Giovanella L, Salvatori M. The role of positron emission tomography and positron emission tomography/computed tomography in thyroid tumours: an overview. *Eur Arch Otorhinolaryngol* 2012; **270:** 1783-7.
4. Cistaro A, Quartuccio N, Mojtahedi A, Fania P, Filosso PL, Campenni A, et al. Prediction of 2 years-survival in patients with stage I and II non-small cell lung cancer utilizing (18)F-FDG PET/CT SUV quantification. *Radiol Oncol* 2013; **47:** 219-23.
5. Maza S, Buchert R, Brenner W, Munz DL, Thiel E, Korfel A, et al. Brain and whole-body FDG-PET in diagnosis, treatment monitoring and long-term follow-up of primary CNS lymphoma. *Radiol Oncol* 2013; **47:** 103-10.
6. Moon E-H, Lim ST, Han Y-H, Jeong YJ, Kang Y-H, Jeong H-J, et al. The usefulness of F-18 FDG PET/CT-mammography for preoperative staging of breast cancer: comparison with conventional PET/CT and MR-mammography. *Radiold Oncol*; 2013; **47:** 390-7.
7. Karantanis D, Bogsrud TV, Wiseman GA, Mullan BP, Subramaniam RM, Nathan MA, et al. Clinical Significance of diffusely increased 18F-FDG uptake in the thyroid gland. *J Nucl Med* 2007; **48:** 896-901.
8. Kurata S, Ishibashi M, Hiromatsu Y, Kaida H, Miyake I, Uchida M, et al. Diffuse and diffuse-plus-focal uptake in the thyroid gland identified by using FDG-PET: prevalence of thyroid cancer and Hashimoto's thyroiditis. *Ann Nucl Med* 2007; **21:** 325-30.
9. Yasuda S, Shohtsu A, Ide M, Takagi S, Takahashi W, Suzuki Y, et al. Chronic thyroiditis: diffuse uptake of FDG at PET. *Radiology* 1998; **207:** 775-8.
10. Lowe VJ, Mullan BP, Hay ID, McIver B, Kasperbauer JL. 18F-FDG PET of patients with Hürthle cell carcinoma. *J Nucl Med* 2003; **44:** 1402-6.
11. Chen Y-K, Ding H-J, Chen K-T, Chen Y-L, Liao AC, Shen Y-Y, et al. Prevalence and risk of cancer of focal thyroid incidentaloma identified by 18F-fluorodeoxyglucose positron emission tomography for cancer screening in healthy subjects. *Anticancer Res* 2005; **25:** 1421-6.
12. Chu QD, Connor MS, Lilien DL, Johnson LW, Turnage RH, Li BDL. Positron emission tomography (PET) positive thyroid incidentaloma: the risk of malignancy observed in a tertiary referral center. *Am Surg* 2006; **72:** 272-5.
13. Choi JY, Lee KS, Kim H-J, Shim YM, Kwon OJ, Park K, et al. Focal thyroid lesions incidentally identified by integrated 18F-FDG PET/CT: clinical significance and improved characterization. *J Nucl Med* 2006; **47:** 609-15.
14. Katz SC, Shaha A. PET-associated incidental neoplasms of the thyroid. *J Am Coll Surg* 2008: **207:** 259-64.
15. Barnabei A, Ferretti E, Baldelli R, Procaccini A, Spriano G, Appetecchia M. Hurthle cell tumours of the thyroid. Personal experience and review of the literature. *Acta Otorhinolaryngol Ital* 2009; **29:** 305-11.
16. Pagano L, Samà MT, Morani F, Prodam F, Rudoni M, Boldorini R, et al. Thyroid incidentaloma identified by ^{18}F-fluorodeoxyglucose positron emission tomography with CT (FDG-PET/CT): clinical and pathological relevance. *Clin Endocrinol* 2011; **75:** 528-34.
17. Bonabi S, Schmidt F, Broglie MA, Haile SR, Stoeckli SJ. Thyroid incidentalomas in FDG-PET/CT: prevalence and clinical impact. *Eur Arch Otorhinolaryngol* 2012; **269:** 2555-60.
18. Ohba K, Sasaki S, Oki Y, Nishizawa S, Matsushita A, Yoshino A, et al. Factors associated with fluorine-18-fluorodeoxyglucose uptake in benign thyroid nodules. *Endocr J* 2012; **60:** 985-90.
19. Bertagna F, Treglia G, Piccardo A, Giovannini E, Bosio G, Biasiotto G, et al. F18-FDG-PET/CT thyroid incidentalomas: a wide retrospective analysis in three Italian centres on the significance of focal uptake and SUV value. *Endocrine* 2013; **43:** 678-85.
20. Huang SC. Anatomy of SUV. Standardized uptake value. *Nucl Med Biol* 2000; **27:** 643-6.
21. Kang BJ, O JH, Baik JH, Jung SL, Park YH, Chung SK. Incidental thyroid uptake on F-18 FDG PET/CT: correlation with ultrasonography and pathology. *Ann Nucl Med* 2009; **23:** 729-37.
22. Kim BH, Na MA, Kim IJ, Kim S-J, Kim Y-K. Risk stratification and prediction of cancer of focal thyroid fluorodeoxyglucose uptake during cancer evaluation. *Ann Nucl Med* 2010; **24:** 721-8.
23. Kim TY, Kim WB, Ryu JS, Gong G, Hong SJ, Shong YK. 18F-fluorodeoxyglucose uptake in thyroid from positron emission tomogram (PET) for evaluation in cancer patients: high prevalence of malignancy in thyroid PET incidentaloma. *Laryngoscope* 2005; **115:** 1074-8.
24. Are C, Hsu JF, Ghossein RA, Schöder H, Shah JP, Shaha AR. Histological aggressiveness of fluorodeoxyglucose positron-emission tomogram (FDG-PET)-detected incidental thyroid carcinomas. *Ann Surg Oncol* 2007; **14:** 3210-5.

25. Bogsrud TV, Karantanis D, Nathan MA, Mullan BP, Wiseman GA, Collins DA, et al. The value of quantifying 18F-FDG uptake in thyroid nodules found incidentally on whole-body PET–CT. *Nucl Med Comun* 2007; **28:** 373-81.

26. Kwak JY, Kim E-K, Yun M, Cho A, Kim MJ, Son EJ, et al. Thyroid incidentalomas identified by 18F-FDG PET: sonographic correlation. *Am J Roentgenol* 2008; **91:** 598-603.

27. Chen W, Parsons M, Torigian DA, Zhuang H, Alavi A. Evaluation of thyroid FDG uptake incidentally identified on FDG-PET/CT imaging. *Nucl Med Commun* 2009; **30:** 240-4.

28. Pampaloni MH, Win AZ. Prevalence and Characteristics of Incidentalomas Discovered by Whole Body FDG PETCT. *Int J Mol Imaging* 2012; **18:** 1-6.

29. Nguyen NC, Kaushik A, Wolverson MK, Osman MM. Is there a common SUV threshold in oncological FDG PET/CT, at least for some common indications? A retrospective study. *Acta Oncol* 2011; **50:** 670-7.

30. de Langen AJ, Vincent A, Velasquez LM, van Tinteren H, Boellaard R, Shankar LK, et al. Repeatability of 18F-FDG uptake measurements in tumors: a metaanalysis. *J Nucl Med* 2012; **53:** 701-8.

31. Makris NE, Huisman MC, Kinahan PE, Lammertsma AA, Boellaard R. Evaluation of strategies towards harmonization of FDG PET/CT studies in multicentre trials: comparison of scanner validation phantoms and data analysis procedures. *Eur J Nucl Med Mol Imaging* 2013; **40:** 1507-15.

32. King D, Stack B, Spring P, Walker R, Bodenner D. Incidence of thyroid carcinoma in fluorodeoxyglucose positron emission tomography-positive thyroid incidentalomas. *Otolaryngol Head Neck Surg* 2007; **137:** 400-4.

33. Bertagna F, Giubbini R. F18-FDG-PET/CT thyroid incidentalomas and their benign or malignant nature: a critical and debated issue. *Ann Nucl Med* 2010; **25:** 151–2.

34. Ohba K, Nishizawa S, Matsushita A, Inubushi M, Nagayama K, Iwaki H, et al. High incidence of thyroid cancer in focal thyroid incidentaloma detected by 18F-fluorodeoxyglucose [corrected] positron emission tomography in relatively young healthy subjects: results of 3-year follow-up. *Endocr J* 2010; **57:** 395-401.

35. Nishimori H. Incidental thyroid "PETomas": clinical significance and novel description of the self-resolving variant of focal FDG-PET thyroid uptake. *Can J Surg* 2011; 54: 83-8.

36. Treglia G, Annunziata S, Muoio B, Salvatori M, Ceriani L, Giovanella L. The role of fluorine-18-fluorodeoxyglucose positron emission tomography in aggressive histological subtypes of thyroid cancer: An overview. *Int J Endocrinol* 2013; **2013:** 1-6.

37. Zaletel K, Gaberscek S, Pirnat E. Ten-year follow-up of thyroid epidemiology in Slovenia after increase in salt iodization. *Croat Med J* 2011; **52:** 615-21.

38. Cooper DS, Haugen BR, Hauger BR, Kloos RT, Lee SL, Mandel SJ, et al. Revised American Thyroid Association management guidelines for patients with thyroid nodules and differentiated thyroid cancer. *Thyroid* 2009; **19:** 1167-214.

39. Boerner AR, Voth E, Theissen P, Wienhard K, Wagner R, Schicha H. Glucose metabolism of the thyroid in Graves' disease measured by F-18-fluorodeoxyglucose positron emission tomography. *Thyroid* 1998; **8:** 765-72.

40. Liu Y. Clinical significance of thyroid uptake on F18-fluorodeoxyglucose positron emission tomography. *Ann Nucl Med* 2009; **23:** 17-23.

41. Ho T-Y, Liou M-J, Lin K-J, Yen T-C. Prevalence and significance of thyroid uptake detected by 18F-FDG PET. *Endocrine* 2011; **40:** 297-302.

research article

Primary central nervous system lymphoma: is absence of intratumoral hemorrhage a characteristic finding on MRI?

Akihiko Sakata[1], Tomohisa Okada[1], Akira Yamamoto[1], Mitsunori Kanagaki[1], Yasutaka Fushimi[1], Toshiki Dodo[1], Yoshiki Arakawa[2], Jun C Takahashi[2], Susumu Miyamoto[2], Kaori Togashi[1]

[1] Department of Diagnostic Imaging and Nuclear Medicine, Kyoto University Graduate School of Medicine, Kyoto, Japan
[2] Department of Neurosurgery, Kyoto University Graduate School of Medicine, Kyoto, Japan

Radiol Oncol 2015; 49(2): 128-134.

Received 12 August 2014
Accepted 6 January 2015

Correspondence to: Tomohisa Okada, M.D., Ph.D., Department of Diagnostic Imaging and Nuclear Medicine, Kyoto University Graduate School of Medicine, 54 Shogoin Kawaharacho, Sakyo-ku, Kyoto, 606-8507, Japan. Phone: +81 75 751 4215; Fax: +81 75 751 4216; E-mail: tomokada@kuhp.kyoto-u.ac.jp

Disclosure: No potential conflicts of interest were disclosed.

Background. Previous studies have shown that intratumoral hemorrhage is a common finding in glioblastoma multiforme, but is rarely observed in primary central nervous system lymphoma. Our aim was to reevaluate whether intratumoral hemorrhage observed on T2-weighted imaging (T2WI) as gross intratumoral hemorrhage and on susceptibility-weighted imaging as intratumoral susceptibility signal can differentiate primary central nervous system lymphoma from glioblastoma multiforme.

Patients and methods. A retrospective cohort of brain tumors from August 2008 to March 2013 was searched, and 58 patients (19 with primary central nervous system lymphoma, 39 with glioblastoma multiforme) satisfied the inclusion criteria. Absence of gross intratumoral hemorrhage was examined on T2WI, and an intratumoral susceptibility signal was graded using a 3-point scale on susceptibility-weighted imaging. Results were compared between primary central nervous system lymphoma and glioblastoma multiforme, and values of $P < 0.05$ were considered significant.

Results. Gross intratumoral hemorrhage on T2WI was absent in 15 patients (79%) with primary central nervous system lymphoma and 23 patients (59%) with glioblastoma multiforme. Absence of gross intratumoral hemorrhage could not differentiate between the two disorders ($P = 0.20$). However, intratumoral susceptibility signal grade 1 or 2 was diagnostic of primary central nervous system lymphoma with 78.9% sensitivity and 66.7% specificity ($P < 0.001$), irrespective of gross intratumoral hemorrhage.

Conclusions. Low intratumoral susceptibility signal grades can differentiate primary central nervous system lymphoma from glioblastoma multiforme. However, specificity in this study was relatively low, and primary central nervous system lymphoma cannot be excluded based solely on the presence of an intratumoral susceptibility signal.

Key words: glioblastoma multiforme; primary central nervous system lymphoma; magnetic resonance imaging

Introduction

Primary central nervous system lymphoma (PCNSL) represents approximately 2–6% of all brain tumors and 1–2% of all non-Hodgkin lymphomas.[1,2] The vast majority of PCNSLs are diffuse large B-cell lymphomas, regardless of the patient's immunological state, and primary T-cell lymphomas are uncommon in the central nervous system (CNS).[3] The incidence of this pathology has recently been on the rise among both immunocompetent and immunocompromised populations.[4]

Histology is required for a definitive diagnosis, but radical surgical excision of PCNSL is not warranted; even partial tumor resection seems to be a negative prognostic factor.[2] Glioblastoma multiforme (GBM), on the other hand, requires maximal excision. Because symptomatic patients with

PCNSL often present with lesions of considerable size, steroid administration is sometime clinically indicated before pathological confirmation, resulting in low diagnostic yields for histological examination.[5] Accurate diagnosis of PCNSL by initial imaging is thus crucial to avoid steroid treatment and facilitate biopsy, rather than resection that does not improve prognosis.

PCNSL has many documented imaging features[1,6-10], but may mimic other diseases or show atypical findings, making preoperative diagnosis of PCNSL imperfect even with current advanced imaging techniques.[11,12] As another imaging method, susceptibility-weighted imaging (SWI) has recently been reported to differentiate PCNSL from GBM, as the most common malignant primary brain tumor, nearly perfectly when intratumoral susceptibility signal (ITSS) that reflects hemorrhage is used.[13-15]

However, some reports have described PCNSL with cerebral hemorrhage even in non-HIV patients[16-18] and hemorrhage may not be particularly rare even among immunocompetent patients. Moreover, the relationship between ITSS and intratumoral hemorrhage observed on conventional imaging modalities such as computed tomography (CT) or T2-weighted imaging (T2WI) in PCNSL cases has not been clarified in detail.[13-15]

Given these considerations, we have retrospectively reviewed all patients with PCNSL and GBM encountered within a fixed period in our hospital to investigate the differential capabilities of gross intratumoral hemorrhage (GITH) on T2WI and ITSS grading on SWI.

Patients and methods

Patients

A retrospective cohort of brain tumors in the pathology archives of our institution from August 2008 to March 2013 was searched for cases of PCNSL and GBM. From the database, we included all patients with pathologically diagnosed PCNSL and GBM who had preoperative CT and MRI studies including T2WI and SWI. From the database, we found 65 patients with pathologically diagnosed PCNSL and GBM who had undergone preoperative CT and MRI studies, including T2WI and SWI. Exclusion criteria were a history of organ transplantation (n = 1) or surgical intervention (*i.e.* biopsy or drainage) before initial MRI (n = 6). In total, 58 patients satisfied these criteria: 19 patients with PCNSL (10 men, 9 women; mean age, 65.1 years; range, 26–83 years) and 39 patients with GBM (24 men, 15 women; mean age, 59.7 years; age range, 16–87 years). Among PCNSL patients, all were diagnosed with B-cell lymphoma (diffuse large B-cell lymphoma, n = 17; precursor B cell lymphoma, n = 1), except 1 case of T-cell lymphoma. No patient had history of acquired immunodeficiency syndrome or other immunodeficiency disorders. One patient with B-cell lymphoma had Sjögren syndrome and was treated with disease-modifying anti-rheumatic drugs. Another patient was treated for multiple sclerosis with steroid pulse therapy for 1 month prior to admission to our hospital. One patient with T-cell lymphoma showed positive results for human T-lymphotropic virus type 1 infection postoperatively, but the lesion was limited to the CNS. Five patients with PCNSL had received steroids prior to MRI to diminish edema. This study was approved by the institutional review board. Given the retrospective design, the requirement for informed consent was waived.

Image acquisition

Patients were imaged using a 3T MRI system (Magnetom Trio Tim or Skyra; Siemens Healthcare, Erlangen, Germany) with a 32-channel head coil. T2WI was acquired using a fast spin-echo sequence under the following conditions: repetition time (TR), 3200 ms; echo time (TE), 79 ms; matrix, 420 × 448; field of view, 206×220 mm; matrix size, 0.49 × 0.49 mm; 35 slices of 3 mm thickness with a 1 mm gap. SWI was acquired with a three-dimensional fully flow-compensated gradient echo sequence using the following parameters: TR, 28 ms; TE, 20 ms; flip angle, 15°; matrix, 320 × 230; field of view, 230 × 179 mm; matrix size, 0.72 × 0.78 mm. Slab size was 76.8 mm or 128 mm, partitioned into 64 slices of 1.2 or 2 mm (n = 28 and 30, respectively). SWI sequences were acquired before contrast administration. Diffusion-weighted imaging (DWI), pre- and post-contrast enhanced T1-weighted images were also routinely acquired. DWI was performed using a single-shot spin-echo (SE) echo planar sequence with following parameters: TR 5000ms, TE 84 ms, flip angle 90°, matrix 160 × 160, field of view 220 × 220 mm, matrix size, 0.49 × 0.49 mm; 35 slices of 3 mm thickness with a 1 mm gap. Diffusion-sensitizing gradients were applied in 3 directions with b factors of 0 and 1000 s/mm^2. Apparent diffusion coefficients (ADCs) were automatically calculated by the operating console of the MR scanner and displayed as corresponding ADC maps. All patients underwent unenhanced CT with an in-

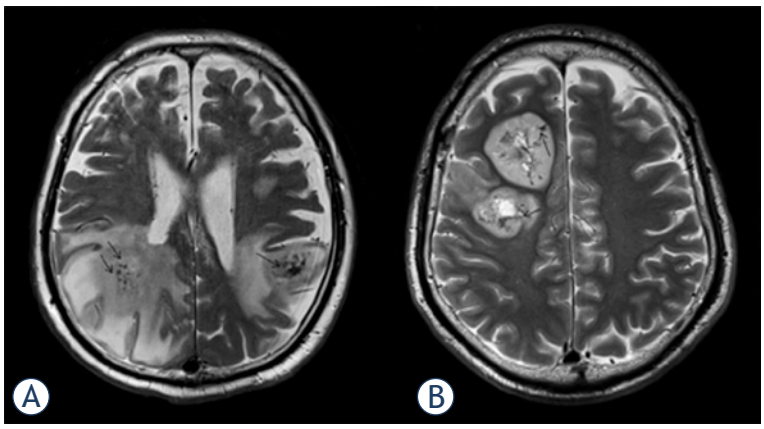

FIGURE 1. Gross intratumoral hemorrhage (arrows) in primary central nervous system lymphoma **(A)** and glioblastoma multiforme **(B)** on T2-weighted image. Both cases show low-intensity areas representing intratumoral hemorrhage.

plane resolution of 0.41 × 0.41 mm and slice thicknesses of 4–8 mm in conventional scans and 5 mm in helical acquisitions using 16- or 64-detector-row CT scanners (Aquilion 16 or Aquilion 64; Toshiba Medical Systems, Ohtawara, Japan).

Image analysis

Qualitative analysis including T2WI and contrast-enhanced T1-weighted images (CE-T1WI) as well as SWI was conducted on a clinical picture archiving and communication system (Centricity, PACS workstation version 3.2; GE Medical Systems, Milwaukee, WI) by two board-certified neuroradiologists (A.S. and T.D.; both with 5 years of experience in diagnostic radiology) who were blinded to the final diagnosis. First, they evaluated the absence of GITH. GITH was defined as nodular or linear hypo-intense foci observed on T2WI (Figure 1). Second, ITSS grading on SWI was conducted independently by the same two neuroradiologists at 1 month after GITH evaluation. As described by Kim *et al.*[12], ITSS was defined as a dot-like or fine linear low signal within a tumor, and graded using a

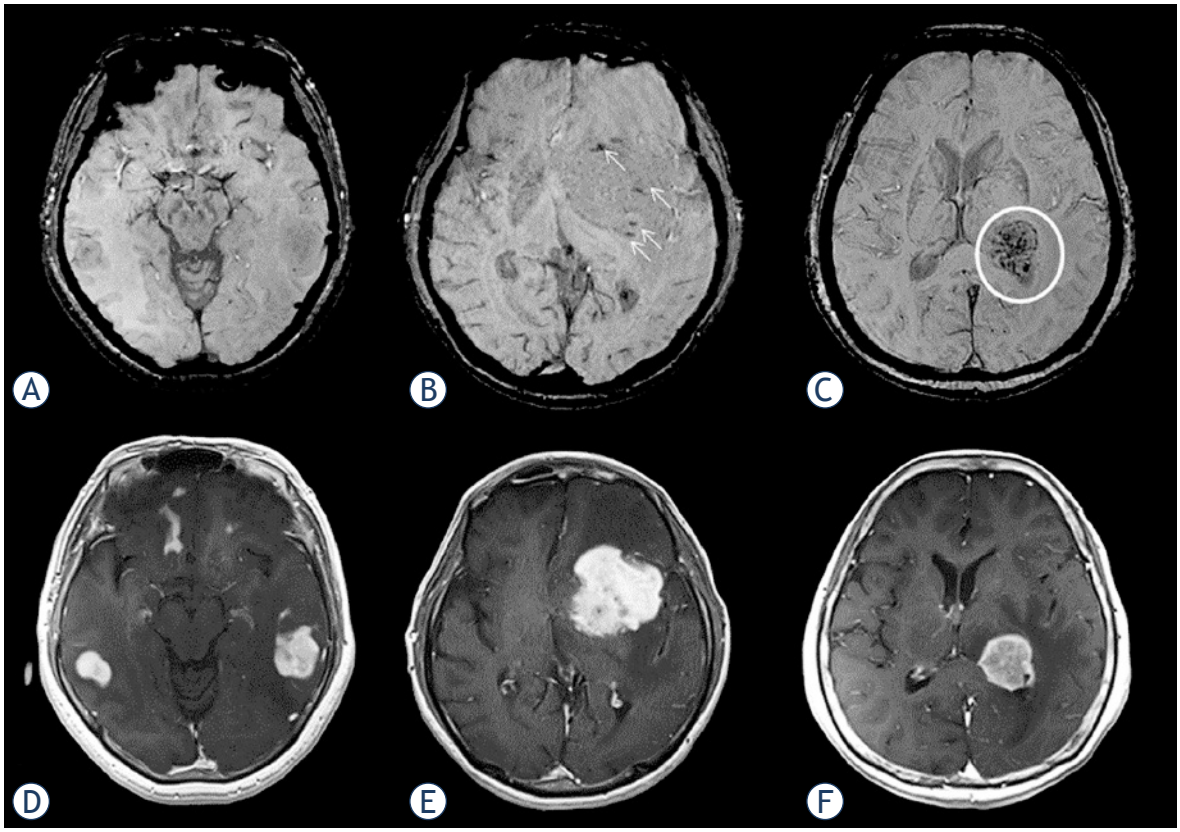

FIGURE 2. Intratumoral susceptibility signals in patients with primary central nervous system lymphoma: **(A)** Grade 1: multifocal tumors in bilateral temporal lobes show no intratumoral susceptibility signal on susceptibility-weighted imaging (SWI). **(B)** Grade 2: tumor in the left basal ganglia shows punctate low-intensity signals (arrows) on SWI. **(C)** Grade 3: tumor in the left thalamus shows multiple linear or nodular low-intensity signals (circle) on SWI. **(D-F)** Contrast-enhanced T1-weighted imaging shows primary central nervous system lymphomas with intense enhancement.

3-point scale: grade 1, no ITSS (Figure 2A); grade 2, 1–10 ITSSs (Figure 2B); and grade 3, ≥ 11 ITSSs (Figure 2C) within a tumor. Corresponding contrast-enhanced T1-weighted images are presented as tumor references (Figure 2D-F). Enhancement patterns on contrast-enhanced T1-weighted image were evaluated as necrotic or non-necrotic: necrotic was defined as solid enhancement with any loss of contrast enhancement.[19] When absence of GITH, ITSS grading or enhancement patterns were discordant between evaluators, the final results were reached by consensus. To exclude low signal intensity caused by calcification (defined as a CT attenuation value >100 Hounsfield units), unenhanced CT was also referred to.

The same neuroradiologists (A.S. and T.D.) evaluated ADC maps using software (Image J version 1.49a; NIH, Bethesda). Firstly, we selected all slices that included tumor. One round- or oval-shaped region of interest (area, approximately 0.3 cm^2) was carefully placed on each slice of the ADC map of the whole tumor to include the area with the lowest ADC value determined by visual inspection. Cystic, necrotic or hemorrhagic areas were carefully avoided by referencing to conventional MR images. Finally, the value of a region of interest with the lowest average ADC value was selected as a minimum ADC (ADCmin) value of the tumor in each case.[20]

Statistical analysis

Patient groups of PCNSL and GBM were compared for age, sex and parameters using a *t*-test and a Pearson's χ^2 test, respectively. Inter-observer variability of GITH and ITSS grading was evaluated using κ statistics. Inter-observer variability of the readers for ADC analysis was evaluated by intraclass correlation (ICC) coefficient (0.00–0.20 poor, 0.21–0.40 fair, 0.41–0.60 moderate, 0.61–0.80 good and 0.81–1.00 excellent correlation). ADCs were averaged between the two observers for further analysis. ADCmin Receiver-operating characteristic (ROC) curve analysis was conducted for GITH, ITSS, enhancement pattern and ADCmin, and sensitivity , specificity, positive predictive value (PPV) and negative predictive value (NPV) were calculated for differentiating PCNSL from GBM.[21] Areas under the curve (AUCs) were statistically compared using a method by Delong *et al*.[22] To analyze whether ADCmin were affected by microhemorrhage, ADCmin values of the groups defined by ITSS were compared using ANOVA in both GBM and PCNSL patients. A value of $P < 0.05$ was considered significant. All statistical analyses were conducted using MedCalc for Windows (version 12.5.0.0; MedCalc Software, Mariakerke, Belgium).

TABLE 1. Gross intratumoral hemorrhage (GITH) frequency in primary central nervous system lymphoma (PCNSL) and glioblastoma multiforme (GBM)

Pathological Diagnosis	GITH	
	Negative (%)	Positive (%)
PCNSL	15 (79)	4 (21)
GBM	23 (59)	16 (41)

TABLE 2. Intratumoral susceptibility signal (ITSS) grading of primary central nervous system lymphoma (PCNSL) and glioblastoma multiforme (GBM)

Pathological Diagnosis	ITSS grading		
	Grade 1 (%)	Grade 2 (%)	Grade 3 (%)
PCNSL	9 (47)	6 (32)	4 (21)
GBM	4 (10)	9 (23)	26 (67)

TABLE 3. Enhancement patterns of primary central nervous system lymphoma (PCNSL) and glioblastoma multiforme (GBM)

Enhancement pattern	Pathological Diagnosis	
	PCNSL	GBM
Non-necrotic	15	2
Necrotic	3	37

Results

No significant differences in age ($P = 0.39$) or sex ($P = 0.72$) were found between patient groups. Inter-observer agreement between the two evaluators was substantial for GITH (κ = 0.75, 95% confidence interval (CI) = 0.58–0.92) and almost perfect for ITSS (κ = 0.88, 95% CI = 0.81–0.96). ICC of ADCmin was 0.693 (95% CI = 0.48–0.82).

CT showed no calcification in any cases. GITH was not observed in 15 patients (79%) with PCNSL and in 23 patients (59%) with GBM (Table 1), and ROC analysis thus failed to reveal any significant difference ($P = 0.20$). ITSS grades 1, 2 and 3 were found in 9, 6 and 4 PCNSL patients, respectively, and in 4, 9 and 26 GBM patients, respectively (Table 2). GITHs were associated with grade 3 ITSS in almost all cases, except for 1 patient with GBM and 1 patient with PCNSL; both of these patients showed grade 2 ITSS. ITSS was not observed (*i.e.*, grade 1) in 9 PCNSL patients (47.4%) and 4 GBM

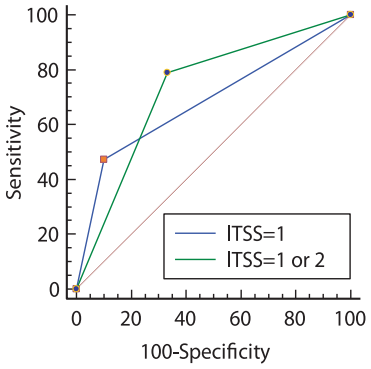

FIGURE 3. Receiver-operating characteristic curve analysis of intratumoral susceptibility signal (ITSS) grading to differentiate primary central nervous system lymphoma from glioblastoma multiforme. ITSS grades≤ 2 is diagnostic of primary central nervous system lymphoma with 78.9% sensitivity and 66.7% specificity, not as high as in previous studies.

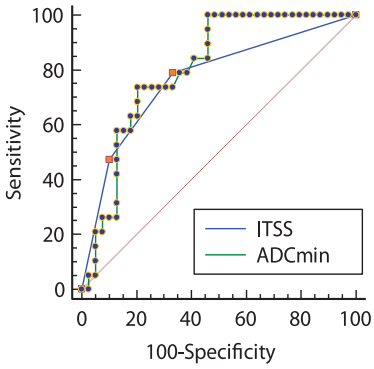

FIGURE 4. Receiver-operating characteristic curve analysis of minimum apparent diffusion coefficient (ADCmin) and intratumoral susceptibility signal (ITSS) grading to differentiate primary central nervous system lymphoma from glioblastoma multiforme. ADCmin ≤ 0.629 mm^2/s is diagnostic of primary central nervous system lymphoma with 100% sensitivity and 53.8% specificity.

patients (10.3%). When ITSS grade 1 was used as the criterion of PCNSL, sensitivity, specificity, PPV, and NPV was 47.4%, 89.7%, 69.2%, and 77.8% respectively, whereas ITSS grade 1 or 2 was diagnostic of PCNSL with 78.9% , 66.7% , 53.6% and 86.7%. The AUC values were 0.686 and 0.728, respectively (p values were 0.0036 and 0.0002, Figure 3). There was not statistically significant difference between the two curves.

Enhancement patterns of GBM and PCNSL were summarized in Table 3: one patient with no contrast-enhancement was excluded from this analysis. Most GBMs showed necrotic pattern, while most PCNSL showed non-necrotic enhancement. Sensitivity, specificity PPV and NPV were 83.3%, 94.9%, 88.2% and 92.5%, respectively.

ADCmin was significantly lower for lymphoma than for GBM ($0.487 \pm 0.09 \times 10^{-3}$ mm^2/s and $0.645 \pm 0.15 \times 10^{-3}$ mm^2/s, respectively; $p = 0.001$ with student t-test). ROC curve analysis of ADCmin found the optimal cutoff value to be 0.629 mm^2/s (sensitivity: 100%, specificity: 53.8%, PPV: 51.4%. and NPV: 100%). There was not statistically significant differences between AUCs of ITSS and ADCmin (p value = 0.68) (Figure 4).

Discussion

Our results demonstrated that ITSS on SWI can aid to differentiate PCNSL from GBM compared with GITH on T2WI. However, in this study cohort, more than half of PCNSL patients showed positive ITSS (*i.e.*, ≥ 2), including 4 patients with ITSS grade 3. The frequency of positive ITSS in PCNSL was much higher than in previous reports, resulting in the lower specificity of 66.7%.

Conventional imaging technique, especially CE-T1WI, is useful for differentiating PCNSL and GBM. Most GBMs show heterogeneous enhancement with variable size of necrotic foci, while PCNSL typically shows homogenous enhancement because of paucity of intratumoral necrosis, especially in immunocompetent patients. However, up to 10% of patients show atypical enhancement patterns in GBM and PCNSL.[1,19] Therefore, further imaging technique is warranted for more appropriate evaluation.

Hemorrhagic and necrotic foci are commonly observed in GBM.[23] Previous studies have also showed that ITSS on T2*-weighted imaging or SWI is more frequently detected in high-grade glioma.[24,25] Conversely, in immunocompetent PCNSL patients, intratumoral hemorrhage before therapy has rarely been observed. On CT and conventional MRI, tumor-associated hemorrhage was reported in 0–8% of PCNSL cases.[1,6,8,10] Based on this rarity, the presence of hemorrhage or calcification is used to exclude PCNSL from the differential diagnosis.

Previous reports on SWI have confirmed non-SWI results.[13-15,21,26] Kim *et al.*, first demonstrated the presence of ITSS, particularly grade 3, could distinguish high-grade glioma from PCNSL with 100% specificity, although their study included only 7 patients with PCNSL.[13] Radbruch *et al.*, also recently reported that ITSS was not observed in any of 14 patients with B-cell PCNSL, with the exception of 1 case of T-cell lymphoma.[14] Peters *et al.*, also showed that SWI is useful for differentiating PCNSL from GBM, although 1 in 4 patients with PCNSL showed grade 2 ITSS.[15] Previous studies have suggested nearly complete absence of ITSS in PCNSL.[13-15,21,26]

However, on pathological examination, necrosis and hemorrhage are occasionally observed in PCNSL.[27] Some case reports have described PCNSL presenting with intracerebral hemorrhage in both immunocompetent and immunocompromised patients.[16-18] In a study of 10 immunocompetent PCNSL patients, small hemorrhage was found on MRI in 4 of 19 lesions (21%).[9] Moreover, Kickingereder *et al.*, have recently reported presence of the ITSS in 6 out of 19 PCNSL patients on 3T MRI.[19] These findings are comparable to our result. SWI is much more sensitive to susceptibility difference than conventional

MRI, including T2*-weighted imaging[24,28,29], and is considered to identify more small hemorrhagic lesions within the tumors. Actually, in the present study, patients with positive ITSS were twice as common as those with GITH in both groups. This is in accordance with the recent report by Ding *et al.*, demonstrating the significant difference in the detecting rate of intra-tumoral hemorrhage in patients with GBM and brain metastasis between the conventional MR imaging and SWI.[21] Therefore, conventional MR including T2*WI seems insensitive to hemorrhagic change, and unsuitable for differentiating GBM from PCNSL based on the absence of intratumoral hemorrhage.

This study showed much higher frequency of positive ITSS in PCNSL patients compared with previous studies. Several factors may contribute to this result. One possible explanation is that SWI in this study used thinner slices than previous studies. Nandigum *et al.*, demonstrated that SWI acquired with thinner slices in a higher magnetic field detected significantly more cerebral microbleeds.[30] Previous SWI studies on PCNSL have reported almost no ITSS[13,14], but used 2.5- or 3-mm slice thicknesses, thicker than used in this study (*i.e.*, 1.2 or 2 mm). Peters *et al.*, used 1-mm slice thickness and found grade 2 ITSS in 1 of 4 patients with PCNSL (diffuse large B-cell lymphoma).[15] Thinner slice thickness thus appears more sensitive to small foci of hemorrhage and may have contributed to higher ITSS grades in our PCNSL cases compared to previous reports. The other technical factor is the difference in head coils used in studies. Previous studies used 8- to 12-channel head coils[13-15], whereas the present study used a 32-channel brain coil, which improves the signal-to-noise ratio (SNR).[31] SWI was acquired at high resolution, but there is a trade-off between resolution and SNR. With lower SNR, lesion detectability is impaired[32,33], which may also have contributed to the differences with previous studies.

Several authors investigate the role of other advanced techniques, especially DWI, in evaluation of differentiation of PCNSL and GBM.[12,34,35] Generally, the ADC values of PCNSL are low, reflecting the high degree of cellularity. However, according to several earlier investigations, the differences in ADC between patients with PCNSL and those with glioblastoma were not always statistically significant.[35] Our results showed there were significant differences between both groups, but its specificity was relatively low, which is consistent with previous studies. We also tested if the presence of ITSS effects ADC values, but the ADC value of the tumor did not differ depending on the amount of microhemorrhage.

Our results showed the diagnostic capability of ITSS for differentiating PCNSL from GBM were comparable to that of ADCmin, however, as a single parameter, both of them were not so specific as previously described.[13-15,21,26] Kickingereder *et al.*, showed that ITSS as an additional imaging parameter allowed correct classification of the atypical GBM (*i.e.* GBM showing homogenous enhancement) and PCNSL.[19] Therefore, considering with the limited diagnostic capability of ITSS, combined analysis of several parameters obtained by other imaging technique, such as PWI[12], ASL[26] and MRS[19] should be considered in the clinical practice.

Some limitations in this study must be considered. The sample size was relatively small. However, the case number is more than or comparable to former studies. Another limitation was that we included patients who were treated with steroids before imaging. Steroid therapy is well known to disrupt cellular morphology, which may affect imaging appearance.[5,36] However, no patients with steroid administration prior to MRI showed positive ITSS, and steroid use had minimal effect on our results. We also included one human T-lymphotropic virus type 1-positive case that may potentially have arisen in an immunocompromised patient. PCNSL in an immunocompromised host with primary CNS T-cell lymphoma is known to have a relatively high incidence of intratumoral hemorrhage[11,37], but the patient in this study showed no GITH or ITSS. Finally, Epstein-Barr virus infection is another important factor that must be considered. Lee *et al.*, recently demonstrated that Epstein-Barr virus -positive PCNSL cases showed intratumoral necrosis or hemorrhage more frequently than cases with Epstein-Barr virus -negative PCNSL, even in the absence of HIV infection.[38] No description of Epstein-Barr virus infection status has been available in previous studies on ITSS[13-15], and this was also the case for this study. PCNSL with GITH or ITSS could potentially be related to Epstein-Barr virus infection, but no conclusion can be drawn within this study.

In conclusion, low ITSS grades can differentiate PCNSL from GBM. However, specificity in this study was relatively low, and PCNSL cannot be excluded based solely on the presence of an ITSS. Careful evaluation using several imaging technique is important.

References

1. Haldorsen IS, Kråkenes J, Krossnes BK, Mella O, Espeland A. CT and MR imaging features of primary central nervous system lymphoma in Norway, 1989-2003. *AJNR Am J Neuroradiol* 2009; **30:** 744-51.
2. Bataille B, Delwail V, Menet E, Vandermarcq P, Ingrand P, Wager M, et al. Primary intracerebral malignant lymphoma: report of 248 cases. *J Neurosurg* 2000; **92:** 261-6.
3. Schlegel U, Schmidt-Wolf IG, Deckert M. Primary CNS lymphoma: clinical presentation, pathological classification, molecular pathogenesis and treatment. *J Neurol Sci* 2000; **181:** 1-12.
4. Olson JE, Janney CA, Rao RD, Cerhan JR, Kurtin PJ, Schiff D, et al. The continuing increase in the incidence of primary central nervous system non-Hodgkin lymphoma: a surveillance, epidemiology, and end results analysis. *Cancer* 2002; **95:** 1504-10.
5. Geppert M, Ostertag CB, Seitz G, Kiessling M. Glucocorticoid therapy obscures the diagnosis of cerebral lymphoma. *Acta Neuropathol* 1990; **80:** 629-34.
6. Zhang D, Hu L-B, Henning TD, Ravarani EM, Zou LG, Feng XY, et al. MRI findings of primary CNS lymphoma in 26 immunocompetent patients. *Korean J Radiol* 2010; **11:** 269-77.
7. Bühring U, Herrlinger U, Krings T, Thiex R, Weller M, Küker W. MRI features of primary central nervous system lymphomas at presentation. *Neurology* 2001; **57:** 393-6.
8. Jenkins CN, Colquhoun IR. Characterization of primary intracranial lymphoma by computed tomography: an analysis of 36 cases and a review of the literature with particular reference to calcification haemorrhage and cyst formation. *Clin Radiol* 1998; **53:** 428-34.
9. Ueda F, Takashima T, Suzuki M, Kadoya M, Yamashita J, Kida T. MR imaging of primary intracranial malignant lymphoma. *Radiat Med* 1995; **13:** 51-7.
10. Coulon A, Lafitte F, Hoang-Xuan K, Martin-Duverneuil N, Mokhtari K, Blustajn J, et al. Radiographic findings in 37 cases of primary CNS lymphoma in immunocompetent patients. *Eur Radiol* 2002; **12:** 329-40.
11. Haldorsen IS, Espeland A, Larsson E-M. Central nervous system lymphoma: characteristic findings on traditional and advanced imaging. *AJNR Am J Neuroradiol* 2011; **32:** 984-92.
12. Yamashita K, Yoshiura T, Hiwatashi A, Togao O, Yoshimoto K, Suzuki SO, et al. Differentiating primary CNS lymphoma from glioblastoma multiforme: assessment using arterial spin labeling, diffusion-weighted imaging, and ą^{8}F-fluorodeoxyglucose positron emission tomography. *Neuroradiology* 2013; **55:** 135-43.
13. Kim HS, Jahng GH, Ryu CW, Kim SY. Added value and diagnostic performance of intratumoral susceptibility signals in the differential diagnosis of solitary enhancing brain lesions: preliminary study. *AJNR Am J Neuroradiol* 2009; **30:** 1574-9.
14. Radbruch A, Wiestler B, Kramp L, Lutz K, Bäumer P, Weiler M, et al. Differentiation of glioblastoma and primary CNS lymphomas using susceptibility weighted imaging. *Eur J Radiol* 2013; **82:** 552-6.
15. Peters S, Knöß N, Wodarg F, Cnyrim C, Jansen O. Glioblastomas vs. lymphomas: more diagnostic certainty by using susceptibility-weighted imaging (SWI). *Rofo* 2012; **184:** 713-8.
16. Rubenstein J, Fischbein N, Aldape K, Burton E, Shuman M. Hemorrhage and VEGF expression in a case of primary CNS lymphoma. *J Neurooncol* 2002; **58:** 53-6.
17. Kim IY, Jung S, Jung TY, Kang SS, Choi C. Primary central nervous system lymphoma presenting as an acute massive intracerebral hemorrhage: case report with immunohistochemical study. *Surg Neurol* 2008; **70:** 308-11.
18. Kimura N, Ishibashi M, Masuda T, Ito M, Takahashi Y, Kumamoto T. Primary central nervous system lymphoma with cortical laminar hemorrhage. *J Neurol Sci* 2009; **287:** 281-4.
19. Kickingereder P, Wiestler B, Sahm F, Heiland S, Roethke M, Schlemmer HP, et al. Primary central nervous system lymphoma and atypical glioblastoma: multiparametric differentiation by using diffusion-, perfusion-, and susceptibility-weighted MR imaging. *Radiology* 2014; **272:** 843-50.
20. Higano S, Yun X, Kumabe T, Watanabe M, Mugikura S, Umetsu A, et al. Malignant astrocytic tumors: clinical importance of apparent diffusion coefficient in prediction of grade and prognosis. *Radiology* 2006; **241:** 839-46.
21. Ding Y, Xing Z, Liu B, Lin X, Cao D. Differentiation of primary central nervous system lymphoma from high-grade glioma and brain metastases using susceptibility-weighted imaging. *Brain and Behavior* 2014; **4:** 841-9.
22. DeLong ER, DeLong DM, Clarke-Pearson DL. Comparing the areas under two or more correlated receiver operating characteristic curves: a nonparametric approach. *Biometrics* 1988; **44:** 837-45
23. Kondziolka D, Bernstein M, Resch L, Tator CH, Fleming JF, Vanderlinden RG, et al. Significance of hemorrhage into brain tumors: clinicopathological study. *J Neurosurg* 1987; **67:** 852-7.
24. Bagley LJ, Grossman RI, Judy KD, Curtis M, Loevner LA, Polansky M, et al. Gliomas: correlation of magnetic susceptibility artifact with histologic grade. *Radiology* 1997; **202:** 511-6.
25. Li C, Ai B, Li Y, Qi H, Wu L. Susceptibility-weighted imaging in grading brain astrocytomas. *Eur J Radiol* 2010; **75:** e81-5.
26. Furtner J, Schöpf V, Preusser M, Asenbaum U, Woitek R, Wöhrer A, et al. Non-invasive assessment of intratumoral vascularity using arterial spin labeling: A comparison to susceptibility-weighted imaging for the differentiation of primary cerebral lymphoma and glioblastoma. *Eur J Radiol* 2014; **83:** 806-10.
27. Deckert M, Paulus W. Malignant lymphoma. In: Louis DN, Ohgaki H, Wiestler OD, Cavenee WK. *WHO classification of tumours of the central nervous system.* 4th ed. Lyon, France: International Agency for Research on Cancer, 2007. p. 188-92.
28. Haacke EM, Mittal S, Wu Z, Neelavalli J, Cheng YC. Susceptibility-weighted imaging: technical aspects and clinical applications, part 1. *AJNR Am J Neuroradiol* 2009; **30:** 19-30.
29. Mittal S, Wu Z, Neelavalli J, Haacke EM. Susceptibility-weighted imaging: technical aspects and clinical applications, part 2. *AJNR Am J Neuroradiol* 2009; **30:** 232-52.
30. Nandigam RN, Viswanathan A, Delgado P, Skehan ME, Smith EE, Rosand J, et al. MR imaging detection of cerebral microbleeds: effect of susceptibility-weighted imaging, section thickness, and field strength. *AJNR Am J Neuroradiol* 2009; **30:** 338-43.
31. Wiggins GC, Triantafyllou C, Potthast A, Reykowski A, Nittka M, Wald LL. 32-channel 3 Tesla receive-only phased-array head coil with soccer-ball element geometry. *Magn Reson Med* 2006; **56:** 216-23.
32. Constable RT, Henkelman RM. Contrast, resolution, and detectability in MR imaging. *J Comput Assist Tomogr* 1991; **15:** 297-303.
33. Kale SC, Chen XJ, Henkelman RM. Trading off SNR and resolution in MR images. *NMR Biomed* 2009; **22:** 488-94.
34. Ahn SJ, Shin HJ, Chang JH, Lee SK. Differentiation between primary cerebral lymphoma and glioblastoma using the apparent diffusion coefficient: comparison of three different ROI Methods. *PLoS One* 2014; **9:** e112948.
35. Matsushima N, Maeda M, Umino M, Suzawa N, Yamada T, Takeda K. Relation between FDG uptake and apparent diffusion coefficients in glioma and malignant lymphoma. *Ann Nucl Med* 2012; **26:** 262-71.
36. Weller M. Glucocorticoid treatment of primary CNS lymphoma. *J Neurooncol* 1999; **43:** 237-9.
37. Kim EY, Kim SS. Magnetic resonance findings of primary central nervous system T-cell lymphoma in immunocompetent patients. *Acta Radiol* 2005; **46:** 187-92.
38. Lee HY, Kim HS, Park JW, Baek HJ, Kim SJ, Choi CG. Atypical imaging features of epstein-barr virus-positive primary central nervous system lymphomas in patients without AIDS. *AJNR Am J Neuroradiol* 2013; **34:** 1562-7.

research article

Doppler ultrasound for diagnosis of soft tissue sarcoma: efficacy of ultrasound-based screening score

Satoshi Nagano[1*], Yuhei Yahiro[1*], Masahiro Yokouchi[1], Takao Setoguchi[2], Yasuhiro Ishidou[3], Hiromi Sasaki[1], Hirofumi Shimada[1], Ichiro Kawamura[3], Setsuro Komiya[1,2]

[1] Department of Orthopaedic Surgery, [2] The Near-Future Locomotor Organ Medicine Creation Course (Kusunoki Kai) and [3] Department of Medical Joint Materials, Graduate School of Medical and Dental Sciences, Kagoshima University, Kagoshima, Japan

Radiol Oncol 2015; 49(2): 135-140.

Received 25 November 2014
Accepted 9 February 2015

Correspondence to: Satoshi Nagano, M.D., Ph.D., Department of Orthopaedic Surgery, Graduate School of Medical and Dental Sciences, Kagoshima University, 8-35-1 Sakuragaoka, Kagoshima City, Kagoshima 890-8520, Japan. Phone: +81 99 275 5381; Fax: +81 99 265 4699; E-mail: naga@m2.kufm.kagoshima-u.ac.jp

* These authors contributed equally to this work.

Disclosure: No potential conflicts of interest were disclosed.

Background. The utility of ultrasound imaging in the screening of soft-part tumours (SPTs) has been reported. We classified SPTs according to their blood flow pattern on Doppler ultrasound and re-evaluated the efficacy of this imaging modality as a screening method. Additionally, we combined Doppler ultrasound with several values to improve the diagnostic efficacy and to establish a new diagnostic tool.

Patients and methods. This study included 189 cases of pathologically confirmed SPTs (122 cases of benign disease including SPTs and tumour-like lesions and 67 cases of malignant SPTs). Ultrasound imaging included evaluation of vascularity by colour Doppler. We established a scoring system to more effectively differentiate malignant from benign SPTs (ultrasound-based sarcoma screening [USS] score).

Results. The mean scores in the benign and malignant groups were 1.47 ± 0.93 and 3.42 ± 1.30, respectively. Patients with malignant masses showed significantly higher USS scores than did those with benign masses ($p < 1 \times 10^{-10}$). The area under the curve was 0.88 by receiver operating characteristic (ROC) analysis. Based on the cut-off value (3 points) calculated by ROC curve analysis, the sensitivity and specificity for a diagnosis of malignant SPT was 85.1% and 86.9%, respectively.

Conclusions. Assessment of vascularity by Doppler ultrasound alone is insufficient for differentiation between benign and malignant SPTs. Preoperative diagnosis of most SPTs is possible by combining our USS score with characteristic clinical and magnetic resonance imaging findings.

Key words: Doppler ultrasound; soft-part tumours; differential diagnosis; ultrasound-based sarcoma screening score

Introduction

The diagnosis of soft-part tumours (SPTs) in orthopaedic primary care is not easy because of the rarity of the disease, few characteristic findings, and lack of simple diagnostic tools. Ultrasonography is a noninvasive imaging tool that is gaining popularity in orthopaedic clinics. It has already been used in daily clinics for evaluation of muscle injury[1], rotator cuff tears[2], entrapment neuropathy[3], and many other conditions.[4] The utility of ultrasound imaging in the screening of SPTs has been discussed in the past by several authors with some modifications.[5-9] To improve the diagnostic accuracy of malignant tumours, more defined and complex methods of ultrasound imaging for SPTs have

TABLE 1. USS score of benign tumors.

Tumor type	Cases	Score (average)	95% CI
PNST	34	1.59	0.36
lipoma et	29	1.41	0.33
Cystic lesion	20	1.20	0.23
PVS/GCT	10	1.60	0.43
Vascular tumor	10	2.30	0.78
Fibroma et	8	1.13	0.42
Other tumor / mass	11	1.09	0.43
Total	122	1.47	0.16

PNST = Peripheral nerve sheath tumor; PVS = Pigmented villonodular synovitis; GCT = Giant cell tumor

TABLE 2. USS score of malignant tumors

Tumor type	Cases	Score (average)	95% CI
UPS/MFH	23	3.87	0.45
Liposarcoma	15	3.13	0.58
WDL	14	2.15	0.5
Synovial sarcoma	3	4.67	0.65
Leiomyosarcoma	3	2.67	0.65
Other sarcoma	9	4.44	0.74
Total	67	3.42	0.31

PS = Unclassified pleomorphic sarcoma; MFH = Malignant fibrous histiocytoma; WDL = Well-differentiated liposarcoma

been reported. For instance, contrast-enhanced ultrasound is reportedly useful for differentiation between malignant and benign SPTs by analysis of contrast-enhancement kinetics[10] or in combination with three-dimensional power Doppler.[11] On the other hand, Chiou *et al.* used a computer-aided diagnosis (CAD) system to improve the diagnosis of malignant SPT.[12] They analysed five features (namely area, boundary transition ratio, circularity, high-intensity spots, and uniformity) with the CAD system and achieved a sensitivity of 88.2% and specificity of 87.5%. Although this new method might be more accurate, it is not feasible for outpatient screening. An accelerated diagnostic process and appropriate treatment of patients with SPTs could be expected with the use of a simple, easy screening method using ultrasound without the requirement for a special technique. Ultrasound may also reduce the performance of unnecessary imaging studies, thus decreasing medical care costs.

Previous reports on diagnostic ultrasound imaging of SPTs describe several methods with which to judge malignancy according to the amount of blood flow seen on Doppler ultrasonography.[8,13,14] Giovagnorio *et al.*[13] classified the blood flow patterns of 51 superficial SPTs into 4 types. By defining hypervascular type III and IV blood flow as malignant criteria, they reported a sensitivity and specificity of 90% and 100%, respectively. Their method is recognised as one of the most useful screening techniques for SPTs.[15]

In the present study, we classified the blood flow pattern of SPTs according to the Doppler ultrasound findings and re-evaluated these previously described results.[13] We also sought to establish new diagnostic criteria, and thus improve the diagnostic efficacy by combining Doppler ultrasound findings with other factors.

Patients and methods

This study included 189 patients with SPTs who underwent surgery in our department and obtained a pathological diagnosis. Ultrasound imaging studies were performed at the initial visit to the orthopaedic outpatient clinic. The patients comprised 87 men and 102 women with an average age of 54 years. In total, 122 patients had benign diseases including SPTs and tumour-like lesions, while 67 patients had malignant SPTs (Table 1). This study was conducted according to the principles of the Declaration of Helsinki and approved by the institutional ethical committee.

A musculoskeletal oncologist performed the ultrasonography examinations using a 12L-RS linear-type probe of 5.0 to 13.0 MHz (Logic e series; General Electric, Fairfield, CT). According to a report by Giovagnorio *et al.*[13], we classified the intratumoural blood flow patterns shown on colour Doppler into four groups: avascular (type I), hypovascular with a single vascular pole (type II), hypervascular with multiple peripheral poles (type III), and hypervascular with internal vessels (type IV).

We also established a scoring system to improve the sensitivity of differential diagnosis of benign and malignant SPTs (ultrasound-based sarcoma screening [USS] score). In addition to three ultrasound findings (echoic intensity, uniformity of internal structure, and Doppler blood flow classification), the tumour diameter was included in the USS score (Table 2). We evaluated all cases using the USS score and analysed its utility in the differential diagnosis of SPTs.

A p value of < 0.05 was considered to indicate a statistically significant difference between two groups using the chi-squared test or Student's t test. Additionally, we established the cut-off value by receiver operating characteristic (ROC) curve analysis (Microsoft Excel; Microsoft Corporation, Redmond, WA).

Results

The rates of malignant tumours were 18% among type I, 63% among type II, 65% among type III, and 79% among type IV using the classification described by Giovagnorio *et al.*[13] (Figure 1A). Using type III and IV vascularity as markers of malignancy, the sensitivity and specificity were 41.8% and 91.0%, respectively. ROC analysis demonstrated that the area under the curve was 0.77 (Figure 1B).

We re-evaluated all cases using the USS score, which comprised four values, to determine whether we could improve the diagnostic accuracy (Figure 2A). The mean scores in the benign and malignant groups were 1.47 ± 0.93 and 3.42 ± 1.30, respectively. Malignant tumours showed significantly higher USS scores than did benign tumours ($p < 1\times10^{-10}$) (Figure 2B). The ratio of malignant tumours to all cases at each USS score (0–6 points) was 0% at 0 points and 8% at 1 point; this increased to 93% and 100% at 5 and 6 points, respectively (Figure 2C). The area under the curve was 0.88 by ROC analysis, suggesting that USS scoring is diagnostically superior to the Doppler classification described by Giovagnorio *et al.*[13] (Figure 2D). Based on the cut-off value (3 points) calculated by ROC curve analysis, the sensitivity and specificity for a diagnosis of malignant SPT was 85.1% and 86.9%, respectively.

Finally, we examined the average score of each pathological tumour type (Table 1,2). Among benign tumours, vascular tumours (haemangioma, angioleiomyoma, etc.) showed significantly higher scores than did all other benign lesions (p = 0.003) (Table 1). Among malignant tumours, well-differentiated liposarcoma (WDL) showed significantly lower scores than did all other malignant tumours (p = 0.0004) (Table 2). However, the score for WDL (2.15 ± 0.95) was significantly higher than that for lipomatous benign lesions (1.41 ± 0.91; p = 0.02).

Discussion

Advances in imaging technology have provided clinicians multiple diagnostic choices for each indi-

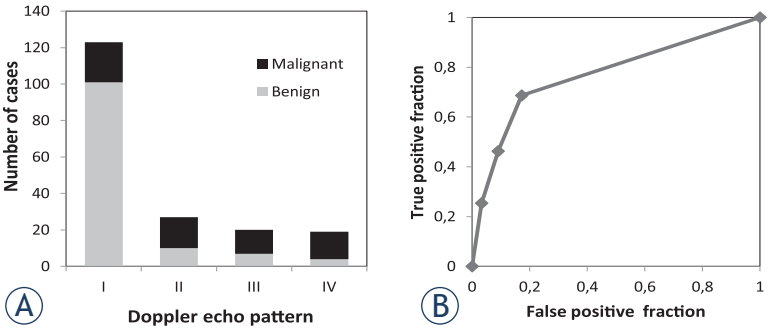

FIGURE 1. Validation of categorisation by Doppler ultrasound pattern. **(A)** All cases were categorised by their vascular pattern using Doppler ultrasound according to the classification described by Giovagnorio *et al*. The type I group included 101 benign tumours and 22 malignant tumours. In contrast, type IV comprised 4 and 15 benign and malignant tumours, respectively. **(B)** Receiver-operating curve analysis of the Doppler ultrasound classification described by Giovagnorio *et al*. The efficacy of the type III and IV pattern for diagnosis of malignant tumours was evaluated. The area under the curve was 0.77.

Values	points
Tumor size	
< 5cm	0
> 5cm	1
Echogenesity	
High/Mid	0
Low	1
Internal texture	
Homogenous	0
Heterogenous	1
Doppler pattern	
I	0
II	1
III	2
IV	3
Total	6

A

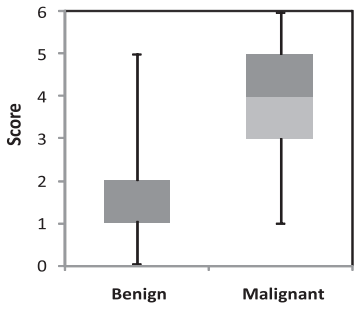

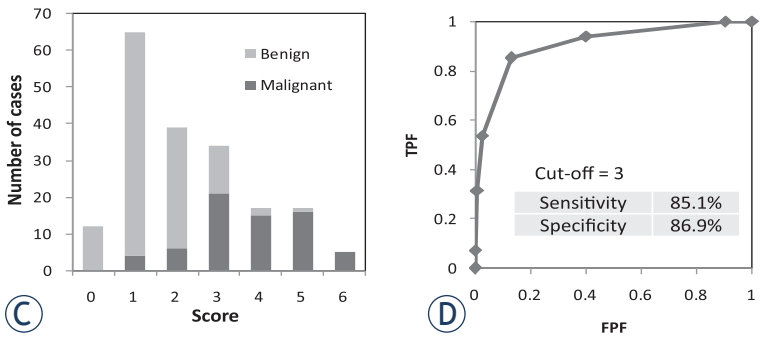

FIGURE 2. Evaluation of new scoring system for soft tissue tumours with ultrasound. **(A)** The new scoring system for differentiation between benign and malignant soft tissue tumours was established by combining four parameters (tumour size, echogenicity, internal structure, and Doppler pattern). The score was designated the ultrasound-based sarcoma screening (USS) score. **(B)** All cases in this study were analysed using the USS score. The average scores of benign and malignant tumours were 1.47 ± 0.90 and 3.71 ± 1.30, respectively. **(C)** Distribution of benign and malignant tumours for each score. As the score increased, the incidence of malignant tumours increased. **(D)** Receiver-operating curve analysis of the USS score revealed a cut-off value of 3 points.

TPF = true-positive fraction; FPF = false-positive fraction

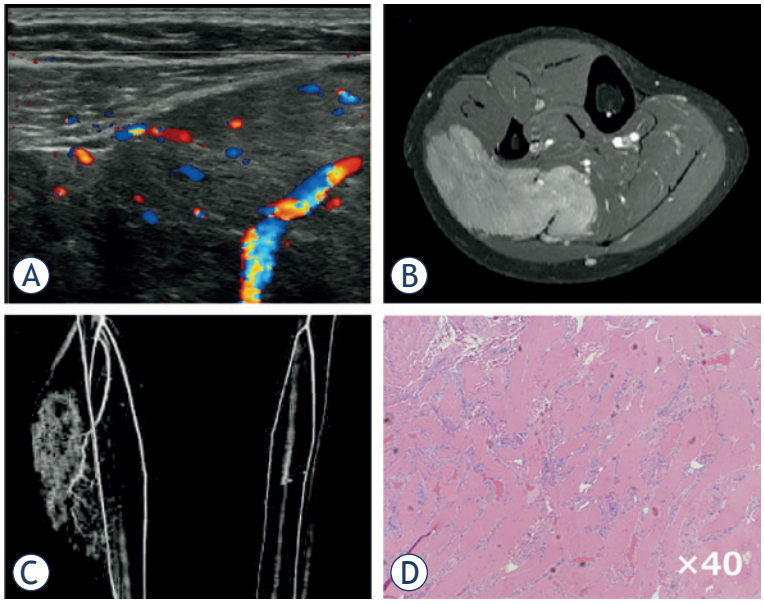

FIGURE 3. Intramuscular haemangioma of gastrocnemius. A 19-year-old woman presented with a swelling and mild pain in her right lower leg. She experienced increased swelling and pain after exercise or long walks. **(A)** Ultrasound revealed an ill-defined mass with a mixed inner texture in the calf muscle. Colour Doppler examination showed multiple vessels within the tumour, corresponding to type IV in the classification described by Giovagnorio et al. **(B)** MRI showed a mass with an irregular border in the soleus muscle. **(C)** CT angiography revealed multiple vessels branching from the tibial artery. **(D)** Pathological analysis of a biopsy specimen demonstrated multiple vessels between the skeletal muscles with no atypia.

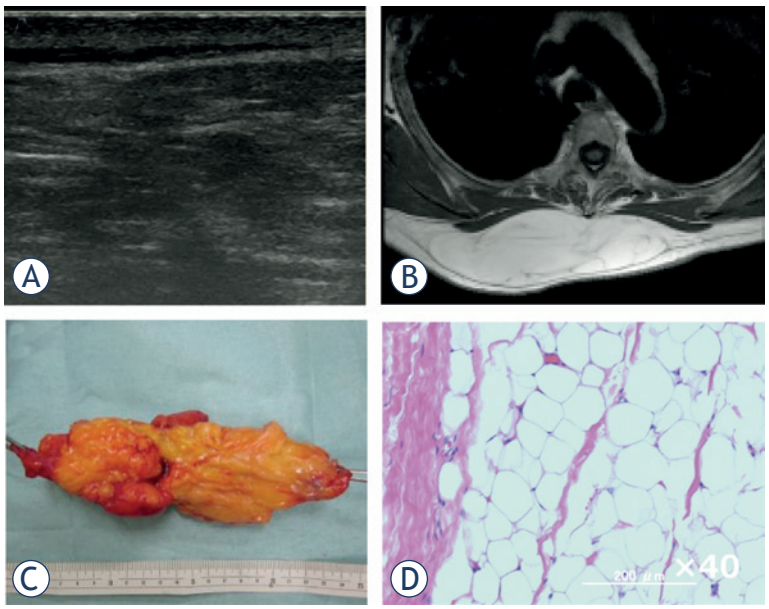

FIGURE 4. Subcutaneous lipoma of the back. A 55-year-old woman presented with a subcutaneous mass on her back. **(A)** Ultrasound revealed a highly echoic mass with a mixed inner texture and no intratumoural vessels by Doppler echo. **(B)** MRI showed a high-intensity mass within the subcutaneous fat tissue on T1-weighted images. **(C)** Gross appearance of the marginally resected tumour. **(D)** Pathological examination of the tumour revealed mature adipocytes with no atypical cells.

vidual patient. Among several imaging modalities, ultrasound is the most feasible method with which to screen for SPTs if the evaluation method is established. Our analysis, which was based on a higher number and greater variety of cases than that by Giovagnorio *et al.*[13], revealed that the specificity for malignant SPT was relatively good (0.91) by Doppler ultrasound alone, but that the sensitivity was poor (0.42). Therefore, we established a novel scoring system (USS score) that can be easily used in orthopaedic outpatient clinics and evaluated whether it can improve the diagnostic sensitivity and specificity without using special equipment. Generally, the probability of malignancy increases as the tumour diameter increases. Grimer[16] reported that a diameter of 5 cm was a significant prognostic factor in patients with soft tissue sarcoma, and recommended that patients should undergo a medical examination if their mass is golf ball-sized or larger (≥ 4.2 cm). We therefore included the tumour size (cut-off of 5 cm) as a simple value incorporated into the USS score. Although a highly significant difference was shown in the USS score between the benign and malignant groups, there were several exceptions. We thus analysed benign cases with USS scores of ≥ 3 points. Among vascular tumours, 40% showed high USS scores (≥ 3), followed by peripheral nerve sheath tumours (PNSTs) (20.6%). This result suggests that these benign tumours require other factors or imaging studies for an accurate diagnosis. Fortunately, these two tumour types exhibit characteristic clinical presentations; *i.e.*, changeable size and symptoms for vascular tumours (Figure 3) and a Tinel-like sign for PNSTs. On the other hand, WDL, known as a low-grade malignancy without metastatic potential[17], exhibited a low USS score (≤ 2 points) in 9 of 13 cases (64.3%) in the present study. Preoperative differential diagnosis between benign lipomatous tumours and WDL is not easy, even with magnetic resonance imaging (MRI). Although the average USS score w as significantly higher in WDL than in benign lipomatous tumours, differential diagnosis between the two groups was not possible. As mentioned above, because WDL does not metastasise and rarely de-differentiates into high-grade liposarcoma, we and others treat such cases by marginal resection, as for benign lipomatous tumours (Figure 4).[17] Adjuvant radiotherapy following resection of WDL was recently shown to reduce local recurrence.[18] Therefore, differentiation of a WDL from a benign tumour is not clinically critical, but differentiation between a high-grade sarcoma

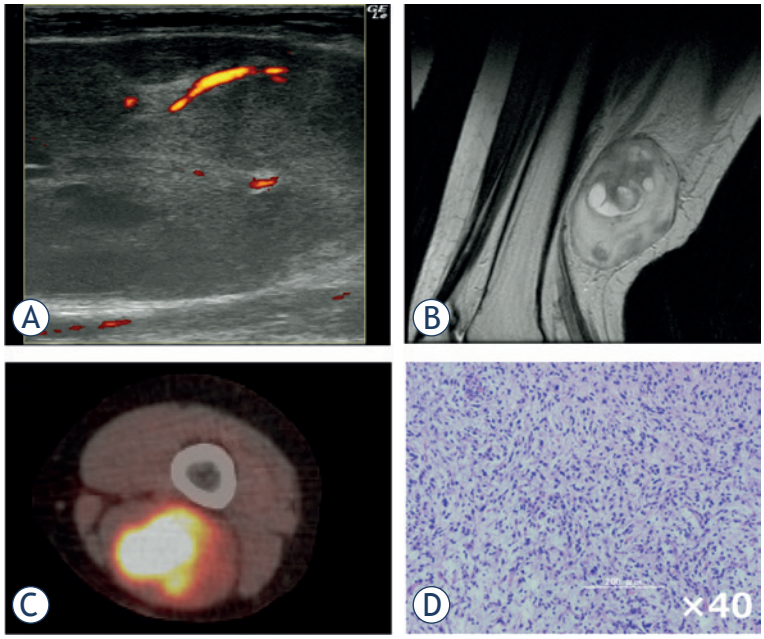

FIGURE 5. Myxofibrosarcoma of the thigh. A 52-year-old woman presented with a firm mass in her popliteal region. **(A)** Ultrasound imaging demonstrated a mixed-echoic mass with an irregular inner texture. Power Doppler revealed a relatively large vessel accompanying multiple small vessels (type IV). **(B)** MRI revealed a mass of both high and low intensity on T2-weighted imaging. **(C)** Positron-emission tomography with fluorodeoxyglucose isotope revealed a tumour with high accumulation and no distant metastases. **(D)** Pathological examination of the biopsy specimen demonstrated abundant atypical tumour cells with nuclear pleomorphism.

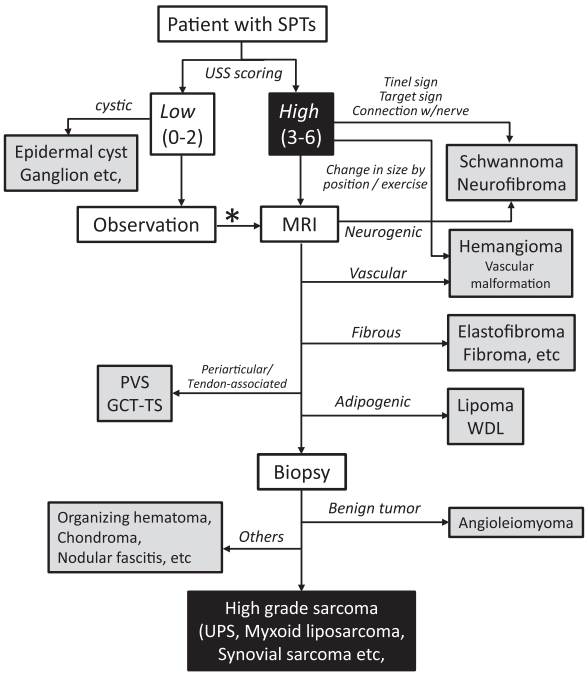

FIGURE 6. Flowchart of diagnosis of soft-part tumours based on ultrasound scoring. This flowchart proposes a screening procedure for soft-part tumours (SPTs). The screening procedure is mainly based on stratification by the ultrasound-based sarcoma screening (USS) score. The USS score is evaluated at the initial visit (0–6 points). If the score is low (0–2 points), the patient can be observed periodically over several months. If the score increases or the tumour size rapidly increases on the second visit or later, the physician may consider performing MRI (*). If the score is high at the initial visit (3–6 points), MRI may be recommended. In this group, peripheral nerve sheath tumours and vascular tumours may be diagnosed based on characteristic clinical symptoms without MRI. MRI can usually be used to diagnose typical fibrous tumours, lipomas, and pigmented villonodular synovitis (PVS) / giant cell tumour of the tendon sheath (GCT-TS). When malignant SPT is suspected, biopsy should be performed to obtain a pathological diagnosis.

UPS = Undifferentiated pleomorphic sarcoma;
WDL = Well-differentiated liposarcoma

(Figure 5) and a benign tumour should be achieved with high accuracy.

The patient's medical history and tumour-related symptoms should be routinely obtained by the physician. We recommend using the USS score in combination with such information to improve the differential diagnostic process. Figure 6 shows a flowchart of the diagnostic process of SPTs based on our analysis. The USS score was used to stratify the cases into high- and low-score groups, which mainly contained malignant and benign cases, respectively. Characteristic symptoms should be combined with ultrasound findings; this will lead to a diagnosis of vascular tumours or PNSTs. If the diagnosis is not conclusive, MRI should be performed. Among benign tumours, MRI can differentiate between fibrous tumours, pigmented villonodular synovitis and histologically related giant cell tumours of the tendon sheath, and lipomatous tumours. Other rare tumours or tumour-like lesions (nodular fasciitis, organising haematoma, or soft tissue chondroma) should be diagnosed by multiple modalities or resectional biopsy. Because the majority of tumours with high USS scores may be malignant, procedures should be chosen carefully for those cases. In the present study, 49 of 73 cases (67%) in the high USS score group were high-grade sarcomas. After careful preoperative assessment, we usually perform a biopsy to obtain a pathological diagnosis for possible cases of malignant SPT. Ultrasound-guided fine-needle aspiration is reportedly useful for soft tissue sarcoma.[19,20] However, because of the shortage of specialised cytologists and the difficulty in obtaining sufficient material, we have not used this method. We are planning to start a prospective study to evaluate the efficacy of fine-needle aspiration as a diagnostic test for SPTs.

In conclusion, our USS score achieved high sensitivity as a screening test for SPT without compromising specificity. Preoperative diagnosis of most SPTs would be possible by combining the USS score with characteristic clinical symptoms and MRI findings.

References

1. Wilson DJ, Parada SA, Slevin JM, Arrington ED. Intrasubstance ruptures of the biceps brachii: diagnosis and management. *Orthopedics* 2011; **34:** 890-6.
2. Murphy RJ, Daines MT, Carr AJ, Rees JL. An independent learning method for orthopaedic surgeons performing shoulder ultrasound to identify full-thickness tears of the rotator cuff. *J Bone Joint Surg Am* 2013; **95:** 266-72.
3. Fowler JR, Maltenfort MG, Ilyas AM. Ultrasound as a first-line test in the diagnosis of carpal tunnel syndrome: a cost-effectiveness analysis. *Clin Orthop Relat Res* 2013; **471:** 932-7.
4. Blankstein A. Ultrasound in the diagnosis of clinical orthopedics: The orthopedic stethoscope. *World J Orthop* 2011; **2:** 13-24.
5. Van der Woude HJ, Vanderschueren G. Ultrasound in musculoskeletal tumors with emphasis on its role in tumor follow-up. *Radiol Clin North Am* 1999; **37:** 753-66.
6. AbiEzzi SS, Miller LS. The use of ultrasound for the diagnosis of soft-tissue masses in children. *J Pediatr Orthop* 1995; **15:** 566-73.
7. Latifi HR, Siegel MJ. Color Doppler flow imaging of pediatric soft tissue masses. *J Ultrasound Med* 1994; **13:** 165-9.
8. Sintzoff SA, Jr., Gillard I, Van Gansbeke D, Gevenois PA, Salmon I, Struyven J. Ultrasound evaluation of soft tissue tumors. *J Belge Radiol* 1992; **75:** 276-80.
9. Griffith JF, Chan DP, Kumta SM, Chow LT, Ahuja AT. Does Doppler analysis of musculoskeletal soft-tissue tumours help predict tumour malignancy? *Clin Radiol* 2004; **59:** 369-75.
10. Stramare R, Gazzola M, Coran A, Sommavilla M, Beltrame V, Gerardi M, et al. Contrast-enhanced ultrasound findings in soft-tissue lesions: preliminary results. *J Ultrasound* 2013; **16:** 21-7.
11. Chiou HJ, Chou YH, Chen WM, Chen W, Wang HK, Chang CY. Soft-tissue tumor differentiation using 3D power Doppler ultrasonography with echo-contrast medium injection. *J Chin Med Assoc* 2010; **73:** 628-33.
12. Chen CY, Chiou HJ, Chou SY, Chiou SY, Wang HK, Chou YH, et al. Computer-aided diagnosis of soft-tissue tumors using sonographic morphologic and texture features. *Acad Radiol* 2009; **16:** 1531-8.
13. Giovagnorio F, Andreoli C, De Cicco ML. Color Doppler sonography of focal lesions of the skin and subcutaneous tissue. *J Ultrasound Med* 1999; **18:** 89-93.
14. Lakkaraju A, Sinha R, Garikipati R, Edward S, Robinson P. Ultrasound for initial evaluation and triage of clinically suspicious soft-tissue masses. *Clin Radiol* 2009; **64:** 615-21.
15. Bianchi S, Martinoli C. *Ultrasound of the musculoskeletal system.* Berlin, New York: Springer; 2007.
16. Grimer RJ. Size matters for sarcomas! *Ann R Coll Surg Engl* 2006; **88:** 519-24.
17. Laurino L, Furlanetto A, Orvieto E, Dei Tos AP. Well-differentiated liposarcoma (atypical lipomatous tumors). *Semin Diagn Pathol* 2001; **18:** 258-62.
18. Cassier PA, Kantor G, Bonvalot S, Lavergne E, Stoeckle E, Le Pechoux C, et al. Adjuvant radiotherapy for extremity and trunk wall atypical lipomatous tumor/well-differentiated LPS (ALT/WD-LPS): a French Sarcoma Group (GSF-GETO) study. *Ann Oncol* 2104; **25:** 1854-60.
19. Trovik CS, Bauer HC, Brosjo O, Skoog L, Soderlund V. Fine needle aspiration (FNA) cytology in the diagnosis of recurrent soft tissue sarcoma. *Cytopathology* 1998; **9:** 320-8.
20. Ayala AG, Ro JY, Fanning CV, Flores JP, Yasko AW. Core needle biopsy and fine-needle aspiration in the diagnosis of bone and soft-tissue lesions. *Hematol Oncol Clin North Am* 1995; **9:** 633-51.

case report

Artery of Percheron infarction: review of literature with a case report

Urska Lamot[1], Ivana Ribaric[2], Katarina Surlan Popovic[1]

[1] Clinical Institute of Radiology, University Medical Centre Ljubljana, Ljubljana, Slovenia
[2] Department of Vascular Neurology and Intensive Therapy, Neurology Clinic, University Medical Centre Ljubljana, Ljubljana, Slovenia

Radiol Oncol 2015; 49(2): 141-146.

Received 21 January 2014
Accepted 20 August 2014

Correspondence to: Asisst. Prof. Katarina Šurlan Popovič, M.D., Ph.D., Clinical Institute of Radiology, University Medical Centre Ljubljana, Zaloška cesta 7, 1525 Ljubljana, Slovenia. E-mail: katarina.surlan@gmail.com

Disclosure: No potential conflicts of interest were disclosed.

Background. Clinical features indicating an ischemic infarction in the territory of posterior cerebral circulation require a comprehensive radiologic examination, which is best achieved by a multi-modality imaging approach (computed tomography [CT], CT-perfusion, computed tomography angiography [CTA], magnetic resonance imaging [MRI] and diffusion weighted imaging [DWI]). The diagnosis of an acute ischemic infarction, where the damage of brain tissue may still be reversible, enables selection of appropriate treatment and contributes to a more favourable outcome. For these reasons it is essential to recognize common neurovascular variants in the territory of the posterior cerebral circulation, one of which is the artery of Percheron.

Case report. A 69 year-old woman, last seen awake 10 hours earlier, presented with two typical clinical features of the artery of Percheron infarction, which were vertical gaze palsy and coma. Brain CT and CTA of neck and intracranial arteries upon arrival were interpreted as normal. A new brain CT scan performed 24 hours later revealed hypodensity in the medial parts of thalami. Other imaging modalities were not performed, due to the presumption that the window for the application of effective therapy was over. The diagnosis of an artery of Percheron infarction was therefore made retrospectively with the re-examination of the CTA of neck and intracranial arteries.

Conclusions. A multi-modality imaging approach is necessary in every patient with suspicion of the posterior circulation infarction immediately after the onset of symptoms, especially in cases where primary imaging modalities are unremarkable and clinical features are severe, where follow-up examinations are indicated.

Key words: Percheron; infarction; imaging

Introduction

The thalami and midbrain have a complex blood supply with a large number of feeding arteries.[1,2] The arterial supply is provided by perforating branches from the posterior cerebral artery and the posterior communicating artery.[3] Although there are significant variations and overlaps, the thalamic vascular supply is classically categorized into 4 territories: anterior, paramedian, inferolateral and posterior.[4-6] In addition to the paramedian thalami, the paramedian thalamic arteries supply the medial areas of the upper brainstem: the interpeduncular nucleus, the decussation of the superior cerebellar peduncles, the medial part of the red nucleus, the third and fourth cranial nerve nuclei and the anterior portion of the periaqueductual grey matter.[3,7]

Consequently, occlusion of the artery of Percheron causes a bilateral paramedian thalamic infarction with or without midbrain infarction.[2,4,5] Additional involvement of the anterior thalamus is uncommon.[5] The prevalence of arteries of Percheron is unknown. Since strokes in these territories are infrequently diagnosed, it is not known whether they are really rare or highly underdiagnosed.[1]

Due to a large number of blood supply variants of the posterior cerebral circulation, an ischemic infarction in this territory presents variable and unspecific clinical symptoms, which requires a comprehensive radiologic examination. This approach enables a diagnosis of an ischemic infarction in the early stage, when treatment with thrombolysis and/or mechanical recanalization is still possible and therefore reversibly damaged brain tissue can be salvaged with prompt revascularization. The goal of this paper is to report a case where the diagnosis of an artery of Percheron infarction was made retrospectively, due to an unspecific clinical presentation and a deficient multi-modality approach.

Clinical presentation

The complex anatomy and function of the human thalamus and its variable vascular supply are responsible for the extremely variable clinical features when this structure is damaged by an ischemic infarction; in addition, the vascular overlap with the underlying midbrain extends the spectrum of these clinical features to include midbrain signs.[5,9] An ischemic stroke in the territory of an artery of Percheron usually presents with three main symptoms, which are found in patients with bilateral paramedian thalamic strokes. These are vertical gaze palsy (65%), memory impairment (58%) and coma (42%).[4,6] Bilateral paramedian thalamic lesions are often accompanied by rostral midbrain lesions, producing a "mesencephalothalamic" or "thalamopeduncular" syndrome.[6,10] In addition to the mentioned triad, the syndrome is characterized by other oculomotor disturbances, hemiplegia, cerebellar ataxia and movement disorders.[6]

Imaging and treatment

Diagnosing an artery of Percheron infarction is critical for directing the appropriate time sensitive management and preventing additional unnecessary procedures.[6,11] Different treatment methods, such as intravenous thrombolysis and endovascular treatment are available. They can be performed if a diagnosis of acute stroke is made.[4] As in our case, the diagnosis is often made in the late stage, when therapy is ineffective and dangerous. Magnetic resonance imaging (MRI) usually allows visualization of the initial infarct in cases of acute cerebral ischemia and is used in stroke centres as the primary or early secondary imaging modality.[4]

Infarction of the artery of Percheron presents as an abnormal signal intensity on MRI and/or hypoattenuation on CT, involving the bilateral paramedian thalami with or without rostral midbrain involvement.[6] Early diagnosis is best made by a diffusion weighted imaging (DWI) sequence using MRI.[11]

Lazzaro *et al*., identified four patterns of ischemic infarctions when the Percheron artery is occluded.[6] Approximately 43% of their patients demonstrated damage to both paramedian thalami and midbrain, while 38% had ischemic damage to paramedian thalami only, without midbrain involvement. In around 14% of patients, the damage involved the anterior thalamic nuclei in addition to paramedian thalami and upper midbrain. The least common pattern (5%) was ischemic damage of the bilateral paramedian and anterior thalami; the midbrain was spared in these cases. They also found that a previously unreported finding (a "V" sign) on fluid attenuated inversion recovery (FLAIR) and DWI sequences was identified in 67% of cases of artery of Percheron infarction with midbrain involvement and this sign supports the diagnosis when present.[5,6] The "V" sign appears as a distinct pattern of V-shaped hyperintensity on axial FLAIR and/or DWI along the pial surface of the midbrain adjacent to the interpeduncular fossa.[6]

The artery of Percheron is rarely visualized with conventional angiography and, to the best of our knowledge, only four authors have successfully demonstrated this variant[5,6]; it is too small to be visualized by computed tomography angiography (CTA) or magnetic resonance angiography (MRA).[11]

Case presentation

A 68 year-old Caucasian woman, last seen awake 10 hours earlier, was found unresponsive in front of her apartment. The patient had a history of hypertension, but, it is unclear if she had used any long-term medication. On physical examination in our Neurological Emergency Room, she was comatose with Glasgow Coma Scale 4 and the following initial vital signs: pulse 60 beats/min, respiratory rate 16 breaths/min and blood pressure 110/53 mmHg. Pupillary light reflex in the right eye was non-reactive and the left eye poorly reactive. The right pupil was dilatated. Passive examination of the ocular movements showed complete vertical gaze palsy. The patient was afebrile and no meningeal signs were present. She flexed the right arm and extended the left leg on painful stimulus. Babinski could not be provoked on the left and

was in flexion on the right. No other pathological signs were present. The following laboratory tests were all unremarkable: complete blood cell count, glycaemia, electrolytes, liver enzymes, creatinine, ammonia, arterial blood gas values, ethanol, benzodiazepine and opioid levels. The international normalized ratio (INR) was 1.15. In this case the neurological examination was misleading due to unspecific clinical signs and symptoms which were unhelpful in the process of achieving the correct working diagnosis.

The initial CT performed 60 minutes after finding the patient (and an unknown time after loss of consciousness) showed no acute haemorrhage or early signs of ischemia, only an old lacunar infarction in the left thalamus (Figure 1). CTA of neck and intracranial arteries was interpreted as normal. A new head CT was performed 24 hours later. It revealed areas of hypodensity (16x 10 mm) in the medial thalami, which were not present on the previous CT examination (Figure 2). The right hypodense area extended into the anterior part of the mesencephalon and cerebral peduncle. The left hypodense area extended only into the anterior part of the mesencephalon. The chronic ischemic change in the posterior part of the left thalamus remained unchanged.

Due to our findings on the second CT, we decided to perform another reading of the CTA examination performed at the time of the patients' admission, which revealed a duplication of the right superior cerebellar artery and a filling defect of the P1 segment of the right posterior cerebral artery (Figure 3).

There was no improvement in the patients' neurological status in the following days and she was included in our palliative care program. On day 5, the patient became febrile with raised inflammatory parameters. Although we applied an antibiotic, the patient's clinical status deteriorated and she died of cardiopulmonary failure on the 13th day of hospitalization. This study was conducted according to the principles of the Declaration of Helsinki and approved by the institutional ethical committee.

Discussion

The large number of variants of the blood supply in the posterior cranial fossa, especially the high variability of presence and size of P1 segments, which give rise to the paramedian arteries, may be a clue that the artery of Percheron is not such an infrequent variant and may be underdiagnosed.[1,6]

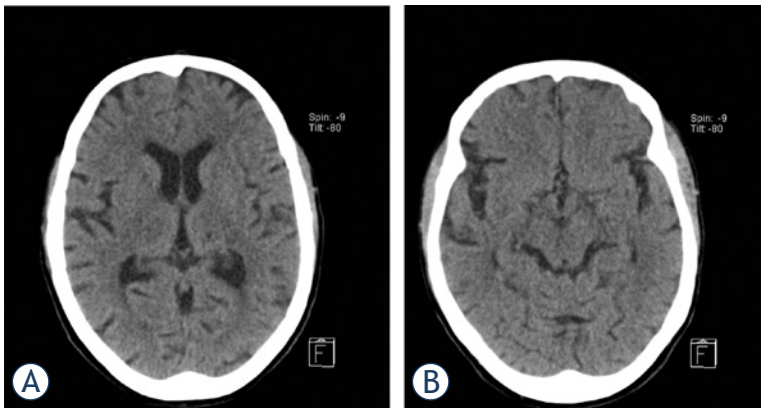

FIGURE 1. The non-contrast head CT scan performed on the day of admission was normal, in particular without early signs of ischemia at the level of both thalami **(A)** the mesencephalon **(B)**.

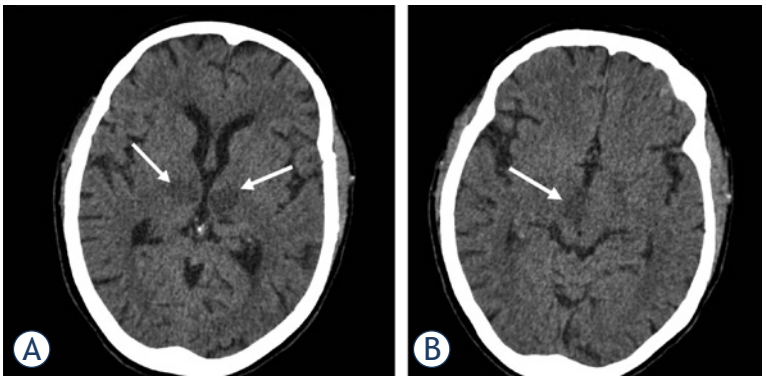

FIGURE 2. Another non-contrast head CT scan was performed 24 hours later and showed symmetrical ill-defined areas of hypodensity in the medial part of both thalami, corresponding to occlusion of the artery of Percheron (white arrows) **(A)**. The hypodense area in the right thalamus extended into the anterior part of the mesencephalon and cerebral peduncle. The hypodense area in the left thalamus extended only into the anterior part of the mesencephalon (white arrow) **(B)**.

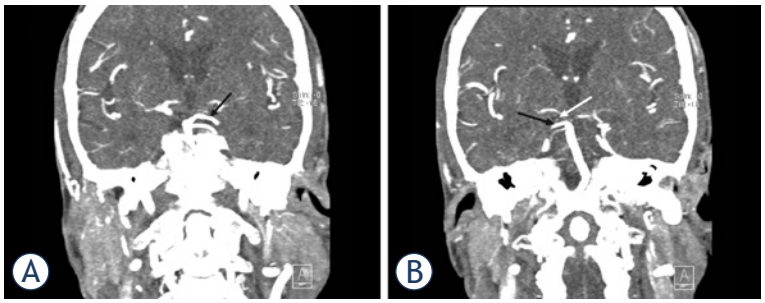

FIGURE 3. Computed tomography angiography (CTA) of the neck and intracranial arteries. The basilar artery and the left posterior cerebral artery (PCA) (black arrow) were both transient **(A)**. At first glance, the right PCA appears to be fully opacified. Detailed examination of the CTA images revealed a filling defect of the P1 segment of the right PCA (white arrow) and another rare anatomic variant: duplication of the right superior cerebellar artery (black arrow), which could have been mistaken for a transient right PCA **(B)**.

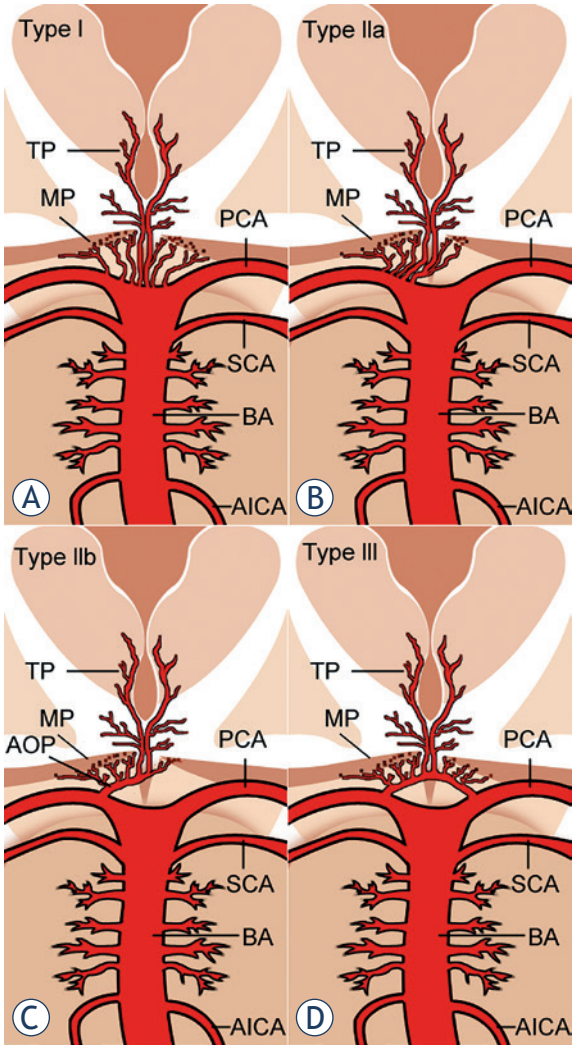

FIGURE 4. Anatomic variations of the arterial supply to the paramedian thalamic-mesencephalic region as described by Percheron: Variant I **(A)**, variant IIa **(B)**, variant IIb **(C)** – the artery of Percheron, variant III **(D)**. Vessels marked by initials: thalamic perforators (TP), midbrain perforators (MP), posterior cerebral artery (PCA), superior cerebellar artery (SCA), basilar artery (BA), anterior inferior cerebellar artery (AICA) and artery of Percheron (AOP).

The characteristic artery of Percheron infarct pattern has been estimated in different studies to occur in 0.1 to 2%[5,7] of all ischemic strokes and in 4% to 18% of all thalamic strokes.[6]

According to Percheron, there are four normal variants of the neurovascular anatomy of the thalami and midbrain.[4,8] Variant I is most common, in which each perforating artery arises from each left and right posterior cerebral artery (Figure 4A).[4,5] Variant IIa is a less common, asymmetrical variant, in which perforating arteries arise directly from the proximal segment of one of the posterior cerebral arteries (Figure 4B).[3-5] In variant IIb, the bilateral perforating thalamic arteries arise from a single arterial trunk called the artery of Percheron, which arises from the P1 segment of one posterior cerebral artery. It supplies the paramedian thalami and the rostral midbrain bilaterally (Figure 4C).[2-5] Variant III is an arcade variant, with several small perforating branches arising from a single arterial arc that bridges the P1 segments of both posterior cerebral arteries (Figure 4D).[3,5]

It is difficult to suspect bithalamic paramedian infarcts because of the complex anatomy, which causes large clinical variability.[4] They are typically characterized by a triad of altered mental status, vertical gaze palsy and memory impairment.[6] Our patient presented with two of the three typical features of this stroke syndrome; that is, vertical gaze palsy and altered mental status.

A head CT was performed on admission to exclude haemorrhage, tumours, other obvious brain lesions and early signs of brain ischemia. A re-examination of the CTA revealed an overlooked anatomical variant, a duplication of the right superior cerebellar artery and a filling defect of the P1 segment of the right posterior cerebral artery. In our previous reading, we had mistaken one of the duplicated right superior cerebellar arteries for a transient P1 segment of the right posterior cerebral artery. Due to the aforementioned findings, we assume that right and left paramedian thalamic arteries aroused from a common trunk, since the P1 segment of the left posterior cerebral artery was transient. A falsely negative CTA of neck and intracranial arteries omitted the consideration of mechanical revascularization, for the possibly effected vessels were not visualized. In such cases where clinical findings are severe we suggest prompt further examination using other imaging modalities. On the basis of clinical, neuroimaging and neurovascular findings, the only possible diagnosis was an ischemic stroke in the territory of the artery of Percheron and this diagnosis was therefore made retrospectively. These findings demonstrate that when an artery of Percheron is suspected, the possibility that other rare anatomic variants of the posterior circulation may be present should also be considered.

In a patient with an acute onset of a neurological deficit and changes in the described locations, a diagnosis of a stroke of an artery of Percheron must be considered.[1] The prognosis of artery of Percheron infarction may be ameliorated by treatment of acute stroke. Patients with acute ischemic stroke are thrombolysed intravenously (applica-

tion of alteplase) unless there are contraindications. Endovascular revascularization applies thrombolytic agents directly into the thrombus or mechanically extracts the cloth.[12] Mechanical trombectomy is considered in patients with a diagnosis of acute stroke, who have an occlusion of a treatable intracranial artery and are within 10.5 hours of onset of posterior circulation symptoms, to allow recanalization within 12 hours.[4,12] The most applicable sites for interventional exploration are carotid T occlusion, M1 and M2 segments of the medial cerebral artery occlusion and vertebra-basilar thrombosis.[12] As in our case, the diagnosis is often made many hours or even days after the clinical onset. At this stage therapy is ineffective and dangerous. Endovascular treatment is only seldom an option in these cases, for these arteries are often too small for visualization during the procedure.

MRI normally allows visualization of the initial infarct in cases of acute cerebral ischemia and is usually used in stroke centres as the primary or early secondary imaging modality. When brain MRI shows an acute stroke, thrombolysis can be performed if the deadline for achieving it is not over.[4] Early diagnosis is best made using a DWI sequence.[1] As in other locations in the brain, the combination of pathologic DWI and normal findings on T2-weighted or FLAIR images suggest an acute stroke. If the lesions are already visible on T2 or FLAIR images, the time window for thrombolysis is over.[1,4] In our case, early MRI and CT perfusion were not performed because, on the basis of the patients' medical history, we presumed the window for thrombolysis was over. Considering our findings, we should perhaps have performed MRI or CT perfusion, since they could have helped in the decision-making process.

To the best of our knowledge, there is only a single report in the literature of a symptomatic patient presenting an acute Percheron stroke with normal early brain MRI.[4] On the basis of this one case, Cassourret[4] *et al.* concluded that a normal initial MRI cannot formally eliminate the diagnosis of acute stroke of the artery of Percheron, although they state that the MRI was of inferior quality because the technical conditions were not optimal. The article suggests that, on the presentation of acute rostral brain stem stroke, accompanied by an inconclusive brain MRI, new brain imaging by MRI should be performed within therapeutic times or interventional explorations focused on the vertebrobasilar territory[4] should be considered.

To the best of our knowledge, the value of CT perfusion in acute Percheron stroke has not been evaluated. The advantage of CT perfusion is that it is able to delineate areas of the brain that may be salvaged by intervention (e.g., thrombolysis or clot retrieval), known as the penumbra, from the parts that are irrevocably destined to go into infarct regardless of therapy, known as the infarct core. What is more, identification of infracted areas is easier than with non-contrast head CT. The weakness of CT perfusion at the level of the midbrain is that we often come across artefacts that reduce the quality of the examination.

It must be born in mind that the artery of Percheron is rarely visualized with conventional angiography[6], since these vessels are too small[1], and to our knowledge only 4 authors have successfully demonstrated this variant.[6] Performing conventional angiography may not be indicated, because lack of visualization of the artery does not exclude its presence (because it is occluded).[2] Although in our case it is unlikely that we would have visualized the artery of Percheron, we should perhaps have performed conventional angiography, since it could have shown the filling defect of the P1 segment of the right posterior cerebral artery, which would have influenced our decision regarding treatment. Conventional cerebral angiography should therefore not be used routinely to diagnose Percheron artery occlusion.[5]

When an ischemic infarction in the territory of the posterior circulation is suspected we firstly perform a native head CT to exclude haemorrhage and enable treatment with intravenous thrombolysis. In the case of negative imaging findings we continue the examination by performing a brain CT-perfusion and CTA of neck and intracranial arteries for the detection of ischemic infarctions not visible on native CT. When regardless the severe clinical picture all the mentioned imaging methods fail to depict the causative pathology for the deterioration of the patient's state, we suggest performing MRI with T1-, T2- and FLAIR sequences and DWI for an exclusion of ischemic infarction in early stages.

We estimate the time to perform a comprehensive multi-modality examination in the evaluation of posterior circulation ischemic infarctions to 45 to 90 minutes, depending on the time from the insult to imaging, size of infarction and technical difficulties, for patients with posterior circulation infarcts usually require mechanical life support devices which make examination with MRI difficult.

The imaging differential of bithalamic lesions is broad and includes arterial and venous occlusion, infiltrative neoplasm, infectious and inflammatory

lesions, and a single large embolus at the basilar tip could result in a similar infarct pattern. However, this would typically manifest as the "top of the basilar" syndrome with additional characteristic posterior circulation infarcts.[6] The final diagnosis is based on the combination of clinical picture, laboratory tests and imaging findings.

Considering all the given information, we suggest that in emergency settings, in which the severity of the clinical features (coma and vertical gaze palsy) does not correlate with the imaging findings, the possibility of an artery of Percheron infarction must be taken into consideration and CT perfusion or MRI performed within therapeutic times, in order to make the correct diagnosis when treatment is still possible.

References

1. Krampla W, Schmidbauer B, Hruby W. Iscmaemic stroke of the artery of Percheron. *Eur Radiol* 2008; **18:** 192-4.
2. Matheus MG, Castillo M. Imaging of acute bilateral paramedian thalamic and mesencephalic infarcts. *AJNR Am J Neuroradiol* 2003; **24:** 2005-8.
3. Godani M, Auci A, Torri T, Jensen S, Sette DM. Coma with vertical gaze palsy: Relevance of angio-CT in acute percheron artery syndrome. *Case Rep Neurol* 2010; **2:** 74-9.
4. Cassourret G, Prunet B, Sbardella F, Bordes J, Maurin O, Boret H. Ishemic stroke of the artery of Percheron with normal initial MRI: a case report. *Case Rep Med* 2010; **2010:** 425734. doi:10.1155/2010/425734.
5. Amin OSM, Shwani SS, Zangana HM, Hussein EMH, Ameen NA. Bilateral infarction of paramedian thalami: a report of two cases of artery of Percheron occlusion and review of the literature. *BMJ Case Rep* 2011; 2011: bcr0920103304. doi: 10.1136/bcr.09.2010.3304.
6. Lazzaro NA, Wright B, Castillo M, Fischbein NJ, Glastonbury CM, Hildenbrand PG, et al. Artery of Percheron infarction: imaging patterns and clinical spectrum. *AJNR Am J Neuroradiol* 2010; **31:** 1283-9.
7. Carrera E, Michael P, Bogousslavsky J. Anteromedian, central, and posterolateral infarcts of the thalamus: three variant types. *Stroke* 2004; **35:** 2826-31.
8. Kraft P, Waschbisch A, Wendel F, Muellges W, Classen J. Why it's important to know Percheron's artery: solitary carotid stenosis as a unique cause of anterior, posterior and bithalamic ischemia. *J Neurol* 2009; **256:** 1558-60.
9. Slamia LB, Jemaa HB, Benammou S, Tlili-Graiess K. Occlusion of the artery of percheron: clinical and neuroimaging correlation. *J Neuroradiol* 2008; **35:** 244-5.
10. Perren F, Clarke S, Bogousslavsky J. The syndrome of combined polar and paramedian thalamic infarction. *Arch Neurol* 2005; **62:** 1212-6.
11. Shea YF, Lin OY, Chang RSK, Luk JKH. Artery of Percheron infarction. *Hong Kong Med J* 2012; **18:** 446. e1-2.
12. Ahmad N, Nayak S, Jadun C, Natarajan I, Jain P, Roffe C. Mechanical thrombectomy for ischaemic stroke: the first UK case series. *PLoS One* 2013; **8:** 1-10.

research article

Feasibility and safety of electrochemotherapy (ECT) in the pancreas: a pre-clinical investigation

Roberto Girelli[1*], Simona Prejanò[2*], Ivana Cataldo[2], Vincenzo Corbo[2], Lucia Martini[3], Aldo Scarpa[2], Bassi Claudio[4]

[1] Pancreatic Unit – Casa di Cura Pederzoli, Peschiera del Garda (VR), Italy
[2] ARC-NET Research Centre and Department of Pathology and Diagnostics, University and Hospital Trust of Verona, Verona, Italy
[3] Laboratory of Preclinical and Surgical Studies and Laboratory of Biocompatibility, Innovative Technologies and Advanced Therapies, Rizzoli Orthopedic Institute Bologna, Italy
[4] Department of Surgery and Oncology, Pancreas Institute, University and Hospital Trust of Verona, Verona, Italy

Radiol Oncol 2015; 49(2): 147-154.

Received 27 December 2014
Accepted 12 February 2015

Correspondence to: Roberto Girelli, M.D., Pancreatic Unit – Casa di Cura Pederzoli, Via Monte Baldo 24-37019 Peschiera del Garda, Verona, Italy. Phone: + 045 644 91 10; Fax: + 045 644 91 15; E-mail: r.girelli@cdcpederzoli.it

Disclosure: No potential conflicts of interest were disclosed.

* These authors contributed equally to this work.

Supported by: FIMP-Italian Ministry of Health (CUP_J33G13000210001)

Background. Pancreatic ductal adenocarcinoma (PDAC) is a lethal disease generally refractory to standard chemotherapeutic agents; therefore improvements in anticancer therapies are mandatory. A major determinant of therapeutic resistance in PDAC is the poor drug delivery to neoplastic cells, mainly due to an extensive fibrotic reaction. Electroporation can be used *in vivo* to increase cancer cells' local uptake of chemotherapeutics (electrochemotherapy, ECT), thus leading to an enhanced tumour response rate. In the present study, we evaluated the *in vivo* effects of reversible electroporation in normal pancreas in a rabbit experimental model. We also tested the effect of electroporation on pancreatic cancer cell lines in order to evaluate their increased sensitivity to chemotherapeutic agents.

Materials and methods. The application *in vivo* of the European Standard Operating Procedure of Electrochemotherapy (ESOPE) pulse protocol (1000 V/cm, 8 pulses, 100 µs, 5 KHz) was tested on the pancreas of normal New Zealand White Rabbits and short and long-term toxicity were assessed. PANC1 and MiaPaCa2 cell lines were tested for *in vitro* electrochemotherapy experiments with and without electroporation. Levels of cell permeabilization were determined by flow cytometry, whereas cell viability and drug (cisplatin and bleomycin) sensitivity of pulsed cells were measured by 3-(4,5-dimethylthiazol-2-yl)-5-(3-carboxymethoxyphenyl)-2-(4-sulfophenyl)-2H-tetrazolium (MTS) assay.

Results. In healthy rabbits, neither systemic nor local toxic effects due to the electroporation procedure were observed, demonstrating the safety of the optimized electric parameters in the treatment of the pancreas *in vivo*. In parallel, we established an optimized protocol for ECT *in vitro* that determined an enhanced anti-cancer effect of bleomycin and cisplatin with respect to treatment without electroporation.

Conclusions. Our data suggest that electroporation is a safe procedure in the treatment of PDAC because it does not affect normal pancreatic parenchyma, but has a potentiating effect on cytotoxicity of bleomycin in pancreatic tumour cell lines. Therefore, ECT could be considered as a valid alternative for the local control of non-resectable pancreatic cancer.

Key words: electroporation; bleomycin; cisplatin; electrochemotherapy; preclinical study; safety; pancreatic adenocarcinoma

Introduction

Pancreatic ductal adenocarcinoma (PDAC) is a highly aggressive disease with a poor 5-year survival, resulting in the fifth leading cause of cancer-related death in Europe.[1-3] PDAC is usually diagnosed in advanced stage, with loco-regional invasion and distant metastasis, and usually results largely drug-resistant. Surgical resection, although is currently the only "curative" chance to prolong survival, is suitable only for a minority of patients (< 20%). Standardized protocols of treatment in resectable patients provide a 6-month-course adjuvant chemotherapy following resection[4], although the survival is still poor.

The optimal treatment for patients with locally advanced pancreatic cancer (LAPC) with no evidence of metastases remains to be defined. The standard treatment for LAPC is based on Chemotherapy (CT)[5-9] and combination of CT and Radiotherapy (RT) with a median overall survival of 10–15 months.[10-12]

Because of the poor results achieved, some new ablative techniques have been considered for local treatment: radiofrequency ablation (RFA), laser ablation, microwave, ethanol injection and irreversible electroporation (IRE).[13] Particularly, RFA has been used in the clinical setting with promising preliminary results.[14-17]

Patients with metastatic disease undergo systemic palliative chemotherapy. Treatment outcomes are typically poor and resistance to standard chemotherapeutic agents remains the major problem.[18-24]

Based on recent preclinical data in mouse models, it has been hypothesised that currently available anticancer drugs cannot access tumour cells at an effective concentration due to the presence of an extensive hypo-vascular fibrotic stroma that acts as a barrier shielding tumour cells from the action of systemic therapeutic agents.[25] Therefore, the improvement of anticancer drug delivery enhances tumour cells sensitivity and hence would provide a better response and a potential prolongation of survival.

Electroporation is a physical method that employs microsecond length electric pulses to alter temporarily the permeability of cell membranes in order to facilitate chemicals and large molecules delivery to the cells.[26-28] Electroporation can be used in all types of isolated cells as well as in tissues. Target cells have to be exposed to an electric field of sufficient strength and for a sufficient time. The magnitude of the electric field depends on cell type, size, orientation and density, pulse duration and number of pulses.[29]

Electrochemotherapy (ECT) combines the administration of non-permeant or low-permeant cytotoxic drugs (bleomycin or cisplatin) with the application to the tumour of permeabilizing electric pulses, to increase local drug uptake and hence its effectiveness.[30, 31]

This combination treatment has proven to be very effective in local control of skin metastatic tumour nodules independently of the histotype[32-39] and it is now routinely employed for this purpose in a number of European countries, in about 140 cancer treatment centres; recently this technique has been developed for the treatment of deep-seated tumours.[40,41]

Electrochemotherapy has been used in previous preliminary studies for the treatment of rats and mice bearing subcutaneous implants of melanoma[30,41-44], sarcoma[30,43-45], and pancreatic tumours[46] with encouraging results. Furthermore, liver tumours of rats and rabbits resulted highly responsive to ECT without impairment of the surrounding normal tissue functionality.[47-48] The effectiveness of intraoperative ECT was demonstrated in hamster pancreatic adenocarcinoma cell line (PC-1) model.[49]

We hypothesize that ECT could be used for the treatment of primary non-resectable pancreatic cancer. The aim of the present study was to investigate the feasibility and safety of electroporation in an experimental rabbit model. *In vivo* local and systemic effects of electric pulses applied to the pancreas were evaluated. Furthermore, we tested ECT *in vitro* on highly drug resistant pancreatic cancer cell lines in order to prove its efficacy in this subset as well.

Materials and methods

Electroporation apparatus

Electroporation was performed using the Cliniporator™ (IGEA S.p.A., Carpi, Modena, Italy). Different protocols of 100 μs square-wave electric pulses were tested *in vitro*; one sequences of 8 electrical pulses, 100 μs of duration, at 1000 V/cm were used for *in vivo* experiments.

Animals and anaesthesia

The experiments were conducted according to the EU Directive 2010/63/EU and to the Guidelines for the welfare and use of animals in cancer research

(Br J Cancer 2010; 102:1555–77). The protocol was approved by the Ethical Committee of the Rizzoli Orthopaedic Institute (ELETTRO-RAB 03/25/2009 prot.10499), and submitted to the Italian Ministry of Health (28/04/2009 prot.10771). We used 9 male Hybrid New Zealand rabbits weighing 2.1 ± 0.5 kg, housed under controlled conditions. General anaesthesia was induced with an intramuscular injection of 44 mg/kg ketamine (Imalgene 1000, Merial Italia S.p.a., Milano), 3 mg/kg xylazine (Rompun: Bayer S.p.a. Milano) and maintained by means of facial mask in spontaneous ventilation (O_2: 1 L/min, N_2O: 0.4 L/min, isoflurane: 2.5% to 3%). Postoperatively, antibiotic and analgesic therapy was administered (Flumequine - Flumexil Fatro, Italy and metamizole Farmolisina Vetem, Italy).

General physiological status of rabbits, including potential onset of anorexia and intestinal blocking, was monitored daily by technician and in charge veterinarian during all the period of the study.

Animal electroporation and sample collection

Animals underwent pancreas and duodenum (gut) electroporation in open surgery according to the standard operating procedure: 8 pulses at 1000 V/cm of amplitude over distance ratio, 100 μs of duration were delivered at 5 KHz using linear N-20-4B electrodes. The electroporated area ranged between 12–15 mm in length. The animals were euthanized 24 hours (n = 2), 72 hours (n = 1), 15 days (n = 3), 30 days (n = 3) after surgery with *i.v.* injection of 2 ml Tanax (Tanax, Intervet International AN Baxmeer NL) under deep general anaesthesia. The pancreas was removed and treated for the morphological and histological analysis. All the specimens were formalin fixed and paraffin embedded. Four mm tissue sections were stained with Haematoxylin and Eosin (H&E) for histopathological evaluation. Post mortem bowel was visually explored for integrity. No histological evaluation was performed on the bowel.

Biochemical analysis

Peripheral blood was collected before surgery (T0) and at each experimental time: 7 days, 15 days and 30 days following electroporation. After blood collection, serum was separated by centrifugation and parameters of hepatic function such as alanine transaminase (ALT), aspartate transaminase (AST), and pancreatic enzymes, such as amylase, were analysed. The animals did not receive any pharmacological prophylaxis for pancreatitis such as octreotide and Gabesato mesylate. Since the *in vivo* study is limited to tissue electroporation and no drug was administered to the animals, for ethical reasons, we did not include control groups.

Cell line and drugs

PANC1 and MiaPaCa2 human pancreatic cancer cell lines were obtained from the American Type Culture Collection (ATCC). Various molecular mechanisms have been taken in account to play a role in drug-resistance development in these specific cell lines. One of these mechanisms is mediated by the overexpression of BRG1, a chromatin modulator responsible for gemcitabine resistance also in locally advanced and metastatic pancreatic cancer.[50]

The two cell lines were cultured in RPMI 1640 medium supplemented with 10% of heat-inactivated foetal calf serum (Gibson, Milan, Italy). Cells were maintained as monolayer in 75 cm^2 tissue culture flasks at 37°C in a humidified atmosphere of 5% CO_2. The cell lines were Mycoplasma free as assessed by MycoAlert assay (Lonza, Milan, Italy). Cells used for experimental purposes were detached using trypsin-EDTA (0.05% trypsin, Lonza) and collected by centrifugation at 300 rpm. Cell diameter for PANC1 and MiaPaCa2 was 16.8 μm and 12.2 μm respectively, as measured by FACS analysis. The following anticancer drugs were used: bleomycin and cisplatin (Sigma, Milan, Italy). Drugs were dissolved in 0.9% bacteriostatic saline and used at indicated concentrations.

Cell viability and permeabilization

Three aliquots of $1x10^5$ cells (in 100μl of RPMI medium) were placed in separate 2 mm gap electroporation cuvettes (Bio-Rad laboratories). Each cuvette was exposed to electric field strength of 0.5 or 1 kV/cm (8 pulses, 100 μs of duration, 5 KHz). After 30 minutes of incubation, pulsed cells were diluted by a factor 100 in RPMI medium and seeded into 96- well tissue culture plates. Unpulsed cells were subjected to same procedure. The acute effect of electroporation on cell viability was determined using MTS assay (Promega) and the Countess Cell Counter (Invitrogen, Milan, Italy). Cell permeabilization was determined at indicated field strength by uptake of fluorescent dye Lucifer yellow (Sigma, Milan, Italy). Briefly, cells incubat-

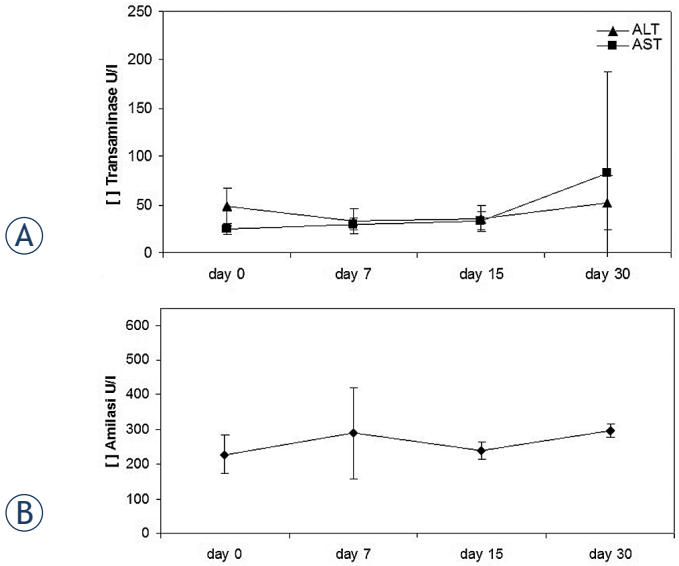

FIGURE 1. Serum levels of the liver enzymes, AST, ALT **(A)** and of the pancreatic amylase **(B)**. Data points represent mean ± (standard error) SE, n = 3-6.

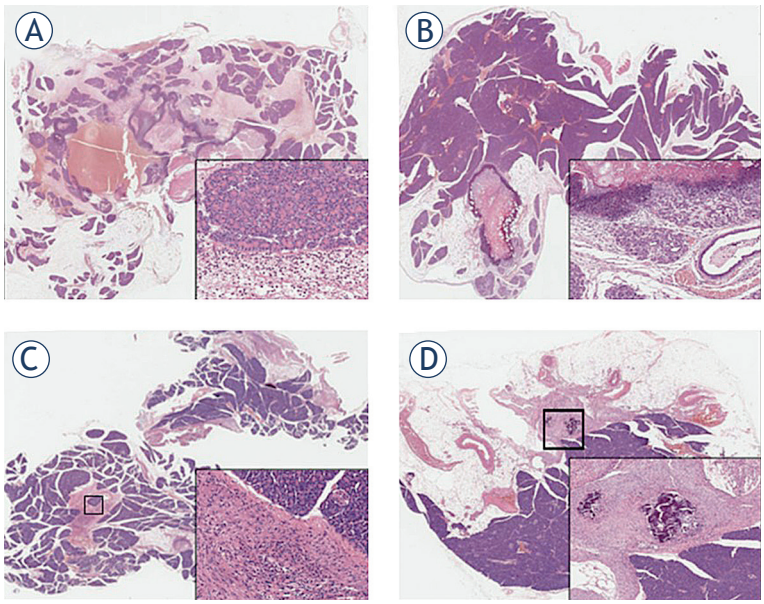

FIGURE 2. Photomicrographs of rabbit pancreata at different times after electroporation. **(A)** 24 hours: necrosis in the treated areas surrounded by significant hyperaemia and oedema. Acinar degranulation and vacuolation with granulocytes and lymphocytes infiltration (inset). **(B)** 72 hours: necrosis is still evident while acinar to ductal metaplasia appears along with intraductal protein plugs (inset). **(C)** 15 days: fibrotic areas are evident; chronic inflammatory cells are present while pancreatic acini are normal (inset). **(D)** 30 days: calcium deposition is detectable in fibrotic areas; pancreatic parenchyma is normal (inset).

ed in the presence of Lucifer yellow at a final concentration of 1 mM were exposed to electric pulses and then incubated at 37°C for 5 min. Cells were then chilled on ice, washed in phosphate-buffered saline (PBS) buffer and examined for fluorescence emission in a FACScalibur flow cytometer (Beckton Dickinson). Median fluorescence emission was determined and percent of permeabilized cells was calculated.

In vitro electrochemotherapy (ECT)

Cell sensitivity of PANC1 and MiaPaCa2 to cisplatin and bleomycin was preliminary tested in order to define an appropriate range of drug concentrations to be used for electrochemotherapy experiments (data not shown). For ECT, cells ($1x10^5$ suspended in 100µl of RPMI medium) were placed between 2 plate electrodes in 2 mm gap cuvette (Bio-Rad laboratories) in the presence of a range of concentration of drugs or isotonic saline and exposed to a defined electric field strength of 1 kV/cm (8 pulses, 100 µs of duration). Aliquots of cells were left unpulsed in presence of drugs or vehicle. Seven concentrations of cisplatin ranging from 1.6 to 26 µM were used for PANC1, whereas 7 concentrations ranging from 1.6 to 40 µM were tested for MiaPaCa2. For bleomycin, 5 concentrations ranging from 0.1 to 6.6 µM were used for MiaPaCa2, whereas 7 concentrations ranging from 0.3 to 130 µM were tested for PANC1. Pulsed and unpulsed cuvettes were incubated in humidified atmosphere at 37°C for 30 min after electric exposure. Then cells were diluted by a factor of 100 in RPMI medium and three aliquots of 100 µl ($1x10^4$ cells) from each cuvette were seeded in 96-well tissue culture plates. Plates were incubated for 72 h and then survival was evaluated by MTS assay (Promega) and the Countess Cell Counter (Invitrogen, Milan, Italy).

Data from the plate reader were analysed using GraphPad Prism version 6. The data were first normalized to the vehicle control and then analysed using the nonlinear regression feature. The curves shown in the figures and the calculated IC50 values were the result of three technical replicates for each cell lines.

Statistical analysis

Comparisons between groups were performed using Student's T test and $p < 0.05$ level was considered significant.

TABLE 1. IC50 of bleomycin and cisplatin for PANC1 and MiaPaCa-2 unpulsed (-) or pulsed (+) with electroporation (EP)

	IC 50 of Bleomycin			IC 50 of Cisplatin		
Cell	- EP	+ EP	P value	- EP	+ EP	P value
PANC1	100 μM	0.59 μM	<0.0001	23 μM	8 μM	<0.0001
MiaPaCa2	3.5 μM	0.2 μM	<0.0001	30 μM	23 μM	0.001

Results

In vivo electroporation of non-pathological rabbit pancreata; general toxicity and histological evaluation

General physiological status of the rabbits was checked daily and no functional deficits as anorexia, intestinal blockage or other clinical status alterations were detected; all the rabbits recovered from general anaesthesia after 1 hour. Transaminase and amylase levels were not statistically modified ($p > 0.05$) over 30 days of the electroporation procedure (day 0, day 7, day 15, day 30) (Figure 1).

Histological evaluation

The results of hystopathological analysis are shown in Figure 2A–D. At short term, 24 h post-electroporation, non-pathological rabbit pancreas showed necrosis in the treated areas surrounded by important hyperaemia and oedema in addition to aspects of acute distress of acinar cells (degranulation and vacuolation). An acute inflammatory reaction was also present (Figure 2A). Acinar to ductal metaplasia appeared after 72 h. Elevation of serum amylase is often, but not always, associated with acute pancreatitis. In our study, we found that the ductal metaplasia is not associated with an increase in the serum level of amylase. It is possible that the ductal metaplasia is the consequence of the transient inflammatory response to the insertion of the needle rather than the inflammatory response of the entire organ.

Moreover, the evidence of intraductal protein plugs, containing degenerating cells, was due to proteins hypersecretion by acinar cells (Figure 2B). After 15 days, fibrotic areas surrounded by normal pancreatic acinar cells were detected. Fat substitution of about 20% of pancreatic parenchyma was also present (Figure 2C). After 30 days, calcium deposition was evident in fibrotic areas (Figure 2D) as a result of mild and transient modification.

When electrical pulses were directly applied to the gut, its integrity was maintained without infection on further clinical complications (data not shown).

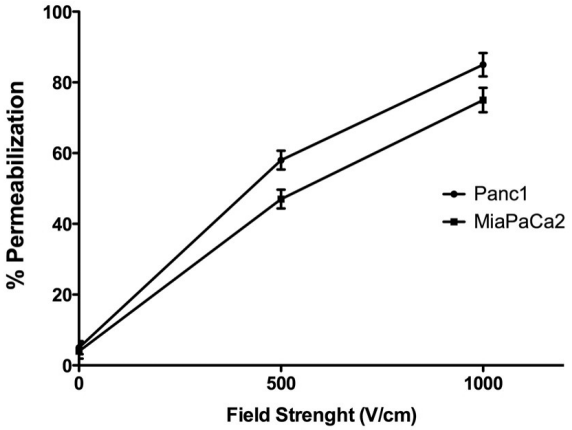

FIGURE 3. Cell lines permeabilization as determined by Lucifer yellow uptake and flow cytometry. Mean ± standard deviation (S.D.) of n = 3 independent experiments; circle symbol, Panc1; square symbol, MiaPaCa2

Cells survival and permeabilization

Before testing the toxicity of anticancer drugs on electropermeabilized cells, we defined the optimal parameters for electrical treatment in order to obtain high cell survival and effective permeabilization. Therefore, both PANC1 and MiaPaCa2 cells were subjected to 8 pulses of 100 μs at two different electric field strength of 0.5 or 1 kV/cm. Percent of viable cells was calculated with respect to untreated cells. Field strength of 0.5 kV/cm did not affect cell viability, whereas a slight reduction of about 4% was observed when both cell lines were exposed to field strength of 1 kV/cm (data not shown). Cell permeabilization was assessed by flow cytometry at 1 kV/cm showing that about 90% and about 75% of cells were permeabilized, for PANC1 and MiaPaCa2 respectively (Figure 3). The optimal electric condition was defined as 1 kV/cm, 8 pulses of 100μs duration. In these conditions, the mean value of viability of the pulsed controls was 95% (range 93–97%) of that of the unpulsed con-

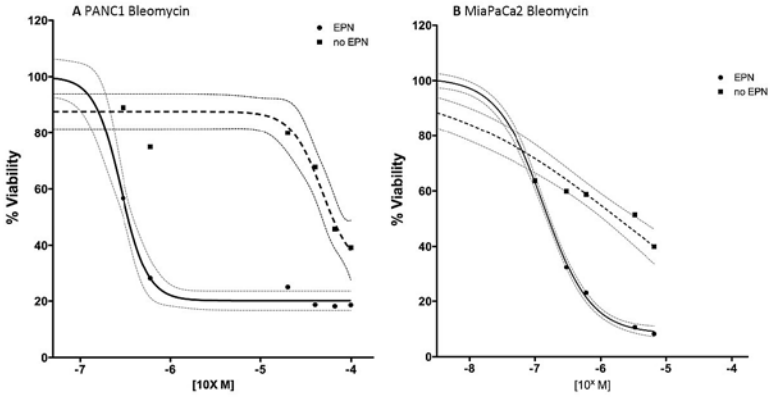

FIGURE 4. Dose-response curve of bleomycin treatment. Cell viability was assessed at 72 hours of drug exposure using 3-(4,5-dimethylthiazol-2-yl)-5-(3-carboxymethoxyphenyl)-2-(4-sulfophenyl)-2H-tetrazolium (MTS) assay (Promega) and the Countess Cell Counter (Invitrogen, Milan, Italy).

Dashed line = no electroporation; solid line = electroporation; grey lines indicate 95 % confident interval [CI]

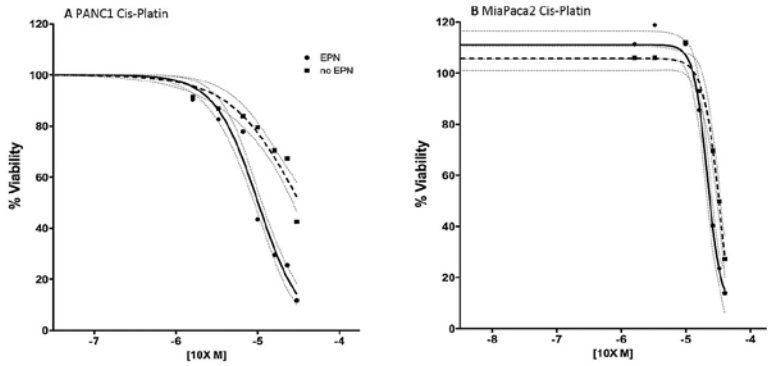

FIGURE 5. Dose-response curve of cisplatin treatment. Cell viability was assessed at 72 hours of drug exposure using 3-(4,5-dimethylthiazol-2-yl)-5-(3-carboxymethoxyphenyl)-2-(4-sulfophenyl)-2H-tetrazolium (MTS) assay (Promega) and the Countess Cell Counter (Invitrogen, Milan, Italy).

Dashed line = no electroporation; solid line = electroporation; grey lines = indicate 95% confident interval [CI]

trols, with a permeabilization level of at least 75% of pulsed cells.

Cell viability following electrochemotherapy

After establishing the optimized parameters for electroporation, 8 pulses of 100μs duration at 1 kV/cm, we investigated the cytotoxicity of two chemotherapeutic agents, bleomycin and cisplatin, against PDAC cell lines. Pulsed PANC1 and MiaPaCa2 cell lines showed enhanced sensitivity to both bleomycin and cisplatin compared to unpulsed cells. Specifically, the IC50 of bleomycin for PANC1 and MiaPaCa2 was reduced by a factor 166 and 18 respectively, after electroporation. Whereas the IC50 of cisplatin was reduced by a factor 2.8 for PANC1 and 1.3 for MiaPaCa2 (Table 1). The cells viability after bleomycin and cisplatin treatment pulsed with electroporation and unpulsed (Figure 4,5).

Discussion

In this study, we demonstrated that a well-defined electroporation protocol does not induce evident signs of local and systemic toxicity when applied to normal pancreas in a pre-clinical model. In addition, the effect of ECT with cisplatin and bleomycin was evaluated in human pancreatic cancer cells lines after. ECT refers to the combined administration of chemotherapy with the local application of electric pulses to the tumour cells in order to increase drug delivery and local cytotoxicity. ECT has been proven effective in the treatment of skin or subcutaneous metastases from solid tumours of different origin. Subsequently to several reports of clinical studies[35-38] assessing the use and the efficacy of ECT in the treatment of various primary skin cancers, head and neck cancer, and skin metastasis of different primary tumours, clinicians and researchers are trying to develop novel approaches to extend ECT to the treatment of deep-seated and visceral tumours.[39-41] Edhemovic *et al*., have recently reported for the first time, the feasibility and safety of the procedure highlighting the effectiveness of ECT in the treatment of patients with liver metastases from primary colorectal cancer. The lack of side effect during and after the procedure, demonstrates the safety of the treatment.[41] Furthermore, Granata *et al.* reported a preliminary experience of feasibility and safety of intraoperative electrochemotherapy in locally advanced pancreatic tumour. Twelve patients with tumours of the head or the body of the pancreas underwent ECT. No side effects or major complications have been recorded. No acute intraoperative or postoperative serious adverse effects were related to ECT, showing that electrochemotherapy is a feasible and safe treatment for patients with locally advanced pancreatic adenocarcinoma.[51]

According to the results reported in further studies, the viability of human tumoural pancreatic cell lines was not modified by electrical pulse alone, while it decreased after exposure to bleomycin and cisplatin. Bleomycin and cisplatin result cytotoxic only at high concentrations. Nevertheless, when

the cells were exposed to both the chemotherapeutic agent and the electric pulses, the cytotoxic effect was achieved at lower drug concentration. Specifically, the potentiating effect of electric pulse was more pronounced for bleomycin than cisplatin, confirming previous observations.[35,41,49,52-54] Todorovic *et al*.[55] observed a similar sensitization effect in murine colon carcinoma cell-line CMT3 and reported the referral range of IC50 value of different murine and human cell lines treated with bleomycin and cisplatin, with and without electroporation. The pancreatic cell lines PANC1 and MiaPaCa2 tested in the present study, demonstrate IC50 values within the range indicated by Todorovic *et al.*

The delivery of electric pulses through needles inserted into the pancreas of rabbits elicits a local inflammatory response in the early days after ECT and completely resolves in 30-days. The blood values of pancreatic amylase and transaminases (ALT and AST) were not significantly increased over the whole observational period. Our data agree with previous results reported by Ramirez LH *et al*., which demonstrate that tissues submitted to electroporation alone, present an immediate inflammatory reaction restricted to electropulsed areas. No diffuse damage of adjacent organs was observed.[48] Similarly, Cemazar M *et al*. analysed *in vivo* the ECT antitumour efficacy in a number of animal models.[56] Our data confirmed that electroporation is a safe procedure in the treatment of pancreatic tumours and ECT could be effective for local control of non-resectable pancreatic cancer. The development of new electrodes and specific software for the assessment of proper preoperative strategies could increase both the safety of ECT and extend its application field.

References

1. Ferlay J, Parkin DM, Steliarova-Foucher E. Estimates of cancer incidence and mortality in Europe in 2008. *Eur J Cancer* 2010; **46:** 765-81.
2. Jemal A, Bray F, Center MM, Ferlay J, Ward E, et al. Global cancer statistics. *CA Cancer J Clin* 2011; **61:** 69-90.
3. Krejs GJ. Pancreatic cancer: epidemiology and risk factors. *Dig Dis* 2010; **28:** 355-8.
4. Neoptolemos IP, Stocken DD, Friess H, Bassi C, M.D., Dunn JA, Hickey H, et al. A randomized trial of chemoradiotherapy and chemotherapy after resection of pancreatic cancer. *NEJM* 2004; **350:** 1200-10.
5. Gastrointestinal Tumour Study Group. Radiation therapy combined with adriamycin or 5-Fluorouracil for the treatment of locally unresectable pancreatic carcinoma. *Cancer* 1985; **56:** 2563-8.
6. Klaassen DJ, MacIntyre JM, Catton GE, Engstrom PF, Moertel CG. Treatment of locally unresectable cancer of the stomach and pancreas: a randomized comparison of 5-fluorouracil alone with radiation plus concurrent and maintenance 5-fluorouracil--an Eastern Cooperative Oncology Group study. *J Clin Oncol* 1985; **3:** 373-8.
7. Chauffert B, Mornex F, Bonnetain F, Rougier P, Mariette C, Bouché O, et al. Phase III trial comparing intensive induction chemoradiotherapy (60 Gy, infusional 5-FU and intermittent cisplatin) followed by maintenance gemcitabine with gemcitabine alone for locally advanced unresectable pancreatic cancer. Definitive results of the 2000-01 FFCD/SFRO study. *Ann Oncol* 2008; **19:** 1592-9.
8. Loehrer PJ Sr, Feng Y, Cardenes H, Wagner L, Brell JM, et al. Gemcitabine alone versus gemcitabine plus radiotherapy in patients with locally advanced pancreatic cancer: An eastern cooperative oncology group trial. *J Clin Oncol* 2011; **29:** 4105-12.
9. Conroy T, Desseigne F, Ychou M., Bouché O, Guimbaud R, Bécouarn Y, et al. For the Groupe Tumeurs Digestives of Unicancer and the PRODIGE Intergroup. FOLFIRINOX versus gemcitabine for metastatic pancreatic cancer. *N Engl J Med* 2011; **364:** 1817-25.
10. Gillen S, Schuster T, Meyer zum Büschenfelde C, Friess H, Kleeff J. Preoperative/neoadjuvant therapy in pancreatic cancer: A systematic review and meta-analysis of response and resection percentages. *PLoS Med* 2010; **7(4):** e1000267 2010.
11. Huguet F, André T, Hammel P, Artru P, Balosso J, Selle F, et al. Impact of chemoradiotherapy after disease control with chemotherapy in locally advanced pancreatic adenocarcinoma in GERCOR Phase II and III studies. *J Clin Oncol* 2007; **25:** 226-331.
12. Krishnan S, Rana V, Janjan NA, Varadhachary GR, Abbruzzese JL, Das P, et al: Induction chemotherapy selects patients with locally advanced, unresectable pancreatic cancer for optimal benefit from consolidative chemoradiation therapy. *Cancer* 2007; **110:** 47-55.
13. Katrina F. Chu and Damian E. Dupuy. Thermal ablation of tumours: biological mechanisms and advances in therapy. *Nature Rev* 2014; **14:** 199-208.
14. Giardino A, Girelli R, Lusenti A, Auriemma A, Bassi C, Cantore M, et al. Triple approach strategy for patients with locally advanced pancreatic carcinoma. *HPB (Oxford)* 2013; **15:** 623-7.
15. Girelli R, Gobbo S, Malleo G, Regi P, Salvia R, Frigerio I, et al. Results of 100 pancreatic radiofrequency ablations in the context of a multimodal strategy for stage III ductal adenocarcinoma. *Langenbecks Arch Surg* 2013; **398:** 63-9.
16. Cantore M, Frigerio I, Giardino A, Girelli R, Mambrini A, Orlandi M, et al: Combined modality treatment for patients with locally advanced pancreatic adenocarcinoma. *Brit J Surg* 2012; **99:** 1083-8.
17. Girelli R, Frigerio I, Salvia R, Barbi E, Tinazzi Martini P, et al. Feasibility and safety of radiofrequency ablation for locally advanced pancreatic cancer. *Brit J Surg* 2010; **97:** 220-5.
18. Shi X, Liu S, Kleeff J, Friess H, Büchler MW. Acquired resistance of pancreatic cancer cells towards 5-Fluorouracil and gemcitabine is associated with altered expression of apoptosis-regulating genes. *Oncology* 2002; **62:** 354-62.
19. Arumugam T, Ramachandran V, Fournier KF, Wang H, Marquis L, Abbruzzese JL, et al. Epithelial to mesenchymal transition contributes to drug resistance in pancreatic cancer. *Cancer Res* 2009; **69:** 5820-8.
20. Tamburrino A, Piro G, Carbone C, Tortora G, Melisi D. Mechanisms of resistance to chemotherapeutic and anti-angiogenic drugs as novel targets for pancreatic cancer therapy. *Front Pharmacol* 2013; **4:** 56.
21. Hermann PC, Huber SL, Herrler T, Aicher A, Ellwart JW, Guba M, et al. Distinct populations of cancer stem cells determine tumor growth and metastatic activity in human pancreatic cancer. *Cell Stem Cell* 2007; **1:** 313-23.
22. Li C, Heidt DG, Dalerba P, Burant CF, Zhang L, Adsay V, et al. Identification of pancreatic cancer stem cells. *Cancer Res* 2007; **67:** 1030-7.
23. Thiery JP, Acloque H, Huang RY, Nieto MA. Epithelial-mesenchymal transitions in development and disease. *Cell* 2009; **139:** 871-90.
24. Bria E, Milella M, Gelibter A, Cuppone F, Pino MS, Ruggeri EM, et al. Gemcitabine-based combinations for inoperable pancreatic cancer: have we made real progress? A meta-analysis of 20 phase 3 trials. *Cancer* 2007; **110:** 525-33.
25. Olson P, Hanahan D. Cancer. Breaching the cancer fortress. *Science* 2009; **324:** 1400-1.
26. Neumann E, Schaefer-Ridder M, Wang Y, Hofschneider PH. Gene transfer into mouse lyoma cells by electroporation in high electric field. *EMBO J* 1982; **1:** 841-5.
27. Neumann E, Kakorin S, Toesing K. Fundamentals of electroporative delivery of drugs and genes. *Bioelectrochem Bioenerg* 1999; **48:** 3-16.

28. Orlowski S, Mir LM. Cell electropermeabilization: a new tool for biochemical and pharmacological studies. *Biochim Biophys Acta* 1993; **1154:** 51-63.

29. Gehl J. Electroporation: theory and methods, perspectives for drug delivery, gene therapy and research. *Acta Physiol Scand* 2003; **177:** 437-47.

30. Mir LM, Orlowski S, Belehradek M and Paoletti C. Electrochemotherapy: potentiation of antitumor effect of bleomycin by local electric pulses. *Eur J Cancer* 1991; **1:** 68-72.

31. Belehradek M, Domenge C, Luboinski B, Orlowski S, Belehradek Jr. J, Mir LM. Electrochemotherapy, a new antitumor treatment - first clinical phase I–II trial. *Cancer* 1993; **72:** 3694-700.

32. Marty M, Sersa G, Garbay JR, Gehl J, Collins CG, Snoj M, et al: Electrochemotherapy – an easy, highly effective and safe treatment of cutaneous and subcutaneous metastases. Results of ESOPE (European Standard Operating Procedures of Electrochemotherapy) study. *Eur J Cancer* 2006; **S4:** 3-13.

33. Sersa G, Stabuc B, Cemazar M, Jancar B, Miklavcic D, Rudolf Z. Electrochemotherapy with CDDP: potentiation of local CDDP antitumor effectiveness by application of electric pulses in cancer patients. *Eur J Cancer* 1998; **34:** 1213-8.

34. Sersa G, Stabuc B, Cemazar M, Miklavcic D, Rudolf Z. Electrochemotherapy with cisplatin: clinical experience in malignant melanoma patients. *Clin Cancer Res* 2000; **6:** 863-7.

35. Matthiessen LW, Johannesen HH, Hendel HW, Moss T, Kamby C, Gehl J. Electrochemotherapy for large cutaneous recurrence of breast cancer: A phase II clinical trial. *Acta Oncol* 2012; **51:** 713-21.

36. Mevio N, Bertino G, Occhini A, Scelsi D, Tagliabue M, Mura F, et al. Electrochemotherapy for the treatment of recurrent head and neck cancers: preliminary results. *Tumori* 2012; **98:** 308-13.

37. Curatolo P, Quaglino P, Marenco F, Mancini M, Nardò T, Mortera C, et al. Electrochemotherapy in the treatment of kaposi sarcoma cutaneous lesions: A two-center prospective phase II trial. *Ann Surg Oncol* 2012; **1:** 192-8.

38. Campana LG, Valpione S, Mocellin S, Sundararajan R, Granziera E, Sartore L, et al. Electrochemotherapy for disseminated superficial metastases from malignant melanoma. *Br J Surg* 2012; **99:** 821-30.

39. Fini M, Salamanna F, Parrilli A, Martini L, Cadossi M, Maglio M, et al. Electrochemotherapy is effective in the treatment of rat bone metastases. *Clin Exp Met* 2013; **30:** 1033-45.

40. Edhemovic I, Gadzijev EM, Brecelj E, Miklavcic D, Kos B, Zupanic A, et al. Electrochemotherapy: a new technological approach in treatment of metastases in the liver. *Technol Cancer Res Treat* 2011; **10:** 475-85.

41. Edhemovic I, Brecelj E, Gasljevic G, Marolt Music M, Gorjup V, Mali B et al. Intraoperative electrochemotherapy of colorectal liver metastases. *J Surg Oncol* 2014; **110:** 320-7.

42. Heller R, Jaroszeski M, Perrot R, Messina J and Gilbert R: Effective treatment of B16 melanoma by direct delivery of bleomycin using electrochemotherapy. *Melanoma Res* 1997; **7:** 10-8.

43. Sersa G., Cemazar M, Miklavcic D, Mir LM. Electrochemotherapy: variable anti-tumor effect on different tumor models. *Bioelectrochem Bioenerg* 1994; **35:** 23-7.

44. Pendez S, Jaroszeski MJ, Gilbert R Hyacinthe M, Dang V, Hickey J, et al. Direct delivery of chemotherapeutic agents for the treatment of hepatoma and sarcoma in rat models. *Radiol Oncol* 1998; **21:** 53-64.

45. Sersa G, Novakovic S, Miklavcic D: Potentiation of bleomycin antitumor effectiveness by electrochemotherapy. *Cancer Lett* 1993; **69:** 81-4.

46. Nanda GS, Sun FX, Hofmann GA, Hofmann RM, Dev SB. Electroporation enhances therapeutic efficacy of anticancer drugs: treatment of human pancreatic tumor in animal model. *Anticancer Res* 1988; **18:** 1361-6.

47. Jaroszeski MJ, Gilbert RA, Heller R. In vivo antitumor effects of electrochemotherapy in a hepatoma model. *Bioch Biophis Acta* 1997; **1334:** 15-8.

48. Ramirez LH, Orlowski S, An D, Gindoula G, Dzodic R, Ardouin P, et al. Electrochemotherapy on liver tumours in rabbit. *Br. J Cancer* 1998; **77:** 2104-11.

49. Jaroszeski MJ, Illingworth P, Pottinger C, Hyacinthe M, Miller R. Electrically mediated drug delivery for treating subcutaneous and orthotopic pancreatic adenocarcinoma in a hamster model. *Anticancer Res* 1999; **19:** 989-94.

50. Liu X, Tian X, Wang F, Ma Y, Kornmann M, Yang Y. BRG1 promotes chemoresistance of pancreatic cancer cells through crosstalking with Akt signalling. *Eur J Cancer* 2014; **50:** 2251-62.

51. Granata V, Fusco R, Piccirillo M. Palaia R, Lastoria A, Petrillo A, et al. Feasibility and safety of intraoperative electrochemotherapy in locally pancreatic tumor: A preliminary experience. *Eur J Inflamm* 2014; **12:** 467-77.

52. Allegretti JP, Panje WR. Electroporation therapy for head and neck cancer including carotid artery involvement. *Laryngoscope* 2001; **111:** 52-6.

53. Bloom DC, Goldfarb PM. The role of intratumour therapy with electroporation and bleomycin in the management of advanced squamous cell carcinoma of the head and neck. *Eur J Surg Oncol* 2005; **31:** 1029-35.

54. Miklavcic D, Sersa G, Brecelj E, Gehl J, Soden D, Bianchi G, Ruggieri P, Rossi CR, Campana LG, Jarm T. Electrochemotherapy: technological advancements for efficient electroporation-based treatment of internal tumors. *Med Biol Eng Comput* 2012; **50:** 1213-25.

55. Todorovic V, Sersa G, Flisar K, Cemazar M. Enhanced cytotoxicity of bleomycin and cisplatin after electroporation in murine colorectal carcinoma cells. *Radiol Oncol* 2009; **43:** 264-73.

56. Cemazar M, Tamzali Y, Sersa G, Tozon N, Mir LM, Miklavcic D, et al. Electrochemotherapy in veterinary oncology. *J Vet Inter Med* 2008; **22:** 826-31.

research article

Efficacy of intensity-modulated radiotherapy with concurrent carboplatin in nasopharyngeal carcinoma

Anussara Songthong, Chakkapong Chakkabat, Danita Kannarunimit, Chawalit Lertbutsayanukul[1]

Division of Radiation Oncology, Department of Radiology, Faculty of Medicine, Chulalongkorn University, King Chulalongkorn Memorial Hospital, Pathumwan, Bangkok, Thailand

Radiol Oncol 2015; 49(2): 155-162.

Received 30 June 2014
Accepted 1 October 2014

Correspondence to: Anussara Songthong, M.D., Division of Radiation Oncology, Department of Radiology, King Chulalongkorn Memorial Hospital, 1873 Rama IV Rd. Pathumwan, Bangkok 10330, Thailand. Phone: +662 256 4334; Fax: +662 256 4590; E-mail: anussara_pr@yahoo.com

Disclosure: No potential conflicts of interest were disclosed.

Background. The aim of the prospective phase II study was to evaluate the efficacy and toxicities of concurrent carboplatin with intensity-modulated radiotherapy (IMRT) in the treatment of nasopharyngeal carcinoma (NPC).

Patients and methods. Between October 2005 and November 2011, 73 stage II–IVB NPC patients received IMRT 70 Gy concurrently with three cycles of carboplatin (AUC 5) every three weeks, followed by three cycles of adjuvant carboplatin (AUC 5) and 5-FU (1,000 mg/m^2/day for four days) every four weeks. All patients were evaluated for tumour response using response evaluation criteria in solid tumour (RECIST) criteria, survival analysis using Kaplan-Meier methods, and toxicities according to common terminology criteria for adverse events (CTCAE) version 4.0.

Results. At three months after chemoradiation, 82.2% and 17.8% of patients achieved complete and partial response, respectively. With a median follow-up of 48.1 months (1.3–97.8 months), 9.6% and 17.8% had local recurrence and distant metastasis, respectively. The median survival was not reached. A three-year overall survival was 83.6% and a progression-free survival was 65.3%. Regarding treatment compliance, 97.2%, 68.5% and 69.8% completed radiation treatment, concurrent carboplatin and adjuvant chemotherapy, respectively. Grade 3–4 acute toxicities were oral mucositis (16.4%), dysphagia (16.4%), xerostomia (15.1%) and haematotoxicity (6.8%).

Conclusions. Carboplatin concurrently with IMRT provided excellent tumour response, manageable toxicities and good compliance. This should be considered as an alternative treatment for NPC patients.

Key words: intensity-modulated radiotherapy (IMRT); carboplatin; nasopharyngeal carcinoma

Introduction

Nasopharyngeal carcinoma (NPC) is one of the most common head and neck neoplasms among Asian people. The overall incidence of NPC in Southeast Asia is 6.5 and 2.6 per 100,000 person-years in males and females, respectively.[1] In Thailand, the age-standardized incidence rates of NPC are approximately 3.7 and 1.2 per 100,000 in males and females, respectively.[2]

Meta-analysis showed that chemotherapy plays an important role in the treatment of this disease.[3] Al Saraff *et al*. (Intergroup 0099) demonstrated significant benefits of additional cisplatin in terms of both disease free survival and overall survival, when used concurrently with radiation followed by a combination of cisplatin and 5-fluorouracil chemotherapy for three cycles.[4] Thus, this regimen has become standard of care for nasopharyngeal carcinoma despite the low compliance rate (55–63%) in this trial. Significant side effects of cisplatin include nausea and vomiting, renal, neurological and ototoxicity. Additionally, during high-dose cisplatin administration, adequate hydration and volume monitoring are needed and require hospital admission. Recently, Chan *et al*. proposed

a low-dose weekly cisplatin that could be administered in an outpatient setting and provides good patient compliance.[5]

Based on similar radiosensitizing properties of carboplatin and cisplatin along with pre-clinical data that demonstrated an enhanced radiation effect from concurrent carboplatin in tumour cells, some physicians use carboplatin as an alternative regimen to avoid serious cisplatin toxicities, especially renal, gastrointestinal and neurotoxicity.[6-10]

Many studies have shown comparable response rates and survival outcomes with acceptable toxicities and better compliance from carboplatin.[11-14] However, the radiation technique in those studies was the conventional technique. More recently, intensity-modulated radiotherapy (IMRT) has been proven in NPC treatment for its efficacy and its advantages over conventional techniques and has been considered as a standard radiation technique for NPC.[15-17]

The objectives of this study are to evaluate efficacy and toxicities using IMRT concurrently with carboplatin, followed by adjuvant carboplatin and 5-fluorouracil (5-FU) chemotherapy for the treatment of NPC.

Patients and methods

Patients and methods

Between October 2005 and November 2011, newly diagnosed NPC patients were accrued for this prospective phase II study after obtaining the institutional review board approval (RA 13/49). The eligibility criteria included those aged 18 years old and above; histologically confirmed non-metastatic nasopharyngeal carcinoma stage II–IVB according to the 7th edition of the American Joint Committee on Cancer Staging System (AJCC 2010); Eastern Cooperative Oncology Group (ECOG) performance status 0–2; adequate hematologic and renal function, defined by with blood cells (WBC) ≥ 4,000/mL, platelet count ≥ 100,000/mL, serum creatinine ≤ 1.5 mg/dL or calculated creatinine clearance ≥ 60 ml/min. Patients with distant metastasis; previous radiation and/or chemotherapy treatment less than six months prior to the study entry; other malignancy except non-melanoma skin cancer or a carcinoma of non-head and neck origin, controlled for at least five years; active infection; major medical or psychiatric condition or pregnancy were excluded.

All eligible patients received a pre-treatment evaluation including complete history and physical examination, endoscopic biopsy, routine laboratory tests for hematologic, renal and hepatic function as well as a dental and nutritional evaluation before the treatment. Radiological investigations consisted of computed tomography (CT) scan or magnetic resonance imaging (MRI) of the nasopharynx, chest radiography, ultrasound of upper abdomen and bone scintigraphy. Positron emission tomography (PET) scan was optional. A pathologic confirmation of NPC was performed and re-classified according to WHO subtype.[18]

Treatment protocol

Each patient underwent contrast-enhanced CT simulation with a long thermoplastic mask. The GTVs and CTVs were contoured according to RTOG guidelines. There were two planning target volumes (PTVs): PTV-high risk (PTV-HR), defined as primary tumour and gross lymphadenopathy with appropriate margin, and PTV-low risk (PTV-LR), defined as PTV-HR plus elective lymph node region. The prescription dose was 50 Gy in 25 fractions to PTV-LR followed by a boost of 20 Gy in 10 fractions, called sequential IMRT (SEQ). Recently, a simultaneous integrated boost (SIB) technique was developed and applied in last few patients with total dose of 70 Gy and 56 Gy in 33 fractions for PTV-HR and PTV-LR, respectively. Normal tissue constraints were used according to our institutional protocol (adopted from RTOG 0225 and 0615 study protocols) and are described in Table 1.

All patients received IMRT concurrently with three cycles of carboplatin (AUC 5) every three weeks, followed by three cycles of adjuvant carboplatin (AUC 5) and 5-FU (1,000 mg/m^2 /day for four days) every four weeks.

During the concurrent and the adjuvant treatment, patients were assessed weekly. Dose modification and proper management were performed according to patients' toxicity grading. The response of the primary tumour and lymph node was evaluated at three months after the last fraction of radiotherapy by endoscopic examination and CT scan. Other imaging was performed if indicated.

Statistical analysis

Data collection consisted of patient characteristics including age, sex and ECOG performance status; disease characteristics including pathologic WHO subtype and TNM staging; and treatment modalities including radiation treatment technique, radiation dose, duration of radiation treatment as well as compliance with radiation and chemotherapy.

TABLE 1. Dose volume constraints of normal tissue

Organ at risk	Maximum dose (Gy)	Dose volume constraints	
		Dose (Gy)	Maximum volume
Spinal cord	50	45	1 cc
Brain stem	60	54	1 cc
One parotid gland		26	50%
Optic nerve	54		
Cochlear		46	50%
Eyes	24		50%
Lens	6		
Mandible	70	53	50%
Oral cavity	60	40	50%
Vocal cord	58	45	50%

Maximum dose (Dmax) defined as radiation dose encompasses 1% of each organ-at-risk volume

All patients were evaluated for tumour response using response evaluation criteria in solid tumour (RECIST) criteria, survival outcomes using Kaplan-Meier methods, and acute and late toxicities according to common terminology criteria for adverse events (CTCAE) version 4.0.

Primary endpoints were progression-free survival (PFS) and overall survival (OS). PFS was defined as the time period since the initial treatment of NPC until disease recurrence or progression or death. OS was defined as the time period between the initial treatment of NPC and any cause of death. Survival analyses were computed using the Kaplan-Meier method and log-rank test. P-value of 0.05 or less was applied to define significance. Statistical Packages for Social Sciences (SPSS) software version 17.0 was used for the statistical analysis. Secondary endpoints were disease control and treatment-related toxicities.

The sample size calculation was based on the proportion of expected death (mortality rate) with 95% confidence interval. We employed 18.1% mortality rate for concurrent radiation with carboplatin according to the results of a randomized study of Chitapanarux *et al*.[13] Allowing 20% dropout p-value of 0.05, 69 participants were planned to be enrolled in the study.

Results

Patient and disease characteristics

A total of 73 patients diagnosed with NPC and treated between October 2005 and November 2011 were accrued. Patient and disease characteristics are listed in Table 2. The mean age was 54.4 years (range 24–76 years). The majority of patients (67.1%) were males. All were in good performance status and had non-serious comorbidities. The histological subtype, according to WHO classification, was non-keratinizing squamous cell carcinoma (NK-SCCA) in every patient, which could be further identified as undifferentiated NK-SCCA in most patients (83.6%). Approximately half of patients had stage III disease.

TABLE 2. Patients and disease characteristics

	N (73)	%
Age, years		
Mean (range)	54.4 (24–76)	
Sex		
Male	49	67.1%
Female	24	32.9%
Performance status		
ECOG 0	67	91.8%
ECOG 1	6	8.2%
WHO classification		
Type II (Non-keratinizing SCCA)	73	100.0%
T stage		
1	15	20.6%
2	26	35.6%
3	23	31.5%
4	9	12.3%
N stage		
0	5	6.8%
1	19	26.0%
2	41	56.2%
3a	5	6.9%
3b	3	4.1%
M stage		
0	73	100.0%
Stage grouping		
II	16	22.0%
III	42	57.5%
IV A	12	16.4%
IV B	3	4.1%

SCCA = Squamous cell carcinoma

Radiation treatment

Whole-neck IMRT was planned using the Eclipse treatment planning system. The majority of patients (91.8%) was treated with the SEQ-IMRT technique. The rest were treated with the SIB-IMRT technique. Seventy-two patients (98.6%) completed a course of radiation. One patient could not complete the course of radiation and the treatment interruption of 38 days occurred in another patient; both resulted from intolerable toxicity. The average PTV-HR and PTV-LR dose were 69.95 Gy (range 58–76 Gy) and 50.82 Gy (range 42–62 Gy), respectively. The median duration of the radiation treatment was 55 days (range 14–93 days).

Chemotherapy

Seventy-two patients (98.6%) received concurrent carboplatin and radiation; 50 patients (68.5%) received all three cycles of chemotherapy as planned. The compliance of chemotherapy treatment is detailed in Table 3.

Clinical outcome

The median follow-up time was 48.1 months (6.1–97.8 months). At three months after completion of radiotherapy, a complete response (CR) was achieved in 60 patients (82.2%) while 13 patients (17.8%) achieved a partial response (PR). Regarding the site of the tumour response, 94.5% of patients achieved CR at the primary (nasopharyngeal) site while 83.6% achieved CR at regional lymph node sites. Patients who achieved PR received a further treatment: a radiotherapy boost of 30 Gy in 10 fractions to any residual disease at the primary site. Patients with small residual lymph node(s) had a radiation boost of 15 Gy in 5 fractions while those with a larger residual disease in the neck underwent a salvage neck dissection. No additional systemic therapy was given after the patients completed three chemotherapy cycles.

During the follow-up period, seven patients (9.6%) and 13 patients (17.8%) experienced local and distant failure, respectively. None of the patients had regional recurrence or both, local/regional and distant failure. The median time to local and distant recurrence was 20.3 months and 22.2 months, respectively. The most common sites of metastasis were bone (8.2%), liver (6.8%) and lung (4.1%).

At the last follow-up, 45 patients (61.6%) were alive without disease while eight patients (10.9%) had disease recurrence. There were 20 deaths (27.4%); 14 patients died from the progression of the disease.

TABLE 3. Compliance of chemotherapy treatment

Number of cycles	N (%)	
	Concurrent carboplatin	Adjuvant carboplatin/5-FU
0	1 (1.4%)	4 (5.5%)
1	2 (2.7%)	8 (11%)
2	20 (27.4%)	10 (13.7%)
3	50 (68.5%)	51 (69.8%)
Total	73 (100%)	73 (100%)

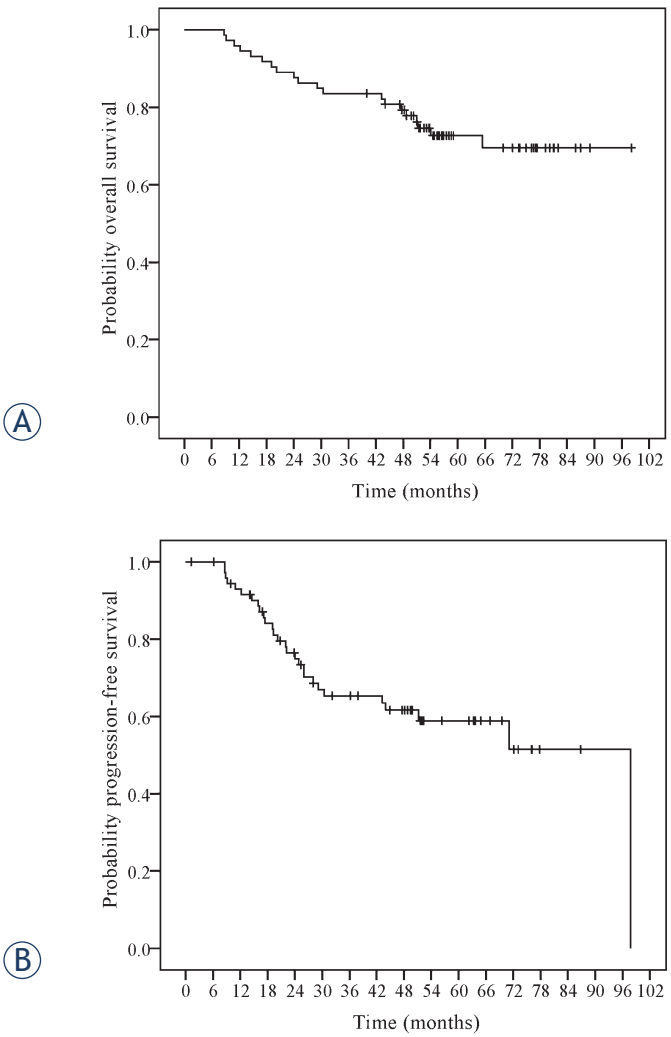

FIGURE 1. Overall and progression-free survival of patients with nasopharyngeal carcinoma treated with intensity-modulated radiotherapy and concurrent carboplatin.

Survival outcome

Median OS was not reached. Median PFS was 71 months. Three-year OS and PFS were 83.6% and 65.3%, respectively and at 5 years they were 72.7% and 58.9%, respectively, as shown in Figure 1.

Toxicities

The toxicities were classified as acute and late toxicities using a 90-day cut-off point after the completion of chemoradiation. Acute toxicity consisted of symptoms developing during the concurrent and the adjuvant treatment. During concurrent chemoradiation, all patients experienced some degrees of acute toxicities, most of which were mild (grade 1–2). The most common grade 3–4 toxicities were

mucositis (16.4%), dysphagia (16.4%) and xerostomia (15.1%). Only two patients (2.7%) had severe nausea and vomiting. Twelve patients (16.4%) needed nasogastric tube insertion. Weight loss of more than 20% (grade 3) occurred in 5 patients (6.8%) during concurrent chemoradiation and in 24 patients (32.9%) during the adjuvant period. During adjuvant chemotherapy, most patients recovered from mucositis, xerostomia and dysphagia. Grade 3 or more hematologic toxicities developed in 6 patients (8.2%). Three (4.1%) and two patients (2.7%) developed grade 3–4 neutropenia and thrombocytopenia, respectively. A renal function impairment was not found. No patient developed grade 5 toxicity during the concurrent and the adjuvant treatment. The incidence of acute toxicities is described in Table 4.

Eighteen patients (28.6%) had grade 3 weight loss at one year after chemoradiation. Most patients regained their weight within two years. Grade 2 xerostomia was found in 10 patients (13.7%) and three patients (4.1%) at 6-month and 12-month follow-up, while no patient had grade 2 xerostomia at the 24-month point. None of the patients experienced grade 3–4 gastrointestinal and dermatologic toxicities during follow-up. There was no renal toxicity among these patients.

TABLE 4. Acute toxicity during treatment

Toxicities	Acute toxicity During chemoradiation		Acute toxicity During adjuvant period	
	0–2	3–5	0–2	3–5
Constitutional symptoms				
Fatigue	72 (98.6%)	1(1.4%)	71(97.3%)	2(2.7%)
Anorexia	71(97.3%)	2(2.7%)	73(100%)	0
Weight loss	68(93.2%)	5(6.8%)	49(67.1%)	24(32.9%)
Gastrointestinal				
Oral mucositis	61(83.6%)	12(16.4%)	73(100%)	0
Xerostomia	62(84.9%)	11(15.1%)	73(100%)	0
Dysphagia	61(83.6%)	12(16.4%)	73(100%)	0
Nausea	71(97.3%)	2(2.7%)	73(100%)	0
Vomiting	71(97.3%)	2(2.7%)	73(100%)	0
Diarrhea	73(100%)	0	73(100%)	0
Dermatitis	73(100%)	0	73(100%)	0
Hematologic				
Anaemia	73(100%)	0	72(98.6%)	1(1.4%)
Neutropenia	68(93.2%)	5(6.8%)	70(95.9%)	3(4.1%)
Thrombocytopenia	72(98.6%)	1(1.4%)	71(97.3%)	2(2.7%)
Creatinine	73(100%)	0	73(100%)	0
Total	73(100%)	0	73(100%)	0

Discussion

Nasopharyngeal carcinoma is one of the most common head and neck cancer in Southeast Asia and has a different natural history and prognosis from other cancers in this region. The current standard treatment of locally advanced NPC is concurrent chemoradiation followed by adjuvant chemotherapy.[3-5] According to a meta-analysis from eight trials involving 1,753 patients, chemotherapy resulted in an absolute survival benefit of 6% (from 56% to 62%) and an event-free survival benefit of 10% (from 42% to 52%) at five years. This study also concluded that the concurrent trials showed significant survival benefit with hazard ratio (HR) of 0.60 (95% CI, 0.48–0.76).[3] Another meta-analysis from 10 randomized clinical studies with a total of 2,450 patients supported that concurrent chemoradiation improved survival by 20% at five years with a pooled HR of 0.48 (95% CI, 0.32–0.72).[19] The landmark study by Al Saraff *et al.* (INT 0099)[4] supported the standard treatment of nasopharyngeal carcinoma using concurrent radiation with cisplatin followed by cisplatin and 5FU with 5-year OS and DFS of 67% and 58%, respectively. Although cisplatin is a widely accepted regimen, its toxicity, including nausea, vomiting, ototoxicity, neurotoxicity and nephrotoxicity, may lead to poor compliance; only 63% and 55% of patients completed concurrent and adjuvant chemotherapy in INT 0099.[4]

Carboplatin has come into interest due to its lesser side effects, especially gastrointestinal and nephrogenic side effects. The advantages of carboplatin are tolerable toxicity leading to better compliance and its capability of out-patient administration, thus reducing hospitalization, cost of the treatment and workload of medical personnel. Eisenberger indicated that 100 mg/m^2/week of carboplatin was well tolerated when given concurrently with radiation in locally advanced head and neck cancers.[20] Unfortunately for NPC, a prospective phase I/II study from Canada of concurrent carboplatin in 47 patients reported probably inferior OS and PFS with acceptable toxicity compared to INT 0099. With the median follow-up of 23.1 months, 3-year OS and PFS were 56% and 58%, respectively.[11] Nevertheless, different WHO histological subtypes may result in different natural history of disease and response between Caucasian and Asian people. The randomized controlled trial from Thailand, comparing carboplatin-based chemotherapy with an INT 0099 regimen in 220 patients demonstrated a non-inferior survival outcome. Three-year OS and DFS in the carboplatin arm were 79.2% and 60.9% compared with 77.7% and 63.4% in the cisplatin arm. They also showed better compliance to treatment in carboplatin arm, 73% versus 59%.[13] Another report from Thailand

TABLE 5. Comparison of treatment schedule, compliance and outcome between studies on concurrent chemoradiation with carboplatin in NPC patients and INT 0099 trial; and RTOG 0225 using IMRT technique

Study		N	Stage	F/U	RT	CMT		Compliance CMT		DFS / PFS	OS
						Concurrent	Adjuvant	Concurrent	Adjuvant		
INT 0099[4]	RCT	147	III 9% IV 91%	NA	Conventional 66–70 Gy	Cis 100 mg/m^2 q 3 wk x 3 cycles	Cis 80 mg/m^2 +5FU 4000 mg/m^2 q 4 wk x 3 cycles	63%	55%	58%(5Y)	67%(5Y)
Parliament[11]	Prospective phase I/II (AJCC 2002)	47	I/II 10.7% III 14.9% IV 74.5%	23.1 mo	Conventional 70 Gy	Carbo 100mg/m^2 q 1 wk x 6 cycles	-	95.7%	-	58%(3Y)	56%(3Y)
Chitapanarux[13]	RCT (AJCC 1997)	206	III 36% IVA 25% IVB 40%	26.3 mo	Conventional 70 Gy	Cis 100 mg/m^2 q 3 wk x 3 cycles	Cis 80 mg/m^2 +5FU 4000 mg/m^2 q 4 wk x 3 cycles	59%	42%	63.4%(3Y)	77.7%(3Y)
			III 31% IVA 23% IVB 46%			Carbo 100mg/m^2 q 1 wk x 6 cycles	Carbo AUC 5 +5FU 4000 mg/m^2 q 4 wk x 3 cycles	77%	72%	60.9%(3Y)	79.2%(3Y)
Dechaphunkul[14]	Prospective (AJCC 2002)	50	IIB 8% III 36% IVA 38% IVB 18%	37.3 mo	Conventional 66–70 Gy	Carbo AUC 6 q 3 wk x 3 cycles	Carbo AUC 5 +5FU 4000 mg/m^2 q 3 wk x 2 cycles	98% (total 5 cycles)		89.7%(3Y)	72.7%(3Y)
RTOG 0225[21]	Prospective Phase II (AJCC 1997)	68	I 13.2% IIA 2.9% IIB 25.0% III 30.9% IVA 16.2% IVB 11.8%	31.2 mo	IMRT 70 Gy	Cis 100 mg/m^2 q 3 wk x 3 cycles	Cis 80 mg/m^2 +5FU 4000 mg/m^2 q 4 wk x 3 cycles	87%	45.6%	72.7% (2Y)	80.2% (2Y)
MSKCC[22]	Prospective Phase II (AJCC 1997)	74	I 7% IIB 16% III 30% IVA/B 47%	35 mo	IMRT 70 Gy (AF and SIB)	Cis 100 mg/m^2 q 3 wk x 2 cycles	Cis 80 mg/m^2 +5FU 4000 mg/m^2 q 4 wk x 3 cycles	92%	NA	67% (3Y)	83% (3Y)
This study	Prospective Phase II (AJCC 2010)	73	II 22.0% III 57.5% IVA 16.4% IVB 4.1%	48.1 mo	IMRT 70 Gy (Seq and SIB)	Carbo AUC 5 q 3 wk x 3 cycles	Carbo AUC 5 +5FU 4000 mg/m^2 q 4 wk x 3 cycles	68.5%	69.8%	Median=71m 65.3% (3Y) 58.9% (5Y)	MS=not reached 83.6% (3Y) 72.7% (5Y)

AF = Accelerated fractionation (here, hyperfractionated concomitant boost); AJCC = American Joint Committee on Cancer Staging; Carbo = Carboplatin; Cis = Cisplatin; CMT = Chemotherapy; DFS = Disease-free survival; F/U = Follow-up time; 5FU = 5-fluorouracil; mo = months; NA = Not available; OS = Overall survival; PFS = Progression-free survival; RCT = randomized-controlled trial; RT = Radiation treatment; SIB = simultaneous integrated boost; wk = week

that included 50 patients using concurrent chemoradiation with carboplatin followed by carboplatin and 5FU in NPC showed good results and tolerability. The 3-year OS and PFS were 72.7% and 89.7%, respectively.[14]

Although the efficacy of concurrent carboplatin with radiation in NPC was demonstrated, these studies used a conventional radiation technique[11,13,14] whereas in current practice, the standard radiation technique for NPC is IMRT, which has demonstrated significantly better salivary flow rate and quality of life in NPC patients compared with conventional techniques.[15-17] Additionally, the recent RTOG phase II trial 0225 and a prospective study from Memorial Sloan Kettering Cancer Center (MSKCC) reported promising results of tumour control and toxicities by using IMRT and concurrent cisplatin.[21,22] In RTOG 0225 with 68 patients, 2-year OS and PFS were 80.2% and 72.7%, respectively. In the MSKCC study with 74 patients, 3-year OS and PFS were 83% and 67%, respectively. In this study, using concurrent carboplatin with IMRT, our 3-year OS and PFS were 83.6% and 65.3%, which were comparable with those previous studies. Moreover, approximately 70% of patients completed three cycles of adjuvant chemotherapy.

Distant metastasis is the major reason of failure in nasopharyngeal carcinoma. The rate of distant metastasis reported in many series was 14.7%–22% in cisplatin-based chemotherapy series compared with 14.3%–29.8% in carboplatin-based series.[4,11-14,18,21,22] In our study, the crude distant metastasis rate was 17.8%, which was comparable with the results from studies using either of the two chemotherapy regimens. The most common sites of metastasis were bone (8.2%), liver (6.8%) and lung (4.1%), giving the 3- and 5-year distant

metastasis-free survival (DMFS) of 82% and 77.1%, respectively.

With regards to toxicity, because different criteria were used for evaluation, comparing the toxicity among several published trials including our study might not be appropriate. Compared with RTOG 0225, which used similar toxicity evaluation criteria, Common Terminology Criteria for Adverse Events (CTCAE), overall acute grade 3 toxicity was 61.8%[21], while it was 24.7% in our study. Acute grade 3 mucositis, defined as confluent pseudomembranous reaction (contiguous patches generally > 1.5 cm in diameter) in CTCAE version 2.0 and as severe pain or interference with oral intake in CTCAE version 4.03, was 29.4% in the RTOG study compared to 16.4% in our study. There was no patient who experienced acute grade 5 mucositis in this trial but one patient (1.3%) did in the RTOG study. According to Dechapunkul, using conventional radiation and RTOG acute toxicity criteria in which grade 3 mucositis was defined as confluent fibrinous mucositis or severe pain requiring narcotics, grade 3–4 mucositis was reported in 42% of total 50 patients.[14] In contrast, in the Chitapanarux study, using conventional radiation technique and RTOG acute toxicity criteria, the rate of mucous membrane toxicity was very low: 0% in the cisplatin arm and 5% in the carboplatin arm. However, the rate of nasogastric tube insertion was as high as 48% and 22% in the cisplatin and carboplatin arm, respectively, compared with 16.4% in our study.

Grade 3 or higher nausea and vomiting rates during chemoradiation in our study were comparable to those of carboplatin studies and was less than cisplatin studies, for example, 2.7% in our study, 0% in Chitapanarux study, 8% in Dechapunkul study versus 19.2% in INT 0099 study.

The rate of grade 3 dermatitis, which was defined as confluent moist desquamation ≥ 1.5 cm diameter and not confined to skin folds or pitting oedema in CTCAE version 2.0 and RTOG toxicity criteria and as moist desquamation other than skin folds and creases or bleeding induced by minor trauma or abrasion in CTCAE 4.03, was 13.2% in the RTOG 0225 study, 3% and 6% in the cisplatin and carboplatin arm in the Chitapanarux study, and none in our study.

Late grade 2 xerostomia at 12-month period in our study was 4.1% compared with 13.5% reported in RTOG 0225 and 24% in the Chitapanarux study.

The treatment schedule, compliance and outcome in each study are demonstrated in Table 5.

One of the major concerns of carboplatin administration is hematologic toxicity. In our study, 8.2% experienced grade 3–4 hematologic toxicity, mainly neutropenia (6.8%) and thrombocytopenia (1.4%), which was comparable to the Chitapanarux study in which 10% and 2% of patients experienced grade 3 neutropenia and thrombocytopenia in the carboplatin arm.

This is the first study to our knowledge that demonstrated the efficacy and feasibility of carboplatin concurrently with IMRT in NPC and that this treatment can be applied as an alternative chemotherapy regimen, especially in vulnerable patients or those not suitable for standard cisplatin regimen.

Conclusions

Carboplatin concurrently with IMRT provided excellent tumour response, manageable toxicities and good compliance. This should be considered as alternative to standard treatment with cisplatin for NPC patients.

References

1. International Agency for Research on Cancer, World Health Organisation, International Association of Cancer Registries. Nasopharyngeal carcinoma. In: Curado MP, Edwards B, Shin HR, Storm H, Ferlay J, Heanue M, et al, editors. *Cancer in five continents, vol IX. IARC Scientific Publication No. 160.* Lyon: IARC; 2007.
2. Nasopharyngeal carcinoma. In: Khuhaprema T, Srivatanakul P, Attsara A, Sriplung H, Wiangnon H, Sumitsawan Y, editors. *Cancer in Thailand.* Bangkok: Ministry of health; 2010. p. 16-17.
3. Baujet B, Audry H, Bourhis J, Chan AT, Onat H, Chua DT, et al. Chemotherapy in locally advanced nasopharyngeal carcinoma: an individual patient data meta-analysis of eight randomized trials and 1753 patients. *Int J Radiat Oncol Biol Pys* 2006; **64:** 47-56.
4. Al-Sarraf M, LeBlanc M, Giri PG, Fu KK, Cooper J, Vuong T, et al. Chemoradiotherapy versus radiotherapy in patients with advanced nasopharygeal cancer: Phase III randomized Intergroup study 0099. *J Clin Oncol* 1998; **16:** 1310-7.
5. Chan AT, Leung SF, Ngan RK, Teo PM, Lau WH, Kwan WH, et al. Overall survival after concurrent cisplatin-radiotherapy compared with radiotherapy alone in locoregionally advanced nasopharyngeal carcinoma. *J Natl Cancer Inst* 2005; **97:** 536-9.
6. Douple EB, Richmond RC, O'Hara JA, Coughlin CT. Carboplatin as a potentiator of radiation therapy. *Cancer Treat Rev* 1985; **12(Suppl A):** 111-24.
7. Coughlin CT, Richmond RC. Biologic and clinical developments of cisplatin combined with radiation: Concepts, utility, projections for new trials, and the emergence of carboplatin. *Semin Oncol* 1989; **16:** 31-43.
8. Calais G1, Alfonsi M, Bardet E, Sire C, Germain T, Bergerot P, et al. Randomized trial of radiation therapy versus concomitant chemotherapy and radiation therapy for advanced-stage oropharynx carcinoma. *J Natl Cancer Inst* 1999; **91:** 2081-6.
9. Calais G, Le Floch O. Concomitant radiotherapy and chemotherapy in the treatment of cancer of the upper respiratory and digestive tracts. *Bull Cancer Radiother* 1996; **83:** 321-9.

10. Muggia FM. Overview of carboplatin: Replacing complementing and extending the therapeutic horizons of cisplatin. *Semin Oncol* 1989; **16(Suppl 5):** 7-13.

11. Paliament M, Jha N, Rapp E, Smith C, MacKinnon J, Nabholtz JM, et al. Concurrent weekly carboplatin and radiotherapy for nasopharyngeal carcinoma: report of a joint phase II study. *Radiother Oncol* 2001; **58:** 131-6.

12. Okita J, Hatta C, Terada T, Saeki N, Ogasawara H, Kakibuchi M, et al. Concurrent chemo-radiotherapy for nasopharyngeal carcinoma. *Auris Nasus Larynx* 2004; **31:** 43-7.

13. Chitapanarux I, Lorvidhaya V, Kamnerdsupaphon P, Sumitsawan Y, Tharavichitkul E, Sukthomya V, et al. Chemoradiation comparing cisplatin versus carboplatin in locally advanced nasopharyngeal cancer: Randomised, non-inferiority, open trial. *Euro J of Cancer* 2007; **43:** 1399-406.

14. Dechaphunkul T, Pruegsanusak K, Sangthawan D, Sanpaeravong P. Concurrent chemoradiotherapy with carboplatin followed by carboplatin and 5- fluorouracil in locally advanced nasopharyngeal carcinoma. *Head Neck Oncol* 2011; **3:** 30.

15. Pow EH, Kwong DL, McMillan AS, Wong MC, Sham JS, Leung LH, et al. Xerostomia and quality of life after intensity-modulated radiotherapy vs conventional radiotherapy for early-stage nasopharyngeal carcinoma: initial report on a randomized controlled clinical trial. *Int Radiat Oncol Biol Phys* 2006; **66:** 981-91.

16. Kam MK, Leung SF, Zee B, Chau RM, Suen JJ, Mo F, et al. Prospective randomized study of intensity- modulated radiotherapy on salivary gland function in early-stage nasopharyngeal carcinoma patients. *J Clin Oncol* 2007; **25:** 4873-9.

17. Peng G, Wang T, Yank KY, Zhang S, Zhang T, Li Q, et al. A prospective, randomized study comparing outcomes and toxicities of intensity-modulated radiotherapy vs. conventional two-dimensional radiotherapy for the treatment of nasopharyngeal carcinoma. *Radiother Oncol* 2012; **104:** 286-93.

18. Chan J, Bray F, McCarron P, Foo W, Lee AWM, Yip T, et al. Nasopharyngeal carcinoma. In: Barnes EL, Eveson JW, Reichart P, Sidransky D, editors. *Pathology and genetics of head and neck tumor. World Health Organization classification of tumours.* Lyon: IARC Press; 2005. p. 85.

19. Langendijk JA, Leemans CR, Buter J, Berkhof J, Slotman BJ. The additional value of chemotherapy to radiotherapy in locally advanced nasopharyngeal carcinoma: a meta-analysis of the published literature. *J Clin Oncol* 2004; **22:** 4604-12.

20. Eisenberger M, Jacobs M. Simultaneous treatment with single-agent chemotherapy and radiation for locally advanced cancer of head and neck. *Semin Oncol* 1992; **4(Suppl11):** 41-6.

21. Lee N1, Harris J, Garden AS, Straube W, Glisson B, Xia P, et al. Intensity-modulated radiation therapy with or without chemotherapy for nasopharyngeal carcinoma: radiation therapy oncology group phase II trial 0225. *J Clin Oncol* 2009; **27:** 3684-90.

22. Wolden SL, Chen WC, Pfister DG, Kraus DS, Berry SL, Zelefsky MJ. Intensity-modulated radiation therapy (IMRT) for nasopharyngeal cancer. Update of the Memorial Sloan-Kettering experience. *Int J Radiat Oncol Biol Phys* 2006; **64:** 57-62.

research article

Preoperative treatment with radiochemotherapy for locally advanced gastroesophageal junction cancer and unresectable locally advanced gastric cancer

Ivica Ratosa, Irena Oblak, Franc Anderluh, Vaneja Velenik, Jasna But-Hadzic, Ajra Secerov Ermenc, Ana Jeromen

Department of Radiotherapy, Institute of Oncology Ljubljana, Ljubljana, Slovenia

Radiol Oncol 2015; 49(2): 163-172.

Received: 14 April, 2014
Accepted: 19 May, 2014

Correspondence to: Assist. Prof. Irena Oblak, M.D., Ph.D., Institute of Oncology Ljubljana, Zaloška c. 2, SI-1000 Ljubljana, Slovenia. Phone: +386 1 5879 661; Fax: +386 1 5879 304; E-mail: ioblak@onko-i.si

Disclosure: No potential conflicts of interest were disclosed.

Background. To purpose of the study was to analyze the results of preoperative radiochemotherapy in patients with unresectable gastric or locoregionally advanced gastroesophageal junction (GEJ) cancer treated at a single institution.

Patients and methods. Between 1/2004 and 6/2012, 90 patients with locoregionally advanced GEJ or unresectable gastric cancer were treated with preoperative radiochemotherapy at the Institute of Oncology Ljubljana. Planned treatment schedule consisted of induction chemotherapy with 5-fluorouracil and cisplatin, followed by concomitant radiochemotherapy four weeks later. Three-dimensional conformal external beam radiotherapy was delivered by dual energy (6 and 15 MV) linear accelerator in 25 daily fractions of 1.8 Gy in 5 weeks with two additional cycles of chemotherapy repeated every 28 days. Surgery was performed 4–6 weeks after completing radiochemotherapy. Following the surgery, multidisciplinary advisory team reassessed patients for the need of adjuvant chemotherapy. The primary endpoints were histopathological R0 resection rate and pathological response rate. The secondary endpoints were toxicity of preoperative radiochemotherapy and survival.

Results. Treatment with preoperative radiochemotherapy was completed according to the protocol in 84 of 90 patients (93.3%). Twenty patients (22.2%) did not undergo the surgery because of the disease progression, serious co-morbidity, poor performance status or still unresectable tumour. In 13 patients (14.4%) only exploration was performed because the tumour was assessed as unresectable or diffuse peritoneal carcinomatosis was established. Fifty-seven patients (63.4%) underwent surgery with the aim of complete removal of the tumour. Radical resection was achieved in 50 (55.6%) patients and the remaining seven (7.8%) patients underwent non-radical surgery (R1 in five and R2 in two patients). In this group of patients (n = 57), pathological complete response of tumour was achieved in five patients (5.6% of all treated patients or 8.8% of all operated patients). Down-staging was recorded in 49 patients (86%), in one patient (1.8%) the stage after radiochemotherapy was unchanged while in seven patients (12.3%) the pathological stage was higher than clinical, mainly due to higher pN stage. No death was recorded during preoperative radiochemotherapy. Most grade 3 and 4 toxicities were due to vomiting, nausea and bone marrow suppression (granulocytopenia). Twenty-six (45.6%) patients died due to GEJ or gastric carcinoma, one died because of septic shock following the surgery and a reason for two deaths was unknown. Twenty-eight patients (49.1%) were disease free at the time of analysis, while 29 patients (50.9%) developed the recurrence, mostly as distant metastases. At two years, locoregional control, disease-free survival, disease-specific survival and overall survival were 82.9%, 43.9%, 56.9% and 53.9%, respectively.

Conclusions. Preoperative radiochemotherapy was feasible in our group of patients and had acceptable toxicity. Majority of patients achieved down-staging, allowing greater proportion of radical resections (R0), which are essential for patients' cure.

Key words: unresectable gastric cancer; gastroesophageal junction cancer; preoperative radiochemotherapy; surgery; toxicity

Introduction

Gastric and gastroesophageal junction (GEJ) cancer are two groups of tumours with different pathogenesis, epidemiology and clinicopathological characteristics.[1,2] In the past years changes in classification based mainly on anatomical localization of the tumour were made, and today GEJ cancer that arises within first 5 cm of the stomach and also extends to the oesophagus, is classified as oesophageal cancer (Siewert type I, II or III).[3] Not all of the authors agree with new staging principles, as new classification does not represent the molecular origin of carcinoma. An appropriate interpretation of results from past therapeutic trials also became difficult, as GEJ carcinomas were formerly classified and treated as gastric carcinomas.[4-6]

Surgery is without doubt the main part of curative treatment of primarily advanced (≥ cT3N+) gastric and GEJ cancer. The best surgical approach for both groups is still a subject of a debate, especially regarding the extension of lymphadenectomy. Panel of experts agree that gastrectomy with D2 lymph node dissection (without resection of the pancreatic tail and without routine splenectomy) is advised as the standard approach in Europe and Asia for gastric and Siewert type III GEJ cancers, while Siewert type I and II should be treated by oesophagectomy (or by extended transhiatal gastrectomy for type II tumours, if needed) with dissection of mediastinal lymph nodes.

Although surgical techniques have been improved, local recurrence rate after complete resection of gastric and GEJ adenocarcinoma is still high.[7-9] Suboptimal surgery and high rates of distant metastases - especially to liver, bone, brain and lung - have led to search for additional therapeutic approaches. The results of INT-0116 and MAGIC trials suggest a survival benefit of postoperative radiochemotherapy or perioperative chemotherapy and subsequently they were accepted as standards of care.[10,11]

Recent evidence shows an important role of radiotherapy in addition to preoperative chemotherapy regimens in GEJ and in gastric cancers as well as in others gastrointestinal cancers.[12] According to the results of the CROSS trial, in which 368 patients with T1N1 or T2-3N0-1 tumours without clinical evidence of metastatic spread (M0) were included, preoperative radiochemotherapy followed by surgery significantly improves disease-free survival (DFS) and overall survival (OS) as compared with surgery alone in patients with distant oesophageal or GEJ squamous-cell carcinoma, adenocarcinoma, or large-cell undifferentiated carcinoma. A pathological complete response (pCR) and radical resection (R0) was achieved in 29% and 92% of patients who underwent resection after radiochemotherapy, compared to the 69% of R0 resections in the group where the patients were treated with surgery only.[13] In ACCORD07 phase III trial patients treated with preoperative chemotherapy had better survival compared to the patients treated with surgery alone (5-year OS 38% vs. 24%). Survival rates from CROSS trial where preoperative radiochemotherapy was used seem to be superior then in ACCORD07 trial where preoperative chemotherapy was used (5-year OS 47% vs. 34% in control arm).[14] Results, published by Stahl *et al*., also pointed to a survival advantage for preoperative radiochemotherapy compared with preoperative chemotherapy in GEJ carcinomas (3-year OS rate 47.4% and 27.7%, respectively). The patients treated with preoperative radiochemotherapy also had lower rate of non-radical resections (4.1% and 14.4%, respectively) and higher rate of pCRs (15.6% and 2%, respectively). Another interesting observation in that study is that the patients who achieved pCR had 100% 3-year OS rate, whereas in other patients the 3-year OS was 47.4%.[15]

In gastric cancer, data demonstrating survival benefits of preoperative radiochemotherapy are less clear. Only several retrospective or prospective, randomized or non-randomized trials (in general with small number of included patients), investigating the role of preoperative radiochemotherapy for gastric cancer have been published. Rates of R0 resection and pCR in resectable gastric cancer patients were as high as 70–78% and 20–30%, respectively.[16-25] Authors concluded that morbidity and mortality were not significantly higher in preoperative radiochemotherapy treatment.[15,26] Valenti *et al*. randomized 72 patients with operable locally advanced gastric cancer (cT3–4/N+) in two groups. The first group was treated with preoperative chemotherapy, the second one with preoperative radiochemotherapy. They did not find differences in the incidence of complications between groups (30.9% vs. 33.3%, respectively). A major pathological response was detected in 33.3% of patients and it was more frequent in the radiochemotherapy group (47.6% vs. 13.3%, $p = 0.0024$).[26] A randomized phase II/III trial (TOPGEAR) is currently recruiting patients with resectable adenocarcinoma of the stomach or GEJ to answer whether preoperative radiochemotherapy is superior to perioperative chemotherapy alone.[27]

Arguments for using the combination of chemotherapy and radiotherapy have a biological expla-

nation: chemotherapy - by acting cytotoxically - reduces the number of cells in tumours and makes them more susceptible to radiotherapy by inhibiting cellular repair mechanisms. Radiotherapy triggered accelerated repopulation of tumour cells reduced by chemotherapy is another example of cooperation of the two modalities. Tumour shrinkage allows enhanced reoxygenation.[28,29] Intact tumour vasculature in the preoperative setting helps in better chemotherapy delivery. The aim of such treatment is also to eradicate subclinical metastatic disease and to sterilize the surgical fields - potentially reducing the risk of local tumour dissemination at resection.[19,21,30] Preoperative radiotherapy treatment fields can be smaller and the radiation delivery itself more accurate.[21] It seems that preoperative treatment with chemotherapy or radiochemotherapy for locally advanced gastric or GEJ cancer can be performed safely, with high compliance, and acceptable toxicity profiles and low perioperative morbidity and mortality rates.[13,26]

Several authors reported benefits of preoperative radiochemotherapy also in unresectable gastric cancer patients showing that tumour downstaging can be achieved, enabling radical resections, in 25–50% of these patients with consequent benefit on their survival.[31-40]

The purpose of this study was to analyze the effectiveness and safety of preoperative radiochemotherapy in patients with unresectable gastric and locoregionally advanced GEJ adenocarcinoma treated at the Institute of Oncology Ljubljana.

Methods

Patient characteristics

Patients with unresectable gastric or locoregionally advanced GEJ adenocarcinoma treated in Slovenia with preoperative radiochemotherapy between January 2004 and July 2012 were included in this retrospective study. According to surgeon's opinion gastric tumours were estimated as unresectable by endoluminal ultrasound (EUS) and/or computer tomography (CT) imaging, and GEJ tumours were estimated as locoregionally advanced by EUS and/or CT.

Patients were presented to a multidisciplinary advisory team, consisting of a surgeon, radiation oncologist and medical oncologist and were considered for preoperative treatment if the following criteria were met: histologically confirmed unresectable gastric or locoregionally advanced GEJ adenocarcinoma, age greater than 18 years and below 80 years, no prior radiotherapy and/or chemotherapy, a performance status of 2 or lower according to World Health Organization (WHO), adequate function of major organs (including cardiac, bone marrow, renal and hepatic function) and adequate collaboration during treatment. All patients underwent a general clinical examination, blood tests, endoscopy of upper gastrointestinal tract with biopsy of the tumour and EUS and/or radiographic imaging (CT of abdomen and/or thorax) to define the extent of the disease. If there was a suspicion of distant metastases (high level of tumour markers or any suspicious lesion on CT scan), positron emission tomography-computed tomography (PET-CT) was performed.

During therapy the patients were clinically examined and referred to haematology and biochemistry blood tests once a week. The therapy-related local and systemic toxicity was assessed according to the National Cancer Institute Common Toxicity Criteria (NCI-CTC) version 4.0.[41] The performance status of patients was determined and their body weight was measured on a weekly basis. All patients received intensive supportive care, including intensive nutrition support.

For the purpose of this study patients' disease stage was classified using medical records, according to the new, 7th edition of the AJCC cancer-staging manual.[3] Ninety patients with stages IIIA–IV of gastric carcinoma (including Siewert III) and IIB–IV of GEJ adenocarcinoma (Siewert I and II) were included in the study (Table 1).

Treatment

All patients were treated preoperatively at the Institute of Oncology Ljubljana. The treatment schedule consisted of induction chemotherapy (one cycle) with 5-fluorouracil (1000 mg/m^2) in 96 h continuous infusion and cisplatin (75 mg/m^2) in a bolus on day 2, followed by concomitant radiochemotherapy four weeks later. Concomitant radiochemotherapy included two cycles of the same type of chemotherapy repeated every 28 days. Chemotherapy administration required hospitalization for appropriate monitoring, hydration, antiemetic therapy and other supportive treatment that included also nutrition support. In case of severe therapy-related toxicity, irradiation and/or chemotherapy doses were modified and adapted to the patient's physical condition or laboratory tests. When necessary, chemotherapy application was delayed, or radiotherapy was temporarily interrupted or terminated.

Radiotherapy started at the beginning of the second cycle. Three-dimensional conformal radiother-

TABLE 1. Patients and tumour characteristics (n = 90)

Characteristic		No.	%
Gender	Male	24	26.7
	Female	66	73.3
PS (WHO)	0	62	68.9
	1	26	28.9
	2	2	2.2
Weight loss before therapy	Yes	67	74.4
	No	23	25.6
Primary tumour localization	Stomach (including GEJ Siewert III)	55	61.1
	GEJ (Siewert I+II)	35	38.9
Clinical T stage	1	0	0
	2	2	2.2
	3	20	22.2
	4a	35	38.9
	4b	33	36.7
Clinical N stage	0	6	6.7
	1	16	17.8
	2	29	32.2
	3	39	43.3
Clinical M stage	0	86	95.6
	1*	4	4.4
Stage grouping at presentation	IIA	2	2.2
	IIB	5	5.6
	IIIA	12	13.3
	IIIB	11	12.3
	IIIC	56	62.2
	IV	4	4.4

GEJ = gastroesophageal junction; PS = Performance status at presentation according to WHO scoring system; * Clinical M1 stage includes only tumours with local peritoneal carcinomatosis

TABLE 2. Surgery characteristics

Surgery		No. of patients	%
No surgery		20	22.2
Only exploratory operation		13	14.4
Subtotal gastrectomy		15	16.7
Total gastrectomy		32	35.6
Multivisceral resection		7	7.8
Transthoracic oesophagectomy		3	3.3
Type of resection	R0	50	55.6
	R1	5	5.6
	R2	2	2.2

apy was delivered by dual energy (6 and 15 MV) linear accelerator in 25 daily fractions of 1.8 Gy in 5 weeks. Planning target volume (PTV) received 45 Gy and encompassed the entire stomach or all tumour extension (if present) and draining lymph nodes (perigastric, coeliac, porta hepatis, gastroduodenal, splenic hilar, suprapancreatic, pancreaticoduodenal and paraaortic to the level of L3/L4) (Figure 1). For GEJ tumours and tumours which originated in the upper third of the stomach the upper margin of at least 3–5 cm was used in the distal oesophagus, and for distal lesions (at or near the gastroduodenal junction), a 5 cm lower margin in the part of duodenum was used. The dose was prescribed to cover the PTV with a 95% reference isodose (95% of the International Commission on Radiation Unit reference point dose). Custom shielding with multileaf collimator was applied to reduce the dose to kidneys (70% of one kidney volume < 20 Gy and 30% of second kidney volume < 20Gy), liver (30% of liver volume < 30Gy) and spinal cord (Dmax < 45 Gy). Dose-volume histogram parameters were used for plan verification regarding target coverage and normal structures sparing. Treatment was verified using a weekly portal imaging.

During the radiochemotherapy treatment, the patients were followed up on weekly basis by clinical examination and laboratory blood tests. Patients' performance status, weight loss and toxicity profiles according to CTCAE v4.0 were registered.[41] Surgery was performed 4–6 weeks after radiochemotherapy in two University Clinical Centers in Slovenia - Ljubljana and Maribor. Following the surgery patients were reassessed by multidisciplinary advisory team for the need of adjuvant chemotherapy.

After the treatment, patients were followed up every 3 months for 2 years and later on every 6 months until 5 years or death. The study was approved by the institutional review board committee and it was carried out according to the Declaration of Helsinki.

Statistical analysis

Statistical analysis was performed using statistical package SPSS, version 20 (SPSS Inc., USA).

The primary endpoints were histopathological R0 resection rate and pathological response rate. The effect of preoperative radiochemotherapy on tumour down-staging was assessed by comparing the pretreatment clinical TNM stage with the postoperative pathologic TNM stage. The secondary endpoints of this study were as follows: toxicity of

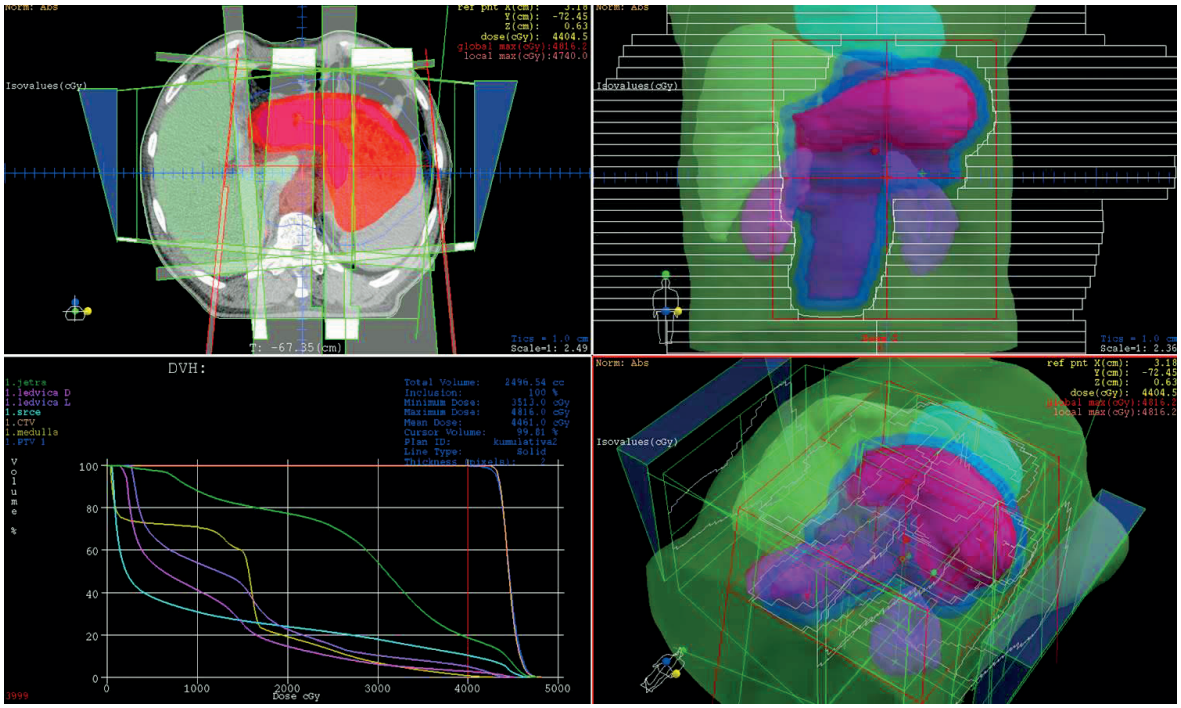

FIGURE 1. Planning target volume and dose–volume histogram for patient with locoregionally advanced gastric cancer.

preoperative radiochemotherapy, early postoperative mortality and locoregional control (LRC, the event was local and/or regional recurrence), DFS (the event was local, regional or systemic recurrence), disease-specific survival (DSS, the event was death due to gastric adenocarcinoma) and OS (the event was death from any cause).

Survival data was calculated from the beginning of preoperative treatment to the November 1st 2013 (close-out date). Survival probability was calculated using Kaplan-Meier estimate[42], and log rank test[43] was used to evaluate the differences between individual groups of patients. Independent prognostic values of variables that appeared as statistically significant on univariate analysis were tested by multivariate Cox regression analysis model. Two-sided tests were used and the differences at $p < 0.05$ were considered as statistically significant.

Results

Eighty-four patients (93.3%) completed preoperative treatment with radiochemotherapy according to the protocol. In six patients (6.7%) RT was interrupted before 45 Gy and none of those patients received the last (third) cycle of chemotherapy. In one patient treatment was interrupted at 12.6 Gy due to pulmonary abscess (as a result of communication between tumour and pulmonary system), in one patient at 14.4 Gy because of febrile neutropenia, in one patient at 33.6 Gy because of progression into the liver and in three patients at 41.4 Gy due to serious side effects of treatment and deterioration of performance status.

Resection rate

Twenty patients (22.2%) did not undergo the surgery. In 8 patients the reason was progression of the disease with the occurrence of distant metastases during or after preoperative treatment, one patient developed ileus of small intestine and one patient died due to the rupture of colon transversum caused by direct tumour infiltration. In six patients tumour was estimated as unresectable and other four patients were not operated on due to poor performance status or serious comorbidity. In 13 patients (14.4%) only exploration was performed because the tumour was assessed as unresectable in 6 and diffuse peritoneal carcinomatosis established in 7 patients (three of them had M1 stage at diagnosis).

Fifty-seven patients (63.4%) underwent surgery with the aim of complete removal of the tumour. Except for one patient (whose surgery was performed in regional hospital) all the operations were performed in two major surgical centres in

TABLE 3. Pathological response rate

	T-stage		N-stage		Overall stage	
Response rate	**n**	**%**	**n**	**%**	**n**	**%**
pCR*	5	8.8	×	×	5	8.8
p-stage < c-stage	42	73.7	37	64.9	49	86
p-stage = c-stage	14	24.6	13	22.8	1	1.8
p-stage > c-stage	1	1.8	7	12.3	7	12.3

c = clinical; p = pathologic; pCR = pathologic complete response

TABLE 4. Toxicity of preoperative radiochemotherapy

Toxicity	NCI grade (% of patients, n = 90)					
	0	**1**	**2**	**3**	**4**	**5**
Radiomucositis	53.4	30	13.3	2.2	1.1	0
Radiodermatitis	0	0	0	0	0	0
Diarhoea	90	6.7	2.2	1.1	0	0
Dysphagia	44.4	37.8	8.9	5.6	3.3	0
Vomiting, nausea	38.8	16.7	18.9	20	5.6	0
Infection	53.4	18.9	11.1	13.3	3.3	0
Weight loss	41.7	44.4	11.1	2.8	×	×
Granulocytopenia	17.8	15.6	37.8	23.3	5.5	0
Anemia	13.3	41.1	41.1	3.3	1.1	0
Trombocytopenia	31.1	47.8	10	5.6	5.6	0

NCI = National Cancer Institute Common Toxicity Criteria for Adverse Events version 4.0 (CTCAE v4.0) [41]

Slovenia - University Medical Centre Ljubljana and Maribor. Distal subtotal resection of the stomach was performed in 15 (16.7%) patients, total resection of the stomach in 32 (35.6%) patients, multivisceral resection in seven (7.8%) patients and transthoracic oesophageal resection in three (3.3%) patients. R0 resection was achieved in 50 (55.6%) of all patients and the remaining seven (7.8%) patients underwent non-radical surgery (R1 in five and R2 in two patients) (Table 2).

Pathological response rate

Among the patients that underwent surgery with the aim of complete tumour removal (n = 57), pCR was achieved in five patients (5.6% of all treated patients or 8.8% of all operated patients). Down-staging was recorded in 44 patients (86%), in one patient (1.8%) the stage after radiochemotherapy was unchanged while in seven patients (12.3%) the pathological stage was higher than clinical, mainly due to higher pN stage (Table 3). We did not find any statistical differences in survival between the groups of patients with tumour/nodes down-staging versus patients with no response to preoperative treatment.

Toxicity of preoperative radiochemotherapy

Five patients (5.6%) did not complete the treatment as planned. Reasons were lung abscess in one patient and serious side effects of the treatment (such as fatigue, neutropenic fever and serious deterioration of performance status) in other four patients. Consequently none of them received the last (third) cycle of chemotherapy.

No death was recorded during preoperative radiochemotherapy. Most grade 3 and 4 toxicities (Table 4) were due to vomiting, nausea and bone marrow suppression. In total, 58% of patients lost their weight during radiochemotherapy, but more than 10% of weight loss was seen in only 13.9% of patients.

Outcome of the disease for patients who underwent surgery

The median follow up for all patients was 18 months (range 4–77 months), but for the subgroup of survivors the median follow up was 20 months (range 5–77 months). Twenty-six (45.6%) patients died due to GEJ or gastric carcinoma, one died because of septic shock following the surgery and a reason for two deaths was unknown. Twenty-eight patients (49.1%) were disease free, while 29 patients (50.9%) developed the recurrence: one patient (1.8%) only local, one patient (1.8%) locoregional, 24 patients (42.1%) only distant metastases and other three patients (5.4%) locoregional recurrence in combination with distant metastases. At two years, LRC, DFS, DSS and OS were 82.9%, 43.9%, 56.9% and 53.9%, respectively.

The GEJ cancer patients (Siewert I + II) who underwent surgery

In the group of the GEJ cancer patients (Siewert I + II) 21 patients completed preoperative treatment and were operated on for the removal of the tumour. R0 resection of the tumour was achieved in 19 patients (90.5%) and the remaining 2 patients (9.6%) underwent non-radical surgery. pCR was achieved in four patients (19%). Down-staging was altogether achieved in 17 patients (81%) (Table 5).

Seven patients (33.3%) died due to GEJ carcinoma, one died because of septic shock after surgery and a reason for one death is unknown. Twelve patients (57.1%) were disease free, in one patient (4.8%) only locoregional recurrence developed and eight patients (38.1%) presented with distant metastases. At 2 years, LRC, DFS, DSS and OS were 82.3%, 47%, 56% and 50.6% respectively.

The initially unresectable gastric cancer patients who underwent surgery

After preoperative radiochemotherapy the surgery for tumour removal was performed in 36 patients with initially unresectable cancer. R0 resection of the tumour was achieved in 31 (86.1%) patients and the remaining 5 (13.9%) patients underwent non-radical surgery. pCR of the tumour was achieved in 1 patient (2.8%) and downstaging was recorded in 32 patients (88.9%) (Table 6).

Nineteen patients (52.8%) died due to gastric cancer; in one patient (2.8%) the reason for death was unknown. Sixteen patients (44.4%) were without any signs of disease, in one patient (2.8%) only locoregional recurrence developed, sixteen patients (44.4%) developed distant metastases only and other three patients (8.4%) developed combination of locoregional recurrence and distant metastases. At 2 years, LRC, DFS, DSS and OS were 79.9%, 43.5%, 58.8% and 57.1%, respectively.

TABLE 5. The GEJ cancer patients (Siewert I + II) who underwent surgery

Characteristic		No.	%
Gender	Male	17	81
	Female	4	19
Age		Median 62 years (44–80 years)	
PS (WHO)	0	17	81
	1	2	9.5
	2	2	9.5
Resectability	R0	19	90.5
	R1	1	4.8
	R2	1	4.8
Response	pCR	4	19
	pT-stage < cT-stage	14	66.7
	pT-stage = cT-stage	6	28.6
	p-Tstage > cT-stage	1	4.8
	pN-stage < cN-stage	12	57.2
	pN-stage = cN-stage	5	23.8
	pN-stage > cN-stage	4	19
	p-stage < c-stage	17	81
	p-stage = c-stage	0	0
	p-stage > c-stage	4	19

pCR = Pathological complete response; PS = Performance status according to WHO scoring system

Discussion

In the 7th edition of the AJCC cancer staging manual, GEJ carcinomas have been classified as oesophageal carcinomas. However, for various reasons, some of the experts believe that their classification should remain under gastric carcinoma. Furthermore, the published literature in this area is not uniform and often deals with both localizations together. Based on various research findings GEJ cancer is currently treated with different modalities: postoperative radiochemotherapy[9,11], perioperative chemotherapy with epirubicin, cisplatin and 5-fluorouracil[8,10] and in few past years preoperative radiochemotherapy is being used increasingly.[14,15] The current approach to the treatment of unresectable gastric cancer patients is based mainly on the preference of the oncologist and perioperative chemotherapy[10], systemic therapy with trastuzumab for tumours with HER2 overexpression[44] or preoperative radiochemotherapy is used.[31-40] It has been shown that preoperative radiochemotherapy in GEJ carcinoma is superior to preoperative chemotherapy.[15] In resectable gastric carcinoma the role of preoperative radiochemotherapy is not so defined, since there are currently no data to clarify the differences of both treatment modalities and results from TOPGEAR study are eagerly awaited.[27] In patients with unresectable gastric cancer, who were offered only palliative treatment in the past, it is even more meaningful to use the combination of radiotherapy and chemotherapy in order to increase the effectiveness of the treatment and hopefully change the unresectable disease into the resectable one with R0 resection.

At our institution the same preoperative treatment for GEJ and gastric carcinomas is used. Radiation therapy is delivered daily in 1.8 Gy per fraction to the total dose of 45 Gy with concomitant chemotherapy using 5-fluorouracil and cisplatin. Surgery for both tumours follows in 4–6 weeks after the completion of preoperative radiochemotherapy. Patients in our study had advanced disease with tumours staged as cT4 and cN+ disease in 75.6% and 93.3% of patients, respectively. Four patients with unresectable gastric carcinoma (4.4%)

TABLE 6. The unresectable gastric cancer patients who underwent surgery

Characteristic		No.	%
Gender	Male	25	69.4
	Female	11	30.6
Age		Median 62 years (43–78 years)	
PS (WHO)	0	28	77.8
	1	8	22.2
Resectability	R0	31	86.1
	R1	4	11.1
	R2	1	2.8
Response	pCR	1	2.8
	pT-stage < cT-stage	28	77.8
	pT-stage = cT-stage	8	22.2
	p-Tstage > cT-stage	0	0
	pN-stage < cN-stage	25	69.4
	pN-stage = cN-stage	8	22.2
	pN-stage > cN-stage	3	8.3
	p-stage < c-stage	32	88.9
	p-stage = c-stage	1	2.8
	p-stage > c-stage	3	8.3

pCR = Pathological complete response; PS = Performance status according to WHO scoring system

had localized peritoneal carcinomatosis diagnosed by laparoscopy or exploratory operation prior to treatment. Despite M1 disease multidisciplinary advisory team indicated preoperative treatment because of excellent general condition of these patients and hope for achieving radical resection. Two patients were later operated on, with R1 resection in first and only exploratory operation in the second patient. All 4 patients died due to gastric cancer within one year from completing the preoperative treatment (median: 4 months, range: 3–12 months).

Eighty-four patients (93.3%) finished preoperative treatment with radiochemotherapy according to the protocol. Only in four patients the treatment was stopped prematurely due to toxic side effects, which did not allow the continuation of therapy (neutropenic fever in one patient and serious deterioration of performance status in other three patients). No death was recorded during preoperative radiochemotherapy. Most grade 3 and 4 toxicities were due to nausea and vomiting (in 25.6% of patients) and bone marrow suppression with granulocytopenia (in 16.9% of patients). Similar toxicities were noted in other studies.[16,22,35] Altogether 58% patients lost their weight during radiochemotherapy, but more than 10% of weight loss was seen in only 13.9% of patients, which we believe is the result of excellent team work between radiation oncologists, nutritionists and intensive supportive therapy that was provided to our patients.

Several studies have demonstrated that preoperative radiochemotherapy does not increase early postoperative mortality.[15,35,45] In our study only one patient (1.8%) died due to septic shock early after the surgery and there were no reports of anastomotic leak or any other complications after surgery.

Only 57 patients (63.4%) in our study underwent surgery for tumour removal. In 50 patients (55.6% of all included or 87.7% of operated patients) R0 resection was obtained. Ajani *et al*. reported that 85% of all included patients underwent surgery and in 70% R0 resection was obtained, but in this study only initially resectable, non-cT4 tumours were included.[17]

There is a general belief that all such patients should be operated in large, multidisciplinary centres, by experienced surgeons in order to achieve better treatment outcome. In our study only one patient was not operated in a large volume surgery centre, which reflects that gastric surgery in our country is centralized.

In 49 (86%) of operated patients tumour and/or nodes down-staging was achieved (when comparing clinical stage and pathological stage), which we believe is a very good result. Ajani *et al*. noted response on preoperative radiochemotherapy in 64% of patients with resectable gastric cancer who were operated and in 55% of all assessable patients.[17] In our study pCR was achieved in only five patients (5.6% of all assessable patients) in comparison with Ajani *et al*. who reported pCR in 30% of all patients.[17] As expected, more pCRs in our study were achieved in patients with GEJ tumour (four) comparing to only one patient with unresectable gastric cancer, as GEJ tumours were less advanced and mostly resectable. The 2-years OS of our patients was 53.9%, which is similar to the results that Ajani *et al*. reported in their study.[16]

If we consider GEJ tumours and gastric tumours separately, we can notice that patients with gastric cancer had worse 2-years LRC than patients with GEJ cancer (79.9% and 82.3%, respectively). This is somehow expected because gastric cancer patients in our study had more advanced disease consid-

ered as unresectable before the start of any treatment. On the other hand, there were no significant differences between GEJ and gastric tumours in DFS, DSS and OS at 2-years. It seems that the well-known worse outcome for GEJ tumours was not so obvious, as GEJ tumours in our study were less advanced.

The biggest limitation of our study is the retrospective data collection. For more accurate conclusions we would need longer follow-up and a larger number of enrolled patients. Maybe patients with GEJ and gastric cancer should be separated (although TOPGEAR study includes both tumour sites, without Siewert I). Furthermore, we need to develop more effective systemic drugs in order to decrease the incidence of distant metastases, which are the most common site of the disease recurrence.

In conclusion, we believe that treatment with preoperative radiochemotherapy was feasible, with acceptable toxicity, and it enabled good down-staging with even the possibility of complete pCR of the disease.

References

1. Rüschoff J. Adenocarcinoma of the GEJ: gastric or oesophageal cancer? *Recent Results Cancer Res* 2012; **196:** 107-13.
2. Ito H, Inoue H, Odaka N, Satodate H, Suzuki M, Mukai S, et al. Comparison of clinicopathological characteristics in the patients with cardiac cancer with or without esophagogastric junctional invasion: a single-center retrospective cohort study. *Int J Surg Oncol* 2013; **2013:** 189459.
3. American Joint Committee on Cancer. *AJCC cancer staging manual.* 7th Edition. New York: Springer-Verlag; 2009.
4. Buergy D, Lohr F, Baack T, Siebenlist K, Haneder S, Michaely H, et al. Radiotherapy for tumors of the stomach and gastroesophageal junction - a review of its role in multimodal therapy. *Radiat Oncol* 2012; **7:** 192.
5. Lutz MP, Zalcberg JR, Ducreux M, Ajani JA, Allum W, Aust D, et al. Highlights of the EORTC St. Gallen International Expert Consensus on the primary therapy of gastric, gastroesophageal and oesophageal cancer - differential treatment strategies for subtypes of early gastroesophageal cancer. *Eur J Cancer* 2012; **48:** 2941-53.
6. Jeromen A, Oblak I, Anderluh F, Velenik V, Vidmar MS, Ratosa I. Results of postoperative radiochemotherapy of the patients with resectable gastroesophageal junction adenocarcinoma in Slovenia. *Radiol Oncol* 2012; **46:** 337-45.
7. D'Angelica M, Gonen M, Brennan MF, Turnbull AD, Bains M, Karpeh MS. Patterns of initial recurrence in completely resected gastric adenocarcinoma. *Ann Surg* 2004; **240:** 808-16.
8. Wayman J, Bennett MK, Raimes SA, Griffin SM. The pattern of recurrence of adenocarcinoma of the oesophago-gastric junction. *Br J Cancer* 2002; **86:** 1223-9.
9. Oblak I, Vidmar SM, Anderluh F, Velenik V, Jeromen A, Hadzic JB. Capecitabine in adjuvant radiochemotherapy for gastric adenocarcinoma. *Radiol Oncol* 2015; 49(2): 163-172.; **48:** 189-96.
10. Cunningham D, Allum WH, Stenning SP, Thompson JN, Van de Velde CJH, Nicolson M, et al. Perioperative chemotherapy versus surgery alone for resectable gastroesophageal cancer. *N Engl J Med* 2006; **355:** 11-20.
11. Macdonald JS, Smalley SR, Benedetti J, Hundahl SA, Estes NC, Stemmermann GN, et al. Chemoradiotherapy after surgery compared with surgery alone for adenocarcinoma of the stomach or gastroesophageal junction. *N Engl J Med* 2001; **345:** 725-30.
12. Oblak I, Velenik V, Anderluh F, Mozina B, Ocvirk J. The correlation between the levels of tissue inhibitor of metalloproteinases 1 in plasma and tumour response and survival after preoperative radiochemotherapy in patients with rectal cancer. *Radiol Oncol* 2013; **47:** 138-44.
13. Van Hagen P, Hulshof MCCM, van Lanschot JJB, Steyerberg EW, van Berge Henegouwen MI, Wijnhoven BPL, et al. Preoperative chemoradiotherapy for esophageal or junctional cancer. *N Engl J Med* 2012; **366:** 2074-84.
14. Ychou M, Boige V, Pignon J-P, Conroy T, Bouché O, Lebreton G, et al. Perioperative chemotherapy compared with surgery alone for resectable gastroesophageal adenocarcinoma: an FNCLCC and FFCD multicenter phase III trial. *J Clin Oncol* 2011; **29:** 1715-21.
15. Stahl M, Walz MK, Stuschke M, Lehmann N, Meyer H-J, Riera-Knorrenschild J, et al. Phase III comparison of preoperative chemotherapy compared with chemoradiotherapy in patients with locally advanced adenocarcinoma of the esophagogastric junction. *J Clin Oncol* 2009; **27:** 851-6.
16. Ajani JA, Mansfield PF, Janjan N, Morris J, Pisters PW, Lynch PM, et al. Multi-institutional trial of preoperative chemoradiotherapy in patients with potentially resectable gastric carcinoma. *J Clin Oncol* 2004; **22:** 2774-80.
17. Ajani JA, Mansfield PF, Crane CH, Wu TT, Lunagomez S, Lynch PM, et al. Paclitaxel-based chemoradiotherapy in localized gastric carcinoma: degree of pathologic response and not clinical parameters dictated patient outcome. *J Clin Oncol* 2005; **23:** 1237-44.
18. Rivera F, Galán M, Tabernero J, Cervantes A, Vega-Villegas ME, Gallego J, et al. Phase II trial of preoperative irinotecan-cisplatin followed by concurrent irinotecan-cisplatin and radiotherapy for resectable locally advanced gastric and esophagogastric junction adenocarcinoma. *Int J Radiat Oncol Biol Phys* 2009; **75:** 1430-6.
19. Oblak I, Anderluh F, Velenik V, Jeromen A, Ratoša I, Skoblar Vidmar M. Preoperative radiochemotherapy in patients with locoregionally inresectable gastric cancer. [Abstract]. *Ann Oncol* 2011; **22(Suppl 5):** V37.
20. Díaz-González JA, Rodríguez J, Hernández-Lizoain JL, Ciérvide R, Gaztañaga M, San Miguel I, et al. Patterns of response after preoperative treatment in gastric cancer. *Int J Radiat Oncol Biol Phys* 2011; **80:** 698-704.
21. Pepek JM, Chino JP, Willett CG, Palta M, Blazer Iii DG, Tyler DS, et al. Preoperative chemoradiotherapy for locally advanced gastric cancer. *Radiat Oncol* 2013; **8:** 6.
22. Ajani JA, Winter K, Okawara GS, Donohue JH, Pisters PWT, Crane CH, et al. Phase II trial of preoperative chemoradiation in patients with localized gastric adenocarcinoma (RTOG 9904): quality of combined modality therapy and pathologic response. *J Clin Oncol* 2006; **24:** 3953-8.
23. Lowy AM, Feig BW, Janjan N, Rich TA, Pisters PW, Ajani JA, et al. A pilot study of preoperative chemoradiotherapy for resectable gastric cancer. *Ann Surg Oncol* 2001; **8:** 519-24.
24. McCloskey SA, Yang GY. Benefits and challenges of radiation therapy in gastric cancer: techniques for improving outcomes. *Gastrointest Cancer Res* 2009; **3:** 15-9.
25. Koukourakis G V. Evidence based radiation therapy for locally advanced resectable and unresectable gastric cancer. *World J Gastrointest Oncol* 2011; **3:** 131-6.
26. Valenti V, Hernandez-Lizoaín JL, Beorlegui MC, Diaz-Gozalez JA, Regueira FM, Rodriguez JJ, et al. Morbidity, mortality, and pathological response in patients with gastric cancer preoperatively treated with chemotherapy or chemoradiotherapy. *J Surg Oncol* 2011; **104:** 124-9.
27. Leong T, Smithers M, Michael M, Gebski V, Boussioutas A, Miller D, et al. TOPGEAR: an international randomized phase III trial of preoperative chemoradiotherapy versus preoperative chemotherapy for resectable gastric cancer (AGITG/TROG/EORTC/NCIC CTG). [Abstract]. 2012 ASCO Annual Meeting. *J Clin Oncol* 2012; 30(Suppl). Abstr. No TPS4141. Available from: http://meetinglibrary.asco.org/content/99024-114. Accessed on 5th April, 2014.
28. Tannock IF. Treatment of cancer with radiation and drugs. *J Clin Oncol* 1996; **14:** 3156-74.
29. Hennequin C, Favaudon V. Biological basis for chemo-radiotherapy interactions. *Eur J Cancer* 2002; **38:** 223-30.

30. Seiwert TY, Salama JK, Vokes EE. The concurrent chemoradiation paradigm--general principles. *Nat Clin Pract Oncol* 2007; **4:** 86-100.

31. Moertel CG, Childs DS, Reitemeier RJ, Colby MY, Holbrook MA. Combined 5-fluorouracil and supervoltage radiation therapy of locally unresectable gastrointestinal cancer. *Lancet* 1969; **2(7626):** 865-7.

32. Yoshimizu N, Saikawa Y, Kubota T, Akiba Y, Yoshida M, Otani Y, et al. Complete response of a highly advanced gastric carcinoma to preoperative chemoradiotherapy with S-1 and low-dose cisplatin. *Gastric Cancer* 2003; **6:** 185-90.

33. Takahashi T, Saikawa Y, Kubota T, Akiba Y, Shigematsu N, Yoshida M, et al. Histological complete response in a case of advanced gastric cancer treated by chemotherapy with S-1 plus low-dose cisplatin and radiation. *Jpn J Clin Oncol* 2003; **33:** 584-8.

34. Shigeoka H, Imamoto H, Nishimura Y, Shimono T, Furukawa H, Imamura H, et al. Complete response to preoperative chemoradiotherapy in highly advanced gastric adenocarcinoma. *World J Gastrointest Oncol* 2010; **2:** 282-6.

35. Roth AD, Allal AS, Bründler M-A, de Peyer R, Mermillod B, Morel P, et al. Neoadjuvant radiochemotherapy for locally advanced gastric cancer: a phase I-II study. *Ann Oncol* 2003; **14:** 110-5.

36. Allal AS, Zwahlen D, Bründler M-A, de Peyer R, Morel P, Huber O, et al. Neoadjuvant radiochemotherapy for locally advanced gastric cancer: long-term results of a phase I trial. *Int J Radiat Oncol Biol Phys* 2005; **63:** 1286-9.

37. Klautke G, Foitzik T, Ludwig K, Ketterer P, Klar E, Fietkau R. Neoadjuvant radiochemotherapy in locally advanced gastric carcinoma. *Strahlenther Onkol* 2004; **180:** 695-700.

38. Schein PS, Smith FP, Woolley P V, Ahlgren JD. Current management of advanced and locally unresectable gastric carcinoma. *Cancer* 1982; **50(11 Suppl):** 2590-6.

39. Hazard L, O'Connor J, Scaife C. Role of radiation therapy in gastric adenocarcinoma. *World J Gastroenterol* 2006; **12:** 1511-20.

40. Henning GT, Schild SE, Stafford SL, Donohue JH, Burch PA, Haddock MG, et al. Results of irradiation or chemoirradiation following resection of gastric adenocarcinoma. *Int J Radiat Oncol Biol Phys* 2000; **46:** 589-98.

41. National Cancer Institute Common Terminology Criteria for Adverse Events version 4.0. Available from: http://evs.nci.nih.gov/ftp1/CTCAE/About.html. Accessed 2nd June, 2013.

42. Kaplan EL, Meier P. Nonparametric estimation from incomplete observations. *J Am Stat Assoc* 1958; **53:** 457-81.

43. Peto R, Pike MC, Armitage P, Breslow NE, Cox DR, Howard S V, et al. Design and analysis of randomized clinical trials requiring prolonged observation of each patient. II. analysis and examples. *Br J Cancer* 1977; **35:** 1-39.

44. Bang Y-J, Van Cutsem E, Feyereislova A, Chung HC, Shen L, Sawaki A, et al. Trastuzumab in combination with chemotherapy versus chemotherapy alone for treatment of HER2-positive advanced gastric or gastro-oesophageal junction cancer (ToGA): a phase 3, open-label, randomised controlled trial. *Lancet* 2010; **376(9742):** 687-97.

45. Burmeister BH, Thomas JM, Burmeister EA, Walpole ET, Harvey JA, Thomson DB, et al. Is concurrent radiation therapy required in patients receiving preoperative chemotherapy for adenocarcinoma of the oesophagus? A randomised phase II trial. *Eur J Cancer* 2011; **47:** 354-60.

research article

Febrile neutropenia in chemotherapy treated small-cell lung cancer patients

Renata Rezonja Kukec[1], Iztok Grabnar[2], Tomaz Vovk[2], Ales Mrhar[2], Viljem Kovac[3], Tanja Cufer[4]

[1] Krka, d.d., Novo mesto, Slovenia
[2] University of Ljubljana, Faculty of Pharmacy, Ljubljana, Slovenia
[3] Institute of Oncology Ljubljana, Ljubljana, Slovenia
[4] University Clinic Golnik, Golnik, Slovenia

Radiol Oncol 2015; 49(2): 173-180.

Received: 24 September 2014
Accepted: 15 October 2014

Correspondence to: Prof. Aleš Mrhar, Ph.D., Faculty of Pharmacy, University of Ljubljana, Aškerčeva 7, 1000 Ljubljana.
E-mail: ales.mrhar@ffa.uni-lj.si

Disclosure: No potential conflicts of interest were disclosed.

Background. Chemotherapy with platinum agent and etoposide for small-cell lung cancer (SCLC) is supposed to be associated with intermediate risk (10–20%) of febrile neutropenia. Primary prophylaxis with granulocyte colony-stimulating factors (G-CSFs) is not routinely recommended by the treatment guidelines. However, in clinical practice febrile neutropenia is often observed with standard etoposide/platinum regimen. The aim of this analysis was to evaluate the frequency of neutropenia and febrile neutropenia in advanced SCLC patients in the first cycle of standard chemotherapy. Furthermore, we explored the association between severe neutropenia and etoposide peak plasma levels in the same patients.

Methods. The case series based analysis of 17 patients with advanced SCLC treated with standard platinum/etoposide chemotherapy, already included in the pharmacokinetics study with etoposide, was performed. Grade 3/4 neutropenia and febrile neutropenia, observed after the first cycle are reported. The neutrophil counts were determined on day one of the second cycle unless symptoms potentially related to neutropenia occurred. Adverse events were classified according to Common Toxicity Criteria 4.0. Additionally, association between severe neutropenia and etoposide peak plasma concentrations, which were measured in the scope of pharmacokinetic study, was explored.

Results. Two out of 17 patients received primary GCS-F prophylaxis. In 15 patient who did not receive primary prophylaxis the rates of both grade 3/4 neutropenia and febrile neutropenia were high (8/15 (53.3%) and 2/15 (13.3%), respectively), already in the first cycle of chemotherapy. One patient died due to febrile neutropenia related pneumonia. Neutropenic events are assumed to be related to increased etoposide plasma concentrations after a standard etoposide and cisplatin dose. While the mean etoposide peak plasma concentration in the first cycle of chemotherapy was 17.6 mg/l, the highest levels of 27.07 and 27.49 mg/l were determined in two patients with febrile neutropenia.

Conclusions. Our study indicates that there is a need to reduce the risk of neutropenic events in chemotherapy treated advanced SCLC, starting in the first cycle. Mandatory use of primary G-CSF prophylaxis might be considered. Alternatively, use of improved risk models for identification of patients with increased risk for neutropenia and individualization of primary prophylaxis based on not only clinical characteristics but also on etoposide plasma concentration measurement, could be a new, promising options that deserves further evaluation.

Key words: small cell lung cancer; platinum-etoposide chemotherapy; etoposide; febrile neutropenia; plasma drug concentration

Introduction

Small cell lung cancer (SCLC) accounts for approximately 13% of all lung cancer diagnoses. It is very aggressive, growing rapidly and spreading early. Seventy percent of SCLC patients have extensive disease at the time of diagnosis. The standard therapeutic approach for extensive disease is chemo-

TABLE 1. Factors associated with FN risk according to EORTC, ASCO, NCCN and ESMO guidelines

Risk factor	EORTC	ASCO	NCCN	ESMO
Older age (≥ 65 years)	■	■	■	■
Comorbidities	Liver, renal or cardiovascular diseases	■	Liver dysfunction, poor renal function	
History of prior FN	■	■	■	
Poor performance status	■	■	■	
Extensive prior treatment including large radiation ports		■	■	Reduced marrow reserve (e.g. ANC < 1.5 × 10^9/l) due to radiotherapy of > 20% marrow
Poor nutritional status	■	■		
Advanced stage of disease	■	■		
Cytopenias due to bone marrow involvement by tumour		■	■	
The presence of open wounds or active infections		■	■	
Lack of antibiotic prophylaxis	■			
Lack of G-CSF use	■			
Female gender	■			
Haemoglobin < 12 g/dl	■			
Administration of combined chemoradiotherapy		■		
Previous chemotherapy			■	
Pre-existing neutropenia			■	
Recent surgery			■	
Further infections in the next treatment cycle considered life-threatening				■
Dose reduction below treshold				■
Delay of chemotherapy				■
Lack of protocol adherence if compromising cure rate, overall or disease-free survival				■
Human immunodeficiency virus				■

ANC = absolute neutrophil count; ASCO = American Society of Clinical Oncology; EORTC = European Organisation for Research and Treatment of Cancer; ESMO = European Society for Medical oncology; FN = febrile neutropenia; G-CSF = granulocyte colony-stimulating factor; NCCN = National Comprehensive Cancer Network

therapy with platinum agent and topoisomerase II inhibitor etoposide.[1]

Chemotherapy causes haematological as well as non-haematological adverse drug reactions. The most serious haematological toxicity is neutropenia, which can cause fatal septicaemia by suppressing the production of neutrophils and by cytotoxic effects on the cells that line the gastrointestinal tract allowing bacterial multiplication and invasion.[2] Febrile neutropenia (FN) is a serious adverse event of chemotherapy characterized as an oral temperature > 38.5 °C or two consecutive readings of > 38 °C for 2 h and an absolute neutrophil count (ANC) < 0.5 × 10^9/l, or expected to fall below 0.5 × 10^9/l.[3] It is associated with high morbidity, mortality, costs, and an increase of the risk for chemotherapy dose delays and/or reductions, or even discontinuation of chemotherapy.[4,5]

Primary prophylaxis with granulocyte colony-stimulating factors (G-CSFs), *i.e.* use with first cycle of chemotherapy, has been shown to significantly reduce the risk of FN; however, its use in all patients is not considered cost-effective.[2,4] According to recommendations of the European Organisation for Research and Treatment of Cancer (EORTC)[6], American Society of Clinical Oncology (ASCO)[7], National Comprehensive Cancer Network (NCCN)[8], and European Society for Medical Oncology (ESMO) clinical practice guidelines[9], the prophylactic G-CSF is recommended when the risk of FN is high (≥ 20%). Treatment-related risk factors classify chemotherapy regimens to high (≥

20%), intermediate (10–20%), or low risk (< 10%) for developing FN.[4,6] When using a chemotherapy regimen associated with an intermediate (10–20%) risk of FN other factors that may increase the overall risk of FN should be considered in making the decision to use prophylactic G-CSF. Guidelines indicate various risk factors, with an older age included in all four guidelines. Additional factors are history of prior FN, poor performance status (PS) and comorbidities[7,8]; for further details see Table 1. Recently, genetic factors which are not mentioned in the guidelines have also been associated with the risk of FN.[4]

According to EORTC and NCCN guidelines etoposide/platinum regimen for SCLC is associated with an intermediate risk of FN, while in the ESMO guidelines which provide only the list of regimens with high risk of FN, etoposide/platinum is not listed. ASCO guidelines do not indicate FN risk for any particular chemotherapeutic regimen. Based on the guidelines, primary prophylaxis with G-CSF in SCLC patients treated with etoposide/platinum regimen is not recommended without a prior identification of a high risk of FN in each individual patient. However, in routine clinical practice FN seems to be frequent in advanced SCLC patients treated with standard etoposide/platinum regimen, who are not entitled to G-CSF prophylaxis.

To get additional information on febrile neutropenia in a first cycle of standard chemotherapy with etoposide/platinum, a post-planned analysis of the frequency of neutropenia and FN in a case series of patients with advanced SCLC, already included in a clinical trial of etoposide pharmacokinetics, was performed. Furthermore, analysis of association of severe neutropenia with previously measured levels of etoposide peak plasma concentration in the same patients during the first cycle of etoposide/cisplatin has been conducted.

Patients and methods

Clinical observation

The post-planned analysis of the frequency and grade of neutropenia and FN was conducted in a case series of patients in the first cycle of standard chemotherapy with etoposide/platinum. These patients were already included in a clinical trial of etoposide pharmacokinetics. Furthermore, association between severe neutropenia and etoposide peak plasma levels was explored.

Eligible patients were at least 18 years old receiving first-line chemotherapy with etoposide/platinum for advanced SCLC confirmed by cytology or histology. Other entry criteria included World Health Organization PS 0–2, adequate haematological parameters and medical conditions allowing chemotherapy, satisfactory liver and renal function. The main exclusion criteria were Gilbert syndrome, Criegler-Najjar syndrome, active gastrointestinal disorders, and concomitant drugs entering the clinically important pharmacokinetic interactions. The Charlson comorbidity index was not assessed; however, patients with some comorbidities, such as liver or kidney dysfunction were excluded by the criteria of pharmacokinetic study. Patients gave written informed consent to participate in the pharmacokinetic study, which was approved by the Slovenian Ethics Committee for Research in Medicine (approval ref. no. 02/11/11) and was carried out according to the Helsinki Declaration.

Patients received a standard myelosuppressive chemotherapeutic regimen of etoposide and cisplatin or carboplatin without any concurrent irradiation. G-CSF prophylaxis was administered according to current guidelines. Planned dose of etoposide was of 100 mg/m^2 intravenously on day 1 through 3. Cisplatin or carboplatin were administered intravenously on day 2 at a planned dose of 80 mg/m^2 or at a target area under the curve (AUC) 5–6 mg min/ml (maximally 350 mg/m^2), respectively. Patients were followed according to routine practice guidelines valid at that period at our university clinic. Neutrophil count was determined on day one of the next 3-week cycle, or earlier in case of clinical symptoms associated with neutropenia. If indicated, patients with severe neutropenia and/or FN were hospitalized at our clinic. Grade 3/4 neutropenia and FN were classified according to Common Toxicity Criteria (NCI-CTC, version 4.0).

The reason for including only the first chemotherapy cycle in our post-planned analysis was relatively high rate of observed neutropenia grade 3/4 or FN in the first cycle while using primary G-CSF prophylaxis according to current guidelines. The following cycles were not included into our analysis due to the fact that G-CSF prophylaxis had been used in the majority of patients in consecutive cycles. In addition, some patients in consecutive cycles received decreased etoposide dose or administration of chemotherapy was delayed.

Pharmacokinetic sampling and drug assay in the scope of pharmacokinetic study

Blood sampling was performed on days 1, 2 and 3 in the first cycle of chemotherapy. Blood samples

TABLE 2. Patients and treatment characteristics with the data on grade 3/4 and febrile neutropenia in the first cycle

Patient n = 17	Age Mean (range)	Sex	PS	Etoposide dose (%)	Neutropenia grade	FN Yes/No	G-CSF prophylaxis	Etoposide peak plasma concentration (3 days mean) (mg/l)
1	60	F	1	100	2	No	No	16.27
2	62	M	0	100	4	No	No	14.43
3	65	M	1	100	1	No	No	16.17
4	60	M	1	100	4	Yes, death	No	27.07
5	64	F	0	100	4	Yes	No	27.49
6	78	M	1	75	0	No	No	15.09
7	51	M	1	100	0	No	Yes	14.73
8	73	M	1	100	1	No	No	17.04
9	63	M	1	100	1	No	No	17.88
10	78	M	1	75	0	No	No	11.93
11	62	M	1	75	0	No	Yes	10.59
12	54	M	0	75	3	No	No	15.14
13	63	F	1	100	3	No	No	17.65
14	64	M	1	100	4	No	No	16.73
15	65	F	0	100	0	No	No	20.25
16	66	M	0	100	4	No	No	23.71
17	62	M	1	100	3	No	No	16.74
	64.1 (51-78)				**Grade 3/4: 8/17 (47.1%) Grade 3/4 (no G-CSF): 8/15 (53.3%) Grade 1/2 or 0: 9/17 (52.9%) Grade 1/2 or 0 (no G-CSF): 7/15 (46.7%)**	**2/17 (11.8%) No G-CSF 2/15 (13.3%)**		**17.6 (range 10.59-27.49)**

FN = febrile neutropenia; G-CSF = granulocyte colony-stimulating factor; PS = performance status; M = male; F = female

(6 ml) were collected at the end of etoposide 60-min infusion. Samples were immediately placed on ice. Plasma was separated by centrifugation at 3000 × g and 4 °C for 10 min and stored at -80 °C until the analysis. Etoposide plasma concentration was determined by high-performance liquid chromatography with fluorimetric detection using a modified method of Krogh-Madsen *et al*.[10] Linearity of the method was 0.125–30 mg/l with a lower limit of quantification of 0.125 mg/l. The method was accurate (all deviations ≤ 10.3%) and reproducible (coefficient of variability ≤ 7.22% intra-day and ≤ 7.33% inter-day).

Results

According to patients baseline characteristics presented in Table 2 our group of 17 patients represents a typical population of advanced SCLC patients treated with chemotherapy, with a mean age of 64.1 years (range, 51–78 years), mostly males (76.5%) and PS ≤ 2. In the first cycle etoposide was administered in a full dose in 13 of all patients (76.5%). Primary G-CSF prophylaxis was administered in only 2 patients (11.8%).

Two out of 17 cases (11.8%) of FN have been observed in the first cycle, one of these two patients died due to FN related pneumonia. Taken into account only 15 patients without primary prophylaxis with G-CSF the rate of FN was even higher, *i.e.* 13.3% (2/15). The whole rate of neutropenia grade 3/4 after the first cycle was also quite high, it was recorded in 8 out of 15 patients not receiving primary G-CSF prophylaxis (53.3%). Of note, in our study neutrophil count has only been determined on day one of the second cycle, unless symptoms potentially related to neutropenia occurred.

TABLE 3. A summary of studies reporting risk of FN by ASCO, EORTC and NCCN guidelines

Reference, year	No of patients entered	Treatment regimen	% pts with grade 3/4 neutropenia	% pts with FN	Concurrent radiotherapy	G-CSF
Roth *et al.*[11], 1992	159	Etoposide 80 mg/m²/d i.v. for 5 days, Cisplatin 20 mg/m²/d i.v. for 5 days, every 3 weeks, 4 cycles	70 (granulocytopenia)	NR	Yes (patients with brain metastases).	No.
Skarlos *et al.*[12], 1994	Regimen A: 73 Regimen B: 74	Regimen A: Etoposide 100 mg/m²/d i.v. days 1-3, Cisplatin 50 mg/m²/d day 1 to 2 Regimen B: Etoposide 100 mg/m²/d i.v. days 1-3, Carboplatin 300 mg/m²/d i.v. day 1, every 3 weeks, 6 cycles	NR	NR	Yes (responding limited disease patients and complete responders with extensive disease)	No.
Kosmidis *et al.*[13], 1994	Regimen A: 73 Regimen B: 74	Regimen A: Etoposide 100 mg/m²/d i.v. days 1-3, Cisplatin 50 mg/m²/d day 1 to 2 Regimen B: Etoposide 100 mg/m²/d i.v. days 1-3, Carboplatin 300 mg/m²/d i.v. day 1, every 3 weeks, 6 cycles	NR	NR	Yes (limited disease patients)	No.

ASCO = American Society of Clinical Oncology; EORTC = European Organisation for Research and Treatment of Cancer; FN = febrile neutropenia; NCCN=National Comprehensive Cancer Network; G-CSF = granulocyte colony-stimulating factor; i.v. = intravenous administration; NR = not reported; pts = patients

In addition, mild grade 1/2 neutropenia or normal neutrophil blood count have been observed in 7/15 (46.7%) of patients without G-CSF prophylaxis on the scheduled day of the second cycle.

Mean etoposide peak plasma concentration in the first cycle of chemotherapy was 17.6 mg/l (from 10.59 to 27.49 mg/l) (Table 2). Of note, the highest levels 27.07 and 27.49 mg/l were determined in two patients with FN. Patients with grade 3/4 neutropenia not experiencing FN had also high mean peak plasma concentrations of 17.4 mg/l (from 14.43 to 23.71 mg/l). Mean etoposide peak plasma concentration in patients with grade 1/2 neutropenia was 16.84 (from 16.17 to 17.88 mg/l), while patients who did not experience neutropenia had etoposide plasma level of 14.5 mg/l (from 10.59 to 20.25 mg/l).

Discussion

According to the guidelines, G-CSF primary prophylaxis is mandatory when the overall risk of FN due to chemotherapy regimen and other factors is ≥ 20%. Etoposide/platinum regimen for SCLC treatment is considered to be associated with 10–20% risk of FN and G-CSF primary prophylaxis is not unambiguously recommended by current guidelines.[6-9] We reviewed studies on the basis of which guidelines classified etoposide/platinum regimen for SCLC treatment into the intermediate risk group for FN.

Taken together, according to EORTC, ASCO, NCCN and ESMO guidelines, information on FN rates in SCLC patients treated with etoposide/platinum regimen is scarce. Only three published studies related to the risk of FN in SCLC patients treated by etoposide/cisplatin are cited[11-13], two of them[12,13] are even very likely the same study. Roth *et al.*[11] reported grade 3/4 granulocytopenia in 70% of patients, while in other two studies[12,13] grade 3/4 neutropenia was not even reported. FN was not reported in any of these studies.[11-13] Of note, in all of these trials concomitant irradiation has been performed in selected patients (Table 3).

Therefore, we performed a comprehensive PubMed literature search to find additional data on grade 3/4 neutropenia and FN rates in SCLC patients treated with first-line intravenous etoposide/platinum regimen (etoposide dosage 240 to 420 mg/m² per cycle) without concurrent radiotherapy and G-CSF primary prophylaxis. In addition to the above 3 mentioned articles[11-13], our literature search found nine studies[14-22] (Table 4). In fact, our search confirmed a substantially high rate of grade 3/4 neutropenia (51-91%) observed in SCLC patients treated with etoposide/platinum chemotherapy given the fact that G-CSF use has been allowed in 3 out of nine trials. In addition, FN rates reported in five of these nine articles[14-22] were in the range of 10–20% referred in the guidelines.[6,8] The reported rates of FN during all, not only the first cycle of the chemotherapy, were in the range from 9.5% to 17%, with the highest rate observed in the trial using relatively high daily dose of etoposide, *i.e.* 140 mg/m² for 3 days.[16,18,19,21,22] Of note, data on neutropenia rates were based on all chemotherapy cycles and not just the first cycle.

In our limited series of patients, severe neutropenia G3/4 and FN were observed in unexpect-

TABLE 4. A summary of comprehensive literature search of studies on FN and grade 3/4 neutropenia

Reference, year	No of patients eligible for evaluation	Treatment regimen	G3/4 neutropenia (% of pts)	FN (% of pts)	G-CSF prophylaxis
Miller *et al.*[14], 1995	156	Etoposide 130 mg/m^2/d i.v. for 3 days, cisplatin 25 mg/m^2/d i.v. for 3 days, every 3 weeks, up to 8 cycles	85.0	NR	No
Pujol *et al.*[15], 2001	109	Etoposide 100 mg/m^2 i.v. days 1-3, cisplatin 100 mg/m^2 i.v. day 1, every 4 weeks, up to 6 cycles	91.0	NR	No
Quoix *et al.*[16], 2001	38	Etoposide 100 mg/m^2 i.v. days 1-3, carboplatin AUC 5 mg/ml/min day 1, every 4 weeks, up to 6 cycles	57.0% cycles (NR per patient)	13.2	No
Schiller *et al.*[17], 2001	402	Etoposide 120 mg/m^2 i.v. days 1-3, cisplatin 60 mg/m^2 i.v. day 1, every 3 weeks, 4 cycles	67.0	NR	Used at the discretion of the treating physician. (no data on use)
Hanna *et al.*[18], 2006	106	Etoposide 120 mg/m^2 i.v. days 1-3, cisplatin 60 mg/m^2 i.v. day 1, every 3 weeks, at least 4 cycles	86.5	10.4	Used in accordance with their package inserts or the 1999 guidelines from the ASCO. (no data on use)
Schmittel *et al.*[19], 2006	35	Etoposide 140 mg/m^2 i.v. days 1-3, carboplatin AUC 5 mg min/ml day 1, up to 6 cycles	51.0	17.0	No
Heigener *et al.*[20], 2009	37	Etoposide 140 mg/m^2 i.v. days 1-3, carboplatin AUC 5 i.v. day 1, every 4, up to 6 cycles	69.4	NR	No
Lara *et al.*[21], 2009	324	Etoposide 100 mg/m^2 i.v. days 1-3, cisplatin 80 mg/m^2 i.v. day 1, every 3 weeks, 4 cycles	68.0	9.5	Use of G-CSF was allowed per investigator discretion. (no data on use)
Zatloukal *et al.*[22], 2010	203	Etoposide 100 mg/m^2 i.v. days 1-3, cisplatin 80 mg/m^2 i.v. day 1, every 3 weeks, 6 cycles	59.6	9.9	No
			Grade 3/4 (range): 51.0-91.0	**FN (range): 9.5-17.0**	

ASCO=American Society of Clinical Oncology; d = day; FN = febrile neutropenia; G-CSF = granulocyte colony-stimulating factor; i.v. = intravenous administration; NR = not reported; pts = patients;

edly high portion of patients not receiving primary G-CSF prophylaxis already in the first cycle of platinum/etoposide chemotherapy; neutropenia G 3/4 developed in more than half patients (53.3%) and FN developed in 2 out of 15 patients. Of note, neutropenia and FN were recorded after the first cycle of the chemotherapy based on the neutrophil count determined only on day one of the second cycle, unless symptoms potentially related to neutropenia occurred. In addition, only 12 out of these 15 patients without G-CSF prophylaxis received the full dose of etoposide. Patient 4 was on long-term treatment with corticosteroids. This patient developed FN with lung infection and died. Taken together, more than half of our patients not receiving primary G-CSF prophylaxis developed at least grade 3/4 neutropenia already in the first cycle, with FN representing a quarter of these eight patients. None of the patients on primary G-CSF prophylaxis developed grade 3/4 neutropenia. Based on this observation most of our consecutive patients included into the prospective etoposide pharmacokinetic study received primary GCS-F prophylaxis and are not included in this analysis.

Compared to the literature search data showing the rate of grade 3/4 neutropenia between 51 and 91% and FN rate between 9.5 and 17% after all cycles in the population of patients not receiving primary prophylaxis with G-CSF the 53.3% rate of grade 3/4 neutropenia and 13.3% rate of FN observed in our patients already in the first cycle without G-CSF prophylaxis is rather high. Taking into account 4 additional patients with grade 1/2 neutropenia recorded on the day one of the second cycle (including one patient taking corticosteroids chronically), the number of grade 3/4 neutropenia in the first cycle might be even higher, if the ANC was measured in the middle of the first chemotherapy cycle.

Despite the fact that the majority of our patients did not classify to high risk FN due to first-line chemotherapy, no concurrent palliative irradiation, good PS, no major comorbidities and normal kidney, liver and bone marrow function, which were all prerequisites for patients to be included into

the pharmacokinetic trial, the rate of FN and 3/4 neutropenia observed after first cycle of the chemotherapy was substantially high. The reason for this might be in the fact that half of our patients were older than 65 years and all of them had advanced disease. Age more than 65 years has not been taken as high-risk criteria per se in our selected population of patients without comorbidities and with a good PS included into the pharmacokinetic trial. Obviously in elderly, fragile population the use of comprehensive geriatric assessment might improve our efforts to better identify patients with an increased risk of cytotoxic drugs complications.[23] However, so far there are no reported prognostic validation studies using comprehensive geriatric assessment for decision on prophylactic use of G-CSF. In addition, we have still not found a score that would help us select these patients in a more comprehensive fashion.

EORTC, ASCO, NCCN and ESMO guidelines indicate various risk factors that predispose to increased risk of FN. Older age is the only factor included in all four guidelines. EORTC guidelines define older age even as patient-related risk factor most consistently associated with an increased FN risk.[6] However, Crawford *et al*. tested various patient's baseline characteristics as possible risk factors for ≥ 1 event of FN, including age, body weight, body surface area, sex, PS, disease stage, and neoplastic disease involvement in the marrow. Surprisingly, only sex was marginally predictive in their study, while patient age was not found to be a risk factor for FN.[24]

The association between neutropenic events and etoposide peak plasma concentration has been well perceived by our analysis. According to the literature etoposide therapeutic trough serum concentration range in cancer patients is 2 to 6 mg/l and peak, 8 to 14 mg/l.[25] In all our groups of patients, *i.e*. patients with FN, grade 3/4 neutropenia, grade 1/2 neutropenia and without neutropenia, mean peak plasma concentration of etoposide was above therapeutic level (*i.e*. 14 mg/l). However, relatedness of mean peak plasma concentration height with severity of neutropenia was observed; concentrations were the highest in patients with FN and declined to the lowest levels observed in patients without neutropenia. Based on the fact that the mean etoposide peak plasma concentration was above therapeutic level also in patients without neutropenia could be anticipated that the frequency of (high-grade) neutropenia would be even higher if neutrophils were measured at the time of the largest expected neutrophil nadir.

On another point, peak plasma etoposide concentrations in two patients (one of them did not receive G-CSF prophylaxis) not experiencing neutropenia were within therapeutic range. Interestingly enough, in patient 7 etoposide plasma concentration was increased (14.73 mg/l) after dosage of etoposide; however, primary G-CSF prophylaxis was received and neutropenia did not develop. These data raised the question of whether high plasma concentrations measured immediately after the first application of etoposide on day one of the three day application course could help in selection of patients for primary G-CSF prophylaxis.

Our analysis is limited by the biases of selected patient population with good PS, without major comorbidities, treated in a controlled situation in the frame of the prospective clinical study. Additionally, the number of the patients is low and neutrophil counts were routinely measured only on the day one of the second cycle and not at the time of the largest expected neutrophil nadir in the middle of the cycle. But, all these limitations do not compromise our conclusion that the risk of FN in advanced SCLC population of patients treated with etoposide/platinum is substantially high. In a real world scenario the probability of FN in these patients might be even higher.

The goal is to develop a comprehensive risk models for FN which can be used as a guide whether or not to incorporate primary G-CSF prophylaxis for each individual patient.[26,27] Some predictive models for neutropenia in the first cycle have already been proposed. However, a prospective study is needed for their validation. On the other hand, individualization of etoposide dosage taking into account pharmacokinetic parameters as well as genetic factors such as genetic polymorphisms, which can also affect drug plasma concentrations, is another option that has to be considered.[28]

Conclusions

According to the guidelines etoposide/platinum regimen for SCLC treatment is not associated with high ≥ 20% risk of FN and primary G-CSF prophylaxis is therefore not mandatory. However, in our case series analysis of selected advanced SCLC patients included in a prospective pharmacokinetic trial, the rate of neutropenic complications in patients not receiving primary G-CSF prophylaxis was substantially high, already in the first cycle. Advanced SCLC patients treated with a standard dose of etoposide in combination with platinum

may have increased plasma etoposide concentrations as reported in our patients and may therefore be at increased risk for high grade neutropenia and FN.

There is a need of greater effort to reduce the risk of neutropenic events starting in the first cycle. To avoid overuse of G-CSF a better prediction of post-chemotherapy neutropenic events, based on etoposide peak plasma concentration, might be of great value. An option could be the development and validation of risk models for severe neutropenia, based on etoposide plasma concentration on day one of the first cycle, a strategy that deserves further evaluation.

References

1. Califano R, Abidin AZ, Peck R, Faivre-Finn C, Lorigan P. Management of Small Cell Lung Cancer. Recent developments for optimal care. *Drugs* 2012; **72:** 471-90.
2. Crawford J, Dale DC, Lyman GH. Chemotherapy-induced neutropenia. Risks, consequences, and new directions for its management. *Cancer* 2004; **100:** 228-37.
3. de Naurois J, Novitzky-Basso I, Gill MJ, Marti Marti F, Cullen MH, Roila F, et al. Management of febrile neutropenia: ESMO clinical practice guidelines. *Ann Oncol* 2010; **21(Suppl 5):** v252-6.
4. Lyman GH, Abella E, Pettengell R. Risk factors for febrile neutropenia among patients with cancer receiving chemotherapy: a systematic review. *Crit Rev Oncol Hematol* 2014; **90:** 190-9.
5. Cooper KL, Madan J, Whyte S, Stevenson MD, Akehurst RL. Granulocyte colony-stimulating factors for febrile neutropenia prophylaxis following chemotherapy: systematic review and meta-analysis. *BMC Cancer* 2011; **11:** 1471-2407.
6. Aapro MS, Bohlius J, Cameron DA, Dal Lago L, Donnely JP, Kearney N, et al. 2010 update of EORTC guidelines for the use of granulocyte-colony stimulating factor to reduce the incidence of chemotherapy-induced febrile neutropenia in adult patients with lymphoproliferative disorders and solid tumors. *Eur J Cancer* 2011; **47:** 8-32.
7. Smith TJ, Khatcheressian J, Lyman GH, Ozer H, Armitage JO, Balducci L, et al. 2006 Update of recommendations for the use of white blood cell growth factors: An evidence-based clinical practice guideline. *J Clin Oncol* 2006; **24:** 3187-205.
8. National Comprehensive Cancer Network. NCCN Guidelines Version 2.2013. Available from: http://www.nccn.org/professionals/physician_gls/f_guidelines.asp#myeloid_growthMyeloid growth factors. Accessed 11 September 2013.
9. Crawford J, Caserta C, Roila F. Haematopoietic growth factors: ESMO clinical practice guidelines for the applications. *Ann Oncol* 2010; **21(Suppl 5):** v248-51.
10. Krogh-Madsen M, Honoré Hansen S, Hartvig Honoré P. Simultaneous determination of cytosine arabinoside, daunorubicin and etoposide in human plasma. *J Chromatogr B* 2010; **878:** 1967-72.
11. Roth BJ, Johnson DH, Einhorn LH, Schacter LP, Cherng NC, Cohen HJ, et al. Randomized study of cyclophosphamide, doxorubicin, and vincristine versus etoposide and cisplatin versus alternation of these two regimens in extensive small-cell lung cancer: a phase III trial of the Southeastern Cancer Study Group. *J Clin Oncol* 1992; **10**: 282-91.
12. Skarlos DV, Samantas E, Kosmidis P, Fountzilas G, Angelidou M, Palamidas Ph, et al. Randomized comparison of etoposide-cisplatin vs. etoposide-carboplatin and irradiation in small-cell lung cancer. A Hellenic Co-operative Oncology Group Study. *Ann Oncol* 1994; **5:** 601-7.
13. Kosmidis PA, Samantas E, Fountzilas G, Pavlidis N, Apostolopoulou F, Skarlos D. Cisplatin/etoposide versus carboplatin/ etoposide chemotherapy and irradiation in small cell lung cancer randomized phase II study. Hellenic Cooperative Oncology Group for Lung Cancer Trials. *Semin Oncol* 1994; **21(Suppl 6):** 23-30.
14. Miller AA, Herndon JE 2nd, Hollis DR, Ellerton J, Langleben A, Richards F 2nd, et al. Schedule dependency of 21-day oral versus 3-day intravenous etoposide in combination with intravenous cisplatin in extensive-stage small-cell lung cancer: a randomized phase III study of the Cancer and Leukemia Group B. *J Clin Oncol* 1995; **13:** 1871-9.
15. Pujol JL, Daurès JP, Rivière A, Quoix E, Westeel V, Quantin X, et al. Etoposide plus cisplatin with or without the combination of 4'-epidoxorubicin plus cyclophosphamide in treatment of extensive small-cell lung cancer: a French Federation of Cancer Institutes multicenter phase III randomized study. *J Natl Cancer Inst* 2001; **93:** 300-8.
16. Quoix E, Breton JL, Daniel C, Jacoulet P, Debieuvre D, Paillot N, et al. Etoposide phosphate with carboplatin in the treatment of elderly patients with small-cell lung cancer: a phase II study. *Ann Oncol* 2001; **12:** 957-62.
17. Schiller JH, Adak S, Cella D, DeVore RF 3rd, Johnson DH. Topotecan versus observation after cisplatin plus etoposide in extensive-stage small-cell lung cancer: E7593-a phase III trial of the Eastern Cooperative Oncology Group. *J Clin Oncol* 2001; **19:** 2114-22.
18. Hanna N, Bunn Jr. PA, Langer C, Einhorn L, Guthrie T Jr, Beck T, et al. Randomized phase III trial comparing irinotekan/cisplatin with etoposide/cisplatin in patients with previously untreated extensive stage disease small-cell lung cancer. *J Clin Oncol* 2006; **24:** 2038-43.
19. Schmittel A, Fischer von Weikersthal L, Sebastian M, Martus P, Schulze K, Hortig P, et al. A randomized phase II trial of irinotekan plus carboplatin versus etoposide plus carboplatin treatment in patients with extended disease small-cell lung cancer. *Ann Oncol* 2006; **17:** 663-7.
20. Heigener DF, Manegold C, Jäger E, Saal JG, Zuna I, Gatzemeier U. Multicenter randomized open-label phase III study comparing efficacy, safety, and tolerability of conventional carboplatin plus etoposide versus dose-intensified carboplatin plus etoposide plus lenograstim in small-cell lung cancer in "extensive disease" stage. *Am J Clin Oncol* 2009; **32:** 61-4.
21. Lara PN Jr, Natale R, Crowley J, Lenz HJ, Redman MW, Carleton JE, et al. Phase III trial of irinotecan/cisplatin compared with etoposide/cisplatin in extensive-stage small-cell lung cancer: clinical and pharmacogenomic results from SWOG S0124. *J Clin Oncol* 2009; **27:** 2530-5.
22. Zatloukal P, Cardenal F, Szczesna A, Gorbunova V, Moiseyenko V, Zhang X, et al. A multicenter international randomized phase III study comparing cisplatin in combination with irinotecan or etoposide in previously untreated small-cell lung cancer patients with extensive disease. *Ann Oncol* 2010; **21:** 1810-6.
23. Maas HAAM, Janssen-Heijnen MLG, Olde Rikkert MGM, Machteld Wymenga AN. Comprehensive Geriatric assessment and its clinical impact in oncology. *Eur J Cancer* 2007; **43:** 2161-9.
24. Crawford J, Glaspy JA, Stoller RG, Tomita DK, Vincent ME, McGuire BW, et al. Final results of a placebo-controlled study of filgrastim in small-cell lung cancer: exploration of risk factors for febrile neutropenia. *Support Cancer Ther* 2005; **3:** 36-46.
25. Clarke's analysis of drugs and poisons. Moffat AC, Osselton MD, Widdop B, Watts J, editors. Available from: http://www.medicinescomplete.com/mc/clarke/current/CLK0691.htm?q=etoposide&t=search&ss=text&p=1#_hit. Accessed 19 September 2013.
26. López-Pousa A, Rifà J, Casas de Tejerina A, González-Larriba JL, Iglesias C, Gasquet JA, et al. Risk assessment model for first-cycle chemotherapy-induced neutropenia in patients with solid tumors. *Eur J Cancer Care* 2010; **19:** 648-55.
27. Lyman GH, Lyman CH, Agboola O. Risk models for predicting chemotherapy-induced neutropenia. *Oncologist* 2005; **10:** 427-37.
28. Režonja R, Knez L, Čufer T, Mrhar A. Oral treatment with etoposide in small cell lung cancer – dilemmas and solutions. *Radiol Oncol* 2013; **47**: 1-13.

case report

Mesenteric ischemia after capecitabine treatment in rectal cancer and resultant short bowel syndrome is not an absolute contraindication for radical oncological treatment

Ana Perpar[1], Erik Brecelj[2], Nada Rotovnik Kozjek[3], Franc Anderluh[1], Irena Oblak[1], Marija Skoblar Vidmar[1], Vaneja Velenik[1]

[1] Department of Radiotherapy, [2] Department of Oncological Surgery, [3] Clinical Nutrition Unit, Institute of Oncology Ljubljana, Ljubljana, Slovenia

Radiol Oncol 2015; 49(2): 181-184.

Received 10 December 2013
Accepted 23 January 2014

Correspondence to: Assist. Prof. Vaneja Velenik, M.D., Ph.D., Department of Radiotherapy, Institute of Oncology Ljubljana, Zaloška cesta 2, 1000 Ljubljana, Slovenia. Phone: +386 1 5879 661; Fax: +386 1 5879 304; E-mail: vvelenik@onko-i.si

Disclosure: No potential conflicts of interest were disclosed.

Background. Thrombotic events, arterial or venous in origin, still remain a source of substantial morbidity and mortality in cancer patients. The propensity for their development in oncology patients is partially a consequence of the disease itself and partially a result of our attempts to treat it. One of the rarest and deadliest thromboembolic complications is arterial mesenteric ischemia. The high mortality rate is caused by its rarity and by its non-specific clinical presentation, both of which make early diagnosis and treatment difficult. Hence, most diagnoses and treatments occur late in the course of the disease. The issue survivors of arterial mesenteric ischemia may face is short bowel syndrome, which has become a chronic condition after the introduction of parenteral nutrition at home.

Case report. We present a 73-year-old rectal cancer patient who developed acute arterial mesenteric thrombosis at the beginning of the pre-operative radiochemotherapy. Almost the entire length of his small intestine, except for the proximal 50 cm of it, and the ascending colon had to be resected. After multi-organ failure his condition improved, and he was able to successfully complete radical treatment (preoperative radiotherapy and surgery) for the rectal carcinoma, despite developing short bowel syndrome (SBS) and being dependent upon home-based parenteral nutrition to fully cover his nutritional needs.

Conclusions. Mesenteric ischemia and resultant short bowel syndrome are not absolute contraindications for radical oncological treatment since such patients can still achieve long-term remission.

Key words: rectal cancer; capecitabine; acute mesenteric ischemia; multiorgan failure; short bowel syndrome

Introduction

Standard treatment for locally advanced and/or node positive rectal cancer is neoadjuvant concomitant radiochemotherapy, surgery and adjuvant chemotherapy. All systemic therapy is 5-FU based.[1,2]

During treatment patients experience side effects, the most common of which are leukopenia, diarrhoea and proctitis, fatigue, nausea and vomiting, dermatitis, paraesthesia and hand-foot syndrome.[3] Most patients require supportive measures and symptomatic therapy to complete treatment. Severe toxicity, *e.g.* thrombotic events or coronary vasospasm, is rare.[3]

We present a patient with locally advanced rectal cancer who developed severe and life-threatening

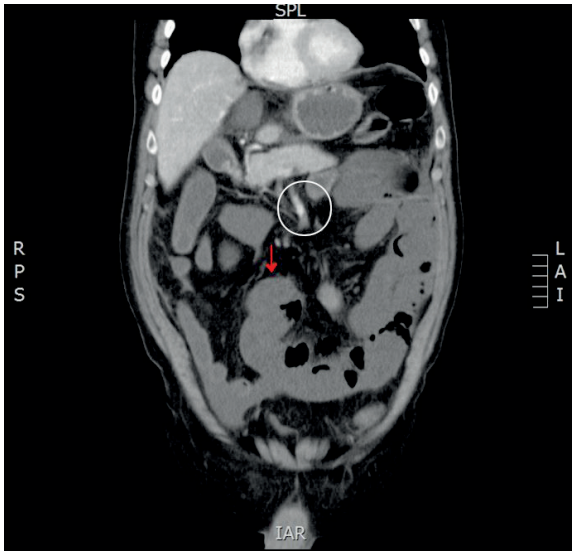

FIGURE 1. Image of a CT slice which confirmed superior mesenteric artery thrombosis (white circle) and resultant ischemia without contrast enhancement of the bowel wall (red arrow). For comparison there are some bowel loops with contrast enhancement of the bowel wall visible in the upper left part of the image.

complications during neoadjuvant treatment with mesenteric thrombosis and short bowel synrome. Good interdepartmental cooperation and multidisciplinary treatment played a key role in the successful treatment first for mesenteric ischemia and then for rectal cancer as well.

To our knowledge, ours is the first case described wherein a patient with acute mesenteric ischemia was able to complete specific treatment for a malignant disease.

Case report

A 73-year-old man presented with a 4-month history of bloody stools and weight loss. He had no previous relevant medical history. Magnetic resonance imaging (MRI) of the pelvis showed a T3N1 tumour of the rectum, 5 cm above the proximal margin of the anal sphincter.

Endoscopic biopsy confirmed a moderately differentiated adenocarcinoma. Abdominal ultrasound and chest x-ray excluded the presence of distant metastases, setting the stage at IIIB.

The patient was referred to an oncology multidisciplinary team, who made the decision to start pre-operative chemoradiotherapy after one cycle of induction chemotherapy with 2,500 mg/12h capecitabine within the framework of a national study. Written informed consent of patients was obtained for the treatments and for the scientific use of the clinical data according to Declarations of Helsinki.

After 10 days of chemotherapy the patient developed severe nausea, headaches, flushing and general weakness. Physical examination showed only tenderness in the upper abdomen. Laboratory tests showed leukocytosis with relative neutrophilia and hypophosphatemia; other results were normal.

Capecitabine was discontinued. Despite symptomatic therapy (with proton pump inhibitors, antiemetics, parenteral nutrition, analgesia and empiric antibiotics) his clinical condition and laboratory results worsened on the fifth day.

Computed tomography (CT) scan showed a thrombus in the superior mesenteric artery approximately 5 cm distal of the aorta; dilated jejunal, ileal and colonic loops with absence of contrast enhancement in the intestinal wall.

The patient was admitted to the intensive care unit, where he received fluid infusion, vasoactive support with noradrenaline, repeated transfusions of thrombocytes, and fresh frozen plasma; the metabolic acidosis was corrected.

After the patient had been declared stable enough for surgery, a laparotomy was performed and the small bowel, except for the proximal 50 cm of it, along with the right colon were resected despite the rectal tumour. A jejunal-transverse anastomosis was constructed. An attempt at revascularization was not considered due to the clearly necrotic appearance of the affected intestine. Histological examination of the resected gut showed gangrene and multiple thrombi in the vessel walls.

In the intensive care unit he developed sepsis, multi-organ failure (with hemodynamic instability, respiratory insufficiency, hepatic and renal failure, coagulopathy) and fistulae as enteric contents started to leak from the laparotomy wound and through two surgical drains.

The decision was made not to operate but to manage the patient conservatively. The patient's condition improved; he was hemodynamically stable, he no longer needed oxygen, his organ function was restored and his fever subsided.

On the nineteenth post-operative day, the patient was extubated and he began physiotherapy.

Additional imaging showed enterocutaneous fistulae among the jejunal loops, skin and enterocolic anastomosis, as well as a pancreatic pseudocyst.

The multidisciplinary team composed of radiation therapists, an oncologic surgeon and an anaes-

thesist specializing in artificial nutrition decided to continue specific oncologic treatment and simultaneously treat gastrointestinal failure with parenteral nutrition.

The rectal carcinoma was treated with short-course pre-operative radiotherapy (5 x 5 Gy) and surgery, during which the fistulae were excised and jejuno-colic re-anastomosis was done. Rectal cancer was treated with total mesorectal excision and permanent colostomy. Post-operatively, the patient developed a paracolic hematoma and a presacral abscess which was drained when he was well enough to be transferred to the regular ward.

The patient remained on home parenteral nutrition (HPN) because of short bowel syndrome. No complications arose during oncologic treatment and the patient is to date in good health and without any signs of recurrence.

Discussion

Cancer patients face an increased risk of thrombosis as a consequence of their disease and/or its treatment. While the majority of thrombotic events occurring in cancer patients are of venous origin, arterial thrombosis is a well-documented, albeit rarer, entity.

Chemotherapy has been identified as a risk factor for thrombosis and may, depending on the agent, damage the endothelium, induce cytokine release, activate platelets and disrupt the balance between the pro- and anti-thrombotic molecules.[4]

The toxic effects of fluorouracil on the endothelium and the serum concentration of anti-thrombotic molecules have been studied[4] and most likely apply to capecitabine, a pro-drug of fluorouracil, as well.

Acute mesenteric ischemia (AMI) is an uncommon entity, affecting less than 0.1% of hospitalised patients.[5] It is most commonly caused by superior mesenteric artery embolism (40–50%) and thrombosis (15–30%).[6,7]

With its high sensitivity (96–100%) and specificity (89–92%), CT angiography remains the gold standard for the diagnosis of mesenteric ischemia. [6,7]

Treatment decisions are affected by the intraoperative appearance of the bowel. Evidently necrotic bowel loops should be resected, while in any other case, treatment is guided by the principle of arterial reperfusion before intestinal resection is considered, which has in a recent series of three cases proven to be a safe and effective method.[5]

There exists no data about the outcome of intestinal resection in patients with untreated rectal cancer.

Our patient's surgery resulted in short bowel syndrome (SBS), which is a consequence of a massive anatomical and/or functional loss of intestine, where a reduced small-bowel surface area leads to malabsorption and dehydration. SBS may occur as a consequence of surgery (25%), irradiation/cancer (24–46%), mesenteric vascular disease (15–22%), Crohn's disease (16–19%) and other benign causes (13–20%).[8,9]

The early management of a patient with SBS is that of a critically ill surgical patient, while later, the primary objective is artificial nutritional support at the patient's home. Enteral intake should be encouraged to minimise dependence on parenteral nutrition.[10]

The patient had type II SBS with a jejunal-colonic anastomosis and from the beginning it was clear that he will remain dependent upon the parenteral supply of adequate energy and nutrients. Despite that the specific oncologic treatment went well with no major complications.

There are three types of intestinal anatomy in SBS, depending on the presence of the colon and ileocecal valve.[11] Presence of the distal ileum/ileocecal valve is essential to slowing the transit and preventing bacterial overgrowth, while the colon is able to absorb water, electrolytes and fatty acids; both functions serve as a deterrent to the development of diarrhoea, an important cause of malnutrition.[11]

Patients with SBS on parenteral nutrition are at risk of many complications: catheter occlusion and breakage; catheter infections and thrombosis of the central venous access, metabolic disturbances and small bowel bacterial overgrowth.[11]

Conclusions

Cancer patients face an increased risk of thrombosis as a result of their disease and its treatment. The risks and benefits of aggressive oncological treatment should always be carefully weighed, especially in patients with a good prognosis.

However, with adequate parenteral nutrition and medical support, SBS is not an absolute contraindication for specific oncologic treatment, especially if said treatment is expected to result in cure and/or long-term remission.

Even though the prognosis of patients with bowel necrosis and systemic inflammatory response is

dismal, long-term survival is still possible with adequate treatment and management.

References

1. Glimelius B, Tiret E, Cervantes A, Arnold D. Rectal cancer: ESMO Clinical Practice Guidelines for diagnosis, treatment and follow-up. *Ann Oncol* 2013; **24(Suppl 6):** vi81-8.
2. Oblak I, Velenik V, Anderluh F, Mozina B, Ocvirk J. The correlation between the levels of tissue inhibitor of metalloproteinases 1 in plasma and tumour response and survival after preoperative radiochemotherapy in patients with rectal cancer. *Radiol Oncol* 2013; **47:** 138-44.
3. Walko CM, Lindley C. Capecitabine: a review. *Clin Ther* 2005; **27:** 23-44.
4. Haddad TC, Greeno EW. Chemotherapy-induced thrombosis. *Thromb Res* 2006; **118:** 555-68.
5. Kuhelj D, Kavcic P, Popovic P. Percutaneous mechanical thrombectomy of superior mesenteric artery embolism. *Radiol Oncol* 2013; **47:** 239-43.
6. Wyers MC. Acute mesenteric ischemia: diagnostic approach and surgical treatment. *Semin Vasc Surg* 2010; **23:** 9-20.
7. Dewitte A, Biais M, Coquin J, Fleureau C, Cassinotto C, Ouattara A, et al. Diagnosis and management of acute mesenteric ischemia. *Ann Fr Anesth Reanim* 2011; **30:** 410-20.
8. Thompson JS, DiBaise JK, Iyer KR, Yeats M, Sudan DL. Postoperative short bowel syndrome. *J Am Coll Surg* 2005; **201:** 85-9.
9. Bakker H, Bozzetti F, Staun M, Leon-Sanz M, Hebuterne X Pertkiewicz M. Home parenteral nutrition in adults: a european multicentre survey in 1997. ESPEN-Home Artificial Nutrition Working Group. *Clin Nutr* 1999; **18:** 135-40.
10. DiBaise JK, Young RJ, Vanderhoof JA. Intestinal rehabilitation and the short bowel syndrome: part 2. *Am J Gastroenterol* 2004; **99:** 1823-32.
11. DiBaise JK, Young RJ, Vanderhoof JA. Intestinal rehabilitation and the short bowel syndrome: part 1. *Am J Gastroenterol* 2004; **99:** 1386-95.

research article

Clinical applicability of biologically effective dose calculation for spinal cord in fractionated spine stereotactic body radiation therapy

Seung Heon Lee[1], Kyu Chan Lee[1], Jinho Choi[1], So Hyun Ahn[1], Seok Ho Lee[1], Ki Hoon Sung[1], Se Hee Kil[2]

[1] Department of Radiation Oncology; [2] Gachon Medical Research Institute, Gachon University Gil Medical Center, Republic of Korea

Radiol Oncol 2015; 49(2): 185-191.

Received 7 November 2014
Accepted 5 January 2015

Correspondence to: Kyu Chan Lee, M.D., Ph.D., Department of Radiation Oncology, Gachon University Gil Medical Center 21, 774 beon-gil, Namdong-daero, Namdong-gu, Incheon, 405-460, Republic of Korea. Phone: +82 32 460 8050; Fax: +82 32 460 3009; E-mail: kyu22@gilhospital.com

Disclosure: No potential conflicts of interest were disclosed.

Background. The aim of the study was to investigate whether biologically effective dose (BED) based on linear-quadratic model can be used to estimate spinal cord tolerance dose in spine stereotactic body radiation therapy (SBRT) delivered in 4 or more fractions.

Patients and methods. Sixty-three metastatic spinal lesions in 47 patients were retrospectively evaluated. The most frequently prescribed dose was 36 Gy in 4 fractions. In planning, we tried to limit the maximum dose to the spinal cord or *cauda equina* less than 50% of prescription or 45 $Gy_{2/2}$. BED was calculated using maximum point dose of spinal cord.

Results. Maximum spinal cord dose per fraction ranged from 2.6 to 6.0 Gy (median 4.3 Gy). Except 4 patients with 52.7, 56.4, 62.4, and 67.9 $Gy_{2/2}$, equivalent total dose in 2-Gy fraction of the patients was not more than 50 $Gy_{2/2}$ (12.1–67.9, median 32.0). The ratio of maximum spinal cord dose to prescription dose increased up to 82.2% of prescription dose as epidural spinal cord compression grade increased. No patient developed grade 2 or higher radiation-induced spinal cord toxicity during follow-up period of 0.5 to 53.9 months.

Conclusions. In fractionated spine SBRT, BED can be used to estimate spinal cord tolerance dose, provided that the dose per fraction to the spinal cord is moderate, e.g. < 6.0 Gy. It appears that a maximum dose of up to 45–50 $Gy_{2/2}$ to the spinal cord is tolerable in 4 or more fractionation regimen.

Key words: biologically effective dose; spine stereotactic body radiation therapy; spinal cord; tolerance dose; linear quadratic model

Introduction

Stereotactic body radiation therapy (SBRT) has been increasingly applied to the management of spinal metastases with encouraging clinical results of rapid and durable pain relief.[1,2] SBRT is also effective for treating radio-resistant metastatic tumours, such as, renal cell carcinoma or malignant melanoma.[3,4]

The spinal cord is the major dose-limiting tissue in spine SBRT. In conventionally fractionated radiation therapy, the tolerance dose for the spinal cord has been reported to be 50 Gy for cord lengths of 5 and 10 cm, and 47 Gy for 20 cm, given a probability of myelopathy of less than 5% within 5 years.[5] Schultheiss reported that the probabilities of myelopathy were 0.03% and 0.2% at 45 Gy and 50 Gy, respectively.[6] For single fraction SBRT, Ryu *et al.* reported a partial volume tolerance of the human spinal cord of at least 10 Gy to 10% of the spinal cord volume when spinal cord volume was defined from 6 mm above and to 6 mm below the

TABLE 1. Patient and tumour characteristics

Age (year, median)	33–86 (56)
Histology (person)	
Lung	13
Colorectal	11
Breast	6
Pancreas	3
Hepatocellular	3
Stomach	2
Cholangiocarcinoma	2
Prostate	2
Renal cell	1
Other	4
Spine level (lesion)	
Cervical	3
Cervicothoracic	4
Thoracic	37
Thoracolumbar	5
Lumbar	14
Number of involved spine segments per PTV (lesion)	
1	24
2	17
3	16
4	3
5	3
Tumour volume (cc, median)	1.0–176.7 (21.0)
PTV volume (cc, median)	17.9–340.8 (59.1)
Number of treated sites per patient (person)	
1	35
2	8
3	4
ESCC grade[20] (lesion)	
0	14
1a	15
1b	9
1c	5
2	18
3	2

ESCC = epidural spinal cord compression; PTV = planning target volume

treatment target.[7] Sahgal *et al.* suggested 10 Gy as a maximum safe threshold for single fraction SBRT to the thecal sac.[8]

In fractionated spine SBRT, however, variable dose schedules are applied and no reliable dose comparison method has been established for the target or the spinal cord. Since Fowler first proposed the term 'biologically effective dose' based on linear-quadratic (LQ) cell survival model in 1989, BED has been used to compare the biologic effects of various radiotherapy schedules.[9] However, because prescription doses in fractionated spine SBRT are usually between 6 and 10 Gy per fraction, several authors have argued that the simple application of BED based on LQ model is not appropriate in SBRT.[10-18] The extrapolations using the LQ model beyond 5–6 Gy per fraction are likely to lack clinically useful precision.[19]

Modern linear accelerator based stereotactic radiotherapy technology using a fine multileaf collimator of 2.5 mm thickness could deliver highly conformal radiation to the target while sparing the spinal cord with the merit of a steep dose gradient just outside the target. The irradiated dose to the spinal cord can be more strictly limited and is usually much lower than the prescription dose in fractionated spine SBRT. We hypothesized that if maximum doses per fraction to the spinal cord are less than 6 Gy, BED based on LQ model could be used to estimate spinal cord tolerance dose in fractionated spine SBRT. We usually implemented fractionated spine SBRT in 4 or 5 fractions to avoid complications such as radiation-induced myelopathy and vertebral compression fracture.

To determine if BED based on LQ model can be used to estimate spinal cord tolerance dose in fractionated spine SBRT of 4 or more fractionation regimen, the plans used for actual fractionated SBRT at our institution were analysed retrospectively and clinical outcomes, including complications, were investigated.

Patients and methods

Sixty-three metastatic spinal lesions in 47 patients were treated by spine SBRT between January 2010 and March 2014. Median patient age was 56 (range 33–86) and 27 patients (57.4%) were male. The thoracic spine was the most frequent site for treatment. Of the 63 lesions, 41 lesions involved single or two contiguous spine segments. When categorized with the epidural spinal cord compression (ESCC) grading system, 43.5% of the lesions belonged to

grade 1c (deformation of the thecal sac with spinal cord abutment), 2 (spinal cord compression, but with cerebrospinal fluid [CSF] visible around the cord) or 3 (spinal cord compression, no CSF visible around the cord) (Table 1).[20] No patients received surgical intervention, vertebroplasty or kyphoplasty, prior to spine SBRT.

All patients underwent CT simulation with an appropriate immobilization technique to obtain SBRT planning images. To delineate targets and spinal cords, T2-weighted and gadolinium contrast T1-weighted MRI sequences with a 3 mm slice thickness including at least one vertebral body above and below the target were obtained and fused to the planning CT image using iPlan software (version 4.1, BrainLAB, Germany). Gross tumour volume (GTV) included gross visible tumour in spine, paraspinal, or epidural area on MR or enhanced planning CT images. Planning target volumes (PTV) were derived from GTVs by encompassing involved vertebral body and including anterior and/or posterior elements of the spine depending on the location of metastatic lesions as described in RTOG 0631.[21] Median PTV volume was 65.6 cc (range, 17.9–340.8 cc). The spinal cord was contoured starting from 6 mm above the superior of the PTV to 6 mm below the inferior of the PTV. However, the spinal cord was always excluded from the PTV, with a 1–2 mm free margin if the GTV did not abut onto the cord. Other organs, such as heart, lungs, oesophagus, large vessels, trachea, liver, and kidneys were delineated depending on tumour vertebral level.

The most frequently prescribed dose was 36 Gy in 4 fractions, followed by 40 Gy in 5 fractions (Table 2). The requirement for clinical implementation was > 80% of the prescription dose to > 90% of the PTV, or a mean PTV dose > 95% of prescription. The spinal cord dose was converted to equivalent total dose in 2-Gy fraction (EQD_2) using the following formula provided below. This model was derived from the LQ model assuming an α/β ratio of 2 for the late effect of spinal cord.

$$EQD_2\ (Gy_{2/2}) = \text{Total dose} \times \left(\frac{\text{Dose per fraction} + \alpha/\beta}{2 + \alpha/\beta} \right)$$

We tried to limit the maximum dose to the spinal cord or *cauda equina* less than 50% of prescription or 45 $Gy_{2/2}$. Maximum dose per fraction to the spinal cord of each plan was investigated.

All patients were treated using the Novalis Tx™ (Varian, USA) equipped with a 2.5 mm multileaf collimator. Thirty-five patients received SBRT to a single treatment site spanning one to five vertebral segments. Eight patients received SBRT to 2 separate sites and 4 patients to 3 sites. Re-SBRT was performed in one patient with hepatocellular carcinoma at 5 months after initial SBRT because of the recurrence of severe pain due to tumour progression.

TABLE 2. Prescription dose to planning target volume and maximum dose to spinal cord

Total dose / fractions	Number	Maximum dose to spinal cord (EQD_2, $Gy_{2/2}$)
26.0 Gy / 4 fractions	1	24.8
28.0 Gy / 4 fractions	1	25.4
30.0 Gy / 4 fractions	1	52.7
32.0 Gy / 4 fractions	2	25.5–56.4
36.0 Gy / 4 fractions	23	12.1–67.9
40.0 Gy / 4 fractions	1	24.3
44.0 Gy / 4 fractions	2	38.9–44.4
32.5 Gy / 5 fractions	6	16.6–43.0
35.0 Gy / 5 fractions	4	25.7–49.0
40.0 Gy / 5 fractions	19	24.2–41.1
42.5 Gy / 5 fractions	1	38.7
42.0 Gy / 6 fractions	2	39.8–62.4

BED = biologically effective dose; EQD_2 = equivalent dose in 2-Gy fractions with an α/β ratio of 2

Patients were followed up clinically and radiographically at 1- to 3-month intervals. A visual analogue scale (VAS) was used to measure pain before and after treatment. Symptomatic responses were scored as defined by RTOG 0631.[21] All available follow up MRIs were reviewed to assess radiographic responses. Radiologic local failure was defined as local tumour growth by MRI. Late complications were scored as described by Common Toxicity Criteria for Adverse Events, version 4.0. Overall survival was estimated by the Kaplan–Meier method. The relationship between radiologic local failure and variable candidate risk factors such as spinal cord to tumour distance, spinal cord to PTV distance, minimum dose administered to tumour, and tumour volume was analyzed by the Mann-Whitney U-test. The retrospective study was approved by the institutional review board committee and was according to the Helsinki Declaration.

Results

Inhomogeneous dose distributions inside the spinal cord and very steep dose gradients around it were observed (Figure 1A). Approximately 10% decrease of dose per millimetre was observed from

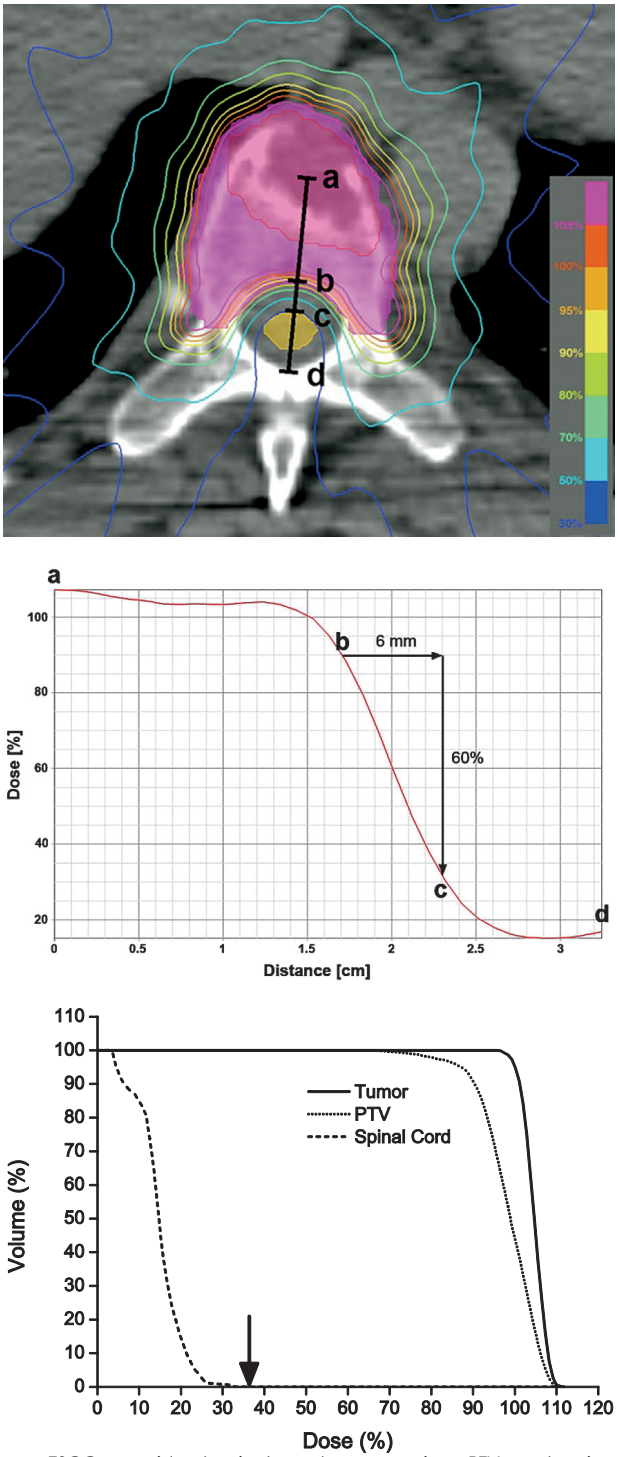

ESCC = epidural spinal cord compression; PTV = planning target volume

FIGURE 1. An example of dose distribution in a patient with disease of the T7 vertebral body only (ESCC grade[20] 0). **(A, B)** Dose profile from the center of the tumour (a) to the posterior edge of the thecal sac (d). Note that the dose gradient around the spinal cord in this case is steepest between (b) and (c), where 90% and 30% isodose lines, and is approximately 10% per millimeter. **(C)** Dose volume histogram of the patient shows much difference of the doses to target and spinal cord. The maximum dose per fraction to the spinal cord (arrow) was 37% (3.0 Gy) of the prescription dose (9.0 Gy).

PTV margin to the surface of spinal cord (Figure 1B). Maximum dose to spinal cord was much lower than prescription dose (Figure 1C). According to PTV shape and spinal cord proximity, maximum spinal cord doses varied from 10.5 Gy to 33.2 Gy (median 20.2 Gy). When they were divided by corresponding fraction numbers, the maximum spinal cord dose per fraction ranged from 2.6 to 6.0 Gy (median 4.3 Gy). Maximum EQD_2 to spinal cords ranged from 12.1 to 67.9 $Gy_{2/2}$ (median 32.0 $Gy_{2/2}$). Six cords were administered more than 45 $Gy_{2/2}$ and doses of them were 48.0, 49.0, 52.7, 56.4, 62.4, and 67.9 $Gy_{2/2}$, respectively. The ratio of maximum spinal cord dose to prescription dose increased up to 82.2% of prescription dose as the ESCC grade increased (Table 3).

Median follow-up period was 7.1 months (0.5–53.9 months) and median overall survival was 10.2 months. During follow-up, 26 patients succumbed to systemic disease progression. VAS results were available for 46 of the 63 lesions. Mean VAS declined from 7.8 before to 2.7 after SBRT. Complete response was achieved for 10 lesions and partial response for 28 lesions.

Follow-up MRIs were available for 27 lesions. Radiologic local failure occurred in 4 lesions (14.8%, Table 4). All patients in the radiologic local failure group (4 patients) had spinal cord compression (ESCC grade 2) before SBRT. In the non-failure group (23 patients), distances between spinal cords and tumours or PTVs ranged from 0 to 14 mm (median 2.3) or from 0 to 3.5 mm (median 1.0), respectively. Spinal cord to tumour distance ($p < 0.001$), spinal cord to PTV distance ($p = 0.003$), and minimum dose administered to tumours ($p = 0.040$) in the local failure group were significantly smaller than those in the non-failure group. No intergroup difference of tumour volumes was observed. There has been no grade 2 or more radiation-induced spinal cord toxicity during follow up period up to 53.9 months. There were three compression fractures (3 of 27, 11.1%); two resulted from progressions of existing fractures and the other was a new fracture. Fractures occurred at 2, 3, and 4 months after treatment, respectively.

Discussion

BED based on the LQ model has been widely accepted for the comparisons of doses administered in different treatment schedules in treating with conventional multifractionated irradiation. However, dose comparisons for fractionated spine

SBRT based on simple BED calculations should be approached with caution. First, BED was developed and validated based on homogenous radiation dose distributions in irradiated areas.[22,23] The radiation dose administered to the spinal cord in SBRT is intrinsically inhomogeneous because it is performed with an intensity modulated radiation beam. The data regarding the tolerance of the rat cervical spinal cord suggested that small volume of rat spinal cord tolerates a greater dose compared to homogeneous radiation.[24,25] Although those observations were not found in swine model, the tolerance dose of spinal cord for partial-volume irradiation closely resembled that for rats, mice and guinea pigs receiving uniform spinal cord irradiation.[26] Therefore, estimated spinal cord tolerance using BED calculation for partial-volume irradiation seems to be more conservative than, or at least comparable to that for uniform irradiation.

Second, BED has been based on the data of conventional fraction size. However, in fractionated SBRT, prescription dose per fraction is relatively high, usually 6–20 Gy. Fundamental arguments have arisen as to whether the LQ model is a valid method for assessing BED when doses per fraction are high. Brenner *et al*. reported that the LQ model is reasonably well validated experimentally and theoretically up to about 10 Gy per fraction, and suggested that its use is reasonable up to about 18 Gy per fraction.[27] However, several authors have argued to the contrary. Iwata *et al.* studied the applicability of the LQ model for dose conversion in high dose per fraction radiotherapy using cell survival data for V79 Chinese hamster lung fibroblasts and EMT6 mouse mammary sarcoma cells.[14] It was found that the LQ model fitted relatively well at doses of 5 Gy or less as compared with the repairable-conditionally repairable model and the multi-target model. Timmerman *et al*. proposed a universal survival curve that hybridizes the LQ model survival curve for the low-dose range and the multi-target model asymptote for the high-dose range.[15] They reported a transition dose at which the LQ model smoothly transits to the terminal asymptote of the multi-target model. The transition dose calculated using 12 non-small-cell lung cancer (NSCLC) cell lines was 6.2 Gy, which means that LQ model may not be applicable for dose ranges of more than 6.2 Gy. Recently, Song *et al.* argued that the usefulness of the LQ model is likely to be limited when tumours are treated with high dose per fraction, usually more than 10 Gy, because LQ model and other modified-LQ models are based on the assumption that radiation-induced cell death in tumours is due solely to DNA strand breaks. They suggested indirect/necrotic cell death as a consequence of vascular damage plays an important role in SBRT.[17,18] As of now, the applicability of BED based on the LQ model to the high dose per fraction radiation remains a controversial issue.

According to the current radiobiological knowledge as mentioned above, BED based on the LQ model seems to be clinically applicable if the dose is limited to 6 Gy or less, especially for normal tissue, not tumour. With current technical developments, dose to the spinal cord can be maintained at much lower levels than the prescription dose due to the steep dose gradient just outside the target. In the present study, the maximum irradiation dose per fraction to the spinal cord varied from 2.6 to 6.0 Gy (median 4.3 Gy) depending on the PTV shape and its proximity to the spinal cord. Because the dose per fraction to the spinal cord was less than 6.0 Gy, it would be reasonable to estimate spinal cord tolerance dose in fractionated SBRT using BED based on LQ model.

Recently, Sahgal *et al.* recommended limiting maximum point dose to 23.0 Gy in 4 fractions

TABLE 3. Spinal cord dose classified using the epidural spinal cord compression (ESCC) grading system[20]

Grade	lesions	D_{max} (Gy, median)	$EQD_{2\ max}$ ($Gy_{2/2}$, median)	D_{max} / prescription dose (%, median)
0	14	12.0–25.5 (18.3)	15.0–38.9 (29.6)	33.4–60.7 (50.5)
1a	15	10.5–25.3 (20.8)	12.1–52.7 (32.0)	29.1–84.3 (52.0)
1b	9	13.9–23.4 (19.3)	16.6–44.4 (33.4)	40.3–56.2 (53.4)
1c	5	16.3–22.3 (17.5)	24.8–36.1 (28.0)	45.9–63.8 (57.1)
2	18	16.5–33.2 (21.8)	24.2–67.9 (36.1)	43.9–81.1 (58.4)
3	2	21.4–26.3 (23.9)	39.3–56.4 (47.9)	59.4–82.2 (70.8)

D_{max} = maximum dose to spinal cord; $EQD_{2\ max}$ = maximum equivalent dose in 2-Gy fractions with an α/β ratio of 2; ESCC = epidural spinal cord compression

TABLE 4. Distances from spinal cord to tumour or planning target volume (PTV), minimum tumour doses, and tumour volumes according to radiologic local failure status

	Failure group (4 lesions)	Non-failure group (23 lesions)	p-value**
Distance between SC and tumour (mm, median)	0*	0–14.0 (2.3)	< 0.001
Distance between SC and PTV (mm, median)	0*	0–3.5 (1.0)	0.003
Minimum tumour dose (Gy, median)	15.4–23.8 (20.0)	15.3–44.7 (25.2)	0.040
Tumour volume (cc, median)	13.7–47.3 (20.8)	1.0–176.7 (20.9)	0.468

SC = spinal cord; * All tumours compressed the spinal cord; ** Statistical significance was determined using the Mann-Whitney U-test

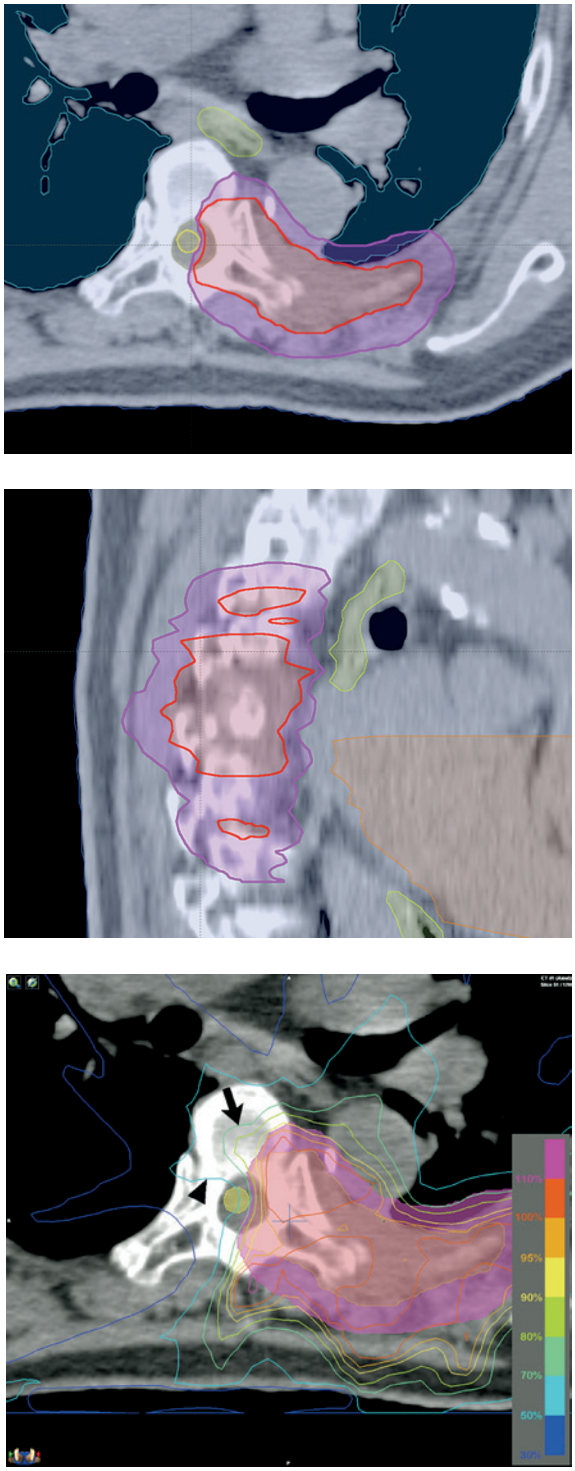

ESCC = epidural spinal cord compression;GTV = gross tumour volume; PTV = planning target volume

FIGURE 2. (A, B) Target volume (GTV: red, PTV: magenta) delineation in a patient with cord compression (ESCC grade[20] 2) and paraspinal mass. Five spine segments were involved in the PTV. **(C)** Dose distribution around the spinal cord. The 70% (arrow) and 50% (arrowhead) isodose lines are shown. The maximum spinal cord dose was 33.2 Gy, which was equivalent to 78.9% of the prescription dose of 42 Gy in 6 fractions.

and 25.3 Gy in 5 fractions for a risk of radiation myelopathy of less than 5%.[28] Dividing the constraint dose by fraction number, maximum point doses per fraction to the thecal sac are 5.75 Gy and 5.06 Gy, respectively. The calculated EQD_2 of thecal sac based on the LQ model for these schedules were 44.6 $Gy_{2/2}$ and 44.7 $Gy_{2/2}$, respectively. These seem to be reasonable because the tolerance dose of spinal cord in conventionally fractionated radiation therapy is 45-50 Gy with fraction size of 1.8 or 2.0 Gy when full thickness of the cord is irradiated. In Sahgal's data, there was no radiation myelitis after irradiation in 4 or 5 fractions, though the patient number is relatively small, 9 cases. In the present study, except 4 patients, all patients were administered a maximum spinal cord dose less than 50 $Gy_{2/2}$ and no radiation myelopathy was observed among 63 cases.

Gerszten *et al*. reported that post-SBRT tumour progressions often occurred at the edge of contoured treatment volumes and the overall mean tumour volume of local failure cases was 40% greater than the average for their series.[29] Chang *et al.* also reported that failure at the epidural space adjacent to the spinal cord is a major reason for tumour progression after spine SBRT.[10] In the present study, minimum tumour dose ($p = 0.040$), which is mainly affected by distance between spinal cord and tumour ($p < 0.001$) or PTV ($p = 0.003$) appeared to have more influence on local failure. Furthermore, when the tumour did not abut the spinal cord, local failure was not observed even in tumours larger than those in local failure group. These results mean that tumoricidal dose was not delivered to tumour because of the proximity of spinal cord in local failure group. BED calculation has clinical impact on choosing appropriate fraction size and number to deliver optimal tumour dose, especially for the lesions close to spinal cord, while limiting spinal cord dose of less than 45–50 $Gy_{2/2}$.

When a tumour abuts the spinal cord, increasing the number of fractions to deliver potentially tumoricidal dose, with lowering spinal cord BED, might be considered. In the patient shown in Figure 2, there was a large paraspinal tumour mass compressing the spinal cord. By increasing the number of fractions to 6 and decreasing the prescription dose per fraction to the PTV to 7 Gy, we tried to spare the spinal cord delivering 42 Gy to the GTV to improve local control. Although maximum EQD_2 of the spinal cord was 62.4 $Gy_{2/2}$, we treated this patient in the palliative setting because local tumour control was important for the quality of life of the patient.

This study has several limitations; it is a retrospective and single center study, cohort was small, and there was no myelopathy case. Rare but severe events like myelopathy require high patient numbers to evaluate safe tolerance doses and it should not give a false sense of security. Although no myelopathy was observed in 6 patients who were administered a maximum spinal cord dose greater than 45 $Gy_{2/2}$, their survival period was only 1.5–6.4 months. They had multiple metastases in liver or lung and had short life expectancy. Therefore, it is not possible to suggest more doses for spinal cord tolerance above this dose level. However, we believe that the data of our study is important for applying BED calculation for spinal cord tolerance dose in various clinical situations. We plan to conduct a multi-center prospective study with more patients.

In conclusion, BED can be used to estimate spinal cord tolerance dose, provided that the dose per fraction to the spinal cord is moderate, e.g. < 6.0 Gy in fractionated spine SBRT. Within this dose range it appears that a maximum dose of up to 45–50 $Gy_{2/2}$ to the spinal cord is tolerable. The minimum tumour dose, which is mainly affected by tumour to spinal cord distance, seems to significantly affect local failure. When a tumour abuts or is closely located to the spinal cord, we suggest adjustment of the fractionation schedule based on BED calculations, while maintaining the desirable dose to the target. Randomized controlled dose escalation study is reserved to verify this suggestion.

Acknowledgments

This work was supported by Gachon University Gil Medical Center (Grant number : 2013-42).

References

1. Ryu S, Jin R, Jin JY, Chen Q, Rock J, Anderson J, et al. Pain control by image-guided radiosurgery for solitary spinal metastasis. *J Pain Symptom Manage* 2008; **35:** 292-8.
2. Wang XS, Rhines LD, Shiu AS, Yang JN, Selek U, Gning I, et al. Stereotactic body radiation therapy for management of spinal metastases in patients without spinal cord compression: a phase 1-2 trial. *Lancet Oncol* 2012; **13:** 395-402.
3. Balagamwala EH, Angelov L, Koyfman SA, Suh JH, Reddy CA, Djemil T, et al. Single-fraction stereotactic body radiotherapy for spinal metastases from renal cell carcinoma. *J Neurosurg Spine* 2012; **17:** 556-64.
4. Stinauer MA, Kavanagh BD, Schefter TE, Gonzalez R, Flaig T, Lewis K, et al. Stereotactic body radiation therapy for melanoma and renal cell carcinoma: impact of single fraction equivalent dose on local control. *Radiat Oncol* 2011; **6:** 34.
5. Emami B, Lyman J, Brown A, Coia L, Goitein M, Munzenrider JE, et al. Tolerance of normal tissue to therapeutic irradiation. *Int J Radiat Oncol Biol Phys* 1991; **21:** 109-22.
6. Schultheiss TE. The radiation dose-response of the human spinal cord. *Int J Radiat Oncol Biol Phys* 2008; **71:** 1455-9.
7. Ryu S, Jin JY, Jin R, Rock J, Ajlouni M, Movsas B, et al. Partial volume tolerance of the spinal cord and complications of single-dose radiosurgery. *Cancer* 2007; **109:** 628-36.
8. Sahgal A, Ma L, Gibbs I, Gerszten PC, Ryu S, Soltys S, et al. Spinal cord tolerance for stereotactic body radiotherapy. *Int J Radiat Oncol Biol Phys* 2010; **77:** 548-53.
9. Fowler JF. The linear-quadratic formula and progress in fractionated radiotherapy. *Br J Radiol* 1989; **62:** 679-94.
10. Chang EL, Shiu AS, Mendel E, Mathews LA, Mahajan A, Allen PK, et al. Phase I/II study of stereotactic body radiotherapy for spinal metastasis and its pattern of failure. *J Neurosurg Spine* 2007; **7:** 151-60.
11. Sahgal A, Ames C, Chou D, Ma L, Huang K, Xu W, et al. Stereotactic body radiotherapy is effective salvage therapy for patients with prior radiation of spinal metastases. *Int J Radiat Oncol Biol Phys* 2009; **74:** 723-31.
12. Ahmed KA, Stauder MC, Miller RC, Bauer HJ, Rose PS, Olivier KR, et al. Stereotactic body radiation therapy in spinal metastases. *Int J Radiat Oncol Biol Phys* 2012; **82:** e803-9.
13. Nelson JW, Yoo DS, Sampson JH, Isaacs RE, Larrier NA, Marks LB, et al. Stereotactic body radiotherapy for lesions of the spine and paraspinal regions. *Int J Radiat Oncol Biol Phys* 2009; **73:** 1369-75.
14. Iwata H, Matsufuji N, Toshito T, Akagi T, Otsuka S, Shibamoto Y. Compatibility of the repairable-conditionally repairable, multi-target and linear-quadratic models in converting hypofractionated radiation doses to single doses. *J Radiat Res* 2013; **54:** 367-73.
15. Park C, Papiez L, Zhang S, Story M, Timmerman RD. Universal survival curve and single fraction equivalent dose: useful tools in understanding potency of ablative radiotherapy. *Int J Radiat Oncol Biol Phys* 2008; **70:** 847-52.
16. Kirkpatrick JP, Brenner DJ, Orton CG. Point/Counterpoint. The linear-quadratic model is inappropriate to model high dose per fraction effects in radiosurgery. *Med Phys* 2009; **36:** 3381-4.
17. Song CW, Kim MS, Cho LC, Dusenbery K, Sperduto PW. Radiobiological basis of SBRT and SRS. *Int J Clin Oncol* 2014; **19:** 570-8.
18. Song CW, Park I, Cho LC, Yuan J, Dusenbery KE, Griffin RJ, et al. Is indirect cell death involved in response of tumors to stereotactic radiosurgery and stereotactic body radiation therapy? *Int J Radiat Oncol Biol Phys* 2014; **89:** 924-5.
19. Joiner MC, Bentzen SM. Fractionation: the linear-quadratic approach. In: Joiner M, van der Kogel A, editors. *Basic Clinical Radiobiology.* London: Hodder Education; 2009. p. 102-19.
20. Bilsky MH, Laufer I, Fourney DR, Groff M, Schmidt MH, Varga PP, et al. Reliability analysis of the epidural spinal cord compression scale. *J Neurosurg Spine* 2010; **13:** 324-8.
21. Ryu S, Pugh SL, Gerszten PC, Yin FF, Timmerman RD, Hitchcock YJ, et al. RTOG 0631 phase II/III study of image-guided stereotactic radiosurgery for localized (1-3) spine metastases: phase II results. *Int J Radiat Oncol Biol Phys* 2011; **81:** S131-2.
22. Fowler JF. Alpha, beta, and surviving fraction. *Int J Radiat Oncol Biol Phys* 1992; **24:** 188-9.
23. Fowler JF. Modelling altered fractionation schedules. *BJR Suppl* 1992; **24:** 187-92.
24. Bijl HP, van Luijk P, Coppes RP, Schippers JM, Konings AW, van der Kogel AJ. Unexpected changes of rat cervical spinal cord tolerance caused by inhomogeneous dose distributions. *Int J Radiat Oncol Biol Phys* 2003; **57:** 274-81.
25. Bijl HP, van Luijk P, Coppes RP, Schippers JM, Konings AW, van Der Kogel AJ. Regional differences in radiosensitivity across the rat cervical spinal cord. *Int J Radiat Oncol Biol Phys* 2005; **61:** 543-51.
26. Medin PM, Foster RD, van der Kogel AJ, Sayre JW, McBride WH, Solberg TD. Spinal cord tolerance to single-fraction partial-volume irradiation: a swine model. *Int J Radiat Oncol Biol Phys* 2011; **79:** 226-32.
27. Brenner DJ. The linear-quadratic model is an appropriate methodology for determining isoeffective doses at large doses per fraction. *Semin Radiat Oncol* 2008; **18:** 234-9.
28. Sahgal A, Weinberg V, Ma L, Chang E, Chao S, Muacevic A, et al. Probabilities of radiation myelopathy specific to stereotactic body radiation therapy to guide safe practice. *Int J Radiat Oncol Biol Phys* 2013; **85:** 341-7.
29. Gerszten PC, Burton SA, Ozhasoglu C, Vogel WJ, Welch WC, Baar J, et al. Stereotactic radiosurgery for spinal metastases from renal cell carcinoma. *J Neurosurg Spine* 2005; **3:** 288-95.

research article

Dynamic CT angiography for cyberknife radiosurgery planning of intracranial arteriovenous malformations: a technical/ feasibility report

Anoop Haridass, Jillian Maclean, Santanu Chakraborty, John Sinclair, Janos Szanto, Daniela Iancu, Shawn Malone

The Ottawa Hospital, Ottawa, Ontario, Canada

Radiol Oncol 2015; 49(2): 192-199.

Received 27 October 2014
Accepted 31 December 2014

Correspondence to: Dr. Jillian Maclean, The Ottawa Regional Cancer Centre, The Ottawa Hospital General Campus, Smyth Rd, Ottawa, Ontario, Canada. Phone: +613 737 7700, +613 737 0212; Fax: +613 247 351; E-mail: jillianmaclean@nhs.net

Disclosure: No potential conflicts of interest were disclosed.

Background. Successful radiosurgery for arteriovenous malformations (AVMs) requires accurate nidus delineation in the 3D treatment planning system (TPS). The catheter biplane digital subtraction angiogram (DSA) has traditionally been the gold standard for evaluation of the AVM nidus, but its 2D nature limits its value for contouring and it cannot be imported into the Cyberknife TPS. We describe a technique for acquisition and integration of 3D dynamic CT angiograms (dCTA) into the Cyberknife TPS for intracranial AVMs and review the feasibility of using this technique in the first patient cohort.

Patients and methods. Dynamic continuous whole brain CT images were acquired in a Toshiba 320 volume CT scanner with data reconstruction every 0.5 sec. This multi-time-point acquisition enabled us to choose the CT dataset with the clearest nidus without significant enhancement of surrounding blood vessels. This was imported to the Cyberknife TPS and co-registered with planning CT and T2 MRI (2D DSA adjacent for reference). The feasibility of using dCTA was evaluated in the first thirteen patients with outcome evaluation from patient records.

Results. dCTA data was accurately co-registered in the Cyberknife TPS and appeared to assist in nidus contouring for all patients. Imaging modalities were complementary. 85% of patients had complete (6/13) or continuing partial nidus obliteration (5/13) at 37 months median follow-up.

Conclusions. dCTA is a promising imaging technique that can be successfully imported into the Cyberknife TPS and appears to assist in radiosurgery nidus definition. Further study to validate its role is warranted.

Key words: arteriovenous malformation; radiosurgery; Cyberknife; dynamic CT angiogram

Introduction

Intracranial arteriovenous malformations (AVM) are congenital vascular abnormalities present in approximately 0.01–0.5% of the population.[1] In AVM, arteries supply a serpiginous collection of vessels, called the nidus, which shunt blood from the feeding arteries directly to the draining veins without an intervening capillary bed. The nidus and draining veins become enlarged and tortuous to cope with the increased flow. Intracranial AVMs are clinically important as there is 1–5% annual risk of haemorrhage.[2,3]

Advances in the treatment of AVMs have resulted in a decrease in associated morbidity and mortality in the last two decades.[4] Although microvascular surgery remains the gold standard treatment, stereotactic radiosurgery (RS) is proving increasingly useful in the treatment of small inoperable deep seated AVMs, those in eloquent areas where the risk of surgical morbidity is high, in medically inoperable patients and as part of

a multi-therapy approach for larger complex AVMs.[5-7]

The goal of RS for AVMs is to treat the nidus to a high dose while simultaneously minimising dose to the surrounding normal tissue. Improvements in image guidance, computing and radiation delivery technology in the last two decades have made it feasible to deliver accurate highly conformal RS plans. However, a successful outcome following RS - optimal AVM obliteration with minimal toxicity - is dependent on accurate definition of the nidus. This has always been challenging and inaccuracies in nidus definition are an important cause for treatment failure.[8,9]

The gold standard for imaging vascular structures, such as the AVM nidus, is the catheter biplane high resolution digital subtraction angiogram (DSA). The excellent temporal resolution of the DSA allows differentiation of the nidus from the feeding arteries and draining veins. However, the 2D nature of DSA images means they are of limited use to contour the nidus in 3D RS planning. Furthermore, DSA images cannot be co-registered in the Cyberknife (CK) RS treatment planning system as stereotactic localisation is frame-based in DSA, whereas CKRS uses skull tracking. Therefore, 3D imaging modalities, such as CT angiograms (CTA) and MR angiograms (MRA) are used for RS planning. Whilst CTA and MRA provide a view of the vascular tree with excellent 3D localization, the drawback of the standard 'static' CTA/MRA is that the images represent a snapshot of the blood flow through the AVM and draining veins at a pre-determined acquisition time. This snapshot is unlikely to be the optimal time-point for viewing the nidus, which can make differentiation of the nidus from the surrounding angio-architecture challenging.

Dynamic CT angiography (dCTA) is a non-invasive vascular imaging technique that has been shown to provide both high temporal and spatial resolution in a 3D volume dataset. The entire cerebral volume can be imaged in a single rotation of the gantry, generating a full CT dataset of the cerebral vasculature every second. The scanner splits each dataset to generate whole brain CTA volume with temporal resolution of 0.5 sec. The utility of dCTA has been described in the evaluation of AVMs[10,11], but there are no published reports of using it to aid RS planning. Potentially dCTA would allow delineation of the nidus on the CT dataset captured at the point when the nidus is clearest. We incorporated dCTA into our CKRS planning protocol in 2010 and present a feasibility report regarding our initial findings in the first cohort of patients.

Patients and methods

All patients with AVMs who were treated with CKRS at our hospital between October 2010 and April 2012 underwent a dynamic CT angiogram as part of the planning process. Written informed consent of patients was obtained for the treatments and for the scientific use of the clinical data according to Declaration of Helsinki.

Procedure for dCTA

Patients were scanned in an Aquilion ONE multidetector volume CT scanner (Toshiba, Medical Systems, Japan) in a supine head first position with IV access as per departmental protocol. This system is equipped with 320 ultra-high resolution detector rows (0.5mm in width), 512 x 512 matrix and images 16cm in z-axis in a single gantry rotation which covers the entire brain. Whole brain CT data is acquired at multiple time points as per dCTA protocol. From this dataset Dynamic (time resolved) CT angiography (dCTA) images were reconstructed enabling the analysis of the blood flow in the entire cranial circulation in a non-invasive way with high spatial and temporal resolution. The radiation dose for the dCTA acquisition is approximately (DLP= Dose length product) 2170 mGycm = effective dose 5 mSv, for comparison radiation dose for non-contrast CT head will be (DLP) 1335 mGycm) = 3 mSv.

Timing bolus

Following acquisition of a scout film, a 15ml timing bolus of the contrast agent (Isovue 370 followed by a 20 ml saline chaser) was power injected and low dose scans of the base of skull area were taken every two seconds to determine time taken for the contrast to arrive at the internal carotid arteries at the skull base. The scan was discontinued when contrast appeared in these vessels and contrast arrival time was determined. The usual timeframe varied between 10–15 seconds and depended on patients cardiac output and placement of IV access.

dCTA

The dCTA scan protocol (Figure 1) was initiated with simultaneous scanning and power injection of IV contrast (40 ml Isovue 370 @5ml/sec followed by a 20 ml saline chaser). A 'mask' scan was acquired at 7 seconds using 300mA and 80KV (Figure 1A). This dataset was used to digitally subtract bone

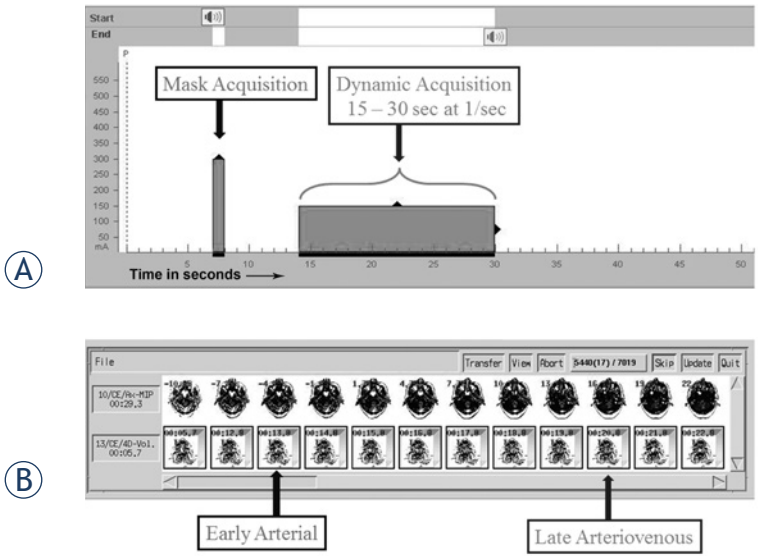

FIGURE 1. The upper panel **(A)** shows planning timeline for dCTA acquisition. Following simultaneous start of IV pump and the scanner, at 7 sec, a volume with 300 mA and 80 kV is taken as a mask for bone subtraction. This is a non-contrast image as the contrast bolus is yet to reach the cranial arteries. The next dynamic acquisition block (100 mA, 80 kV, 1 volume/sec for 16 volumes) will have different a start time, depending on the variable contrast arrival time at the internal carotid arteries at the base of skull as determined by the timing bolus. This will acquire 16 volumes starting 1 sec before the contrast arrival time. The lower panel **(B)** shows series of volumes following dCTA acquisition. Together they will show the timeline of contrast flow (dynamic CTA) thus permitting selection of the best volume showing the AVM nidus for CK planning.

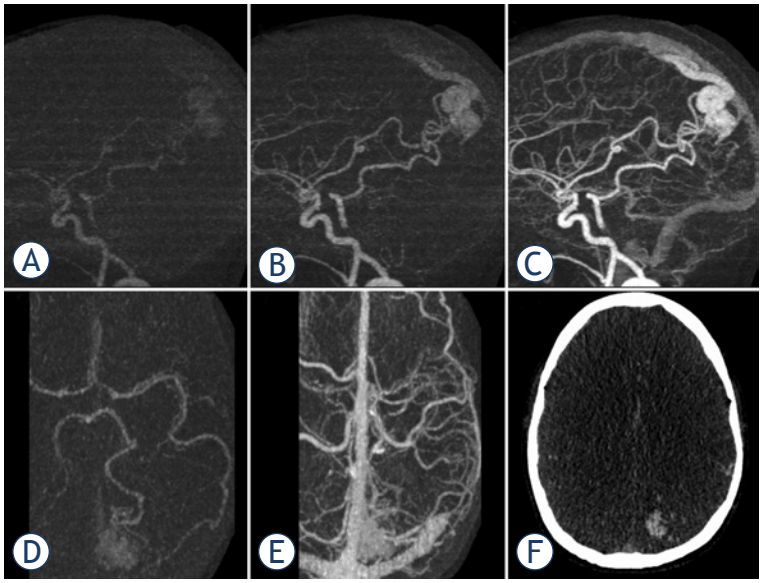

FIGURE 2. Sagittal reformatted dynamic subtracted images **(A, B, C)** show temporal flow of contrast through intracranial vessels and nidus of left occipital AVM. **(A)** very early arterial phase showing the AVM nidus before filling of contrast into the normal brain arteries due to rapid shunting through the AVM. Axial reformatted images in the arterial **(D)** and venous **(E)** phases demonstrate the difficulty in assessing the AVM nidus in the presence of enhancing surrounding vasculature. **(F)** an axial slice of non-subtracted dCTA volume co-registered in the CK system and used for SRS contouring.

from the angiogram datasets and was performed at higher mA to allow clearer definition of the intracranial vasculature. The scanner was setup for dynamic acquisition one second before the contrast arrived at the skull base (as determined from the timing bolus) at 100mA and 80 KV (Figure 1A). The whole brain volume from skull base to vertex was imaged once every second for 16 seconds and the complete data volume was reconstructed every 0.5 seconds (temporal resolution 2 images/sec). The duration of the scan allowed imaging to start with no contrast, continuing to the phase of peak arterial enhancement (Figure 2A) and ending with the venous return phase (Figure 2C).

Non-subtracted and bone subtracted dCTA datasets were created and reviewed by the neuroradiologist (SC) to determine the temporal phase of imaging where the AVM nidus was best visualised (Figure 1B and Figure 2F) without significant contrast in the draining veins and adjacent non-AVM vasculature. The optimum time-point for nidus visualisation varied between subjects depending on AVM flow rate.

Treatment planning

The entire CT dataset (320 slices) at the time point where the nidus was clearest was reformatted to the CKRS treatment planning specifications (1x1x1mm cubic voxels) and imported as a DICOM file to the CK Multiplan TP system (Accuray, Sunnyvale CA). The dCTA was co-registered with the non-contrast planning CT and T2 weighted MRI to contour the target and the surrounding organs at risk. Coregistration between planning CT, dCTA and MRI was visually assessed in the standard split-screen manner using bone and ventricle landmarks. The 2D DSA was available for reference on an adjacent workstation. All imaging modalities were used to accurately delineate the nidus. Contouring was jointly performed by the neurosurgeon, radiation oncologist and neuroradiologist. Single fraction RS treatments were prescribed and the plan and the prescription isodose was finalized by the radiation oncologist to achieve coverage of the nidus and respect published normal tissue constraints.[12]

Review of clinical use

Tolerability and apparent utility of the dCTA was assessed prospectively. Follow up imaging was performed 6 monthly using MRA, followed by a confirmatory catheter angiogram if the MRA in-

TABLE 1. Patient characteristics and outcomes

Pt	Region	Age	Dose Gy	Isodose Tx (%)	Prev bleed	Prev RT	Success?	Comments	Follow-up (months)
1	L basal ganglia	10	15	84	Yes	No	N	Embolization after 33 months	45
2	L thalamus	40	15	82	Yes	Yes	N	RS 15 years previous (lost to follow-up)	45
3	R occipital	50	18	85	No	No	C		45
4	L cerebellum	49	15	84	Yes	No	P	Large AVM – only deep nidus treated, for embolization of remainder	44
5	L vein of galen	22	15	80	Yes	No	P		44
6	R parietal	70	18	82	No	No	C		38
7	Corpus callosum	22	16.5	75	No	No	C		37
8	Sup cerebellum	61	20	80	Yes	No	C		34
9	L occipital AVM	36	18	80	No	No	C		32
10	Pineal	29	16	85	No	No	C		30
11	Sup cerebellum	58	21	82	Yes	No	P		30
12	R CP angle	40	15	77	No	No	P		29
13	R thalamus	11	15	78	Yes	Yes	P	RS 5 years previously	28

C = complete obliteration; L/R = left and right; N = no obliteration; P = partial obliteration; Pt = patient

dicated obliteration. Nidus obliteration rates and toxicity were evaluated from imaging and patient charts.

Results

Between October 2010 and April 2012, 13 consecutive patients with inoperable AVMs were treated with CKRS at our hospital. Median age was 40 years (range 10–70). All patients tolerated the full dCTA protocol without adverse event and accurate co-registration of dCTA images with the CT and MRI within the CK planning system was performed in all cases.

Treatments were all delivered as a single fraction. Median marginal RS dose delivered was 16Gy (range 15–21Gy at the 75–85% isodose). Median target volume was 1.31cc (range 0.4–2.93cc). Ten patients were treated with RS because the AVM was in an eloquent or inoperable area, two patients as part of staged multimodality treatment following surgery and one patient because of medical co-morbidities. Seven patients had prior intracranial haemorrhage. Two patients with thalamic AVMs had been previously treated at other centers with RS for AVM. Re-treatment in these cases occurred after a latency of five and fifteen years. Table 1 summarises the patient cohort and outcomes at a median follow-up of 37 months (range 28–45 months).

The RS team found that all imaging modalities were complementary. The dCTA data could be accurately co-registered within the CK Multiplan TPS and it was possible to visualize the nidus on both MRI and dCTA in all 3 planes. The sagittal and coronal images were compared to the reference 2D Angiography images in the adjacent work station. dCTA was felt by all three clinicians to be beneficial to help define the boundaries of the nidus in every case. On MRI alone it was often difficult to distinguish nidus from adjacent angiomatous change and draining veins often obscured the nidus on both MRI and on 2D Angiography. Careful selection of the optimal dCTA data set where there was minimal uptake in large draining veins and that excluded surrounding angiomatous change helped the RS team clarify boundaries of the nidus. In our experience the dCTA was also helpful to define portions of nidus extending into CSF space in periventricular AVMs and in cases where AVM nidus extended into adjacent sulci. Representative cases are illustrated in Figures 2–4.

Example cases

Case 1 (patient 9)

A 36 year old female with a previous history of cervix cancer was investigated for headaches and found to have a 20 mm AVM in the left occipital area (Figure 2). The option of surgical management with risk of visual morbidity was discussed and

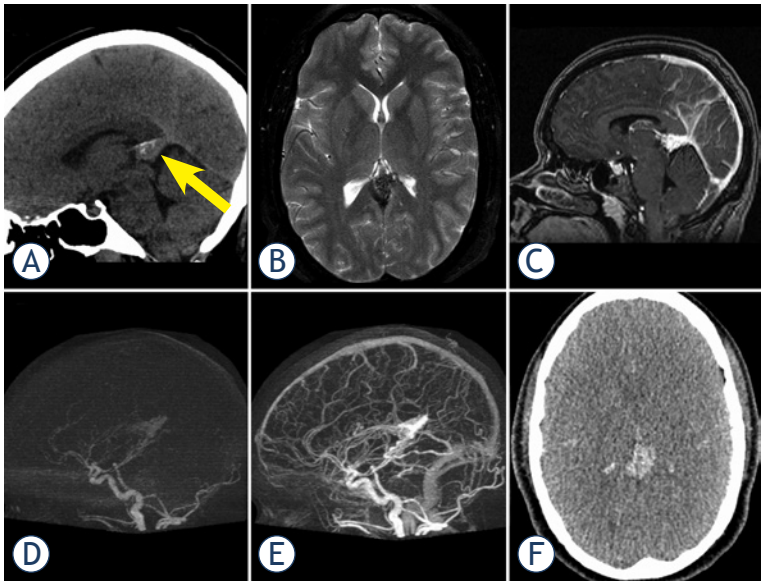

FIGURE 3. (A) Sagittal reformatted non-contrast CT head image showing iso-dense lesion in tentorial notch (arrow). **(B)** Axial T2 weighted MR image (3B) showing nidus with adjacent draining vein. **(C)** Sagittal reformatted image from T1 weighted VIBE image showing enhancing nidus with adjacent draining veins and venous sinuses. **(D-E)** Sagittal reformatted subtracted dCTA images in arterial **(D)** and venous **(E)** phase showing the AVM nidus in the arterial phase and occluded straight sinus. **(F)** Axial image from early arterial volume showing the nidus without contamination from surrounding enhancing vessels (full CT dataset from this temporal imaging phase imported into CBK for contouring).

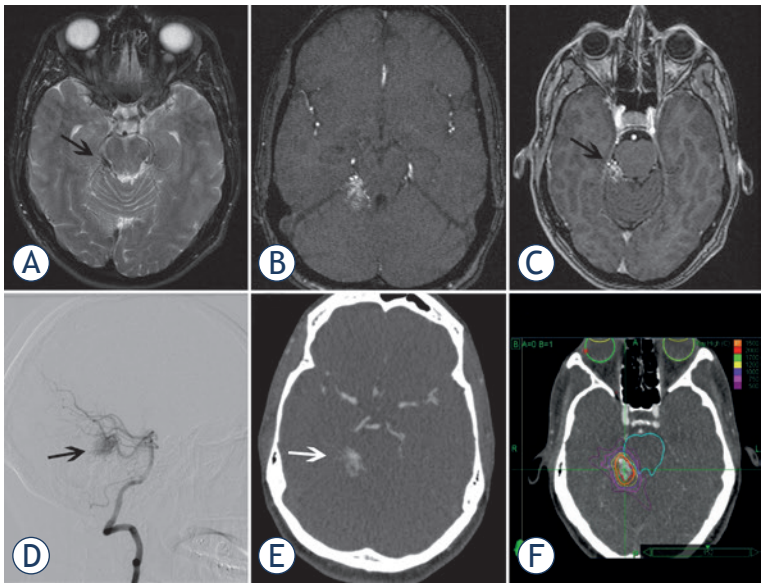

FIGURE 4. (A) Axial T2 image showing abnormal vasculature in right CP angle (black arrow). **(B)** Axial source image from the time of flight MR angiogram showing the nidus. **(C)** Source image from contrast enhanced axial T1weighted VIBE sequence showing enhancing AVM nidus with enhancement of adjacent vasculature. **(D)** arterial phase image of conventional catheter angiogram with injection from the left vertebral artery showing the AVM nidus (black arrow). This is a projectional 2-D image that cannot be coregistered in CBK. **(E)** sample axial image from the corresponding dCTA used for CK planning. **(F)** radiation target volume and isodose lines in CK planning system.

patient declined. The patient had CKRS to a dose of 18 Gy to the 80% isodose and the nidus was completely obliterated at 22 months.

Case 2 (patient 10)

A 29 year old female investigated for headaches against a background of recent haemorrhagic stroke in a close relative, was found to have a 22 mm AVM in the pineal region (Figure 3). The AVM was located in a region deemed not amenable to surgery. The patient had CKRS to a dose of 16 Gy to the 85% isodose. The nidus was obliterated 28 months following treatment.

Case 3 (patient 11)

A 40 year old asymptomatic patient was found to have a 15 mm AVM in the right CP angle (Figure 4) when being screened for aneurysms. The patient received 15 Gy to the 77% isodose with CKRS with partial obliteration of the nidus after 22 months.

Discussion

Accurate delineation of the AVM nidus is paramount to successful RS. The steep dose gradients delivered by RS mean that inaccurate targeting will result in a subtherapeutic dose to regions of the AVM and increase the likelihood of treatment failure. Conversely, treating a larger volume than required increases the risk of toxicity. However, it can be challenging to effectively distinguish the nidus from its feeding and draining vessels as reported by Buis *et al.*[13], who evaluated intraobserver variability in contouring AVMs for RS. They reported a mean agreement ratio of 0.45 amongst six observers and showed that differences were most marked in those with treatment failure. Improved definition of the nidus through the use of multiple imaging modalities should increase the likelihood of successful AVM RS.

DSA remains the gold standard for visualisation of the nidus in view of the excellent spatial and temporal resolution, but the 2D nature of standard DSA limits its use in 3D RS contouring. Furthermore, it is not possible to coregister the DSA within CKRS planning software as CK is not frame-based and the DSA is therefore viewed on an adjacent imaging workstation. This introduces errors. Therefore centres generally co-register CTA or MRA to provide 3D cross-sectional data. However, even with timed contrast boluses and acquisition, the temporal resolution of standard CTA/MRA is limited to a snapshot view of the

AVM. While this produces good cross-sectional imaging, the enlarged draining veins and contrast in adjacent non-AVM vasculature usually obscure parts of the nidus.

Several groups have reported the use of 3D reconstructions of DSA. Veeravagu *et al.*, reported smaller AVM target volumes for CKRS when contours were performed using a combination of 3D rotational angiography, CT and MRI versus CT and MRI alone.[14] They concluded that the addition of 3D angiography into the planning protocol resulted in more precise target contouring, although patient outcome data and analysis of possible image distortion levels would strengthen their data. Zhang *et al.*, reported similar results several years earlier using in-house software to create a 3D reconstruction of DSA images.[15] Columbo *et al.*, recently described a novel method of automatic nidus contouring using coregistered 3D rotational angiography (performed with direct intraarterial contrast injection).[16] After establishing the radiological density of a region of nidus, the treatment planning software automatically contoured GTV based on corresponding voxel values, although manual correction was possible. They did not describe their validation process for this technique, but did report complete angiographic obliteration rates after ≥ three years in 65 of 80 patients (81.2%).

Various other non-invasive methods have been described that appear to assist in nidus definition in RS treatment planning or post-treatment follow-up. 3D time of flight (TOF) MRA has been advocated for the assessment of AVM nidus obliteration dynamics following CKRS[17], although Bednarz *et al.*, concluded that DSA and TOF MRA were complementary for nidus RS delineation as imaging artefact on MRA could obscure the nidus.[18] High sensitivity (81%) and specificity (100%) has been reported for dynamic MRA in the post-treatment evaluation of AVMs treated with RS.[19]

The use of dCTA for imaging AVMs was first described by Matsumo *et al.*[10], who imaged four patients with AVM (within a study of various brain lesions) and reported that dCTA effectively distinguished the nidus from the feeding and draining vessels within the scanned range. Willems *et al.*, recently evaluated dCTA versus DSA to evaluate AVMs using a scoring system.[11] They reported that dCTA could be used to effectively diagnose and classify the shunt but, in some circumstances there were discrepancies on classifying the angioarchitecture with dCTA compared to DSA due to difficulty in determining the nature of certain vessels. However, they focused upon 3D maximum intensity projection (MIP) views of the dCTA in their comparison rather than the cross-sectional images we have used. Indeed, they went on to discuss the benefit of using the cross-sectional data to distinguish the nidus from surrounding vessels.

In this feasibility report we have shown that dCTA data can be easily imported into the CKRS planning system and co-registered to the planning CT and MRI. This allows contouring to be performed on 3D cross-sectional images of the nidus at the point when it is clearest. In all of our 13 cases it was possible to identify the optimum dCTA volume, directly import this 3D dataset into the CKRS software and accurately coregister with other modalities which allowed the nidus to be visualized in all 3 planes for contouring. The sagittal and coronal images can still be compared to the reference 2D angiography images on the adjacent work station. The AVMs in this report were of small volume which demands even greater accuracy than for larger lesions. Direct contouring on the dCTA on the CKRS planning software certainly was an advantage compared to our previous technique where contours were drawn on static CT/MRI images with reference to the DSA on an adjacent screen. It is important to carefully choose the right arterial phase of the dCTA and use the non-subtracted volume to allow confident definition of the nidus on the dCTA. However, at this point in our analysis it would be premature to conclude that dCTA replaces the need for DSA in RS planning and we found the combination of imaging modalities to be complementary.

The primary purpose of this study was to report our initial findings on the feasibility of using dCTA to assist in targeting AVMs for RS on the Cyberknife TPS. Accordingly, our data is descriptive. We do not claim to have validated dCTA in nidus contouring. Formal validation of a new imaging technique in contouring is challenging. Although comparison of volumes contoured with and without the dCTA may show differences, such differences alone do not themselves reflect whether the dCTA improves contouring accuracy. Improvement in contouring agreement between observers using a new imaging technique is often used as a surrogate for improved accuracy. However, we did not pursue this approach as we contour as a multidisciplinary group with different areas of primary expertise (radiology, neurosurgery and radiation oncology) and our final targets reflect a consensus opinion. Long-term patient outcomes will be the ultimate validation,

but patient numbers are too low and follow-up too short to accurately assess treatment success rates at this point as the latency period to complete obliteration following RS can be 4–5 years. We did evaluate preliminary patient outcomes to establish whether it is reasonable to continue to study dCTA in AVM RS treatment planning and the data available so far is comparable to other published outcomes at this follow-up period. Complete nidus obliteration rates three years post-RS of 58%, 39% and 40% have been reported by various authors[7,20,21], with successful obliteration rates increasing as follow-up continues. Six of our first thirteen patients (46%) contoured using dCTA had complete nidus obliteration at a median follow-up of 37 months. Five other patients have had partial responses and the nidus size continues to progressively decrease suggesting they may completely obliterate with further follow-up. Due to the small nidus volume in our cohort, we would hope for complete obliterations in approximately 80% of patients after 4–5 years follow-up. Clearly we do not suggest that our current outcomes themselves validate dCTA in contouring at this point, but we continue to prospectively collect long-term patient outcome and toxicity data. Two patients, both with complete nidus obliterations, required delayed steroid therapy, one for simple edema and one for a thrombosed draining vein, an unusual but documented potential complication of RS for AVM.[22] Review of this patients RS contours showed that the addition of the dCTA had in fact reduced the volume of draining vein included in the target.

Conclusions

It is feasible to integrate dCTA into a CKRS planning protocol for AVM delineation. This technique combines the better spatial resolution of 3D CT volumes with the ability to select the best temporal phase of contrast filling. In our preliminary evaluation, we found dCTA to be a complementary addition to the other standard imaging modalities used to contour the AVM nidus and particularly useful for CK planning as DSAs cannot be imported into the CK TPS. We have now incorporated dCTA into our standard treatment planning protocol and will continue to prospectively collect longer-term follow-up data in more patients for validation.

References

1. Fleetwood IG, Steinberg GK. Arteriovenous malformations. *Lancet* 2002; **359:** 863-73.
2. Brown RD Jr., Wiebers DO, Forbes GS. Unruptured intracranial aneurysms and arteriovenous malformations: frequency of intracranial hemorrhage and relationship of lesions. *J Neurosurg* 1990; **73:** 859-63.
3. Ondra SL, Troupp H, George ED, Schwab K. The natural history of symptomatic arteriovenous malformations of the brain: a 24-year follow-up assessment. *J Neurosurg* 1990; **73:** 387-91.
4. van Beijnum J, van der Worp HB, Buis DR, Al-Shahi Salman R, Kappelle LJ, Rinkel GJ, et al. Treatment of brain arteriovenous malformations: a systematic review and meta-analysis. *JAMA* 2011; **306:** 2011-9.
5. Kano H, Kondziolka D, Flickinger JC, Yang HC, Flannery TJ, Niranjan A, et al. Stereotactic radiosurgery for arteriovenous malformations, Part 4: management of basal ganglia and thalamus arteriovenous malformations. *J Neurosurg* 2012; **116:** 33-43.
6. Kano H, Kondziolka D, Flickinger JC, Yang HC, Flannery TJ, Niranjan A, et al. Stereotactic radiosurgery for arteriovenous malformations, Part 5: management of brainstem arteriovenous malformations. *J Neurosurg* 2012; **116:** 44-53.
7. Kano H, Lunsford LD, Flickinger JC, Yang HC, Flannery TJ, Awan NR, et al. Stereotactic radiosurgery for arteriovenous malformations, Part 1: management of Spetzler-Martin Grade I and II arteriovenous malformations. *J Neurosurg* 2012; **116:** 11-20.
8. Ellis TL, Friedman WA, Bova FJ, Kubilis PS, Buatti JM. Analysis of treatment failure after radiosurgery for arteriovenous malformations. *J Neurosurg* 1998; **89:** 104-10.
9. Pollock BE, Flickinger JC, Lunsford LD, Maitz A, Kondziolka D. Factors associated with successful arteriovenous malformation radiosurgery. *Neurosurgery* 1998; **42:** 1239-44; Discussion 44-7.
10. Matsumoto M, Kodama N, Endo Y, Sakuma J, Suzuki K, Sasaki T, et al. Dynamic 3D-CT angiography. *Am J Neuroradiol* 2007; **28:** 299-304.
11. Willems PW, Taeshineetanakul P, Schenk B, Brouwer PA, Terbrugge KG, Krings T. The use of 4D-CTA in the diagnostic work-up of brain arteriovenous malformations. *Neuroradiology* 2012; **54:** 123-31.
12. Timmerman RD. An overview of hypofractionation and introduction to this issue of seminars in radiation oncology. *Semin Radiat Oncol* 2008; **18:** 215-22.
13. Buis DR, Lagerwaard FJ, Barkhof F, Dirven CM, Lycklama GJ, Meijer OW, et al. Stereotactic radiosurgery for brain AVMs: role of interobserver variation in target definition on digital subtraction angiography. *Int J Radiat Oncol Biol Phys* 2005; **62:** 246-52.
14. Veeravagu A, Hansasuta A, Jiang B, Karim AS, Gibbs IC, Chang SD. Volumetric analysis of intracranial arteriovenous malformations contoured for CyberKnife radiosurgery with 3-dimensional rotational angiography vs computed tomography/magnetic resonance imaging. *Neurosurgery* 2013; **73:** 262-70.
15. Zhang XQ, Shirato H, Aoyama H, Ushikoshi S, Nishioka T, Zhang DZ, et al. Clinical significance of 3D reconstruction of arteriovenous malformation using digital subtraction angiography and its modification with CT information in stereotactic radiosurgery. *Int J Radiat Oncol Biol Phys* 2003; **57:** 1392-9.
16. Colombo F, Cavedon C, Casentini L, Francescon P, Causin F, Pinna V. Early results of CyberKnife radiosurgery for arteriovenous malformations. *J Neurosurg* 2009; **111:** 807-19.
17. Wowra B, Muacevic A, Tonn JC, Schoenberg SO, Reiser M, Herrmann KA. Obliteration dynamics in cerebral arteriovenous malformations after cyberknife radiosurgery: quantification with sequential nidus volumetry and 3-tesla 3-dimensional time-of-flight magnetic resonance angiography. *Neurosurgery* 2009; **64:** A102-9.
18. Bednarz G, Downes B, Werner-Wasik M, Rosenwasser RH. Combining stereotactic angiography and 3D time-of-flight magnetic resonance angiography in treatment planning for arteriovenous malformation radiosurgery. *Int J Radiat Oncol Biol Phys* 2000; **46:** 1149-54.

19. Gauvrit JY, Oppenheim C, Nataf F, Naggara O, Trystram D, Munier T, et al. Three-dimensional dynamic magnetic resonance angiography for the evaluation of radiosurgically treated cerebral arteriovenous malformations. *Eur Radiol* 2006; **16:** 583-91.

20. Zacest AC, Caon J, Roos DE, Potter AE, Sullivan T. LINAC radiosurgery for cerebral arteriovenous malformations: a single centre prospective analysis and review of the literature. *J Clin Neurosci* 2014; **21:** 241-5.

21. Blamek S, Tarnawski R, Miszczyk L. Linac-based stereotactic radiosurgery for brain arteriovenous malformations. *Clin Oncol (R Coll Radiol)* 2011; **23:** 525-31.

22. Yen CP, Khaled MA, Schwyzer L, Vorsic M, Dumont AS, Steiner L. Early draining vein occlusion after gamma knife surgery for arteriovenous malformations. *Neurosurgery* 2010; **67:** 1293-302; discussion 302.

special communication

The cost of systemic therapy for metastatic colorectal carcinoma in Slovenia: discrepancy analysis between cost and reimbursement

Tanja Mesti[1], Biljana Mileva Boshkoska[2], Mitja Kos[3], Metka Tekavčič[4], Janja Ocvirk[1]

[1] Department of Medical Oncology, Institute of Oncology Ljubljana, Ljubljana, Slovenia
[2] Faculty of information studies, Novo mesto, Slovenia
[3] Faculty of Pharmacy, University of Ljubljana, Ljubljana, Slovenia
[4] Faculty of Economics, University of Ljubljana, Ljubljana, Slovenia

Radiol Oncol 2015; 49(2): 200-208.

Received: 14 August 2014
Accepted: 2 October 2014

Correspondence to: Tanja Mesti, M.D., M.Sc., Institute of Oncology Ljubljana, Zaloška 2, Ljubljana. Phone: +386 1 5879 220; Fax: +386 1 5879 305; E-mail: tmesti@onko-i.si

Disclosure: No potential conflicts of interest were disclosed.

Background. The aim of the study was to estimate the direct medical costs of metastatic colorectal cancer (mCRC) treated at the Institute of Oncology Ljubljana and to question the healthcare payment system in Slovenia.

Methods. Using an internal patient database, the costs of mCRC patients were estimated in 2009 by examining (1) mCRC direct medical related costs, and (2) the cost difference between payment received by Slovenian health insurance and actual mCRC costs. Costs were analysed in the treatment phase of the disease by assessing the direct medical costs of hospital treatment with systemic therapy together with hospital treatment of side effects, without assessing radiotherapy or surgical treatment. Follow-up costs, indirect medical costs, and nonmedical costs were not included.

Results. A total of 209 mCRC patients met all eligibility criteria. The direct medical costs of mCRC hospitalization with systemic therapy in Slovenia for 2009 were estimated as the cost of medications (cost of systemic therapy + cost of drugs for premedication) + labor cost (the cost of carrying out systemic treatment) + cost of lab tests + cost of imaging tests + KRAS testing cost + cost of hospital treatment due to side effects of mCRC treatment, and amounted to €3,914,697. The difference between the cost paid by health insurance and actual costs, estimated as direct medical costs of hospitalization of mCRC patients treated with systemic therapy at the Institute of Oncology Ljubljana in 2009, was €1,900,757.80.

Conclusions. The costs paid to the Institute of Oncology Ljubljana by health insurance for treating mCRC with systemic therapy do not match the actual cost of treatment. In fact, the difference between the payment and the actual cost estimated as direct medical costs of hospitalization of mCRC patients treated with systemic therapy at the Institute of Oncology Ljubljana in 2009 was €1,900,757.80. The model Australian Refined Diagnosis Related Groups (AR-DRG) for cost assessment in oncology being currently used is probably one of the reasons for the discrepancy between pay-outs and actual costs. We propose new method for more precise cost assessment in oncology.

Key words: cost of treatment; metastatic colorectal cancer; cost of targeted therapy; monitoring costs

Introduction

Colorectal cancer is one of the most common cancers in the developed world. Morbidity and mortality caused by this form of cancer are increasing in Slovenia. In 2009 1,568 people were diagnosed with colorectal cancer.[1,2] The increasing incidence also corresponds to increasing mortality because 50 to 60% of cases of the disease are discovered in an advanced stage, of which 20 to 30% have metastasized.

Patients in Slovenia with metastasized colorectal cancer (mCRC) that are physically or medically capable are mostly treated at the Institute of Oncology Ljubljana, where treatment takes place following guidelines adopted in line with globally recognized oncological guidelines, although the combinations of medications vary. [3,4]

The costs of treating mCRC have risen quickly over the past decade, especially with the introduction of targeted medications for treating mCRC. With the introduction of the new targeted medications cetuximab and bevacizumab to mCRC treatment, the costs of standard care per person have increased from $500 to $250,000.[5]

There are no studies of defining mCRC treatment costs in Slovenia, and so we decided to take the first step and calculate what mCRC treatment costs amount to. For our analysis, we collected the costs of active patient mCRC treatment with systemic therapy at the Institute of Oncology Ljubljana in 2009 and compared them with payments by the Health Insurance Institute of Slovenia (ZZZS) with the goal to show if there is any discrepancy. The Institute of Oncology Ljubljana was the only healthcare facility in Slovenia where treatment of mCRC was carried out.

Patients and methods

First we used retrospective analysis from an inventory of patient diseases and defined the database of treatment for patients treated at the Institute of Oncology Ljubljana in 2009 with systemic therapy for mCRC, and then we carried out a retrospective analysis of average *direct medical costs* of patient treatment for mCRC with systemic therapy from the *perspective of the hospital.* The study was approved by the institutional review board committee and was according the Declaration of Helsinki.

The study included costs of acute hospital procedures, whereas costs of non-acute hospital procedures were excluded.

For individual patients we took into account the information from the database shown in Table 1.

TABLE 1. Data in the database

No.	Data
1	Age
2	Sex
3	Number of hospital procedures for 2009
4	Localization of primary cancer: colon, rectum, colon-rectum transition
5	Localization of mCRC metastasis: liver, lungs, liver and lungs, local recurrence of disease, other
6	Line of treatment with systemic therapy in 2009: first, second, third, fourth, and number of lines of systemic therapy received by an individual patient in 2009 (one course, two or more lines)
7	Systemic therapy regimen: number of hospital applications and dose of individual medications in regimen and price of medicine
8	Number, dose, and price of medication for premedication per individual application
9	Number, dose, and price of medication for hydration per individual application
10	Laboratory tests carried out for an individual patient during hospital treatment due to systemic therapy, type, number, and price of lab tests
11	Imaging tests carried out for an individual patient during hospital treatment due to systemic therapy, type, number, and price of imaging tests
12	Hospital services per patient due to side effects of systemic therapy
13	KRAS testing before the start of treatment with systemic therapy for mCRC patients before the first line of therapy (yes/no)
14	*Labor* costs for carrying out systemic therapy per hospitalization

mCRC = metastatic colorectal cancer

Group characteristics

We analysed a homogenous group of 294 patients that underwent hospital treatment with systemic therapy. From the group of 409 mCRC patients that were treated at the Institute of Oncology Ljubljana, we excluded patients that took part in additional forms of treatment such as surgical procedures and radiotherapy (internal data from the gastrointestinal cancer team, Institute of Oncology Ljubljana) and 115 patients treated with systemic therapy only as outpatients, because evaluating the costs of outpatient therapy does not take place in the same way as evaluating the costs of hospital treatment. Evaluation of outpatient services takes place according to a point system (the Uniform List of Health Services, or green book), and hospital services are evaluated according to the diagnosis-related group (DRG) system.

The group included 123 men and 86 women. Approximately two-thirds (66%) were under 65-year old. Approximately 60% of patients (122) had primary localization of the tumour in the colon, and one-third in the rectum (69). The most frequent localization of metastasis was the liver (125 patients). One-fifth of patients had metastasis in the lungs or simultaneously in the lungs and liver, local recurrence of disease was present in nine patients, and the remaining one-third of patients had

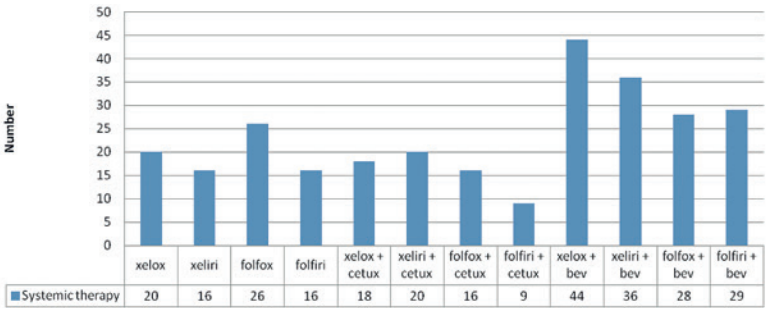

FIGURE 1. Distribution of systemic therapy.

TABLE 2. Definition of costs

Costs	Definition
Medication[a]	Medication cost = dose and number of applications of medication calculated according to medication supply price[b]
Lab tests	Test costs = (number of points[c] of test + number of points scored (venous blood draw)) × cost price of a point[d]
Imaging tests	Test costs = number of points[c] × cost price of a point[d]
Applying medication	Sum of the labor cost of nurses, physician, pharmacist, pharmaceutical technician, and administrative and technical staff with regard to the average time used for application, and average value of an hour of labor for an individual involved in applying medication.
Work during hospitalization	Sum of the labor cost of nurses, physician, average time used per patient, and average value of an hour of labor for an individual during hospitalization[e]
Testing primary cancer or metastasis for KRAS mutation	Cost of molecular analysis + labor cost
Hospital treatment for side effects of systemic therapy	Sum of the cost of medications used (parenteral antibiotics, peroral antibiotics, parenteral feeding, hydration, other medication), tests (lab and imaging), and labor during hospitalization.

[a] Excludes cost of Xeloda (capecitabine) because patients receive it with a prescription at an external pharmacy and then continue their therapy at home.

[b] Supply of medications at the Institute of Oncology Ljubljana takes place through a public procurement process as defined by law (Public procurement Act, *Official Gazette of the Republic of Slovenia*, no. 16/08).

[c] The green book or Uniform List of Health Services contains a point value for health services based on the need for staff and time used expressed in minutes for carrying out these services. It is a very old and outdated document that contains a description of all health exams, care, and tests with precise codes, description of health services and of staffing and time standards, whereby all services are evaluated with points. This document is still used in calculating health services performed and in checking billing accuracy even though many modern services are not included in it.

[d] The cost price of a point is defined retroactively for 2009 by individual diagnostic unit (Analysis of costs and physical indicators for 2009, Institute of Oncology Ljubljana) based on values from the green book. The cost price of a point per individual diagnostic unit represents the quotient between the total costs of an individual diagnostic unit for an individual year and the number of points realized.

[e] Systemic treatment that includes capecitabine (capecitabine, oxaliplatin [XELOX], capecitabine, irinotecan [XELIRI], XELOX/bevacizumab, XELIRI/bevacizumab, XELOX/cetuximab, XELIRI/cetuximab) involves one-day hospitalization, and systemic treatment that includes 5-FU (infusional fluorouracil, leucovorin, oxaliplatin [FOLFOX], fluorouracil, leucovorin, oxaliplatin, irinotecan [FOLFIRI], FOLFOX/bevacizumab, FOLFIRI/bevacizumab, FOLFOX/cetuximab, FOLFIRI/cetuximab) involves three-day hospital treatment.

metastasis in the lymph nodes, bones, or pancreas and peritoneal carcinoma.

The patients were treated with standard combinations of systemic therapy. Most patients received XELOX (capecitabine, oxaliplatin) + bevacizumab, which is understandable considering that capecitabine as a *per oral* form of fluoropyrimidine offers better quality of life for patients and visits to an oncologist are at three-week intervals, in contrast to 5-fluorouracil, which is an infusion form of fluoropyrimidine that is applied in 46 h infusions every two weeks. Paired chemotherapy with cetuximab was received by half as many patients as paired chemotherapy with bevacizumab, primarily because of the presence of KRAS mutation in the primary cancer tissue. The distribution of systemic therapy is presented in Figure 1.

Definition of medications and procedures

Chemotherapeutics included fluoropyrimidine (5-fluororacil, capecitabine), irinotecan, and oxaliplatin, which we used in various regimens (fluorouracil, leucovorin, oxaliplatin, irinotecan [FOLFIRI], infusional fluorouracil, leucovorin, oxaliplatin [FOLFOX], capecitabine, irinotecan [XELIRI], capecitabine, oxaliplatin [XELOX]) and in combination with targeted medications: cetuximab, bevacizumab.[6] The premedication included the following medications: dexamethasone 20 mg, granisetron 1 mg, and clemastine 2 mg. In the hydration we used 0.9% NaCl 2,000 ml or 5% glucose 2,000 ml (for only chemotherapy), or 0.9% NaCl 2,700 ml or 5% glucose 2,700 ml (for chemotherapy + targeted medication). Laboratory tests were divided into standard tests - a complete blood count (CBC), blood differential test, liver function tests, kidney function tests (nitrogen retention), electrolytes, C-reactive protein (CRP), and tumour markers (Carcinoembryonic antigen [CEA], carbohydrate antigen [CA 19–9]) and additional Laboratory tests that we carried out as needed: urinalysis, iron, ferritin, and transferrin. The imaging tests we included were: X-ray (lungs, abdomen, spine, pelvis), CT (thoracic cavity, abdomen), MRI (liver, lesser pelvis, head), bone scintigraphy, abdominal ultrasound, and PET-CT.

Definition of costs

Because direct medical costs are fixed costs and variable costs that are directly connected to health condition or health treatment, in this analysis we

defined direct medical costs as the sum of the following costs per patient per hospitalization (Table 2):[7]

- Cost of medications (cost of systemic therapy + cost of medications for premedication and hydration);
- Cost of labor to carry out systemic treatment (cost of labor per application + cost during time of hospitalization);
- Cost of lab tests carried out;
- Cost of imaging tests carried out;
- Cost of molecular test: defining KRAS mutation;
- Cost of hospital treatment due to side effects of mCRC treatment.

Results

Total direct medical costs of mCRC hospital treatment with systemic therapy in 2009

In 2009 the direct medical costs for mCRC hospital treatment with systemic therapy amounted to €3,914,697.00.

Direct medical costs for systemic therapy (chemotherapy + targeted medication) and medication for premedication and hydration amounted to €2,927,679.70.

Direct medical costs for laboratory tests amounted to €50,736.14, and direct medical costs for imaging tests €160,050.45.

Costs for testing for the presence of KRAS mutations amounted to €32,026.19.

Costs for the labor of applying medications amounted to €262,142.96, and costs for labor during the time of hospitalization were €733,110.64, which means that the cost of labor for carrying out systemic treatment amounted to €995,253.60.

Costs for hospital treatment due to side effects of systemic therapy amounted to €25,668.50. Only nine patients were treated, with an average length of hospital treatment of 12.9 days. The most common reason was diarrhoea (five patients), followed by sepsis without neutropenia (three patients). One patient had an allergic reaction to cetuximab. The reason there was such a low number of patients included in hospital care for side effects of systemic therapy is the good premedication and support therapy that the patients receive alongside systemic therapy, and especially hospital treatment of side effects of systemic therapy at specialized healthcare facilities.

The distribution of all direct medical costs is presented in Figure 2. Approximately seven-tenths

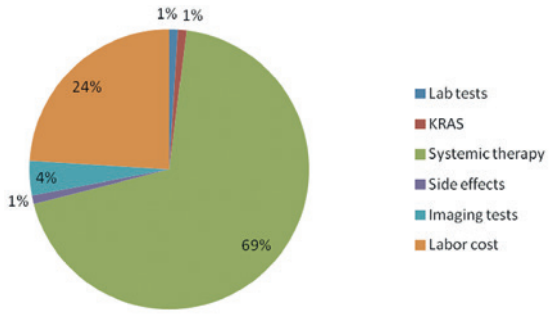

FIGURE 2. Distribution of direct medical costs (%).

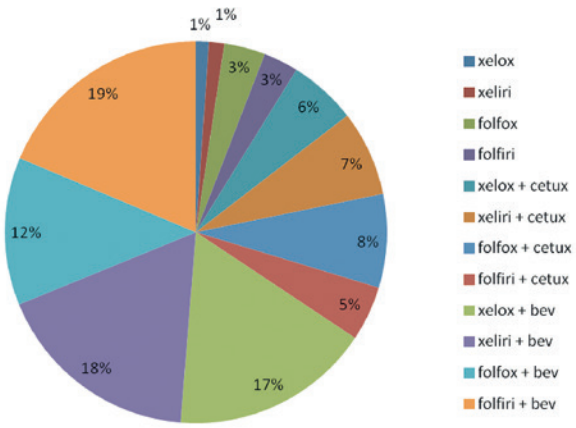

FIGURE 3. Distribution of systemic therapy costs by regimen (%).

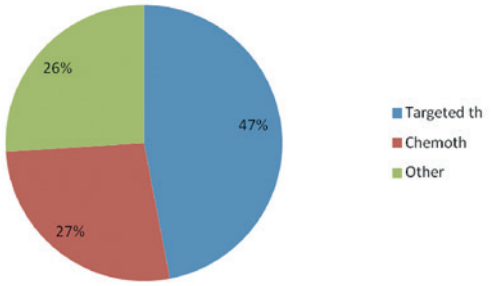

FIGURE 4. Proportion of targeted therapy costs to other costs

(69%) of all direct medical costs were systemic therapy costs, which was also expected. One-fourth of the costs were the cost of carrying out systemic treatment. The greatest costs in the group of laboratory test costs were due to standard laboratory tests (84%). Thirteen percent of laboratory test costs were due to determining levels of iron, ferritin, and transferrin, and only 3% due to urinalysis.

With regard to percentages, the greatest costs were for combined systemic treatment; specifically, for chemotherapy in combination with bevaci-

zumab, which was the most frequently used systemic mCRC treatment in 2009. Individually, out of all costs of medications for systemic treatment (chemotherapy and targeted medications), 19% of all costs were incurred for paired chemotherapy using FOLFIRI in combination with bevacizumab, 18% using XELIRI in combination with bevacizumab, and 17% using XELOX in combination with bevacizumab (Figure 3).

Targeted medications (cetuximab/bevacizumab) represent approximately 50% of the overall direct costs (€1,851,003.30), and the cost of chemotherapy is about 30% of all direct medical costs (€1,047,680.60). All other costs (laboratory tests, imaging tests, labor costs, costs of KRAS testing, and hospital treatment for side effects of systemic treatment) amount to 27% of direct medical costs, mostly due to the labor cost for carrying out systemic treatment (Figure 4).

Average direct medical costs of hospital mCRC therapy with systemic therapy in 2009 per hospitalization

In the group of 209 patients treated with systemic therapy in 2009, altogether *1,605 hospital procedures* were carried out, and on average a patient was hospitalized 7.67 times.

Average direct medical costs of systemic treatment amounted to €2,439.10 per hospitalization.

The average costs of systemic therapy amounted to €1,806.00 per hospitalization

The average labor cost for carrying out systemic treatment amounted to €620.10 per hospitalisation.

Altogether, there were 1,629 standard laboratory tests and 1,547 additional lab tests (urine: 840, iron, ferritin, transferrin: 707) and 600 imaging tests (x-ray: 252, CT: 220, US: 59, MRI: 38, PET CT: 31, bone scintigraphy: 10).

The average cost for laboratory tests amounted to €15.97 per test, and for imaging tests €266.75 per test. On average, 1.98 lab tests and 0.37 imaging tests were conducted per hospitalization.

The average cost of systemic treatment amounted to €18,730.60 per patient.

The average cost of systemic treatment regardless of hospitalization but with regard to the number of rounds of systemic therapy received (two hospitalizations are necessary for one round with a combination of systemic therapy that includes 5-FU amounted to €3,323.17 per patient per round. Altogether, 1,178 rounds of systemic therapy were received.

Comparison of hospital treatment costs recognized by the ZZZS with direct medical costs of hospital treatment of mCRC at the Institute of Oncology Ljubljana in 2009

The average value of DRG weights was 1.12 with a value of €2,739.63 for patients treated for mCRC with systemic therapy in 2009 at the Institute of Oncology Ljubljana (altogether there were 910 DRG cases). On average, each patient was hospitalized 4.35 times. Among the group of DRG cases that were present less than 10% in the calculation, there were 68, with a total weight number of 113.10 and an average value weight of 1.66.

The average value of one DRG weight for 2009 at the Institute of Oncology Ljubljana was €2,446.10.

The value of one DRG weight at the Institute of Oncology Ljubljana is higher in comparison with other providers of secondary activity because tertiary activity is also carried out.

The basic value of one DRG weight (for secondary treatment without added value for tertiary) amounted to €1,976.00 in 2009, which means that in 2009 the ZZZS paid the Institute of Oncology Ljubljana around €2,013,939.20 (if the average value of the DRG weight is 1.12) for patients that received hospital treatment for mCRC with systemic therapy.

Direct medical costs of hospital treatment for mCRC with systemic therapy at the Institute of Oncology Ljubljana in 2009, estimated as the cost of medications (cost of systemic therapy + cost of

TABLE 3. Estimate and actual value of costs for 2009

Cost estimate (2009)	Total cost (€)	DRG case / hospitalization (€)	DRG case / round of systematic treatment (€)
Costs estimated by ZZZS	2,013,939.20	2,213.12	2,213.12
Direct medical costs	3,914,697.00	2,439.10	3,323.17
Difference	**1,900,757.80**	**225.98**	**1,110.1**

DRG = diagnosis-related group

medications for premedication) + labor cost (cost of carrying out systemic treatment) + cost of lab tests performed + cost of imaging tests performed + cost of KRAS testing + cost of hospital treatment due to side effects of mCRC treatment, amounted to €3,914,697.

The difference between paid and actual costs, estimated as the direct medical costs of hospital treatment for mCRC with systemic therapy at the Institute of Oncology Ljubljana, was €1,900,757.80 in 2009.

The estimate and actual value of costs for hospital treatment of mCRC with systemic therapy at the Institute of Oncology Ljubljana in 2009 is presented in Table 3.

The average value of a DRG case amounted to around €2,213.12. Direct medical costs per hospitalization amounted to €2,439.10. Direct medical costs per patient amounted to €18,730.60.

Discussion

Costs of treating colorectal cancer

The most data on costs of treating metastatic cancers are provided by the United States, which have a profit-oriented healthcare system. This trend is also on the rise in Europe.

Analysis of the costs of mCRC, which are defined as the entire costs of the disease together with costs of treatment (costs during diagnosis, treatment, and follow-up) for a group of 6,746 mCRC patients treated between 2004 and 2009 showed that 52.2% of costs were incurred because of hospital treatment of patients, 22.2% of these because of surgical treatment and 47.7% because of outpatient treatment, 10.6% of costs connected with mCRC were incurred because of chemotherapy, and 11.1% were due to targeted medications.[8]

Costs connected with mCRC were defined as the percentage share of total costs and also contained the cost of chemotherapy and targeted medications (cetuximab, panitumumab, and bevacizumab). The cost of chemotherapy rose from 6.9% of total costs in 2004 to 8.1% in 2008. The cost of targeted medications rose from 4.8% in 2004 to 9.4% in 2008. Costs connected with mCRC were $9,978 per month. It is interesting that costs in the mCRC treatment phase were the lowest. The most costs were in the death phase ($26,649), followed by the diagnostic phase ($16,340). Ferro *et al*. determined that there was growth in the total costs of mCRC treatment from 1996 onwards, specifically due to increased choice among possible medications. Targeted medications have increased the cost of treating mCRC by a full 340-fold.[9]

The main cause of the overall costs of mCRC treatment are hospital treatment of patients ($37,369) and outpatient treatment ($34,582), which include chemotherapy. Monthly costs in the diagnostic phase ($12,205) were similar to in the death phase ($13,328), and costs in the treatment phase were considerably lower ($4,722).[10]

Information from England, where Bending determined the direct costs of treating bowel cancer to the National Health Service, where they used the clinical path to determine screening costs, diagnostic costs, treatment costs, and follow-up costs, indicate that the entire annual costs of treating bowel cancer were approximately £1.1 billion. The greatest share of the costs were in the diagnostic phase (£291 million). Treatment costs defined as primary treatment costs (surgery and pharmacotherapy) were approximately £201 million, £129 million for primary treatment of colon cancer, and £72 million for treatment of colon cancer.[11]

In Slovenia, some oncology studies have been carried out that have determined cost effectiveness. Piškur *et al.* analysed the cost effectiveness of the hormone medications anastrozole and tamoxifen for breast cancer.[12] Obradović *et al.* analysed the cost effectiveness of determining the UGT1A1 genotype for irinotecan in monotherapy for colorectal cancer.[13]

In Slovenia to date there has been no analysis that defines mCRC treatment costs, and therefore there are no data from comparable studies in Slovenia.

Evaluating the costs of hospital treatment

In Slovenia the main share of healthcare expenditures are provided from public funds. In 2008 these expenditures comprised of public sources amounted to 72.3% of all funds.[14]

In 2004 Slovenia moved from financing hospitals on the basis of services (the criterion was the green book), to length of stay-based financing on the model of paying DRG to those providing specialized hospital activities. Acute hospital treatments in the DRG model are categorized by diagnoses and procedures performed according to the Australian modification of the tenth revision of the International Statistical Classification of Diseases and Related Health Problems (ICD-10-AM), adapted to Slovenian circumstances, and confirmed by the Health Council.

The DRG system is the most common payment method internationally. This is a payment system that was developed by a group of hospital administration experts at Yale University in the United States by setting up twenty-three main diagnostic groups containing 467 diagnoses. Since 1982, the DRG system has been used as a system for financing health services in the American Medicare program.[15] Various countries have adopted the DRG system with adaptations to their national environments (Canada, Australia, the Scandinavian countries, France, Italy, Austria, and Germany). In Slovenia the DRG system was introduced in 2003 based on the model used in Australia (Australian Refined Diagnosis Related Groups, AR-DRG). The model is based on the principle of "the money follows the patient." At the Institute of Oncology Ljubljana, as at all other hospitals carrying out acute hospital care, since 2004 assessment of health treatment has taken place following the DRG system. DRG are defined through diagnoses and procedures carried out following ICD-10-AM and other information such as length of treatment, age, sex, weight upon admission, and hours of mechanical ventilation.

The DRG system is essentially a method of classifying patients into groups based on different levels of demandingness for whom approximately the same funds are used. An individual acute hospital treatment for a patient is categorized into one DRG case. The price of an individual group of similar cases is expressed in relative terms, and is weighted with regard to price, or the price of an average case. The weight is expressed based on a coefficient of 1. More demanding or expensive DRGs have a weight greater than 1, and less demanding or cheaper ones have a weight less than 1. According to the current method, the ZZZS sends the price of one weight to all hospitals in Slovenia, on the basis of which the hospitals then calculate the services they carry out. Together with the weight of this DRG case and based on the price of one weight, they can calculate the price of a particular acute hospital treatment and, based on the weight of an individual case and the value of the weight, they can define the price of a case.

This method of evaluating hospital treatments—the DRG system or groups of comparable cases—obviously has its disadvantages. Disadvantages of the DRG model may include excessive reduction of costs by limiting necessary tests and choosing less appropriate medications, admitting patients that do not need hospitalization, and false representation of diagnoses and treatments with higher prices, or the provider adapting the data for greater profit with worse medical treatment.[16] Obviously this is not the case for non-profit providers such as the Institute of Oncology Ljubljana, where direct medical costs are higher than those actually paid by the ZZZS.

In his master's thesis, Jurij Stariha draws attention to the lack of uniformity in DRG weight for comparable groups of cases in various hospitals in Slovenia.[17] In principle, for equivalent cases (i.e., cases in which the same amount of resources is used) hospitals should receive the same payment defined by the price of handling an individual case or the weight of the DRG case and the price of one weight. Stariha showed that in 2007 there was not a uniform weight for all providers, which means that providers received different payment for handling equivalent DRG cases. The confirmation that there is a lack of connection of price weight with indicators of operation shows that the current system of financing is not optimal, and so providers or hospitals adapt the value of the weight that they receive.

From the analysis of the DRG system by the Public Health Institute (2003–2008) it is also clear that the current system of financing is not the best and that the level of weight is in great need of adjustment.[18]

According to Marušič *et al*.[15], in order to define standard costs of cases the improvement process ought to take into account clinical paths that precisely describe the handling of a particular case following evidence-based principles of modern medicine. For less frequent cases, actual average costs can be used. It is important to adapt statistical data by taking into account the relationship between the costs of work performed and the differences in length of hospital stay. The DRG model cannot represent all of the complexities of hospital organization. Likewise, a very complicated individual case cannot be classified such that the costs are rejected. In defining weighting, it is not possible to take into account the likelihood of very rare complications, which result in very high additional costs.

Monitoring costs by business process activities as better model for cost assessment in oncology

Currently in Slovenia the AR-DRG 4.2 version of the classification system from 2000 is still being used, even though the updated AR-DRG 6.0 from 2008 (Australian Government, Department of Health and Ageing) is available.

The old version of AR-DRG being used in Slovenia is one of the reasons for the discrepancy between pay-outs and actual costs. Of course, the comparison is not optimal because this study did not include complete costs, but it can be concluded that the discrepancy would be even greater if it took into account the entire cost. Regardless of the version of the evaluation system, it is necessary to adapt the weighting to the actual costs. Oncology is an area of medicine that is developing and changing extremely quickly, which is shown in everyday news on treating cancer. One of the most dynamic areas in oncology in the last decade has been treating mCRC. Classifications and cost evaluation systems for treatments are quite rigid and changes in these areas take place slowly, which is reflected in non-objective evaluation of the costs of mCRC treatment.

Classifying and financing procedures following the DRG model should orient providers towards cost-effective treatment, but not also toward quality. Marušič, Ceglar, and Prevolnik-Rupel suggest including financing criteria such as user satisfaction and treatment outcome for the most common procedures. In this manner, the dimension of quality will be built into payment.[15]

The solution to the problem could be that which was proposed by the Public Health Institute in its DRG analysis (2003–2008): it is necessary to carry out a cost analysis among providers and to define the nationally acceptable average for cancer treatment. However, it is especially emphasized that that it is necessary to define oncology treatment at the Institute of Oncology Ljubljana as the oncology center in Slovenia where most patients with mCRC are treated as a separate entity. Specifically, the price of DRG in Slovenia is based on evaluating the cases of three pilot hospitals, which was carried out based on data on hospital costs in 2001: the Ljubljana Medical Center, Maribor General Hospital, and Jesenice General Hospital. In 2003, based on cost analysis data from the study of pilot hospitals and the Australian weights in the National Hospital Cost Data Collection Round 6 (2001–2002), weights were calculated and then the demandingness of individual cases was determined in Slovenia.[15]

Considering that in the costs we include every monetized use of business elements in achieving the effects of a business process, which in addition to costs in the narrowest sense also includes all elements that are deducted from the profits for a given period, the ideal cost system should ensure completely precise data on all costs with regard to all business effects that a company achieves.[19] The costs, which should ensure one hundred percent reliable information, would far exceed the benefits because they would be too high. Because of this, a company must seek the optimal level of information precision, which can be achieved by monitoring costs by business process activities.

Monitoring costs by business process activities makes it possible to classify general costs and is based on constant improvement of individual parts of the business process; this therefore handles costs at the level of an individual activity, because the activity is the thing that creates the cost. The process of determining and monitoring costs by business process activities takes place such that it is necessary to first define the areas that will be included in defining the costs; for example, the costs of the overall oncological process (pre-hospital testing, pre-hospital care or screening and limiting tests, operation costs, anaesthesia, postoperative costs, material used for this, radiotherapy costs, systemic therapy costs) or for only one area of care. This is followed by defining sources included in analysing the costs that were defined in the previous stage. The third phase defines the specific activities carried out by each of the sources; for example, precisely defining the services that the internal oncology department carries out, a description of the services by staff in an individual department, and the time needed for a particular health service. In the final phase it is necessary to assign a cost to each part. For this we use direct costs, for example, for medicines, services such as lab tests, imaging tests, the material use costs using material, including consumables and technology used, staff, and total direct and indirect labor costs, including employee benefits.[20]

In this manner we can discover and eliminate all unnecessary activities in a healthcare organization so that those that are essential from the viewpoint of treatment and operations will be carried out with maximum efficiency. This will make it possible to achieve lower overall healthcare costs.

This analysis is based on a treatment reality of mCRC that has since remained virtually unchanged. Hence, it can be assumed that the results are still valid today.

Conclusions

The costs paid to the Institute of Oncology Ljubljana by health insurance for treating mCRC with systemic therapy do not match the actual cost of treat-

ment. In fact, the difference between the payment and the actual cost estimated as direct medical costs of hospitalization of mCRC patients treated with systemic therapy at the Institute of Oncology Ljubljana in 2009 was €1,900,757.80.

Classifications and cost evaluation systems for treatments are quite rigid and changes in these areas take place slowly, which is reflected in non-objective evaluation of the costs of mCRC treatment.

The model AR-DRG for cost assessment in oncology being currently used is probably one of the reasons for the discrepancy between pay-outs and actual costs. We propose new method for more precise cost assessment in oncology. Monitoring costs by business process activities makes it possible to classify general costs and is based on constant improvement of individual parts of the business process; this therefore handles costs at the level of an individual activity, because the activity is the thing that creates the cost.

We conclude that the only solution is establishing better communication between oncology, economics, and pharmacoeconomics, which also demands considerably greater transparency of data and accessibility, and only after this it is possible to develop a suitable model for defining costs in oncology.

Acknowledgement

The work of the second author is supported by Creative Core FISNM-3330-13-500033 'Simulations' project funded by the European Union, The European Regional Development Fund.

References

1. Zakelj MP, Zadnik V, Zagar T, Zakotnik B. *Survival of cancer patients, diagnosed in 1991-2005 in Slovenia*. Ljubljana: Institute of Oncology Ljubljana, Epidemiology and Cancer Registry, Cancer Registry of Republic of Slovenia; 2009. p. 229.
2. Treglia G, Taralli S, Salsano M, Muoio B, Sadeghi R, Giovanella L. Prevalence and malignancy risk of focal colorectal incidental uptake detected by 18F-FDG-PET or PET/CT: a meta-analysis. *Radiol Oncol* 2015; 49(2): 200-208.; **48:** 99-104.
3. Ocvirk J. Advances in the treatment of metastatic colorectal carcinoma. *Radiol Oncol* 2009; **43:** 1-8.
4. Ocvirk J, Heeger S, McCloud P, Hofheinz RD. A review of the treatment options for skin rash induced by EGFR-targeted therapies: Evidence from randomized clinical trials and a meta-analysis. *Radiol Oncol* 2013; **47:** 166-75.
5. Reeder CE, Gordon D. Managing oncology costs. *Am J Manag Care.*, 2006; **12:** 3-16.
6. Van Cutsem EJD, Oliveira J. On behalf of the ESMO Guidelines Working Group. Advanced colorectal cancer: ESMO Clinical Recommendations for diagnosis, treatment and follow-up. *Ann Oncol* 2008; **19(Suppl 2):** ii33-4.
7. Mesti T. [The cost of systemic therapy for metastatic colorectal carcinoma at Institute of Oncology Ljubljana in the year 2009]. Master's thesis. [Slovenian]. University of Ljubljana, Faculty of Economics; 2011. Available at: http://www.cek.ef.uni-lj.si/magister/mesti4363.pdf
8. Song X, Zhao Z, Barber B, Gregory C, Zhun C, Sue G. Cost of illness in patients with metastatic colorectal cancer. *J Med Econ* 2011; **14:** 1-9.
9. Ferro SA, Myer BS, Wolff DA, Poniewierski MS, Culakova E, Cosler LE, et al. Variation in the cost of medications for the treatment of colorectal cancer. *Am J Manag Care* 2008; **14:** 717-25.
10. Paramore LC, Thomas SK, Knopf KB. Estimating costs of care for patients with newly diagnosed metastatic colorectal cancer. *Clin Colorectal Cancer*, 2006; **6:** 52-8.
11. Bending WM, Trueman P, Lowson KV, Pilgrim H, Tappenden P, Chilcott J, et al. Estimating the direct costs of bowel cancer services provided by the National Health Service. *Int J Technol Assess Health Care* 2010; **26:** 362-9.
12. Piškur P, Sonc M, Čufer T, Borštnar S, Mrhar A. Pharmacoeconomic aspects of adjuvant anastrozole or tamoxifen in breast cancer: A Slovenian perspective. *Anticancer Drugs*, 2006; **17:** 719-24.
13. Obradovič M, Mrhar A, Kos M. Cost effectiveness of UGT1A1 genotypes in second line, high dose, once every three week irinotecan monotherapy treatment of colorectal cancer. *Pharmacogenomics* 2008; **9:** 539-49.
14. Organisation for Economic Cooperation and Development. *Health data. 2008, May*. Available from: http://www.oecd-ilibrary.org/economics/country-statistical-profile-slovenia_20752288-table-svn. Accessed 10 August 2011.
15. Marušič D, Ceglar J, Prevolnik-Rupel V. [Reimbursement of health care services with special attention paid to drg reimbursement system in Slovenia]. [Slovenian]. *Zdrav Varst* 2009; **48:** 177-83.
16. Busse R. Moving from passive to active provider payment systems: DRG-based financing. *International conference markets in European health systems: opportunities, challenges and limitations;* 2009. Available from: http://www.cef-see.org/health/#. Accessed 20 May 2009.
17. Stariha J. [*The adequacy of funding for acute hospital treatment after a system comparable groups of cases.*] [Slovenian]. Master's thesis. University of Primorska, Faculty of Management; 2009. Available at: http://www.ediplome.fm-kp.si/Stariha_Jurij_20091028.pdf. Accessed 10 August 2010.
18. Zupanc I. [*DRG: questions and answers about the classification system and the financing of hospitals.*][Slovenian].Ljubljana: Inštitut za varovanje zdravja RS; 2008.
19. Tekavčič M. [*Cost management*]. [Slovenian]. Ljubljana : Gospodarski vestnik, ISBN/ISSN: 867061149X; 1997.
20. Grandlich C. Using activity-based costing in surgery. *AORN J*, 2004; **79:** 18-192.

Radiol Oncol 2014; 49(2): 107-114.
doi:10.2478/raon-2014-0029

Ocena prepustnosti krvno-možganske pregrade s pomočjo perfuzijske računalniške tomografije

Avsenik J, Bisdas S, Šurlan Popović K

Izhodišča. Krvno-možganska pregrada je selektivna ovira difuzije na nivoju endotela možganskega žilja. Med preostale funkcije krvno-možganske pregrade sodijo transport, signaliziranje in regulacija osmoze. Povezave endotelnih celic z okoljnimi astrociti, periciti in nevroni so ključne za njihov razvoj, strukturno celovitost in delovanje. Pri boleznih, kot so možganska kap, vnetne bolezni osrednjega živčevja in nevrodegenerativne bolezni, pride do okvare krvno-možganske pregrade in posledično do povečane prepustnosti.

Zaključki. Prepustnost krvno-možganske pregrade lahko ocenimo s pomočjo perfuzijske računalniške tomografije. To je radiološka preiskava, ki vključuje zajemanje slike v t.i. kino tehniki med intravensko aplikacijo jodnega kontrastnega sredstva. Danes perfuzijsko slikanje najpogosteje uporabljamo pri bolnikih z možganskimi tumorji ter v diagnostiki možganske kapi.

Radiol Oncol 2015; 49(2): 115-120.
doi:10.1515/raon-2015-0012

Ocenitev radioloških in metabolnih sprememb kostnih zasevkov z ^{18}FDG-PET/CT po sistemskem zdravljenju

Gunalp B, Oner AO, Ince S, Alagoz E, Ayan A, Arslan N

Izhodišča. Namen raziskave je bila retrospektivna analiza radioloških in metabolnih sprememb kostnih zasevkov po sistemski kemoterapiji s pomočjo ^{18}FDG-PET/CT ter določitev vloge teh kazalcev pri oceni odgovora na zdravljenje.

Bolniki in metode. Retrospektivno smo s pomočjo ^{18}FDG-PET/CT analizirali radiološke in metabolne značilnosti kostnih zasevkov pri 30 bolnikih, ki so jih napotili na oceno odgovora na zdravljenje po sistemski terapiji. Pri vseh bolnikih smo integrirano preiskavo ^{18}FDG-PET/CT opravili pred začetkom in po koncu zdravljenja.

Rezultati. Pri skupini bolnikov z odgovorom na zdravljenje so bili osnovni morfološki radiološki vzorci tarčnih sprememb: litični, sklerotični, mešani in CT negativni. Po zdravljenju se je morfološki vzorec vseh opazovanih lezij spremenil v sklerotičnega, izmerjene atenuacijske vrednosti so se povišale, ocenjena metabolna aktivnost pa se je znižala (p = 0,012). Dokazali smo korelacijo med ocenjenim upadom metabolne aktivnosti ter povišanjem izmerjenih atenuacijskih vrednosti tarčnih sprememb (r = -0,55) (p = 0,026). Pri skupini bolnikov brez odgovora na zdravljenje pa so bili osnovni morfološki radiološki vzorci tarčnih sprememb: litični, blastični, mešani in CT negativni. Po zdravljenju so skoraj vse tarčne lezije obdržale osnovni morfološki vzorec, samo ena CT negativna lezija se je spremenila v litično. Izmerjene atenuacijske vrednosti v lezijah so se znižale (p = 0,012), ocenjena metabolna aktivnost pa se je povišala (p = 0,012). Dokazali smo povezavo med ocenjeno povišano metabolno aktivnostjo ter zmanjšanjem izmerjenih atenuacijskih vrednosti (r = -0,65) (p = 0,032). Izjema so bile lezije, pri katerih je bil osnovni morfološki vzorec blastični. -Te so kazale napredovanje bolezni v smislu povečanja velikosti, povišane izmerjene metabolne aktivnosti ter izmerjenih atenuacijskih vrednosti.

Zaključki. Raziskava kaže, da je ocena metabolne aktivnosti tarčnih lezij (na primeru kostnih zasevkov) bolj zanesljiv kazalec odgovora na zdravljenje kot so morfološko radiološki vzorci teh sprememb.

Radiol Oncol 2015; 49(2): 121-127.
doi:10.2478/raon-2014-0039

Ščitnične patološke spremembe, slučajno najdene pri preiskavi z ^{18}F-FDG PET-CT. Retrospektivna raziskava, v kateri sta sodelovala dva centra PET-CT

Jamšek J, Žagar I, Gaberšček S, Grmek M

Izhodišča. Kadar s preiskavo PET-CT slučajno najdemo kopičenje ^{18}F-FDG v ščitnici, smo pred diagnostičnim izzivom. Maksimalna vrednost privzema izotopa (SUV_{max}) nam je lahko v pomoč pri razlikovanju med benigno in maligno naravo takih ščitničnih sprememb.

Bolniki in metode. Retrospektivno smo ovrednotili rezultate 5.911 preiskav z ^{18}F-FDG PET-CT, ki smo jih v dveh zdravstvenih ustanovah opravili v letih 2010 in 2011. Slučajno odkritim spremembam s patološko povišanim kopičenjem ^{18}F-FDG v ščitnici smo določili vrednost SUV_{max}, bolnike s takimi spremembami pa napotili na pregled k tirologu. Tu so opravili vse potrebne preiskave, po potrebi tudi aspiracijsko biopsijo s tanko iglo. Bolnikom, pri katerih je rezultat preiskave z aspiracijsko biopsijo s tanko iglo dopuščal možnost maligne bolezni ščitnice, smo svetovali operativno zdravljenje.

Rezultati. Kopičenje ^{18}F-FDG v ščitnici smo slučajno odkrili v 3,89 % pri 230 izmed 5.911 bolnikov, pri katerih smo naredili PET-CT preiskavo. Maligno spremembo v ščitnici, ki se je kazala s fokalno povišanim kopičenjem v ščitnici, smo diagnosticirali pri 10 izmed 66 bolnikov (v 15,2 %). V prvem centru ugotovljena vrednost SUV_{max} 36 benignih ščitničnih lezij je bila 5,6 ± 2,8; pri 5 malignih pa 15,8 ± 9,2 ($p < 0,001$). SUV_{max} vrednost 20 benignih ščitničnih lezij, diagnosticiranih v drugem centru, je bila 3,7 ± 2,2; pri 5 malignih pa 5,1 ± 2,3 ($p = 0,217$). Pri vseh 29 bolnikih s slučajno najdenim difuzno povišanim kopičenjem ^{8}F-FDG v ščitnici smo ugotovili benigne spremembe.

Zaključki. Povišano kopičenje ^{18}F-FDG v ščitnici smo slučajno odkrili pri 3,89 % bolnikov, pri katerih smo naredili PET-CT preiskavo. Maligno bolezen ščitnice smo diagnosticirali v 15,2 % ščitničnih lezij, ki so imele fokalno povišano kopičenje ^{18}F-FDG. Vrednost SUV_{max} predstavlja le enega izmed parametrov, ki je v pomoč pri opredeljevanju narave ščitničnih sprememb.

Radiol Oncol 2015; 49(2): 128-134.
doi:10.1515/raon-2015-0007

Primarni limfom centralnega živčnega sistema. Ali je odsotnost znotrajtumorske krvavitve karakterisičen znak pri slikanju z magnetno resonanco?

Sakata A, Okada T, Yamamoto A, Kanagaki M, Fushimi Y, Dodo T, Arakawa Y, Takahaski JC, Miyamoto S, Togashi K

Izhodišča. Dosedanje raziskave so pokazale, da je krvavitev pogosta radiološka najdba pri možganskih tumorjih, histološko opredeljenih kot glioblastomi, nasprotno pa jo zelo redko vidimo pri primarnih limfomih centralnega živčnega sistema. Namen raziskave je bil z oceno krvavitve v tumorju na T2 poudarjenih sekvencah in z oceno tumorskega signala dovzetnosti na magnetno dovzetno poudarjenih slikanjih (SWI) razlikovati med primarnimi limfomi centralnega živčnega sistema in glioblastomi.

Bolniki in metode. V retrospektivno raziskavo smo vključili 58 bolnikov z možganskim tumorjem (19 s primarnim limfomom centralnega živčnega sistema, 39 z glioblastomom) v obdobju od avgusta 2008 do marca 2013, ki so izpolnjevali vključitvene kriterije. Odsotnost krvavitve v tumorju smo ocenjevali na T2 poudarjeni sekvenci in s tumorskim signalom dovzetnosti, ki smo ga razdelili na 3 stopnje na sekvenci SWI. Primerjali smo dobljene rezultate v primarnih limfomih centralnega živčnega sistema in glioblastomih. Vrednosti $P < 0,05$ smo obravnavali kot statistično značilne.

Rezultati. Krvavitve v tumorju na T2 poudarjeni sekvenci ni bilo pri 15 bolnikih (79 %) s primarnim limfomom centralnega živčnega sistema in pri 23 bolnikih (59 %) z glioblastomom. Z odsotnostjo krvavitve v tumorju torej nismo razlikovali med obema vrstama možganskih tumorjev ($P = 0,20$). Nasprotno pa je tumorski signal dovzetnosti 1. ali 2. stopnje pokazal 78,9 % občutljivost in 66,7 % specifičnost ($P < 0,001$) ter je bil značilen za primarne limfome centralnega živčnega sistema ne glede na odsotnost krvavitve v tumorju.

Zaključki. Z nizko stopnjo tumorskega signala dovzetnosti lahko razlikujemo med primarnimi limfomi centralnega živčnega sistema in glioblastomi. Kljub temu je specifičnost naše raziskave nizka in primarne limfome centralnega živčnega sistema ne moremo radiološko izključiti zgolj na podlagi vrednosti tumorskega signala dovzetnosti.

Radiol Oncol 2015; 49(2): 135-140.
doi:10.1515/raon-2015-0011

Diagnosticiranje mehkotkivnih sarkomov z dopplerskim ultrazvokom. Učinkovitost presejalnega točkovalnika z ultrazvokom

Nagano S, Yahiro Y, Yokouchi M, Setoguchi T, Ishidou Y, Sasaki H, Shimada H, Kawamura I, Komiya S

Izhodišča. Znana je uporaba ultrazvoka v postopku presejanja mehkotkivnih tumorjev. Takšne tumorje smo razvrstili glede na vzorec prekrvavljenosti z dopplerskim ultrazvokom ter ponovno ocenili učinkovitost te slikovne diagnostične preiskave kot presejalne metode. Dopplerski ultrazvok smo združili tudi z ostalimi dobljenimi podatki pri ultrazvočni preiskavi, da bi izboljšali učinkovitost diagnosticiranja in da bi uvedli novo diagnostično orodje.

Preiskovanci in metode. V preiskavo smo vključili 189 histološko potrjenih mehkotkivnih tumorjev (122 benignih primerov vključno z benignimi mehkotkivnimi tumorji in podobnimi tumorskimi spremembami ter 67 malignih primerov mehkotkivnih tumorjev). Preiskava z ultrazvokom je vključevala oceno prekrvavljenosti z barvnim dopplerskim ultrazvokom. Vzpostavili smo točkovalnik za bolj učinkovito razlikovanje malignih od benignih mehkotkivnih tumorjev (ultrazvočni presejalni točkovalnik sarkoma).

Rezultati. Srednja vrednost skupine benignih primerov je bila 1,47 ± 0,93, skupine malignih primerov pa 3,42 ± 1,30. Preiskovanci z malignimi spremembami so imeli pomembno višje vrednosti ultrazvočnega presejalnega točkovalnika sarkoma kot preiskovanci z benignimi lezijami. Z analizo značilnosti delujočega sprejemnika je bila površina pod krivuljo 0,88. Z določitvijo vrednosti (3 točke), izračunano z analizo krivulje značilnosti delujočega sprejemnika, je bila senzitivnost 85,1 % in specifičnost 86,9 %.

Zaključki. Ocena prekrvavljenosti samo z dopplerskim ultrazvokom ni zadostna za razlikovanje med benignimi in malignimi mehkotkivnimi tumorji. Predoperativna diagnoza večine mehkotkivnih tumorjev je možna z združevanjem našega ultrazvočnega presejalnega točkovalnika sarkoma s kliničnimi in magnetnoresonančnimi značilnostmi.

Radiol Oncol 2015; 49(2): 141-146.
doi:10.2478/raon-2014-0037

Akutna ishemična možganska kap v povirju Percheronove arterije. Pregled literature s kliničnim primerom

Lamot U, Ribarič I, Šurlan Popović K

Izhodišča. Klinični simptomi in znaki, ki podajo sum na ishemično možgansko kap v področju posteriorne cirkulacije, zahtevajo celovito radiološko obravnavo. To najbolje dosežemo z združevanjem različnih radioloških slikovnopreiskovalnih metod, kot so računalniška tomografija, perfuzijska računalniška tomografija, računalniška tomografska angiografija, magnetnoresonančno slikanje in difuzijsko poudarjeno slikanje. Diagnozo akutne možganske kapi v obdobju, ko je možgansko tkivo še povratno prizadeto, omogoča ustrezen izbor zdravljenja ter prispeva k boljšemu izidu bolezni. Zaradi navedenih razlogov je nujno, da prepoznamo anatomske različice prekrvavitve v posteriorni možganski cirkulaciji, kot je tudi Percheronova arterija.

Prikaz primera. Pri 69-letni bolnici, ki so jo še videli pri polni zavesti pred 10 urami, se je akutna ishemična kap v področju Percheronove arterije klinično pokazala z dvema značilnima znakoma: odsotnostjo okulocefalnega refleksa in komo. Opravljeni preiskavi ob sprejemu, nativna računalniška tomografija glave in računalniška tomografska angiografija vratnega in možganskega žilja, smo sprva ocenili kot normalni. Ponovna nativna računalniška tomografija glave, ki smo jo opravili 24 ur kasneje, je prikazala hipodenzno področje v medialnih predelih obeh talamusov. Ostalih radioloških slikovnopreiskovalnih metod nismo opravili, saj smo predvideli, da je časovno okno za zdravljenje s trombolizo že preteklo. Združevanje vseh dostopnih radioloških slikovnopreiskovalnih metod bi morda prispevalo k diagnozi ishemične kapi še v akutnem obdobju bolezni. Diagnozo ishemične možganske kapi v povirju Percheronove arterije smo tako postavili retrospektivno, s ponovnim pregledom računalniške tomografske angiografije vratnega in možganskega žilja.

Zaključki. Združevanje različnih dostopnih radioloških slikovnopreiskovalnih metod je nujno pri vsakem bolniku s sumom na ishemično kap v področju posteriorne možganske cirkulacije nemudoma po nastanku simptomov. To še posebej velja za primere, ko so izvidi prvotno opravljenih radioloških slikovnih preiskav brez posebnosti, torej v nasprotju z hudimi nevrološkimi klinični znaki.

Radiol Oncol 2015; 49(2): 147-154.
doi:10.1515/raon-2015-0013

Izvedljivost in varnost elektrokemoterapije pri raku trebušne slinavke. Predklinična raziskava

Girelli R, Prejanò S, Cataldo I, Corbo V, Martini L, Scarpa A, Claudio B

Izhodišča. Žlezni rak trebušne slinavke je največkrat smrtna bolezen, kjer je standardno sistemsko zdravljenje neuspešno. Glavni razlog za neobčutljivost trebušne slinavke na zdravljenje je fibroza, ki ovira pristop zdravil. Iščejo nove načine zdravljenja. Elektrokemoterapija je način lokalnega zdravljenja, kjer lahko z aplikacijo električnih pulzov povečamo privzem citostatika, kar poveča njegovovo učinkovitost. Namen raziskave je bil proučiti in vivo učinke elektroporacije na normalni zajčji trebušni slinavki, ki je bila eksperimentalni model. Proučili smo tudi citotoksičnost bleomicina in cisplatina ob njihovi elektroporaciji na celične linije trebušne slinavke. Pri tem smo uporabili celični liniji trebušne slinavke PANC1 in MiaPaCa2.

Materiali in metode. Za elektroporacijo trebušne slinavke smo uporabili standardni protokol elektroporacije, t.j. 1000 V/cm, 8 pulzov, 100 µs, 5 KHz, na belih zajcih Nove Zelandije ter sledili takojšnje in dolgoročne stranske pojave. Stopnjo permeabilizacije celic smo merili s pretočno citometrijo, viabilnost celic in njihovo kemosenzitivnost pa s testom 3-(4,5-dimetiltiazol-2-yl)-5-(3-karboksimetoksifenil)-2-(4-sulfofenil)-2H-tetrazolim (MTS).

Rezultati. Elektroporacija trebušne slinavke zdravih zajcev ni imela lokalnih ali sistemskih toksičnih učinkov na živali. Rezultati zatorej dokazujejo potencialno varnost elektrokemoterapije. In vitro raziskava pa dokazuje povečano kemosenzitivnost dveh celičnih linij trebušne slinavke na zdravljenje z eletrokemoterapijo, tako z bleomicinom kot tudi cisplatinom.

Zaključki. Podatki nakazujejo varnost aplikacije električnih pulzov v zdravi trebušni slinavki. Z aplikacijo takih električnih pulzov lahko vplivamo na citotoksičnost bleomicina ali cisplatina pri njihovi uporabi v elektrokemoterapiji.

Radiol Oncol 2015; 49(2): 155-162
doi:10.2478/raon-2014-0044

Učinkovitost intenzitetno modulirane radioterapije in sočasne kemoterapije s karboplatinom pri raku nosnega žrela

Songthong A, Chakkabat C, Kannarunimit D, Lertbutsayanukul C

Izhodišča. Namen prospektivne klinične raziskave faze II je bil oceniti učinkovitost in toksičnost sočasnega zdravljenja s karboplatinom in intenzitentno modulirano radioterapijo (IMRT) pri bolnikih z rakom nosnega žrela.

Bolniki in metode. Med oktobrom 2005 in novembrom 2011 je 73 bolnikov z rakom nosnega žrela stadija II-IVB prejelo 70 Gy IMRT sočasno s tremi krogi karboplatina (AUC 5) na 3 tedne. Nato so bolniki v štiritedenskih intervalih dodatno prejeli tri kroge karboplatina (AUC 5) in 5-FU-ja (1.000 mg/m2, dnevi 1–4). Pri vseh bolnikih smo ocenili odgovor tumorja na zdravljenje s kriteriji RECIST, preživetje s Kaplan-Meierjevo metodo in toksičnost po običajnih terminoloških kriterijih za neželene učinke zdravljenja (CTCAE) verzije 4.0.

Rezultati. Tri mesece po kemoradioterapiji sta bila popoln in delen odgovor dosežena pri 82,2 % oz. 17,8 % bolnikov. Po srednjem času sledenja 48,1 mesecev (razpon 1,3–97,8 mesecev) je imelo 8,2 % bolnikov lokalno ponovitev bolezni in 17,8 % oddaljene zasevke. Srednje preživetje ni bilo doseženo. Celokupno preživetje po treh letih opazovanja je bilo 83,6 % in preživetje brez napredovanja bolezni 65,3 %. Obsevanje je zaključilo 97,2 % bolnikov, sočasno kemoterapijo s karboplatinom 69,9 % in dodatno kemoterapijo 68,5 %. Akutna toksičnost stopnje 3–4 se je kazala kot oralni mukozitis (16,4 %), disfagija (16,4 %), kserostomija (15,1 %) in hematotoksičnost (6,8 %).

Zaključki. Bolniki z rakom nosnega žrela, ki so sočasno prejeli karboplatin in IMRT, so imeli odličen odgovor tumorja na zdravljenje, toksičnost je bila obvladljiva in zdravljenje dobro tolerirano. Takšno zdravljenje predstavlja alternativo standardnemu zdravljenju s cisplatinom.

Radiol Oncol 2015; 49(2): 163-172.
doi:10.2478/raon-2014-0027

Predoperativno zdravljenje z radiokemoterapijo pri bolnikih z neresektabilnim rakom želodca in lokoregionalno napredovalim rakom gastroezofagealnega prehoda

Ratoša I, Oblak I, Anderluh F, Velenik V, But-Hadžić J, Šečerov Ermenc A, Jeromen A

Izhodišča. Namen raziskave je bil analizirati izide zdravljenja s predoperativno radiokemoterapijo pri bolnikih z neresektabilnim rakom želodca in lokoregionalno napredovalim rakom gastroezofagealnega (GE) prehoda, zdravljenih na Onkološkem inštitutu v Ljubljani.

Bolniki in metode. V retrospektivno raziskavo smo vključili bolnike z neresektabilnim žleznim rakom želodca in lokoregionalno napredovalim žleznim rakom GE prehoda, ki smo jih med januarjem 2004 in junijem 2012 zdravili s predoperativno radiokemoterapijo. V shemi zdravljenja so bili trije krogi kemoterapije s 5-fluorouracilom in cisplatinom in 28 dni obsevanja, ki smo ga pričeli sočasno z drugim krogom kemoterapije. Bolnike smo obsevali s tridimenzionalno konformno tehniko na linearnem pospeševalniku, s fotoni energij 6 in 15 MV. Protokol obsevanja je predvideval v 5 tednih 25 dnevnih frakcij obsevanja po 1,8 Gy. Bolniki so bili operirani 4–6 tednov po zaključenem predoperativnem zdravljenju. Multidisciplinarni konzilij zdravnikov se je po operaciji posameznega bolnika individualno odločil še za dopolnilno zdravljenje s kemoterapijo. Primarna cilja raziskave sta bila stopnja radikalne patohistološke resekcije (R0) in stopnja patološkega odgovora na predoperativno zdravljenje. Sekundarna cilja raziskave pa sta bila ugotoviti preživetje bolnikov in zaznati stranske učinke predoperativne radiokemoterapije.

Rezultati. Po protokolu je predoperativno zdravljenje zaključilo 84 od 90 bolnikov (93,3 %). Pri dvajsetih bolnikih (22,2 %) kirurška odstranitev tumorja ni bila možna zaradi napredovanja bolezni, pridruženih bolezni, slabega splošnega stanja zmogljivosti ali zaradi tumorja, ki kljub predoperativnemu zdravljenju ni bil resektabilen v času operacije. Pri 13 bolnikih (14,4 %) smo zato zaradi neresektabilnosti tumorja ali difuzne karcinomatoze peritoneja naredili kirurško eksploracijo. S ciljem popolne odstranitve tumorja pa je bilo operiranih 57 (63,4 %) bolnikov. Resekcijo R0 smo naredili pri 50 bolnikih (55,6%), neradikalno operacijo (R1 ali R2) pa pri 7 bolnikih (7,8 %), ki so sodelovali v raziskavi. Od vseh operiranih bolnikov (n = 57) je popolni patološki odgovor doseglo 5 bolnikov (5,6 % od vseh zdravljenih bolnikov ali 8,8 % od vseh operiranih bolnikov). Zmanjšanje tumorja in/ali bezgavk je bilo doseženo pri 49 bolnikih (86 %), nespremenjen stadij pri enem (1,8 %) in povišanje stadija, predvsem na račun povečanja števila patoloških bezgavk, pa pri 7 (12,3 %) operiranih bolnikih. Slabost, bruhanje ali supresija kostnega mozga so predstavljali največji delež stopnje 3 ali 4 stranskih učinkov zdravljenja. Smrti zaradi predoperativne radiokemoterapije nismo zabeležili. En bolnik je umrl zaradi septičnega šoka po operaciji, vzrok smrti dveh bolnikov ni znan. 26 bolnikov (45,6 %) je umrlo zaradi raka želodca ali raka GE prehoda. 28 (49,1 %) bolnikov je bilo v času analize podatkov brez bolezni, medtem ko smo ponovitev bolezni – večinoma zaradi oddaljenih zasevkov – ugotavljali pri 29 bolnikih (50,9 %). 2-letna lokoregionalna kontrola bolezni je bila 82,9 %, preživetje brez bolezni 43,9 %, bolezensko specifično preživetje 56,9 % in celokupno preživetje 53,9 %.

Zaključki. Predoperativna radiokemoterapija je omogočila zmanjšanje velikosti tumorja in/ali bezgavk, večji odstotek radikalnih resekcij ter zato več možnosti ozdravitve bolnikov. Toksičnost zdravljenja je bila sprejemljiva.

Radiol Oncol 2015; 49(2): 173-180.
doi:10.2478/raon-2014-0050

Febrilna nevtropenija pri kemoterapevtskem zdravljenju bolnikov z drobnoceličnim pljučnim rakom

Režonja Kukec R, Grabnar I, Vovk T, Mrhar A, Kovač V, Čufer T

Izhodišča. Zdravljenje drobnoceličnega pljučnega raka s kombinacijo kemoterapevtikov etopozida in cisplatina naj bi bilo povezano s srednjim (10–20 %) tveganjem za febrilno nevtropenijo. Onkološke smernice rutinske uporabe rastnih dejavnikov ob tem zdravljenju ne priporočajo, vendar v klinični praksi pri standardnem zdravljenju z etopozidom in cisplatinom pogosto srečujemo primere febrilne nevtropenije. Namen raziskave je bil oceniti pogostnost nevtropenije in febrilne nevtropenije pri bolnikih z razsejanim drobnoceličnim pljučnim rakom po prvem krogu standardne kemoterapije ter pri istih bolnikih raziskati povezavo med nevtropenijo visoke stopnje in maksimalnimi plazemskimi koncentracijami etopozida.

Metode. Analizirali smo skupino 17 bolnikov z razsejanim drobnoceličnim pljučnim rakom zdravljenih s kombinacijo citostatikov etopozida in cisplatina. Ti bolniki so bili že vključeni v farmakokinetično raziskavo zdravljenja z etopozidom. Zbrali smo podatke o nevtropeniji stopnje 3 in 4 ter febrilni nevtropeniji po prvem krogu zdravljenja. Vrednosti nevtrofilcev smo določili prvi dan drugega kroga zdravljenja, razen, če so se simptomi povezani z nevtropenijo pojavili prej. Neželene učinke smo klasificirali s pomočjo kriterijev Nacionalnega inštituta za zdravljenje raka (NCI-CTC), verzija 4,0. Dodatno smo raziskali povezavo med nevtropenijo visoke stopnje in maksimalnimi plazemskimi koncentracijami etopozida, ki so bile izmerjene kot sestavni del farmakokinetične raziskave.

Rezultati. Dva od 17 bolnikov sta prejela primarno zaščito z rastnimi dejavniki. Pri 15 bolnikih brez primarne zaščite je bil delež bolnikov z nevtropenijo stopnje 3 in 4 ter delež s febrilno nevtropenijo visok (8/15 [53,3 %] in 2/15 [13,3 %]) glede na dejstvo, da se podatki nanašajo samo na prvi krog zdravljenja. En bolnik je zaradi pljučnice povezane s febrilno nevtropenijo umrl. Domnevno so nevtropenični dogodki ob standardnem odmerku etopozida in cisplatina povezani s povečanimi plazemskimi koncentracijami etopozida. Najvišji koncentraciji etopozida (27,07 in 27,49 mg/l) sta namreč bili določeni pri bolnikoma, ki sta razvila febrilno nevtropenijo. Povprečna maksimalna plazemska koncentracija etopozida v prvem krogu je bila sicer 17,6 mg/l.

Zaključki. Rezultati naše študije nakazujejo potrebo po zmanjševanju tveganja za nevtropenične dogodke pri kemoterapevtskem zdravljenju drobnoceličnega pljučnega raka, začenši v prvem krogu zdravljenja. Ena izmed možnosti je obvezna primarna zaščita z uporabo rastnih dejavnikov. Druga možnost pa so izboljšani modeli za določanje tveganja z namenom ugotoviti, kateri bolniki imajo povečano tveganje za nevtropenijo. Individualizacija primarne zaščite, ki temelji ne samo na kliničnih lastnostih, ampak tudi na vrednostih plazemskih koncentracij etopozida, predstavlja dodatno možnost, ki bi jo bilo smiselno upoštevati.

Radiol Oncol 2015; 49(2): 181-184.
doi:10.2478/raon-2014-0024

Ishemija mezenterija po zdravljenju s kapecitabinom pri raku danke in posledičnim sindromom kratkega črevesja ni absolutna kontraindikacija za radikalno onkološko zdravljenje

Perpar A, Brecelj E, Rotovnik Kozjek N, Anderluh F, Oblak I, Skoblar Vidmar M, Velenik V

Izhodišča. Arterijski ali venski trombotični zapleti so resna obolevnost in pomemben vzrok smrtnosti pri bolnikih z rakom. Nagnjenost do razvoja teh zapletov je delno posledica bolezni, delno pa naših poskusov zdravljenja raka. Eden najredkejših in najbolj nevarnih trombemboličnih zapletov je ishemija mezenterija. Visoka smrtnost je posledica redkosti zapleta in neznačilnih simptomov, ki otežijo zgodnjo diagnozo in zdravljenje; zaplet običajno odkrijemo in zdravimo pozno. Bolniki, ki preživijo ishemijo mezenterija, imajo lahko sindrom kratkega črevesja, ki je po uvedbi parenteralne prehrane na domu postal kronična bolezen.

Prikaz primera. Predstavljamo 73-letnega bolnika z rakom danke, pri katerem smo ugotovili akutno trombozo mezenterične arterije na začetku predoperativne radiokemoterapije. Potrebna je bila resekcija ascendentnega kolona in skoraj celotnega tankega črevesja razen proksimalnih 50 cm. Bolnik je imel multiorgansko odpoved, nato pa se je njegovo stanje izboljšalo. Uspešno je zaključil radikalno zdravljenje raka danke (predoperativno radioterapijo in operacijo). Še vedno prejema parenteralno prehrano na domu, ker je preostanek črevesja prekratek, da bi zadostil bolnikovim prehranskim potrebam.

Zaključki. Ishemija mezenterija in sindrom kratkega črevesja, ki je njena posledica, nista absolutni kontraindikaciji za radikalno onkološko zdravljenje, še posebej, če s tem lahko dosežemo ozdravitev.

Radiol Oncol 2015; 49(2): 185-191.
doi:10.1515/raon-2015-0008

Klinična uporabnost izračuna biološke učinkovite doze za hrbtenjačo pri zdravljenju s stereotaktičnim obsevanjem telesa

Lee SH, Lee KC, Choi J, Ahn SH, Lee SH, Sung KH, Kil SH

Izhodišča. Namen raziskave je bil ugotoviti, ali lahko izračun biološko učinkovite doze (BED), ki temelji na linearno-kvadratnem modelu, uporabljamo za ocenjevanje tolerančne doze hrbtenjače pri stereotaktičnem obsevanju telesa (SBRT) ob uporabi štirih ali več frakcij.

Bolniki in metode. Retrospektivno smo ocenili 63 metastatskih sprememb hrbtenjače pri 47 bolnikih. Najpogosteje predpisana doza je bila 36 Gy v 4 frakcijah. Pri načrtovanju smo poskušali omejiti najvišji predpisani odmerek na hrbtenjačo ali na caudo equino na manj kot 50% ali 45 Gy2/2. Pri izračunu BED smo uporabili najvišjo točko doze na hrbtenjačo.

Rezultati. Največja doza na hrbtenjačo v eni frakciji je bila v razponu 2,6–6,0 Gy (mediana 4,3 Gy). Enakovredna skupna doza v frakcijah po 2 Gy ni bila večja od 50 Gy2/2 (12,1–67,9; mediana 32,0), razen pri 4 bolnikov s 52,7, 56,4, 62,4 in 67,9 Gy2/2. Razmerje med najvišjo in predpisano dozo na hrbtenjačo se je povečalo do 82,2 % predpisane doze, ko se je povečala stopnja kompresije epiduralnega dela hrbtenjače. Pri nobenem bolniku se v obdobju spremljanja od 0,5 do 53,9 mesecev ni razvila druga stopnja toksičnosti hrbtenjače povzročene z obsevanjem.

Zaključki. Pri SBRT v več frakcijah BED lahko uporabljamo za oceno tolerančne doze na hrbtenjačo pod pogojem, da je doza ene frakcije na hrbtenjačo zmerna, <6,0 Gy. Kaže se, da je največja doza do 45–50 Gy2/2 na hrbtenjačo sprejemljiva pri obsevanju s 4 ali več frakcijami.

Radiol Oncol 2015; 49(2): 192-199.
doi:10.1515/raon-2015-0006

Dinamična računalniško tomografska angiografija pri načrtovanju radiokirurškega zdravljenja intrakranialnih arteriovenskih malformacij z robotskim nožem (cyberknife). Tehnično poročilo in izvedljivost

Haridass A, Maclean J, Chakraborty S, Sinclair J, Szanto J, Iancu D, Malone S

Izhodišča. Pri uspešni radiokirurgiji arteriovenskih malformacij je potrebno natančno očrtati nidus za obsevanje v 3D načrtovalnem sistemu. Za oceno AVM nidusa je za zlati standard veljal kateterski biplanirni digitalni subtrakcijski angiogram (DSA). DSA je zaradi dvodimenzionalnosti omejeval svojo vlogo pri očrtovanju; prav tako ga ni bilo mogoče uvoziti v delovno postajo pri načrtovanju zdravljenja z robotskim nožem. Predstavljamo tehniko pridobivanja in integracije 3D dinamičnih računalniško tomografskih angiogramov (dCTA) v delovno postajo pri načrtovanju obsevanja z robotskim nožem za intrakranialne arteriovenske malformacije ter oceno izvedljivosti uporabe te tehnike v prvi kohorti bolnikov.

Metode. Dinamične zaporedne računalniško tomografske slike celotnih možganov smo pridobili z volumsko slikovno CT napravo Toshiba 320. Podatke smo rekonstruirali vsakih 0,5 sekund. Na ta način smo veččasovno točkovno zajeli podatke in izbrali CT slike z najbolj jasnim nidusom. Krvnih žil v okolici ni bilo potrebno pomembno ojačiti. Podatke smo uvozili v postajo za načrtovanje zdravljenja z robotskim nožem in jih sočasno registrirali z načrtovalnim CT in T2 MRI ter 2D DSA dodali kot referenco. Ocenili smo zmožnost uporabe dCTA pri prvih 13 bolnikih in iz njihovih kartotek ocenili tudi rezultate zdravljenja.

Rezultati. Podatke dCTA smo pravilno zajeli v postajo za načrtovanje zdravljenja z robotskim nožem in videti je, da so bili v pomoč pri očrtanju nidusa pri vseh bolnikih. Slikovni načini so se dopolnjevali. Po srednjem času 37 mesecev spremljanja je imelo 85 % bolnikov popolno (6/13) ali napredujočo delno (5/13) obliteracijo nidusa.

Zaključki. dCTA je obetajoča slikovna tehnika, ki jo lahko uspešno uporabimo za uvoz v postajo za načrtovanje zdravljenja z robotskim nožem. Videti je, da pomaga pri opredelitvi nidusa za potrebe radiokirurgije. Potrebne so nadaljnje raziskave za potrditev njene vloge.

Radiol Oncol 2015; 49(2): 200-208.
doi:10.2478/raon-2014-0046

Stroški zdravljenja razsejanega raka debelega črevesa in danke v Sloveniji. Analiza neskladij med stroški in priznanimi plačili

Mesti T, Boshkoska BM, Kos M, Tekavčič M, Ocvirk J

Izhodišča. Naredili smo oceno dejanskih stroškov zdravljenja razsejanega raka debelega črevesa in danke (rRDČD) v Sloveniji za leto 2009. Onkološki inštitutu Ljubljana je bil edina ustanova, kjer smo to bolezen v Sloveniji zdravili. Stroške smo primerjali s plačilom Zavoda za zdravstveno zavarovanje Slovenije.

Metode. Z retrospektivno analizo bolnikovih podatkov iz notranje baze podatkov smo (1) določili neposredne medicinske stroške zdravljenja rRDČD leta 2009 ter (2) določili razliko med prejetim plačilom Zavoda za zdravstveno zavarovanje Slovenije in dejanskimi stroških sistemskega zdravljenja. V obdobju zdravljenja bolezni smo analizirali neposredne medicinske stroške akutnega bolnišničnega sistemskega zdravljenja, skupaj s stroški bolnišničnega zdravljenja zaradi morebitnih stranskih učinkov. Izvzeli smo stroške možnega obsevanja ali kirurškega zdravljenja. Prav tako smo izvzeli indirektne medicinske stroške, nemedicinske stroške in stroški spremljanja.

Rezultati. Skupina 209 bolnikov je izpolnjevala vključitvene kriterije. Neposredne medicinske stroške bolnišničnega zdravljenja rRDČD s sistemsko terapijo na Onkološkem inštitutu Ljubljana za leto 2009 smo ocenili kot strošek zdravil (strošek sistemske terapije + strošek zdravil za premedikacijo) + strošek dela (strošek izvedbe sistemskega zdravljenja) + strošek laboratorijskih preiskav + strošek slikovnih preiskav + strošek testiranja KRAS + strošek bolnišnične obdelave zaradi stranskih učinkov zdravljenja rRDČD. Znašali so 3.914.697 €.

Razlika med izplačanimi stroški Zavoda za zdravstveno zavarovanje Slovenije ter dejanskimi stroški, ocenjenimi kot neposredni medicinski stroški bolnišničnega zdravljenja rRDČD s sistemsko terapijo na Onkološkem inštitutu Ljubljana za leto 2009, je bila 1.900.757,80 €.

Zaključki. Stroški, ki jih je plačal Zavod za zdravstveno zavarovanje Slovenije Onkološkemu Inštitutu Ljubljana za zdravljenje rRDČD s sistemsko terapijo, se ne ujemajo z dejanskimi stroški zdravljenja. Razlika med izplačanimi in dejanskimi stroški za leto 2009 je bila 1.900.757,80 €. Verjetno je eden od razlogov za razhajanja med izplačili in dejanskimi stroški avstralski model (AR-DRG), ki ga v Sloveniji uporabljamo za oceno stroškov v onkologiji. Predlagamo novo metodo za natančnejšo oceno stroškov.

Spoštovani!

UP Fakulteta za vede o zdravju bo v času **od 18. do 22. maja 2015** v okviru projekta **UP IN SVET** organizirala mednarodno delavnico za študente z naslovom **»CANCER WORKSHOP – Od preprečevanja do novih pristopov zdravljenja«**. Delavnica bo potekala na Univerzi na Primorskem, v prostorih Fakultete za vede o zdravju, Polje 42, 6310 Izola, v popoldanskem času.

Cilj delavnice je dobiti **celovit vpogled v značilnosti raka iz biološkega in medicinskega vidika** s posebnim poudarkom na preprečevanju te bolezni, molekularnih poteh, ki sodelujejo pri nastanku in napredovanju te bolezni, diagnostiki ter pristopih novih oblik zdravljenja. V okviru večdnevne delavnice bo tako predstavljenih več vsebinskih sklopov, v okviru katerih bodo svoje poglede na problematiko podali številni ugledni strokovnjaki in raziskovalci s področja.

Delavnica je namenjena **pretežno študentom Univerze na Primorskem**, lahko pa se je udeležijo tudi ostali zainteresirani, ki jih tematika zanima.

Udeležba na delavnici je **BREZPLAČNA!** Program najdete na spletni strani UP FVZ http://www.fvz.upr.si/sl/napovednik-izobrazevanje

Prijave zbiramo na elektronski naslov: cancerworkshop@fvz.upr.si najkasneje **do petka, 8. maja 2015.** Prijava je obvezna tudi v primeru, da se želite udeležiti samo določenega dela programa oz. posameznega dne.

Veseli bomo, če informacijo o dogodku posredujete svojim kolegom, poslovnim partnerjem in drugim morebitnim zainteresiranim v svojih okoljih.

Vljudno vabljeni!

UP IN SVET – Mednarodna vpetost Univerze na Primorskem: operacijo delno financira Evropska unija iz Evropskega socialnega sklada ter Ministrstvo za izobraževanje, znanost in šport. Operacija se izvaja v okviru Operativnega programa razvoja človeških virov za obdobje 2007-2013, razvojne prioritete: 3.: Razvoj človeških virov in vseživljenjskega učenja; prednostne usmeritve 3.3.: Kakovost, konkurenčnost in odzivnost visokega šolstva.

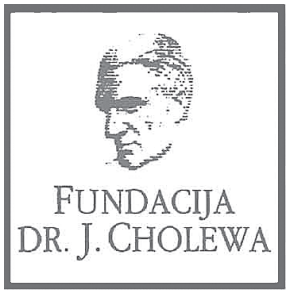

FUNDACIJA DOC. DR. JOSIP CHOLEWA

RAZPISUJE

DENARNO POMOČ ZA SOFINANCIRANJE MATERIALNIH STROŠKOV PRI ZNANSTVENO-RAZISKOVALNIH DELIH S PODROČJA ONKOLOGIJE.

PRIJAVA NAJ VSEBUJE:

1. KRATKO OBRAZLOŽITEV ZNANSTVENO-RAZISKOVALNEGA DELA S FINANČNO KONSTRUKCIJO

2. KRATKO BIOGRAFIJO IN BIBLIOGRAFIJO PROSILCA/PROSILCEV

PRIJAVE, PROSIMO, POŠLJITE DO **30. 9. 2015** NA NASLOV
ZDRUŽENJE FUNDACIJA DOC.DR. JOSIP CHOLEWA,
DUNAJSKA CESTA 106, 1000 LJUBLJANA

Uporabljena moška slovnična oblika se enakovredno nanaša na oba spola.

FUNDACIJA "DOCENT DR. J. CHOLEWA"
JE NEPROFITNO, NEINSTITUCIONALNO IN NESTRANKARSKO
ZDRUŽENJE POSAMEZNIKOV, USTANOV IN ORGANIZACIJ, KI ŽELIJO
MATERIALNO SPODBUJATI IN POGLABLJATI RAZISKOVALNO
DEJAVNOST V ONKOLOGIJI.

Activity of "Dr. J. Cholewa" Foundation for Cancer Research and Education – a report for the second quarter of 2015

The “Docent Dr. J. Cholewa Foundation for Cancer Research and Education” is a non-profit, non-political and non-government organisation that helps professionals, institutions and individuals obtaining financial help for cancer research and education in the Republic of Slovenia. It carries the name of Dr. Josip Cholewa, one of the first researchers in cancer in Slovenia and the founder of the “Banovinski Inštitut za raziskovanje in zdravljenje novotvorb”, that later became the Institute of Oncology in Ljubljana, Slovenia. Already in the twenties of the previous century, his research was based on multidisciplinary approach to prevention, detection and treatment of cancer, as a harbinger of all the progress observed in a large part of the world until now.

High quality cancer research demands a lot of financial support and many excellent ideas cannot be put into practical use for the simple lack of it. The most important activity of the Foundation is to provide at least some of the financial support needed by qualified individuals and organisations interested in cancer research. The Foundation aims to help with the transmission of the latest diagnostic and therapy procedures to the everyday research and clinical environment in Slovenia. This part of Foundation’s activity represents the most direct benefit for the ever increasing number of patients with various types of cancer in Slovenia, since the incidence rates of many cancer, like colon, prostate and breast cancer, have kept rising in recent decades.

The Foundation continues to provide financial support to "Radiology and Oncology”, an international scientific journal that is edited and published in Ljubljana, Slovenia. It publishes scientific research articles, reviews, case reports, short reports and letters to the editor about research and studies in experimental and clinical oncology, supportive therapy, radiology, radiophyics, prevention and early diagnostics of different types of cancer. It is an open access journal freely available in pdf format and with a respectable Science Citation Index Impact factor. All the abstracts in “Radiology and Oncology” are available in Slovenian and the journal can thus provide sufficient scientific information from various fields of high quality cancer research to interested lay public in Slovenia.

The “Docent Dr. J. Cholewa Foundation for Cancer Research and Education” has thus an important role in support of many scientists involved in cancer research, cancer education and in many of the related fields in the Republic of Slovenia. The next meeting of its Executive Board is to take place in late May this year, when its activity in 2014 and its future activity are to be discussed and reviewed.

Borut Štabuc, MD, PhD
Tomaž Benulič, MD
Viljem Kovač, MD, PhD
Andrej Plesničar, MD. MSc

TANTUM VERDE®

Lajšanje bolečine in oteklin pri vnetju v ustni votlini in žrelu, ki nastanejo zaradi okužb in stanj po operaciji in kot posledica radioterapije (t.i. radiomukozitis).

CSC ANGELINI

Imetnik dovoljenja za promet
CSC Pharma d.o.o.
Jana Husa 1a
1000 Ljubljana

www.tantum-verde.si

Tantum Verde 1,5 mg/ml oralno pršilo, raztopina

Kakovostna in količinska sestava
1 ml raztopine vsebuje 1,5 mg benzidaminijevega klorida, kar ustreza 1,34 mg benzidamina. V enem razpršku je 0,17 ml raztopine. En razpršek vsebuje 0,255 mg benzidaminijevega klorida, kar ustreza 0,2278 mg benzidamina. En razpršek vsebuje 13,6 mg 96 odstotnega etanola, kar ustreza 12,728 mg 100 odstotnega etanola, in 0,17 mg metilparahidroksibenzoata (E218).

Terapevtske indikacije
Samozdravljenje: lajšanje bolečine in oteklin pri vnetju v ustni votlini in žrelu, ki so lahko posledica okužb in stanj po operaciji. Po nasvetu in navodilu zdravnika: lajšanje bolečine in oteklin v ustni votlini in žrelu, ki so posledica radiomukozitisa.

Odmerjanje in način uporabe
Uporaba 2- do 6-krat na dan (vsake 1,5 do 3 ure). Odrasli: 4 do 8 razprškov 2- do 6-krat na dan. Otroci od 6 do 12 let: 4 razprški 2- do 6-krat na dan. Otroci, mlajši od 6 let: 1 razpršek na 4 kg telesne mase; do največ 4 razprške 2 do 6-krat na dan.

Kontraindikacije
Znana preobčutljivost za zdravilno učinkovino ali katerokoli pomožno snov.

Posebna opozorila in previdnostni ukrepi
Pri manjšini bolnikov lahko resne bolezni povzročijo ustne/žrelne ulceracije. Če se simptomi v treh dneh ne izboljšajo, se mora bolnik posvetovati z zdravnikom ali zobozdravnikom, kot je primerno. Zdravilo vsebuje aspartam (E951) (vir fenilalanina), ki je lahko škodljiv za bolnike s fenilketonurijo. Zdravilo vsebuje izomalt (E953) (sinonim: izomaltitol (E953)). Bolniki z redko dedno intoleranco za fruktozo ne smejo jemati tega zdravila. Uporaba benzidamina ni priporočljiva za bolnike s preobčutljivostjo za salicilno kislino ali druga nesteroidna protivnetna zdravila. Pri bolnikih, ki imajo ali so imeli bronhialno astmo, lahko pride do bronhospazma. Pri takih bolnikih je potrebna previdnost.

Medsebojno delovanje z drugimi zdravili in druge oblike interakcij
Pri ljudeh raziskav o interakcijah niso opravljali.

Nosečnost in dojenje
Tantum Verde z okusom mentola 3 mg pastile se med nosečnostjo in dojenjem ne smejo uporabljati.

Vpliv na sposobnost vožnje in upravljanja s stroji
Uporaba benzidamina lokalno v priporočenem odmerku ne vpliva na sposobnost vožnje in upravljanja s stroji.

Neželeni učinki
Bolezni prebavil Redki: pekoč občutek v ustih, suha usta.
Bolezni imunskega sistema Redki: preobčutljivostna reakcija.
Bolezni dihal, prsnega koša in mediastinalnega prostora Zelo redki: laringospazem.
Bolezni kože in podkožja Občasni: fotosenzitivnost. Zelo redki: angioedem.

Rok uporabnosti
4 leta. Zdravila ne smete uporabljati po datumu izteka roka uporabnosti, ki je naveden na ovojnini. Posebna navodila za shranjevanje Za shranjevanje pastil niso potrebna posebna navodila. Plastenko z raztopino shranjujte v zunanji ovojnini za zagotovitev zaščite pred svetlobo. Shranjujte pri temperaturi do 25°C. Shranjujte v originalni ovojnini in nedosegljivo otrokom.

ERBITUX®
CETUXIMAB

See the difference

Individualizirano zdravljenje za bolnike z metastatskim kolorektalnim rakom

Merck Serono Onkologija | *Ključ je v kombinaciji*

Erbitux 5 mg/ml raztopina za infundiranje
Skrajšan povzetek glavnih značilnosti zdravila

Sestava: En ml raztopine za infundiranje vsebuje 5 mg cetuksimaba in pomožne snovi. Cetuksimab je himerno monoklonsko IgG_1 protitelo. **Terapevtske indikacije:** Zdravilo Erbitux je indicirano za zdravljenje bolnikov z metastatskim kolorektalnim rakom z ekspresijo receptorjev EGFR in nemutiranim tipom RAS v kombinaciji s kemoterapijo na osnovi irinotekana, kot primarno zdravljenje v kombinaciji s FOLFOX in kot samostojno zdravilo pri bolnikih, pri katerih zdravljenje z oksaliplatinom in zdravljenje na osnovi irinotekana ni bilo uspešno in pri bolnikih, ki ne prenašajo irinotekana. Zdravilo Erbitux je indicirano za zdravljenje bolnikov z rakom skvamoznih celic glave in vratu v kombinaciji z radioterapijo za lokalno napredovalo bolezen in v kombinaciji s kemoterapijo na osnovi platine za ponavljajočo se in/ali metastatsko bolezen. **Odmerjanje in način uporabe:** Zdravilo Erbitux pri vseh indikacijah infundirajte enkrat na teden. Pred prvo infuzijo mora bolnik prejeti premedikacijo z antihistaminikom in kortikosteroidom najmanj 1 uro pred uporabo cetuksimaba. Začetni odmerek je 400 mg cetuksimaba na m^2 telesne površine. Vsi naslednji tedenski odmerki so vsak po 250 mg/m^2. **Kontraindikacije:** Zdravilo Erbitux je kontraindicirano pri bolnikih z znano hudo preobčutljivostno reakcijo (3. ali 4. stopnje) na cetuksimab. Kombinacija zdravila Erbitux s kemoterapijo, ki vsebuje oksaliplatin, je kontraindicirana pri bolnikih z metastatskim kolorektalnim rakom z mutiranim tipom RAS ali kadar status RAS ni znan. **Posebna opozorila in previdnostni ukrepi:** Pojav hude reakcije, povezane z infundiranjem, zahteva takojšnjo in stalno ukinitev terapije s cetuksimabom. Če pri bolniku nastopi blaga ali zmerna reakcija, povezana z infundiranjem, lahko zmanjšate hitrost infundiranja. Priporočljivo je, da ostane hitrost infundiranja na nižji vrednosti tudi pri vseh naslednjih infuzijah. Če se pri bolniku pojavi kožna reakcija, ki je ne more prenašati, ali huda kožna reakcija (≥ 3. stopnje po kriterijih CTCAE), morate prekiniti terapijo s cetuksimabom. Z zdravljenjem smete nadaljevati le, če se je reakcija izboljšala do 2. stopnje. Če ugotovite intersticijsko bolezen pljuč, morate zdravljenje s cetuksimabom prekiniti, in bolnika ustrezno zdraviti. Zaradi možnosti pojava znižanja nivoja elektrolitov v serumu se pred in periodično med zdravljenjem s cetuksimabom priporoča določanje koncentracije elektrolitov v serumu. Pri bolnikih, ki prejemajo cetuksimab v kombinaciji s kemoterapijo na osnovi platine, obstaja večje tveganje za pojav hude nevtropenije. Takšne bolnike je potrebno skrbno nadzorovati. Pri predpisovanju cetuksimaba je treba upoštevati kardiovaskularno stanje in indeks zmogljivosti bolnika in sočasno dajanje kardiotoksičnih učinkovin kot so fluoropirimidini. Če je diagnoza ulcerativnega keratitisa potrjena, je treba zdravljenje s cetuksimabom prekiniti ali ukiniti. Cetuksimab je treba uporabljati previdno pri bolnikih z anamnezo keratitisa, ulcerativnega keratitisa ali zelo suhih oči. Cetuksimaba ne uporabljajte za zdravljenje bolnikov s kolorektalnim rakom, če imajo tumorje z mutacijo RAS ali pri katerih je tumorski status RAS neznan. **Interakcije:** Pri kombinaciji s fluoropirimidini se je v primerjavi z uporabo fluoropirimidinov, kot monoterapije, povečala pogostnost srčne ishemije, vključno z miokardnim infarktom in kongestivno srčno odpovedjo ter pogostnost sindroma dlani in stopal. V kombinaciji s kemoterapijo na osnovi platine se lahko poveča pogostnost hude levkopenije ali hude nevtropenije. V kombinaciji s kapecitabinom in oksaliplatinom (XELOX) se lahko poveča pogostnost hude driske. **Neželeni učinki:** Zelo pogosti (≥ 1/10): hipomagneziemija, povečanje ravni jetrnih encimov, kožne reakcije, blage ali zmerne reakcije povezane z infundiranjem, mukozitis, v nekaterih primerih resen. Pogosti (≥ 1/100 do < 1/10): dehidracija, hipokalciemija, anoreksija, glavobol, konjunktivitis, driska, navzeja, bruhanje, hude reakcije povezane z infundiranjem, utrujenost. **Posebna navodila za shranjevanje:** Shranjujte v hladilniku (2 °C - 8 °C). **Pakiranje:** 1 viala z 20 ml ali 100 ml raztopine. **Način in režim izdaje:** Izdaja zdravila je le na recept-H. **Imetnik dovoljenja za promet:** Merck KGaA, 64271 Darmstadt, Nemčija.

Datum zadnje revizije besedila: junij 2014.

Pred predpisovanjem zdravila natančno preberite celoten Povzetek glavnih značilnosti zdravila.

Samo za strokovno javnost.

Podrobnejše informacije so na voljo pri predstavniku imetnika dovoljenja za promet z zdravilom:
Merck d.o.o., Ameriška ulica 8, 1000 Ljubljana, tel.: 01 560 3810, faks: 01 560 3830, el. pošta: info@merck.si

www.merckserono.net
www.Erbitux-international.com

PM-ONC-04/2014 /29.08.2014

Merck Serono

Merck Serono is a division of Merck

MERCK

SKRAJŠAN POVZETEK GLAVNIH ZNAČILNOSTI ZDRAVILA

Ime zdravila ALIMTA 100 mg prašek za koncentrat za raztopino za infundiranje in ALIMTA 500 mg prašek za koncentrat za raztopino za infundiranje **Kakovostna in količinska sestava** ALIMTA 100 mg: vsaka viala vsebuje 100 mg pemetrekseda (v obliki dinatrijevega pemetrekseda). Po pripravi vsebuje vsaka viala 25 mg/ml pemetrekseda. Pomožne snovi: Vsaka viala vsebuje približno 11 mg natrija, manitol, klorovodikova kislina, natrijev hidroksid. ALIMTA 500 mg: vsaka viala vsebuje 500 mg pemetrekseda (v obliki dinatrijevega pemetrekseda). Po pripravi vsebuje vsaka viala 25 mg/ml pemetrekseda. Pomožne snovi: Vsaka viala vsebuje približno 54 mg natrija, manitol, klorovodikova kislina, natrijev hidroksid. **Terapevtske indikacije:** ALIMTA je v kombinaciji s cisplatinom indicirana za zdravljenje bolnikov z neresektabilnim malignim plevralnim mezoteliomom, ki jih še nismo zdravili s kemoterapijo. ALIMTA je v kombinaciji s cisplatinom indicirana kot zdravljenje prvega izbora za bolnike z lokalno napredovalim ali metastatskim nedrobnoceličnim karcinomom pljuč, ki nima pretežno ploščatocelične histologije. ALIMTA je indicirana kot monoterapija za zdravljenje lokalno napredovalega ali metastatskega nedrobnoceličnega pljučnega karcinoma, ki nima pretežno ploščatocelične histologije pri bolnikih, pri katerih bolezen ni napredovala neposredno po kemoterapiji na osnovi platine. ALIMTA je indicirana kot monoterapija za zdravljenje drugega izbora bolnikov z lokalno napredovalim ali metastatskim nedrobnoceličnim pljučnim karcinomom, ki nima pretežno ploščatocelične histologije. **Odmerjanje in način uporabe:** *Odmerjanje:* ALIMTO smemo dajati le pod nadzorom zdravnika, usposobljenega za uporabo kemoterapije za zdravljenje raka. *ALIMTA v kombinaciji s cisplatinom:* Priporočeni odmerek ALIMTE je 500 mg/m^2 telesne površine (TP), dan kot intravenska infuzija v 10 minutah prvi dan vsakega 21-dnevnega ciklusa. Priporočeni odmerek cisplatina je 75 mg/m^2 TP, infundiran v dveh urah približno 30 minut po zaključku infuzije pemetrekseda prvi dan vsakega 21 dnevnega ciklusa. Bolniki morajo prejeti zadostno antiemetično zdravljenje, pred in/ali po prejemanju cisplatina jih moramo tudi ustrezno hidrirati. *ALIMTA kot samostojno zdravilo:* Priporočeni odmerek ALIMTE je 500 mg/m^2 TP, dan kot intravenska infuzija v 10 minutah prvi dan vsakega 21 dnevnega ciklusa. *Režim premedikacije:* Da zmanjšamo incidenco in resnost kožnih reakcij, dajemo kortikosteroid dan pred dajanjem pemetrekseda, na dan dajanja pemetrekseda in naslednji dan. Kortikosteroid naj ustreza 4 mg deksametazona, danega peroralno dvakrat dnevno. Za zmanjšanje toksičnosti morajo bolniki dnevno jemati tudi peroralno folno kislino ali multivitaminski pripravek, ki jo vsebuje (350 do 1000 mikrogramov). V sedmih dneh pred prvim odmerkom pemetrekseda morajo vzeti vsaj pet odmerkov folne kisline, odmerjanje pa morajo nadaljevati ves čas zdravljenja in še 21 dni po zadnjem odmerku pemetrekseda. Bolniki morajo prejeti tudi intramuskularno injekcijo vitamina B12 (1000 mikrogramov) v tednu pred prvim odmerkom pemetrekseda in enkrat vsake tri cikluse zatem. Kasnejše injekcije vitamina B12 lahko dajemo isti dan kot pemetreksed. **Kontraindikacije:** Preobčutljivost za zdravilno učinkovino ali katerokoli pomožno snov. Dojenje. Sočasno cepljenje proti rumeni mrzlici. **Posebna opozorila in previdnostni ukrepi:** Pemetrekseda lahko zavre delovanje kostnega mozga, kar se kaže kot nevtropenija, trombocitopenija in anemija (ali pancitopenija). Mielosupresija običajno predstavlja toksičnost za omejitev odmerka. Pri bolnikih, ki pred zdravljenjem niso prejemali kortikosteroidov, so poročali o kožnih reakcijah. Uporabe pemetrekseda pri bolnikih z očistkom kreatinina < 45 ml/min ne priporočamo. Bolniki z blagim do zmernim popuščanjem delovanja ledvic naj se izogibajo jemanju nesteroidnih protivnetnih zdravil (NSAID), denimo, ibuprofena in acetilsalicilne kisline 2 dni pred dajanjem pemetrekseda, na dan dajanja in še 2 dni po dajanju pemetrekseda. Vsi bolniki, ki jih lahko zdravimo s pemetreksedom, naj se izogibajo jemanju NSAID-ov z dolgimi razpolovnimi časi izločanja vsaj 5 dni pred dajanjem pemetrekseda, na dan dajanja in še vsaj 2 dni po dajanju pemetrekseda. Poročali so o resnih ledvičnih primerih, vključno z akutno ledvično odpovedjo, s pemetreksedom samim ali v povezavi z drugimi kemoterapevtiki. Pri bolnikih s klinično pomembno tekočino tretjega prostora moramo razmisliti o drenaži izliva pred dajanjem pemetrekseda. Kot posledico toksičnosti pemetrekseda v kombinaciji s cisplatinom za prebavila so opažali hudo dehidracijo, zato moramo bolnike pred prejemanjem terapije in/ali po njej ustrezno hidrirati, prejeti morajo zadostno antiemetično zdravljenje. Občasno so v kliničnih študijah pemetrekseda, običajno ob sočasnem dajanju z drugo citotoksično učinkovino, poročali o resnih srčnožilnih dogodkih, vključno z miokardnim infarktom in možganskožilnimi dogodki. Odsvetujemo uporabo živih oslabljenih cepiv. Spolno zrelim moškim odsvetujemo zaploditev otroka v času zdravljenja in še 6 mesecev zatem. Priporočamo ukrepe proti zanositvi ali vzdržnost. Zaradi možnosti, da zdravljenje s pemetreksedom povzroči trajno neplodnost, naj se moški pred začetkom zdravljenja posvetujejo o shranjevanju semena. Ženske v rodni dobi morajo v času zdravljenja s pemetreksedom uporabljati učinkovito kontracepcijo. Poročali so o primerih radiacijske pljučnice pri bolnikih, ki so jih zdravili z radiacijo pred, med ali po zdravljenju s pemetreksedom. Poročali so o radiacijskem izpuščaju pri bolnikih, ki so se zdravili z radioterapijo pred tedni ali leti. **Medsebojno delovanje z drugimi zdravili in druge oblike interakcij:** Sočasno dajanje nefrotoksičnih zdravil (denimo, aminoglikozidov, diuretikov zanke, spojin platine, ciklosporina) lahko potencialno povzroči zakasnjeni očistek pemetrekseda. Sočasno dajanje snovi, ki se tudi izločajo s tubulno sekrecijo (denimo, probenecid, penicilin), lahko potencialno povzroči zakasnjeni očistek pemetrekseda. Pri bolnikih z normalnim delovanjem ledvic lahko visoki odmerki nesteroidnih protivnetnih zdravil (NSAID-i, denimo, ibuprofen) in acetilsalicilna kislina v visokih odmerkih zmanjšajo eliminacijo pemetrekseda in tako lahko povečajo pojavnost neželenih učinkov pemetrekseda. Pri bolnikih z blagim do zmernim popuščanjem delovanja ledvic se moramo izogibati sočasnemu dajanju pemetrekseda z NSAID-i (denimo, ibuprofenom) ali acetilsalicilne kisline v visokih odmerkih 2 dni pred dajanjem pemetrekseda, na dan dajanja in še 2 dni po dajanju pemetrekseda. Sočasnemu dajanju NSAID-ov z daljšimi razpolovnimi časi s pemetreksedom se moramo izogibati vsaj 5 dni pred dajanjem pemetrekseda, na dan dajanja in še vsaj 2 dni po dajanju pemetrekseda.Velika različnost med posamezniki v koagulacijskem statusu v času bolezni ter možnost medsebojnega delovanja med peroralnimi antikoagulacijskimi učinkovinami ter kemoterapijo proti raku zahtevata povečano pogostnost spremljanja INR. **Kontraindicirana sočasna uporaba:** Cepivo proti rumeni mrzlici: tveganje za smrtno generaliziranо bolezen po cepljenju. **Odsvetovana sočasna uporaba:** Živa oslabljena cepiva (razen proti rumeni mrzlici): tveganje za sistemsko, potencialno smrtno bolezen. **Neželeni učinki** Klinične študije malignega plevralnega mezotelioma *Zelo pogosto:* znižani nevtrofili/granulociti, znižani levkociti, znižan hemoglobin, znižani trombociti, nevropatija-senzorna, diareja, bruhanje, stomatitis/faringitis, slabost, anoreksija, zaprtje, izpuščaj, alopecija, povišan kreatinin, znižan očistek kreatinina, utrujenost. *Pogosti:* dehidracija, motnje okusa, konjuktivitis, dispepsija. Klinične študije nedrobnoceličnega pljučnega karcinoma - ALIMTA monoterapija, zdravljenje 2. izbora: *Zelo pogosti:* znižan nevtrofili/granulociti, znižani levkocitit, znižan hemoglobin, diareja, bruhanje, stomatitis/faringitis, slabost, anoreksija, izpuščaj/luščenje, utrujenost. *Pogosti:* znižani trombociti, zaprtje, povišanje SGPT (ALT), povišanje SGOT (AST), srbenje, alopecija, povišana telesna temperatura. Klinične študije nedrobnoceličnega pljučnega karcinoma - ALIMTA v kombinaciji s cisplatinom, zdravljenje 1. izbora: *Zelo pogosti:* znižan hemoglobin, znižani nevtrofili/granulociti, znižani levkocitit, znižani trombociti, slabost, bruhanje, anoreksija, zaprtje, stomatitis/faringitis, diareja brez kolostomije, alopecija, izpuščaj/luščenje, povišan kreatinin, utrujenost. *Pogosti:* nevropatija-senzorična, motnje okusa, dispepsija/zgaga. Klinične študije nedrobnoceličnega pljučnega karcinoma - ALIMTA monoterapija, vzdrževalno in nadaljevalno zdravljenje: *Zelo pogosti:* znižan hemoglobin, slabost, anoreksija, utrujenost. *Pogosti:* znižani levkociti, znižani nevtrofilci, nevropatija-senzorična, bruhanje, mukozitis/stomatitis, povišanje ALT (SGPT), povišanje AST (SGOT), izpuščaj/luščenje, bolečina. Občasno so v kliničnih študijah pemetrekseda poročali o primerih resnih srčnožilnih in možganskožilnih dogodkov, vključno z miokardnim infarktom, angino pektoris, cerebrovaskularnim insultom in prehodnimi ishemičnimi atakami; primerih kolitisa ter o primerih interstizijske pljučnice z respiratorno insuficience, primerih edema, o ezofagitisu/radiacijskem ezofagitisu in o primerih sepse. Redkeje pa o primerih potencialno resnega hepatitisa in pancitopenije. Po uvedbi zdravila na trg so poročali o primerih akutne odpovedi ledvic s pemetreksedom samim ali v povezavi z drugimi kemoterapevtiki, primerih radiacijske pljučnice pri bolnikih, ki so jih zdravili z radiacijo pred, med ali po njihovem zdravljenju s pemetreksedom, primerih radiacijskega izpuščaja pri bolnikih, ki so se v preteklosti zdravili z radioterapijo, o primerih periferne ishemije, ki je včasih vodila v nekrozo okončin, redkih primerih buloznih stanj, kot sta Stevens-Johnsonov sindrom in toksična epidermalna nekroliza, ki so bila v nekaterih primerih usodna in o redkih primerih hemolitične anemije. Poročali so o redkih primerih anafilaktičnega šoka. **Imetnik dovoljenja za promet** Eli Lilly Nederland B.V., Grootslag 1 5, NL 3991 RA, Houten, Nizozemska. Datum zadnje revizije besedila 27.02.2014. Način izdaje zdravila: H.

Pomembno obvestilo: Pričujoče gradivo je namenjeno samo za strokovno javnost. Zdravilo Alimta se izdaja le na recept. Pred predpisovanjem zdravila Alimta vas vljudno prosimo, da preberete celotni Povzetek glavnih značilnosti zdravila Alimta. Podrobnejše informacije o zdravilu Alimta in o zadnji reviziji besedila Povzetka glavnih značilnosti zdravila so na voljo na sedežu podjetja Eli Lilly (naslov podjetja in kontaktni podatki spodaj) in na spletni strani European Medicines Agency (EMA): www.ema.europa.eu. in na spletni strani European Commission http://ec.europa.eu/health/documents/community-register/html/alfregister.htm.

SIALM00067(1), 14.4.2015

Eli Lilly Farmacevtska družba, d.o.o.
Dunajska 167, 1000 Ljubljana, Slovenija
Telefon: +386 (0)1 5800 010
Faks: +386 (0)1 5691 705

ŠE VEDNO ODKRIVAM

Pri bolnikih z metastatskim, na kastracijo odpornim rakom prostate, ki nimajo simptomov ali imajo blage simptome po neuspešnem zdravljenju z deprivacijo androgenov in pri katerih kemoterapija še ni klinično indicirana.[1]

ZYTIGA zagotavlja [2, 3]

34,7 mesecev statistično značilno **mediano celokupno preživetje**

4,4 mesecev statistično značilno **podaljšanje preživetja**

48 % **zmanjšanje tveganja za** radiološko potrjeno **napredovanje bolezni**

4+ leta **ugoden varnostni profil** tudi po daljšem obdobju spremljanja bolnikov

SKRAJŠANO NAVODILO ZA PREDPISOVANJE ZDRAVILA

▼ Za to zdravilo se izvaja dodatno spremljanje varnosti. Zato je pomembno, da poročate neželene učinke povezane s tem zdravilom. **Ime zdravila:** ZYTIGA 250 mg tablete **Kakovostna in količinska sestava:** 250 mg abirateronacetata; pomožne snovi: mikrokristalna celuloza, premreženi natrijev karmelozat, laktoza monohidrat, magnezijev stearat, povidon, brezvodni koloidni silicijev dioksid, natrijev lavrilsulfat. **Indikacije:** uporaba skupaj s prednizonom ali prednizolonom za zdravljenje na kastracijo odpornega metastatskega raka prostate pri odraslih bolnikih, ki nimajo ali imajo blage simptome po neuspešnem zdravljenju z deprivacijo androgenov in pri katerih kemoterapija še ni klinično indicirana; ter pri odraslih bolnikih, pri katerih je bolezen napredovala med ali po zdravljenju s kemoterapijo z docetakselom. **Odmerjanje:** priporočeni odmerek: 1.000 mg (štiri 250 mg tablete v enem odmerku), 10 mg prednizona ali prednizolona/dan, najmanj dve uri po obroku. Pri bolnikih s hudo okvaro jeter ali ledvic je potrebna previdnost. **Kontraindikacije:** preobčutljivost na zdravilno učinkovino ali katero koli pomožno snov, uporaba zdravila pri ženskah, huda okvara jeter. **Posebna opozorila:** Pri uporabi zdravila pri bolnikih z anamnezo kardiovaskularne bolezni je potrebna previdnost. Pri bolnikih z iztisnim deležem levega prekata < 50% ali s srčnim popuščanjem razreda III ali IV po NYHA varnost uporabe zdravila ni dokazana. Pred začetkom zdravljenja je treba urediti hipertenzijo, zastajanje tekočin in odpraviti hipokaliemijo. Če kadarkoli med zdravljenjem pride do pojava hude hepatotoksičnosti je treba z zdravljenjem prenehati in se ga ne sme ponovno uvesti. Pri bolnikih, ki prejemajo prednizon ali prednizolon in so v stresni situaciji, je lahko pred in med stresno situacijo ter po njej indiciran zvečan odmerek kortikosteroidov. Pri bolnikih z napredovanim metastatskim rakom prostate (rezistentnim na kastracijo) lahko pride do zmanjšanja kostne gostote. Jemanje zdravila v kombinaciji z glukokortikoidi lahko ta učinek poveča. Pri bolnikih z rakom prostate, zdravljenih s ketokonazolom, lahko pričakujemo nižjo stopnjo odziva na zdravljenje. Uporaba glukokortikoidov lahko poslabša hiperglikemijo. Varnost in učinkovitost sočasne uporabe zdravila ZYTIGA in citotoksične kemoterapije ni bila ugotovljena. Bolniki z redko dedno intoleranco za galaktozo, laponsko obliko zmanjšane aktivnosti laktaze ali malabsorpcijo glukoze/galaktoze ne smejo jemati tega zdravila. Zdravilo vsebuje tudi več kot 1 mmol (oziroma 27,2 mg) natrija na odmerek (v štirih tabletah), kar je treba upoštevati pri bolnikih na dieti z nadzorovanim vnosom natrija. Pri bolnikih, ki se zdravijo z zdravilom ZYTIGA, se lahko pojavita anemija in spolna disfunkcija. Pri bolnikih, ki se sočasno zdravijo z zdravili, za katera je znano, da so povezana z miopatijo/ rabdomiolizo, je potrebna previdnost. Zaradi tveganja za manjšo izpostavljenost zdravilu ZYTIGA se med zdravljenjem izogibajte uporabi močnih induktorjev CYP3A4, razen v primerih, ko ni druge možnosti zdravljenja. **Interakcije:** zdravila se ne sme jemati s hrano, ker se bistveno poveča absorpcija abirateronacetata. Pri sočasni uporabi z zdravili, ki jih aktivira ali presnavlja CYP2D6, zlasti tistih z majhno terapevtsko širino je potrebna previdnost. Med zdravljenjem se uporabi močnih induktorjev CYP3A4 izogibajte, razen v primerih, ko ni druge možnosti zdravljenja. **Nosečnost in dojenje:** Ženske, ki so noseče in ženske, ki bi lahko bile noseče, morajo v primeru stika ali rokovanja z zdravilom, nositi zaščitne rokavice. V študijah na živalih so ugotovili toksične učinke na sposobnost razmnoževanja. **Neželeni učinki:** okužba sečil, sepsa, adrenalna insufucienca, hipokaliemija, hipertrigliceridemija, srčno popuščanje, angina pektoris, aritmija, atrijska fibrilacija, tahikardija, miokardni infarkt, hipertenzija, alergijski alveolitis, driska, dispepsija, zvišana koncentracija ALT, AST, izpuščaj, miopatija, rabdomioliza, hematurija, periferni edemi, zlomi. **Imetnik DzP:** Janssen-Cilag International NV, Turnhoutseweg 30, 2340 Beerse, Belgija, Predstavnik v Sloveniji: Johnson & Johnson d.o.o., Šmartinska 53, Ljubljana **Režim izdajanja zdravila:** Rp/Spec. **Datum zadnje revizije besedila:** 04. 03. 2015

Povzetek glavnih značilnosti zdravila s podrobnejšimi informacijami o zdravilu je dostopen pri zastopniku imetnika dovoljenja za promet.

Literatura
1. Povzetek glavnih značilnosti zdravila Zytiga 250 mg tablete.
2. Ryan C et al. Lancet Oncol 2015;16: 152–60.
3. Rathkopf DE et al. Eur Urol 2014;66: 815–825.

janssen PHARMACEUTICAL COMPANIES of Johnson & Johnson

Johnson & Johnson d.o.o.
Šmartinska cesta 53, 1000 Ljubljana,
T: 01 401 18 30, F: 01 401 18 03
E: jac_slo@its.jnj.com

ZYT-SLO-A-086-130315

Zytiga® abirateronacetat

PRELOMNA ZNANSTVENA ODKRITJA S PODROČJA ONKOLOGIJE PRELIVAMO V BIOMEDICINSKE INOVACIJE

- Doprinos k premagovanju raka - **naše vodilo**
- Dostopnost naših zdravil proti raku - **naša zaveza**
- Raziskovanje na področju imunoonkologije - **naša pot**

v prizadevanjih, da bi ljudem z rakom prinesli NOVO UPANJE.

Za več informacij o naših onkoloških kliničnih preskušanjih obiščite **www.merck.com/clinicaltrials**

MSD
Bodite dobro

Napredovali bazalnocelični karcinom (nBCK)*: bolezen, ki ne prizadene le kože

Posledice napredovalega bazalnoceličnega karcinoma so za bolnika lahko zelo resne, še posebej, ko je kirurško zdravljenje ali zdravljenje z obsevanjem neprimerno ali neučinkovito.

Kaj ostane, ko so druge možnosti zdravljenja izčrpane?

* nBCK = lokalno napredovali ali simptomatski metastatski bazalnocelični karcinom

SKRAJŠAN POVZETEK GLAVNIH ZNAČILNOSTI ZDRAVILA

Samo za strokovno javnost

▼ Za to zdravilo se izvaja dodatno spremljanje varnosti. Tako bodo hitreje na voljo nove informacije o njegovi varnosti. Zdravstvene delavce naprošamo, da poročajo o katerem koli domnevnem neželenem učinku zdravila.

Ime zdravila: Erivedge 150 mg trde kapsule **Kakovostna in količinska sestava:** Ena trda kapsula vsebuje 150 mg vismodegiba. Pomožna snov z znanim učinkom: Ena trda kapsula vsebuje 71,5 mg laktoze monohidrata na kapsulo. **Terapevtske indikacije:** Zdravilo Erivedge je indicirano za zdravljenje odraslih bolnikov s simptomatskim metastatskim bazalnoceličnim karcinomom in z lokalno napredovalim bazalnoceličnim karcinomom, neprimernim za operacijo ali radioterapijo. **Odmerjanje in način uporabe:** Zdravilo Erivedge sme predpisati le zdravnik specialist, ki ima izkušnje z vodenjem zdravljenja pri odobreni indikaciji, oziroma se ga sme predpisati le pod nadzorstvom takšnega zdravnika. Odmerjanje: Priporočeni odmerek je ena 150 mg kapsula enkrat na dan. Trajanje zdravljenja: V kliničnih preskušanjih se je zdravljenje z zdravilom Erivedge nadaljevalo do napredovanja bolezni ali nesprejemljivih toksičnih učinkov. Glede na posameznikovo prenašanje zdravila so dovoljevali prekinitve zdravljenja do 4 tednov. Korist nadaljevanja zdravljenja je treba redno ocenjevati. Optimalno trajanje zdravljenja je različno za vsakega posameznega bolnika. Posebne skupine bolnikov: Bolnikom, starim 65 let ali več, odmerka ni treba prilagoditi. Varnosti in učinkovitosti zdravila Erivedge pri bolnikih z okvarjenim delovanjem ledvic ali jeter niso raziskovali. Zdravila Erivedge se zaradi pomislekov glede varnosti ne sme uporabljati pri otrocih in mladostnikih, mlajših od 18 let. Način uporabe: Zdravilo Erivedge je namenjeno za peroralno uporabo. Kapsule je treba zaužiti cele z vodo, s hrano ali brez nje. Kapsul ne smemo odpreti, da preprečimo nenamerno izpostavljenost bolnikov in zdravstvenega osebja. **Kontraindikacije:** Preobčutljivost za zdravilno učinkovino ali katero koli pomožno snov, nosečnice in doječe ženske, ženske v rodni dobi, ki ne upoštevajo Programa preprečevanja nosečnosti med uporabo zdravila Erivedge ter sočasna uporaba šentjanževke. **Posebna opozorila in previdnostni ukrepi:** Embrio-fetalna smrt ali hude prirojene napake: Pri nosečnici uporabljeno zdravilo Erivedge lahko povzroči embrio-fetalno smrt ali hude prirojene napake. Svetovanje: *Za ženske v rodni dobi:* Zdravilo Erivedge je kontraindicirano pri ženskah v rodni dobi, ki ne upoštevajo Programa za preprečevanje nosečnosti med uporabo zdravila Erivedge. *Za moške:* Vismodegib se nahaja v semenu. *Za zdravstvene delavce:* Zdravstveni delavci morajo bolnike poučiti tako, da razumejo in sprejmejo vse zahteve Programa za preprečevanje nosečnosti med uporabo zdravila Erivedge. Kontracepcija: *Ženske v rodni dobi:* Ženske bolnice morajo uporabljati dva priporočena načina kontracepcije med zdravljenjem z zdravilom Erivedge in še 24 mesecev po zadnjem odmerku tega zdravila. *Moški:* Moški bolnik mora med jemanjem zdravila Erivedge in še 2 meseca po zadnjem odmerku tega zdravila med spolnim odnosom s partnerko vedno uporabiti kondom (s spermicidom, če je na voljo), tudi če je imel vazektomijo. Test nosečnosti: Pri ženskah v rodni dobi mora zdravstveni delavec opraviti zdravniško nadzorovan test nosečnosti v 7 dneh pred začetkom zdravljenja in vsak mesec med zdravljenjem. Testi nosečnosti morajo imeti minimalno občutljivost 25 mi.e./ml, v skladu z lokalno dostopnostjo. Bolnice, ki dobijo amenorejo med zdravljenjem z zdravilom Erivedge, morajo s testi nosečnosti nadaljevati vsak mesec medtem, ko se zdravijo. Omejitve za predpisovanje in izdajanje zdravila ženskam v rodni dobi: Prvo predpisovanje in izdaja zdravila Erivedge morata biti opravljena v 7 dneh po negativnem testu nosečnosti. Recepti za zdravilo Erivedge morajo biti omejeni na 28 dni zdravljenja, za nadaljevanje zdravljenja je potreben nov recept. Izobraževalno gradivo: Da bi zdravstvenim delavcem in bolnikom pomagal preprečiti izpostavljenost zarodka in ploda zdravilu Erivedge, bo imetnik dovoljenja za promet z zdravilom priskrbel izobraževalna gradiva (Program preprečevanja nosečnosti med uporabo zdravila Erivedge). Vplivi na postnatalni razvoj: Pri živalih je vismodegib povzročil hude, ireverzibilne spremembe v rasti zob in zaprtje epifizne rastne plošče. Ti izsledki kažejo na mogoče tveganje za nizko rast in deformacije zob pri dojenčkih in otrocih. Krvodajalstvo: Bolnice in bolniki med jemanjem zdravila Erivedge in še 24 mesecev po zadnjem odmerku tega zdravila ne smejo darovati krvi. Darovanje sperme: Bolniki med zdravljenjem z zdravilom Erivedge in 2 meseca po zadnjem odmerku ne smejo darovati sperme. Medsebojno delovanje: Treba se je izogibati sočasnemu zdravljenju z močnimi induktorji CYP, saj ni mogoče izključiti tveganja za znižane plazemske koncentracije in zmanjšano učinkovitost vismodegiba. Ploščatocelični karcinom kože: Bolniki z napredovalim bazalnoceličnim karcinomom imajo povečano tveganje za razvoj ploščatoceličnega karcinoma kože. Pri bolnikih z napredovalim bazalnoceličnim karcinomom, ki so se zdravili z zdravilom Erivedge, so poročali o primerih ploščatoceličnega karcinoma kože. Ni bilo dokazano, da je ploščatocelični karcinom kože povezan z zdravilom Erivedge. Zato je treba vse bolnike med zdravljenjem z zdravilom Erivedge rutinsko kontrolirati, ploščatocelični karcinom kože pa zdraviti v skladu s standardnim zdravljenjem. Dodatni previdnostni ukrepi: Bolnikom je treba naročiti, da tega zdravila nikoli ne dajo drugim osebam. Po končanem zdravljenju morajo bolniki neuporabljene kapsule takoj zavreči v skladu z lokalnimi predpisi. Pomožne snovi: Kapsule zdravila Erivedge vsebujejo laktozo monohidrat. Bolniki z redkimi prirojenimi motnjami, kot so intoleranca za galaktozo, primarna hipolaktazija ali malabsorpcija glukoze-galaktoze, ne smejo jemati tega zdravila. To zdravilo vsebuje manj kot 1 mmol (23 mg) natrija na odmerek, kar v bistvu pomeni 'brez natrija'. **Medsebojno delovanje z drugimi zdravili in druge oblike interakcij:** Vplivi sočasno danih zdravil na vismodegib: Če je vismodegib uporabljen sočasno z zaviralcem protonske črpalke, antagonistom receptorjev H_2 ali z antacidom, se njegova sistemska izpostavljenost lahko zmanjša, vpliv tega na učinkovitost vismodegiba pa ni znan. Pri bolnikih s pomanjkanjem kisline v želodčnem soku obstaja možnost za enak vpliv. Študije *in vitro* kažejo, da je vismodegib substrat efluksnega prenašalca P-glikoproteina (P-gp) in encimov, ki presnavljajo zdravila - CYP2C9 in CYP3A4. Če je vismodegib uporabljen sočasno z zdravili, ki zavirajo P-gp, CYP2C9 ali CYP3A4, se lahko sistemska izpostavljenost vismodegibu in incidenca neželenih učinkov vismodegiba povečata. Ko damo vismodegib s spodbujevalci CYP, se lahko izpostavljenost vismodegibu zmanjša. Vpliv vismodegiba na sočasno dana zdravila: *Kontraceptivni steroidi:* Izsledki študije medsebojnega delovanja zdravilo-zdravilo pri bolnikih z rakom so pokazali, da sistemska izpostavljenost etinilestradiolu in noretindronu ni spremenjena, ko ju dajemo sočasno z vismodegibom. Študija medsebojnega delovanja je trajala samo 7 dni in ne moremo izključiti, da je pri daljšem zdravljenju vismodegib spodbujevalec encimov, ki presnavljajo kontraceptivne steroide. Spodbujanje lahko vodi v zmanjšanje sistemske izpostavljenosti kontraceptivnim steroidom in zmanjšanje učinkovitosti kontracepcije. *Učinki na specifične encime in prenašalce:* Študije *in vitro* kažejo, da ima vismodegib zmožnost, da deluje kot zaviralec beljakovine BCRP. Podatkov *in vivo* o medsebojnem delovanju ni. Ni mogoče izključiti, da lahko vismodegib povzroči povečano izpostavitev zdravilom, ki se prenašajo s to beljakovino, kot so rosuvastatin, topotekan in sulfasalazin. Sočasno jih je treba dajati s previdnostjo in morda bo potrebna prilagoditev odmerka. Za zaviralni učinek vismodegiba je bila od izoforme CYP *in vitro* najbolj občutljiva izoforma CYP2C8. Izsledki študije medsebojnega delovanja pri bolnikih z rakom so pokazali, da se sistemska izpostavljenost rosiglitazonu med sočasno uporabo z vismodegibom ne spremeni. Tako lahko zaviranje encimov CYP s strani vismodegiba *in vivo* izključimo. *In vitro* je vismodegib zaviralec OATP1B1. Ni mogoče izključiti, da lahko vismodegib poveča izpostavljenost substratom OATP1B1, npr. bosentanu, glibenklamidu, repaglinidu, valsartanu in statinom. Še posebno je potrebna previdnost, če vismodegib dajemo skupaj s katerim koli statinom. **Neželeni učinki:** Neželeni učinki, ki so se pojavili pri bolnikih, zdravljenih z zdravilom Erivedge v kliničnih preskušanjih: *Zelo pogosti:* zmanjšanje teka, disgevzija, agevzija, navzea, driska, zaprtost, bruhanje, dispepsija, alopecija, pruritus, izpuščaj, mišični krči, artralgija, bolečine v okončini, amenoreja, zmanjšanje telesne mase, utrujenost in bolečina. *Pogosti:* zvišanje jetrnih encimov, dehidracija, hiponatriemija, hipogevzija, bolečine v zgornjem delu trebuha, bolečine v trebuhu, madaroza, nenormalna rast dlak, bolečine v hrbtu, mišično-skeletna bolečina v prsnem košu, mialgija, bolečina ledveno, mišično-skeletne bolečine, in astenija. Poročanje o domnevnih neželenih učinkih: Poročanje o domnevnih neželenih učinkih zdravila po izdaji dovoljenja za promet je pomembno. Omogoča namreč stalno spremljanje razmerja med koristmi in tveganji zdravila. Od zdravstvenih delavcev se zahteva, da poročajo o katerem koli domnevnem neželenem učinku zdravila na: Univerzitetni klinični center Ljubljana, Interna klinika, Center za zastrupitve, Zaloška cesta 2, SI-1000 Ljubljana, Faks: + 386 (0)1 434 76 46, e-pošta: farmakovigilanca@kclj.si. **Režim izdaje zdravila:** Rp/Spec **Imetnik dovoljenja za promet:** Roche Registration Limited, 6 Falcon Way, Shire Park, Welwyn Garden City, AL7 1TW, Velika Britanija **Verzija: 2.0/15 Informacija pripravljena:** april 2015

PG-32-15-ERI-TG

DODATNE INFORMACIJE SO NA VOLJO PRI:
Roche farmacevtska družba d.o.o.,
Vodovodna cesta 109, 1000 Ljubljana

Erivedge®
vismodegib
Preobrat v zdravljenju

Instructions for authors

The editorial policy

Radiology and Oncology is a multidisciplinary journal devoted to the publishing original and high quality scientific papers and review articles, pertinent to diagnostic and interventional radiology, computerized tomography, magnetic resonance, ultrasound, nuclear medicine, radiotherapy, clinical and experimental oncology, radiobiology, radiophysics and radiation protection. Therefore, the scope of the journal is to cover beside radiology the diagnostic and therapeutic aspects in oncology, which distinguishes it from other journals in the field.

The Editorial Board requires that the paper has not been published or submitted for publication elsewhere; the authors are responsible for all statements in their papers. Accepted articles become the property of the journal and, therefore cannot be published elsewhere without the written permission of the editors.

Submission of the manuscript

The manuscript written in English should be submitted to the journal via online submission system Editorial Manager available for this journal at: **www.radioloncol.com**.

In case of problems, please contact Sašo Trupej at saso.trupej@computing.si or the Editor of this journal at gsersa@onko-i.si

All articles are subjected to the editorial review and when the articles are appropriated they are reviewed by independent referees. In the cover letter, which must accompany the article, the authors are requested to suggest 3-4 researchers, competent to review their manuscript. However, please note that this will be treated only as a suggestion; the final selection of reviewers is exclusively the Editor's decision. The authors' names are revealed to the referees, but not vice versa.

Manuscripts which do not comply with the technical requirements stated herein will be returned to the authors for the correction before peer-review. The editorial board reserves the right to ask authors to make appropriate changes of the contents as well as grammatical and stylistic corrections when necessary. Page charges will be charged for manuscripts exceeding the recommended length, as well as additional editorial work and requests for printed reprints.

Articles are published printed and on-line as the open access (**www.degruyter.com/view/j/raon**).

All articles are subject to 700 EUR + VAT publication fee. Exceptionally, waiver of payment may be negotiated with editorial office, upon lack of funds.

Manuscripts submitted under multiple authorship are reviewed on the assumption that all listed authors concur in the submission and are responsible for its content; they must have agreed to its publication and have given the corresponding author the authority to act on their behalf in all matters pertaining to publication. The corresponding author is responsible for informing the coauthors of the manuscript status throughout the submission, review, and production process.

Preparation of manuscripts

Radiology and Oncology will consider manuscripts prepared according to the Uniform Requirements for Manuscripts Submitted to Biomedical Journals by International Committee of Medical Journal Editors (www.icmje.org). The manuscript should be written in grammatically and stylistically correct language. Abbreviations should be avoided. If their use is necessary, they should be explained at the first time mentioned. The technical data should conform to the SI system. The manuscript, excluding the references, tables, figures and figure legends, must not exceed 5000 words, and the number of figures and tables is limited to 8. Organize the text so that it includes: Introduction, Materials and methods, Results and Discussion. Exceptionally, the results and discussion can be combined in a single section. Start each section on a new page, and number each page consecutively with Arabic numerals.

The Title page should include a concise and informative title, followed by the full name(s) of the author(s); the institutional affiliation of each author; the name and address of the corresponding author (including telephone, fax and E-mail), and an abbreviated title (not exceeding 60 characters). This should be followed by the abstract page, summarizing in less than 250 words the reasons for the study, experimental approach, the major findings (with specific data if possible), and the principal conclusions, and providing 3-6 key words for indexing purposes. Structured abstracts are required. Slovene authors are requested to provide title and the abstract in Slovene language in a separate file. The text of the research article should then proceed as follows:

Introduction should summarize the rationale for the study or observation, citing only the essential references and stating the aim of the study.

Materials and methods should provide enough information to enable experiments to be repeated. New methods should be described in details.

Results should be presented clearly and concisely without repeating the data in the figures and tables. Emphasis should be on clear and precise presentation of results and their significance in relation to the aim of the investigation.

Discussion should explain the results rather than simply repeating them and interpret their significance and draw conclusions. It should discuss the results of the study in the light of previously published work.

Charts, Illustrations, Images and Tables
Charts, Illustrations, Images and Tables must be numbered and referred to in the text, with the appropriate location indicated. Charts, Illustrations and Images, provided electronically, should be of appropriate quality for good reproduction. Illustrations and charts must be vector image, created in CMYK color space, preferred font "Century Gothic", and saved as .AI, .EPS or .PDF format. Color charts, illustrations and Images are encouraged, and are published without additional charge. Image size must be 2.000 pixels on the longer side and saved as .JPG (maximum quality) format. In Images, mask the identities of the patients. Tables should be typed double-spaced, with a descriptive title and, if appropriate, units of numerical measurements included in the column heading. The files with the figures and tables can be uploaded as separate files.

References
References must be numbered in the order in which they appear in the text and their corresponding numbers quoted in the text. Authors are responsible for the accuracy of their references. References to the Abstracts and Letters to the Editor must be identified as such. Citation of papers in preparation or submitted for publication, unpublished observations, and personal communications should not be included in the reference list. If essential, such material may be incorporated in the appropriate place in the text. References follow the style of Index Medicus. All authors should be listed when their number does not exceed six; when there are seven or more authors, the first six listed are followed by "et al.". The following are some examples of references from articles, books and book chapters:
Dent RAG, Cole P. In vitro maturation of monocytes in squamous carcinoma of the lung. *Br J Cancer* 1981; **43:** 486-95.
Chapman S, Nakielny R. *A guide to radiological procedures*. London: Bailliere Tindall; 1986.
Evans R, Alexander P. Mechanisms of extracellular killing of nucleated mammalian cells by
macrophages. In: Nelson DS, editor. *Immunobiology of macrophage.* New York: Academic Press; 1976. p. 45-74.

Authorization for the use of human subjects or experimental animals
When reporting experiments on human subjects, authors should state whether the procedures followed the Helsinki Declaration. Patients have the right to privacy; therefore the identifying information (patient's names, hospital unit numbers) should not be published unless it is essential. In such cases the patient's informed consent for publication is needed, and should appear as an appropriate statement in the article. Institutional approval and Clinical Trial registration number is required.
The research using animal subjects should be conducted according to the EU Directive 2010/63/EU and following the Guidelines for the welfare and use of animals in cancer research (Br J Cancer 2010; 102: 1555 – 77). Authors must state the committee approving the experiments, and must confirm that all experiments were performed in accordance with relevant regulations.
These statements should appear in the Materials and methods section (or for contributions without this section, within the main text or in the captions of relevant figures or tables).

Transfer of copyright agreement
For the publication of accepted articles, authors are required to send the License to Publish to the publisher on the address of the editorial office. A properly completed License to Publish, signed by the Corresponding Author on behalf of all the authors, must be provided for each submitted manuscript.
The non-commercial use of each article will be governed by the Creative Commons Attribution-NonCommercial-NoDerivs license.

Conflict of interest
When the manuscript is submitted for publication, the authors are expected to disclose any relationship that might pose real, apparent or potential conflict of interest with respect to the results reported in that manuscript. Potential conflicts of interest include not only financial relationships but also other, non-financial relationships. In the Acknowledgement section the source of funding support should be mentioned. The Editors will make effort to ensure that conflicts of interest will not compromise the evaluation process of the submitted manuscripts; potential editors and reviewers will exempt themselves from review process when such conflict of interest exists. The statement of disclosure must be in the Cover letter accompanying the manuscript or submitted on the form available on **www.icmje.org/coi_disclosure.pdf**

Page proofs
Page proofs will be sent by E-mail to the corresponding author. It is their responsibility to check the proofs carefully and return a list of essential corrections to the editorial office within three days of receipt. Only grammatical corrections are acceptable at that time.

Open access
Papers are published electronically as open access on **www.degruyter.com/view/j/raon**, also papers accepted for publication as E-ahead of print.

*anaplastična limfomska kinaza

XALKORI®
KRIZOTINIB

BISTVENI PODATKI IZ POVZETKA GLAVNIH ZNAČILNOSTI ZDRAVILA

▼XALKORI 200 mg, 250 mg trde kapsule
Za to zdravilo se izvaja dodatno spremljanje varnosti. Tako bodo hitreje na voljo nove informacije o njegovi varnosti. Zdravstvene delavce naprošamo, da poročajo o kateremkoli domnevnem neželenem učinku zdravila. Glejte poglavje 4.8 povzetka glavnih značilnosti zdravila, kako poročati o neželenih učinkih.
Sestava in oblika zdravila: Ena kapsula vsebuje 200 mg ali 250 mg krizotiniba. **Indikacije:** Zdravljenje odraslih bolnikov s predhodno zdravljenim, napredovalim nedrobnoceličnim pljučnim rakom (NSCLC - *non-small cell lung cancer*), ki je ALK (anaplastična limfomska kinaza) pozitiven. **Odmerjanje in način uporabe:** Zdravljenje mora uvesti in nadzorovati zdravnik z izkušnjami z uporabo zdravil za zdravljenje rakavih bolezni. *Preverjanje prisotnosti ALK:* Pri izbiri bolnikov za zdravljenje z zdravilom XALKORI je treba opraviti točno in validirano preverjanje prisotnosti ALK. *Odmerjanje:* Priporočeni odmerek je 250 mg dvakrat na dan (500 mg na dan), bolniki pa morajo zdravilo jemati brez prekinitev. Če bolnik pozabi vzeti odmerek, ga mora vzeti takoj, ko se spomni, razen če do naslednjega odmerka manjka manj kot 6 ur. V tem primeru bolnik pozabljenega odmerka na sme vzeti. *Prilagajanja odmerkov:* Glede na varnost uporabe zdravila pri posameznem bolniku in kako bolnik zdravljenje prenaša, utegne biti potrebna prekinitev in/ali zmanjšanje odmerka zdravila na 200 mg dvakrat na dan; če je potrebno še nadaljnje zmanjšanje, pa znaša odmerek 250 mg enkrat na dan. Prilagajanje odmerkov pri *hematološki in nehematološki* (povečanje vrednosti AST, ALT, bilirubina; ILD/pnevmonitis; podaljšanje intervala QTc, bradikardija) *toksičnosti:* glejte preglednici 1 in 2 v povzetku glavnih značilnosti zdravila. *Okvara jeter:* Pri blagi in zmerni okvari je zdravljenje treba izvajati previdno, pri hudi okvari se zdravila ne sme uporabljati. *Okvara ledvic:* Pri blagi in zmerni okvari prilagajanje začetnega odmerka ni priporočeno. Pri hudi okvari ledvic (ki ne zahteva peritonealne dialize ali hemodialize) je odmerek 250 mg peroralno enkrat na dan; po vsaj 4 tednih zdravljenja se lahko poveča na 200 mg dvakrat na dan. *Starejši bolniki (≥ 65 let):* V primerjavi z mlajšimi bolniki niso opazili nobenih splošnih razlik v varnosti ali učinkovitosti. *Pediatrična populacija:* Varnost in učinkovitost nista bili dokazani. *Način uporabe:* Kapsule je treba pogoltniti cele, z nekaj vode, s hrano ali brez nje. Ne sme se jih zdrobiti, raztopiti ali odpreti. Izogibati se je treba uživanju grenivk, grenivkinega soka ter uporabi šentjanževke. **Kontraindikacije:** Preobčutljivost na krizotinib ali katerokoli pomožno snov. Huda okvara jeter. **Posebna opozorila in previdnostni ukrepi:** *Določanje statusa ALK:* Pomembno je izbrati dobro validirano in robustno metodologijo, da se izognemo lažno negativnim ali lažno pozitivnim rezultatom. *Hepatotoksičnost:* Zaradi jemanja zdravila je prišlo do hepatotoksičnosti s smrtnim izidom. Delovanje jeter, vključno z ALT, AST in skupnim bilirubinom, je treba preveriti enkrat na teden v prvih 2 mesecih zdravljenja, nato pa enkrat na mesec in kot je klinično indicirano. Ponovitve preverjanj morajo biti pogostejše pri povečanjih vrednosti stopnje 2, 3 ali 4. *Intersticijska bolezen pljuč/pnevmonitis:* Lahko se pojavi huda, življenjsko nevarna in/ali smrtna intersticijska bolezen pljuč (ILD - *interstitial lung disease*)/ pnevmonitis. Bolnike s simptomi, ki nakazujejo na ILD/pnevmonitis, je treba spremljati, zdravljenje pa prekiniti ob sumu na ILD/pnevmonitis. *Podaljšanje intervala QT:* Opažali so podaljšanje intervala QTc. Pri bolnikih z obstoječo bradikardijo, podaljšanjem intervala QTc v anamnezi ali predispozicijo zanj, pri bolnikih, ki jemljejo antiaritmike ali druga zdravila, ki podaljšujejo interval QT, ter pri bolnikih s pomembno obstoječo srčno boleznijo in/ali motnjami elektrolitov je treba zdravilo uporabljati previdno; potrebno je redno spremljanje EKG, elektrolitov in delovanja ledvic; preiskavi EKG in elektrolitov je treba opraviti čimbližje uporabi prvega odmerka, potem se priporoča redno spremljanje. *Bradikardija:* Lahko se pojavi simptomatska bradikardija (lahko se razvije več tednov po začetku zdravljenja); izogibati se je treba uporabi krizotiniba v kombinaciji z drugimi zdravili, ki povzročajo bradikardijo; pri simptomatski bradikardiji je treba prilagoditi odmerek. *Nevtropenija in levkopenija:* V kliničnih preskušanjih so poročali o nevtropeniji, levkopeniji in febrilni nevtropeniji (pri manj kot 1 % bolnikov); spremljati je treba popolno krvno sliko (pogostejše preiskave, če se opazijo abnormalnosti stopnje 3 ali 4 ali če se pojavi povišana telesna temperatura ali okužba). *Perforacija v prebavilih:* V kliničnih študijah so poročali o perforacijah v prebavilih, v obdobju trženja pa o smrtnih primerih perforacij v prebavilih. Krizotinib je treba pri bolnikih s tveganjem za nastanek perforacije v prebavilih uporabljati previdno; bolniki, pri katerih se razvije perforacija v prebavilih, se morajo prenehati zdraviti s krizotinibom; bolnike je treba poučiti o prvih znakih perforacije in jim svetovati, naj se nemudoma posvetujejo z zdravnikom. *Vplivi na vid:* Opažali so motnje vida; če so trdovratne ali se poslabšajo, je treba razmisliti o oftalmološkem pregledu. *Histološka preiskava, ki ne nakazuje adenokarcinoma:* Na voljo so le omejeni podatki pri NSCLC, ki je ALK pozitiven in ima histološke značilnosti, ki ne nakazujejo adenokarcinoma. **Medsebojno delovanje z drugimi zdravili in druge oblike interakcij:** Zdravila, ki lahko povečajo koncentracije krizotiniba v plazmi (atazanavir, indinavir, nelfinavir, ritonavir, sakvinavir, itrakonazol, ketokonazol, vorikonazol, klaritromicin, telitromicin, troleandomicin), tudi grenivke in grenivkin sok. Zdravila, ki lahko zmanjšajo koncentracije krizotiniba v plazmi (karbamazepin, fenobarbital, fenitoin, rifabutin, rifampicin, šentjanževka). Zdravila, katerih koncentracije v plazmi lahko krizotinib spremeni (midazolam, alfentanil, cisaprid, ciklosporin, derivati ergot alkaloidov, fentanil, pimozid, kinidin, sirolimus, takrolimus, bupropion, efavirenz, peroralni kontraceptivi, raltegravir, irinotekan, morfin, nalokson, digoksin, dabigatran, kolhicin, pravastatin, metformin, prokainamid). Zdravila, ki podaljšujejo interval QT ali ki lahko povzročijo Torsades de pointes (kinidin, disopiramid, amiodaron, sotalol, dofetilid, ibutilid, metadon, cisaprid, moksifloksacin, antipsihotiki). Zdravila, ki povzročajo bradikardijo (verapamil, diltiazem, antagonisti adrenergičnih receptorjev beta, klonidin, guanficin, digoksin, meflokin, antiholinesteraze, pilokarpin). **Plodnost, nosečnost in dojenje:** Ženske v rodni dobi se morajo izogibati zanositvi. Med zdravljenjem in najmanj 90 dni po njem je treba uporabljati ustrezno kontracepcijo (velja tudi za moške). Zdravilo lahko škoduje plodu in se ga med nosečnostjo ne sme uporabljati, razen če klinično stanje matere ne zahteva takega zdravljenja. Matere naj se med jemanjem zdravila dojenju izogibajo. Zdravilo lahko zmanjša plodnost moških in žensk. **Vpliv na sposobnost vožnje in upravljanja s stroji:** Lahko se pojavijo simptomatska bradikardija (npr. sinkopa, omotica, hipotenzija), motnje vida ali utrujenost; potrebna je previdnost. **Neželeni učinki:** Najresnejši neželeni učinki so hepatotoksičnost, ILD/pnevmonitis, nevtropenija in podaljšanje intervala QT. Najpogostejši neželeni učinki (≥ 25 %) so motnje vida, navzea, driska, bruhanje, zaprtje, edem, povečane vrednosti transaminaz in utrujenost. Ostali zelo pogosti (≥ 1/10 bolnikov) neželeni učinki so: nevtropenija, anemija, pomanjkanje apetita, nevropatija, disgevzija, omotica. **Način in režim izdaje:** Predpisovanje in izdaja zdravila je le na recept, zdravilo pa se uporablja samo v bolnišnicah. Izjemoma se lahko uporablja pri nadaljevanju zdravljenja na domu ob odpustu iz bolnišnice in nadaljnjem zdravljenju. **Imetnik dovoljenja za promet:** Pfizer Limited, Ramsgate Road, Sandwich, Kent, CT13 9NJ, Velika Britanija.
Datum zadnje revizije besedila: 22.01.2015
Pred predpisovanjem se seznanite s celotnim povzetkom glavnih značilnosti zdravila.

XAR-01-15

Pfizer

Pfizer Luxembourg SARL, GRAND DUCHY OF LUXEMBOURG, 51, Avenue J.F. Kennedy, L – 1855,
Pfizer, podružnica Ljubljana, Letališka cesta 3c, 1000 Ljubljana

SAMO ZA STROKOVNO JAVNOST

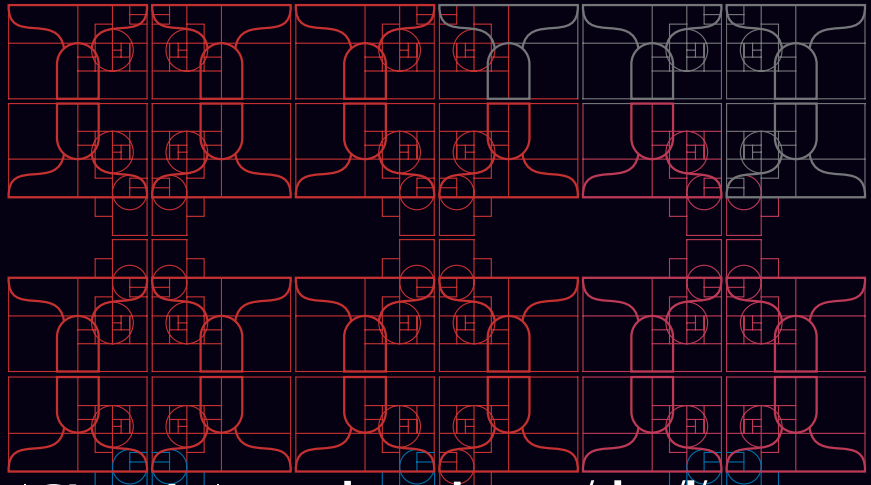

Radiology and Oncology | Ljubljana | Slovenia | www.degruyter.com/view/j/raon

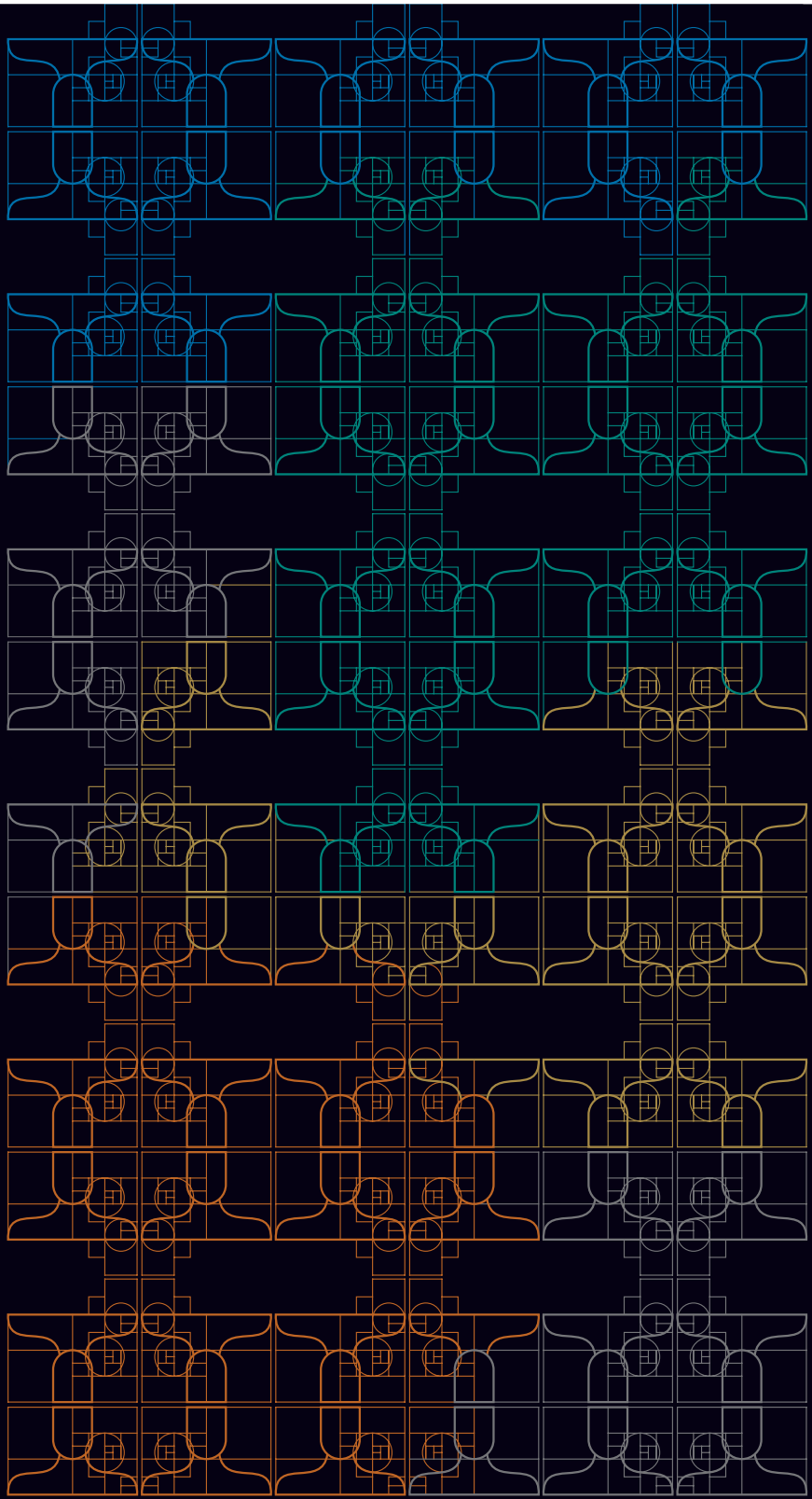

ISSN 1318 - 2099